UNIDIRECTIONAL FIBERS AND POLYURETHANE ELASTOMER
MATRIX BASED COMPOSITES - SYNTHESIS AND PROPERTIES

A. Chakar   DTIC QUALITY INSPECTED 4

Translation of "Composites à base de matrice
élastomère polyuréthanne et des fibres uni-
directionelles, Synthèse et propriétés,"
Lyon, France, Institut National des Sciences Appliquées,
Docteur-Ingénieur Thesis, No. IDI 18309, 1983, pp. 1-213.

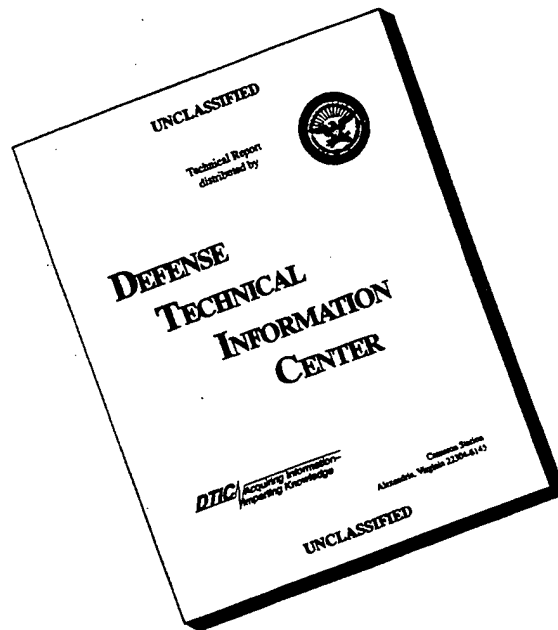19960306 048

1 JAN 1985
RECEIVED
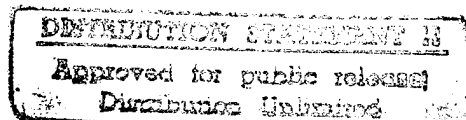
NATIONAL AERONAUTICS AND SPACE ADMINISTRATION
WASHINGTON D.C. 20546   AUGUST 1984

DEPARTMENT OF DEFENSE
PLASTICS TECHNICAL EVALUATION CENTER
ARRADCOM, DOVER, N. J. 07801

DISCLAIMER NOTICE

THIS DOCUMENT IS BEST
QUALITY AVAILABLE. THE
COPY FURNISHED TO DTIC
CONTAINED A SIGNIFICANT
NUMBER OF PAGES WHICH DO
NOT REPRODUCE LEGIBLY.

1. Report No. NASA TM-77501	2. Government Accession No.	3. Recipient's Catalog No.
4. Title and Subtitle UNIDIRECTIONAL FIBERS AND POLYURETHANE ELASTOMER MATRIX BASED COMPOSITES SYNTHESIS AND PROPERTIES		5. Report Date AUGUST 1984
		6. Performing Organization Code
7. Author(s) A. Chakar		8. Performing Organization Report No.
		10. Work Unit No.
9. Performing Organization Name and Address SCITRAN Box 5456 Santa Barbara, CA 93108		11. Contract or Grant No. NASw 3582
		13. Type of Report and Period Covered Translation
12. Sponsoring Agency Name and Address National Aeronautics and Space Administration Washington, D.C. 20546		14. Sponsoring Agency Code

15. Supplementary Notes

Translation of "Composites à base de matrice élastomère polyuréthanne et des fibres unidirectionelles, Synthèse et propriétés," Lyon, France, Institut National des Sciences Appliquées, Docteur-Ingénieur Thesis, No. IDI 18309, 1983, pp. 1-213. (84A 11992) ORIG. LANG.

16. Abstract

This work provides a synthesis and study of elastomers. The first part investigates polyurethane formulations prepared from commercial diisocynate prepolymers or prepared in a laboratory. The second part characterizes the composite material prepared with three types of formulations. This study make it possible to study composites using a polyurethane matrix and provided data on commercial polyurethane formulations.

17. Key Words (Selected by Author(s))	18. Distribution Statement Unclassified and Unlimited	
19. Security Classif. (of this report) Unclassified	20. Security Classif. (of this page) Unclassified	21. No. of Pages 199	22. Price

OUTLINE

INTRODUCTION

PART ONE - POLYURETHANE EXLASTOMER MATRICES

PART TWO - REINFORCED UNIDIRECTIONAL POLYURETHANES

APPENDIX - EXPERIMENTAL PART

GENERAL CONCLUSION

REFERENCES

TABLE OF CONTENTS

iv

Summary:

The purpose of this work is to provide a synthesis and study
of elastomers, then to fabricate and characterize elastomer-fiber
reinforcement composites used for making flexible and absorbent
structures.

To obtain castable elastomer matrices whose vitreous transition
temperature may vary from -80°C to 110°C and exhibiting good adhe-
sion with the fiber, we turned to the polyurethane family.

Our study is divided into two major parts:

1) In the first part, we studied various polyurethane formula-
tions prepared from commercial diisocynate prepolymers or prepared
in a laboratory. This enabled us to determine the choices accord-
ing to the applications;

-If an elastomer matrix with a low vitreous transition is desired,
several L-Adiprenes (DupOnt ref.) hardened with an aromatic diamine,
"Moca", may be used (L 42, L 00). Conversely, the L 315 formulation
risks being too rigid with a modulus which varies considerably with
the temperature.

Moca has the disadvantage of being carcinogenic; the other
amines currently proposed are much less efficient and the L or M
adiprenes hardened with alcohols have a much too high Tg. Yet,
laboratory formulations from polyoxytetramethylene with $M_n > 2000$,
diphenyl methane diisocyanate MDI and butanediol are totally inter-
esting. Use of the hardener di (β-hydroxyethyl) hydroquinone HQEE
instead of butanediol may produce more efficient products, provided that
the use of an operating temperature of 100°C instead of 80°C is not overlooked.

-if one wants to have an absorbent matrix with a Tg between -20°
and ambient temperatures, all L or M adiprenes hardened with alco-
hols are perfectly suitable. The L 100 hardened with a butanediol

+ triol mixture at a very high absorption peak, but in a narrow temperature range. M or L 315 adiprenes hardened in the same conditions have a lower absorption peak, but wider temperature range.

Polyurethanes containing 1.2 (G 2000) polybutadiene also belong to this material range.

-Polyester - based polyurethanes (such as butanediol polyadipate, Cyanamid cyanoprenes) have intermediary properties.

2) The second part of the study pertains to the characterization of composite materials prepared with 3 different types of formulations.

We studied the polyurethane matrix in the presence of tissues, via extraction, infrared spectroscopy and calorimetric measurements. The chemical reaction from this is disturbed very little by the presence of fiberglas and even less by carbon or Kevlar. At present, we have no explanation for this phenomenon.

The static mechanical properties are determined via bending tests on 3 points, as a function of the temperature. Examinations of fracture topography in a scanning microscope show that the adhesion with the carbon and Kevlar fibers is inadequate and this may be associated with the preceding phenomenon. The deviation in the values of the longitudinal and transverse modulii from those of the mathematical models is greater in the case of carbon composites.

The viscoelastic properties are obtained by dynamic mechanical measurements as a function of the temperature (Rheovibron). The problem of the existence of a second transition beyond Tg in unidirectional composite materials has been extensively elicited in literature. We also observe this second transition on our composites.

We tried to show that this was not a thermodynamic transition, but would be due to "slip phenomena along the fibers".

3) <u>In conclusion</u>, this study made us more familiar with commercial polyurethane formulations and above all it enabled us to take up the study of composites using a polyurethane matrix. We were able to offer SNIAS Marignanne with glass composites based on commercial formulations to be tested on mechanical structures. This study also enabled us to focus on the problem of preparing such materials and on the advantage of having prepolymers with inhibited isocyanate functions, a subject which we shall expound in this text.

This is the text of the Docteur-ingenieur thesis writ-
ten by Mr. A. Chakar and upheld on June 9, 1983 in
Lyon

(Jury: Mrs. Gallicher, Mr. J. Azeau, Mr. Baulé, Mr. J.
Golé, Mr. J.P. Pascault and Mr. J. Schultz).

x

INTRODUCTION

Composite materials may replace other traditional materials, due to their specific properties (performance/density ratio) and their corrosion behavior.

They are used in the aeronautics industry, but also in numerous other sectors: civil engineering, petroleum industry, electrotechnics and anything involving transport means (land or sea).

The purpose of this work is to provide a synthesis and study of elastomers, then to fabricate and characterize elastomer composites with long reinforcement fibers which are used for making flexible and absorbent structures.

To obtain castable elastomer matrix whose vitreous transition temperature may vary from -80°C to +10°C and exhibiting good adhesion with fiber, we turned to the polyurethane (PUR) family.

Our study is divided into two main parts. In the first part, we shall study various formulations for polyurethanes synthesized from commercial diisocyanate prepolymers or prepared in the laboratory. The mechanical and calorimetric properties will be defined as a function of the chemical composition and type.

The second part will characterize the composite materials prepared using a few previously selected polyurethanes.

Three types of formulations will therefore be studied. Unidirectional glass fabrics will be the main long fiber reinforcement. We also used T300 carbon and K 49 aramide fabrics. /2

In this part, we will study the quality of the matrix in the presence of fibers via extraction, infrared spectroscopy (IR) and calorimetric measurements. The viscoelastic properties will be obtained using dynamic mechanical measurements as a function of the temperature.

The static mechanical properties will be determined via bending tests on three points as a function of the temperature.

The problem of the existence of a second transition beyond the vitreous transition in unidirectional composite materials has been widely elicited in literature. We also observed this second transition on our composites. We will show that this is not a thermodynamic transition, and that it is due to "slip" phenomena along the fibers.

COMPOSITES MADE UP OF A POLYURETHANE ELASTOMER MATRIX AND UNIDIRECTIONAL FIBERS SYNTHESIS AND PROPERTIES

A. Chakar

PART-ONE

POLYURETHANE ELASTOMER MATRIX

I- Bibliographic Introduction

I-1 - General

The term "polyurethane" is very commonly used to describe a   /5*
wide variety of polymer materials, including reticulated elastomers
and thermoplastic elastomers as well as paints, adhesives, cast
pieces (RIC: Reaction - Injection - Casting) or foams.

This is a conventional term to the extent that this type of
polymer is not obtained by polymerizing "urethane" monomer mole-
cules.

Generally, these polymers come from the polycondensation of
diisocyanate groupings with diol molecules of fairly high molecu-
lar weight. Polyureas are obtained with diamine molecules.

The beginnings of polyurethane technology is recent. The
chemistry of organic isocyanates dates back to 1849 when Wurtz
prepared aliphatic isocyanates by reacting organic sulfates with
cyanates. The commercial use of isocyanates goes back to World War
II, when the Bayer Laboratories accelerated their polyurethane (PUR)
production. Since then, various methods of synthesis have been
investigated to prepare PURs.

I-2 - Polyurethane Synthetic Reactions

The urethane group therefore comes from the chemical reaction
between an isocyanate grouping (NCO) and a mobile hydrogen, as in
alcohol (-OH) or in an amine ($-NH_2$).

---

*Numbers in the margin indicate pagination in the original text.

1

$$R - N = C = O \quad + \quad R' - H \; \rightleftharpoons \; R - N - C - R' \qquad (1)$$
$$\underset{\text{isocyanate}}{\underbrace{}} \qquad \underset{\substack{\text{mobile}\\ \text{hydrogen}}}{\underbrace{}} \qquad \underset{\text{urethane}}{\underbrace{}}$$

(with H and O shown below the urethane carbons)
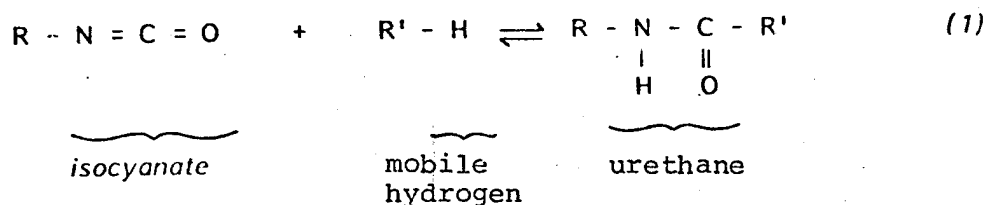
The (diisocyanate + diol) or (diisocyanate + diamine) reaction /6 aroused great interest, because polymerization does not form by-products [1].

$$OCN - R - NCO \quad + \quad HO - R' - OH$$
$$\downarrow$$
$$\left[C - NH - R - NH - C - OR' - R \right]_n$$

(with O below each C)
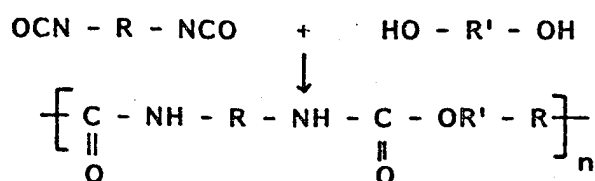
I-2-1) <u>Isocyanate Reactions</u>

The reactivity of isocyanates is due to the presence of two consecutive and polarizable bonds, which may have two mesomer forms:

$$R - N = C = O \longleftrightarrow R - \overset{(-)}{N} = \overset{(+)}{C} - O \longleftrightarrow R - \overset{(-)}{N} - \overset{(+)}{C} = O \qquad (2)$$
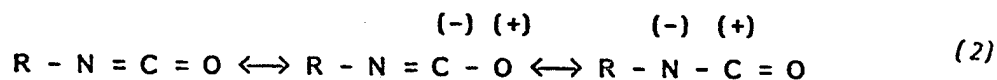
The reaction on an isocyanate is therefore due to a nucleophile attack of the electrophile center:

$$R - N = C = O + \underset{\text{alcohol}}{R' - OH} \longrightarrow \left[R - N - \overset{(-)}{\underset{\underset{\underset{H \qquad R'}{\diagup (+) \diagdown}}{O}}{C}} = O \right] \longrightarrow R - \underset{H}{N} - \underset{OR'}{C} = O \qquad (3)$$

2
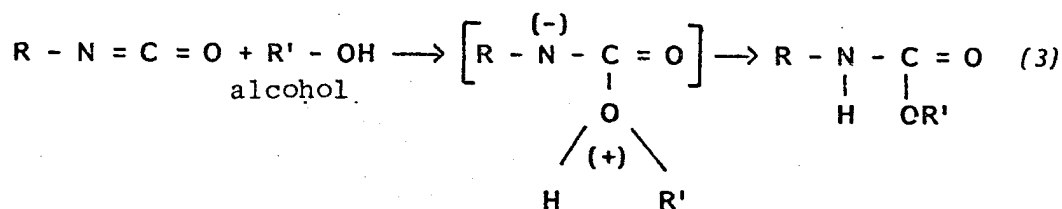
Alcohol reacts with its labile atom (-OH) to the carbon in the NCO grouping. The reaction is exothermic.

The aromatic isocyanates are more reactive than aliphatic isocyanates, but the steric component of the NCO function or of the mobile hydrogen compound tends to delay this reaction [2].

I-2-2) Polycondensation Reactions   /7

Polyurethanes are obtained by the polycondensation of compounds containing at least two active hydrogens per mole with an isocyanate having at least two functions (NCO) per mole. Thus, a linear polymer may be obtained by the reaction of a diol with a diisocyanate [3]. The reaction (1) is reversible and may be catalyzed by tertiary amines (R, R', R")N or tin salts.

Figure 1 shows the synthesis phases (in terms of the chemical reaction) of linear and segmented polyurethanes. Depending on the sequence size and distribution, polymer properties vary within fairly broad limits.

Note, however, that the use of these reagents does not necessarily give linear, fusible and soluble elastomers.

Actually, the isocyanate functions are capable of giving   /8
various chemical reactions, as we can see in Table I below.

An NCO grouping can react to an urethane to give allophanates, /9
or biurets which will be as many branching points capable of reaching the polymer reticulation [4]. In the presence of catalysts (basic catalysts especially), the aromatic isocyanates in particular dimerize into urethidione, trimerize into isocyanurate or polymerize at a lower temperature into products of high molecular weight.

Acid or basic impurities should be avoided. They cannot directly react to diisocyanate or diol, but often tend to favor secondary reactions [5].

macrodiol   diisocyanate

HO ∿∿∿ OH   OCN - R - NCO

OCN - R - NCO∿∿∿ OCN - R - NCO ∿∿∿ OCN - R - NCO

diisocyanate prepolymer

chain extender
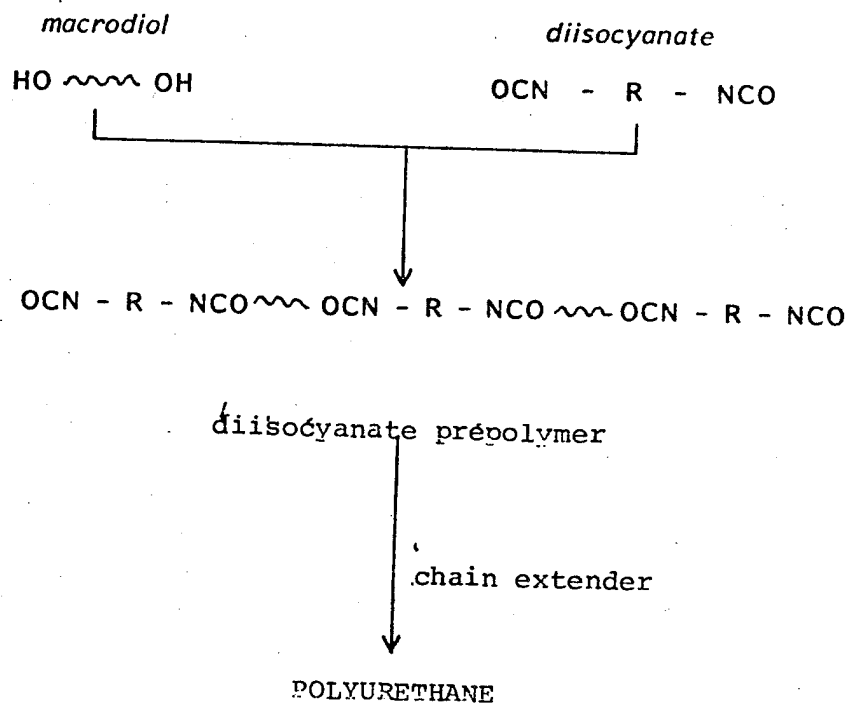
POLYURETHANE

Fig 1 - Diagram of Polyurethane Synthesis

When the polymer synthesis passes through the free (NCO) pre-polymer stage, this prepolymer shall be prepared in temperature and catalytic conditions such that only the expected reaction occurs, without the secondary reactions just described.

The reactions created by this process are therefore complex. If water is present in the system, in addition, it reacts to iso-cyanate to possibly form an amine and carbonic anhydride. The amine formed is then able to react. This is the basic reaction for making foam.

The chemistry of polyurethanes is therefore complex. The synthesis of these polymers involves a large number of reactions which can be guided by a careful selection of the operating conditions.

4

Table 1

POSSIBLE REACTIONS OF ISOCYANATE FUNCTIONS

1. $- R - N = C = O + R' - OH \rightleftharpoons R - NH - \underset{\underset{O}{\|}}{C} - OR'$

    isocyanate   alcohol   urethane

2. $- R - N = C = O + R' - NH_2 \longrightarrow R - NH - \underset{\underset{O}{\|}}{C} - NH - R'$

    amine   substituted urea

3. $- R - N = C = O + R - NH - \underset{\underset{O}{\|}}{C} - OR' \longrightarrow - R - NH - \underset{\underset{O}{\|}}{C} - \underset{\underset{R}{|}}{N} - \underset{\underset{O}{\|}}{C} - OR'$

    urethane   allophanate

4. $- R - N = C = O + R - \underset{\underset{O}{\|}}{NHC} - NHR' \longrightarrow R - NH - \underset{\underset{O}{\|}}{C} - \underset{\underset{R'}{|}}{N} - \underset{\underset{O}{\|}}{C} - NHR$

    substituted urea   substituted biuret

5. $- R - N = C = O + H_2O \longrightarrow RNH_2 + CO_2$

    amine

6. $- n(R - N = C = O) \rightleftharpoons \{\underset{\underset{R}{|}}{N} - \underset{\underset{O}{\|}}{C}\}_n$

    linear polymer

7. $- 3(R - N = C = O) \longrightarrow$

    isocyanurate

8. $- 2(R - N = C = O) \longrightarrow$

    uréthidione

5
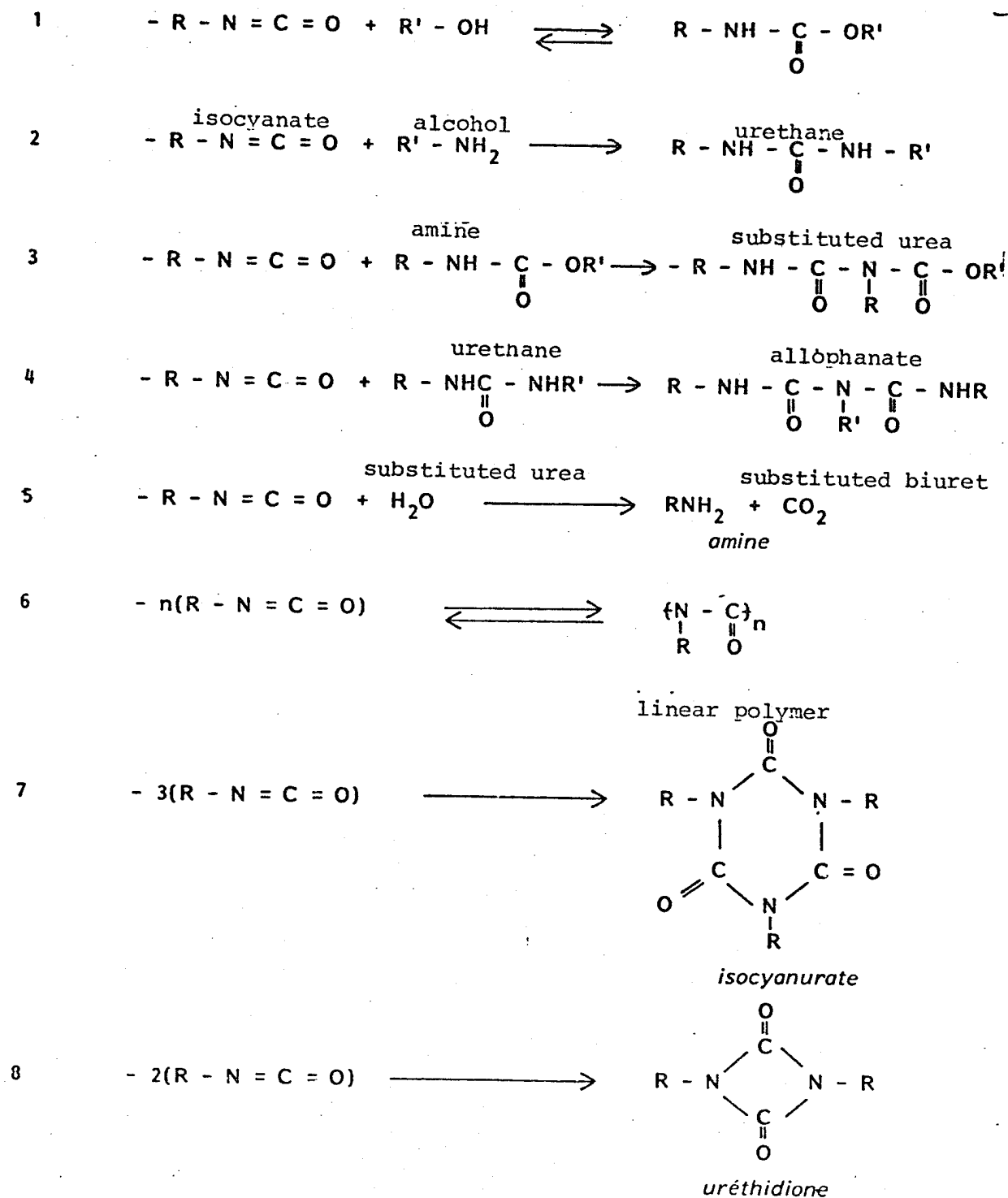
I-2-3) Conditions for Polyurethane Synthesis

A widely used synthesis process, commonly called a "one shot" process consists of directly mixing various reagents. However, due to the considerable difference in the reactivity between macrodiol and the chain extender, in most cases, a two-phase synthesis is required [6,2].

In these conditions, macrodiol reacts to diisocyanate to form a prepolymer with an NCO ending (Figure 1). During the second phase, the reaction of the residual NCO functions occurs with a chain extender which may be a diol or an amine of low molecular weight. These two phases may be executed in mass or in solution.

The BAYER group focused on the technique of polymerizing in   /10 the melted state to obtain homopolymers with high molecular weights. In general, this method is not used for polymers which melt at temperatures above 220°C. Beyond this temperature, the reaction's balance favors the thermal dissociation of urethane which restores isocyanate.

The tests of polymerization in solution did not lead to results due to the absence of a nonreactive and sufficiently polar solvent for dissolving polyurethane. This limited the development of this technique until very recently.

Currently, solvents such as toluene, methylene chloride and benzene are used to prepare polyurethanes, but for the last phases of the reaction, the polymer is not in solution. Polar solvents such as dimethylformamide, dimethylsulfoxide and dimethylacetamide are not inert with respect to the NCO functions [7]. Note that the evaporation of the synthetic solvents causes technical and economic problems.

6

I-3 Structure-Properties Relationships

I-3-1) Demonstration of the Heterophased Structure of Polyurethanes

Polyurethane synthesis creates numerous different patterns in
the chain. Due to their polarity, the urethane groups are involved
in the interactions between chains whose impact on the mechanical
properties has been proven many times [8-11]. These interactions
are of a polar nature (hydrogen bonds) or of an apolar nature (Van
der Waals). Many authors predicted and showed that the break in
the hydrogen bonds may be the cause of a relaxation [12-15]. In
this case, the (NH) group of the urethane function serves as a giver
whereas the carbonyl group of the urethane function serves as a
proton receiver.

The so-called flexible sequences are essentially made up of mac-
rodiols (polyether or most often polyester) and the so-called rigid
sequences of the chain extender reaction and the isocyanate group-
ings (NCO).

The usual properties of polyurethane elastomers are due to the
thermodynamic nonmiscibility of their sequences resulting in the
formation of a two-phase flexible and rigid structure (Figure 2)
made up of flexible sequences and rigid sequences of the macromole-
cule, in variable proportions [16-25]. Accordingly, the rigid
sequences are able to combine into nodules, thus creating the retic-
ulation which gives these polymers their elastometeric property.
The flexible sequences intercalated between these rigid sequences
play the role of a spring.

This phenomenon of phase separation was the subject of several /12
studies. This was demonstrated in the electronic microscopic anal-
yses by S.L. COOPER [17], J. KOUTSKY [26], Y. CAMBERLIN [27] or in
the x-ray diffusion at small angles by SAMUELS and WILKES [22]. The
rigid ranges scattered in the flexible die exhibit dimensions on the
order of 50 to 150 $\overset{o}{A}$.

——— Rigid Sequence

ℓℊ Flexible Sequence

Figure 2 - Structural Model of a Polyurethane
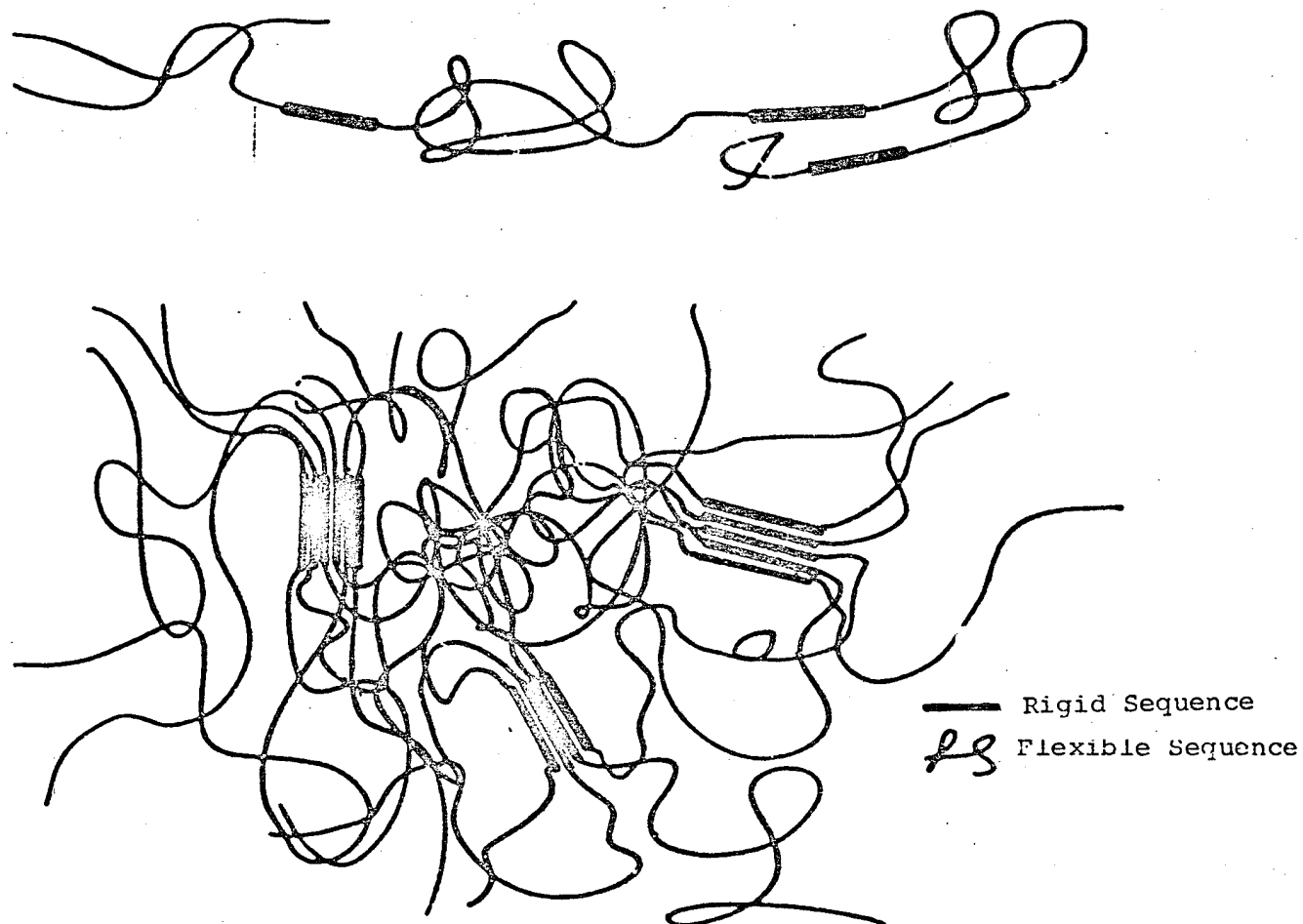
The study of miscibility between rigid segments (RS) and flexible segments (FS) was recently conducted in our laboratory by Y. CAMBERLIN et al. [28]. It was shown that the relative miscibility between RS and FS is an important parameter which conditions the quality of the phase separation and thereby the final properties of the material. We will return to this point in part I-3-2).

8

I-3-2) Relationships Between the Structures of the Formulation
    Components and the Properties of Materials

In approaching the problem of selecting materials, it is important to study the relationships between the chemical structure, the morphology, the properties. First, we will try to describe the role played by the various components in the corresponding polyurethane properties.

a) Flexible Segments (Oligomers, Diol α-ω).

The flexible segments are those which give the polyurethanes their flexibility. The polyethers and aliphatic polyesters are used the most. They exhibit low vitreous transitions (below ambient temperatures) and are generally amorphous or have a melting point below 100°C.

The mean molecular weight $\overline{Mn}$ of the flexible segments influences the elastomer properties of the PURs. An increase in $\overline{Mn}$ lowers the modulus and increases the elongation at rupture. The flexible segments of $\overline{Mn} \leq 600$ give the rigid materials very few elastomers [29].

Table II shows the results of the work of S. LIN et al. [30] as a function of the flexible segments.

Table II
INFLUENCE OF FLEXIBLE SEGMENT % AND TYPE ON THE PROPERTIES
OF POLYURETHANE ELASTOMERS [30]
/13

Formulation	Vibrathane B-635 [a) (g)	Vibrathane 6020 [b) (g)	Butane diol (1-4) (g)	Hardness Shore A	Shore D	Elongation at rupture (%)	Tension modulus (MPa)
1	100		7,16	92	37	345	38,1
2	100		8,31	93	37	338	42,2
3	100		8,78	94	37	462	39,8
4		100	5,70	85	35	500	43,5
5		100	6,64	85	36	555	44,3
6		100	7,43	86	35	531	44,1

a) MDI prepolymer containing $\overline{M}n$ polyether (POTM): 530 (Uniroyal Ref.)

b) MDI prepolymer containing $\overline{M}n$ polyester : 665 (Uniroyal Ref.)

b) Rigid segments (diisocyanate + chain extender):

The rigid segments in polyurethanes give larger forces and interchain bonds than the forces of flexible inter-segment bonds. This is due to the high concentration of the polar groupings and to the numerous possibilities of creating hydrogen bonds. Certain rigid segments may be semi-crystalline and give melting temperatures $T_f > 150°C$.

The influence of the percentage and the type of rigid segments on the mechanical properties of PURs, particularly the modulus, the hardness and the tearing strength, is very high, especially in terms of behavior and high temperature performance.

Influence of the Diisocyanate Reagent
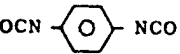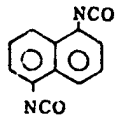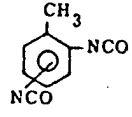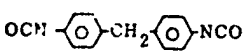
The influence of the chemical structure of the diisocyanate on the physical properties of the elastomer polyurethane was the subject of several studies [31-34]. The aromatic diisocyanates, with a symmetrical chemical structure, give high moduluses and hardnesses to the corresponding elastomers (Table III). The bulky structure of 1,5-NDI seems to give the material a higher modulus and hardness than the p-PDI structure with a single aromatic core, or with a more flexible structure of MDI. The molecules with asymmetric structures such as 2,4/2,6-TDI (isomer mixture) give the materials lower properties.

Influence of the Chain Extender

The most commonly used chain extenders are diols and diamines. Diols are used for rigid "polyurethane" segments, whereas diamines essentially form rigid "urea polyurethane" segments. This fundamental difference generally results in differences in the physical properties between the two types of corresponding materials, due

10

Table III

INFLUENCE OF THE DIISOCYANATE STRUCTURE ON THE PHYSICAL PROPERTIES OF ELASTOMER POLYURETHANES [34]

Diisocyanate	Tension Modulus (MPa)	Elongation at Rupture (%)	Tearing Strength	Modulus at 300% (MPa)	Hardness (°IRHD)
pPDI [a] OCN—⬡—NCO	44,1	600	52,5	15,8	72
1,5 - NDI [b]	29,4	500	35,3	20,6	80
2,4/2,6 TDI [c]	31,4	600	26,5	2,5	40
MDI [d] OCN—⬡—CH₂—⬡—NCO	54,4	600	47,1	11,0	61
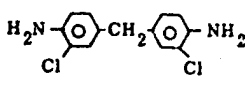
a) p-PDI: p.phenylene diisocyanate; b) 1,5-NDI = 1,5-napthalene diisocyanate

c) 2,4/2,6-TDI: mixture of isomers from toluene diisocyanate

d) MDI: diphenylmethane diisocyanate

to the presence of strong hydrogen bond interactions in the urea
groupings. Table IV shows a few results for a polyether/TDI-based
polyurethane.

Table IV

COMPARISON OF DIOL AND DIAMINE CHAIN EXTENDERS* FOR
POLYURETHANES [35]

Chain Extender (Elongation Process)	tension modulus (MPa)	modulus at 300%(MPa)	elongation at rupture	Hardness (°IRHD)
Moca [a]	31,7	12,6	450	90
Moca/MDA/m-PDA [b,c] 60 / 20 / 20	31,7	7,3	450	62
1,4-Bd/TMP [d,e] (1,0/0,3)	8,9	2,1	560	57
1,4-Bd /TMP (3,0/1,3)	10,4	2,9	470	60

a) Moca : 3,3' dichloro-4,4' diamino diphényl méthane
b) MDA : méthylène dianiline ; c) m-PDA : m.phénylène diamine
d) 1,4-Bd : 1,4-butanediol
e) TMP : triméthylol propane

In the case of diol chain extenders, a proportion of triol
may be used to reticulate the network formed to improve the proper-
ites. However, these materials have lower qualities than those of
the diamine chain extenders.

Recently, a study was conducted by S. LIN et al. [30] on the
properties of polyether or polyester/MDI-based polyurethanes and
diols as chain extenders. The authors compared these results with
those obtained for the diamine chain extender systems plus TDI-based
prepolymers. Their conclusions stressed the fact that with polyure-
thanes prepared from MDI-based diisocyanate prepolymers, a wide line

*Translator's note: "chain extender" refers to chain elongation
process.

of products is obtained as a function of the type of chain extender
diol used. Despite their lower hardness, the wide variety in their
physical properties makes them comparable to polyurethane elastomers
prepared from TDI diisocyanate prepolymers and amines as chain ex-
tenders (Table V). D. KLEMBER and K.C. FRISCH [37] recently studied
the properties of polyurethanes prepared from an MDI diisocyanate pre-
polymer and using an aromatic diol: (β-hydroxyethyl) hydroquinone
(HGEE): use of HQEE and its derivative HER {resorcinol di (β-hydroxy-
ethyl)ether} whose melting temperature is 89°C, as replacement mole-
cules has already demonstrated good elastomer properties.

Table V

COMPARISON OF THE PHYSICAL PROPERTIES OF THE PUR SYSTEMS [30]

Polyurethane	Bd 1.4	Moca	Elongation at Rupture (5)	Tension Modulus (MPa)
polyether - MDI prepolymer	8.31/phr	----	338	42.2
polyether - TDI prepolymer	--	12.5/phr	450	44.3

I-3-3) Research in Our Laboratory on the Miscibility of Flexible and Rigid Segments

The research now being conducted may be divided into three parts:

a) Study of the Model Rigid Segments

A line of model rigid segments containing MDI and butanediol,
of various lengths and having various chain ends was synthesized
[38] and studied via differential calorimetry. The chain end may
be of different types (methyl, ethyl, octyl, ocatadecyl, etc.).
An example of prepared rigid segments [38] is presented below:

R - O - C - N -⟨O⟩- CH$_2$ -⟨O⟩- N - C - O - R : SR1   (rigid segment
    ‖ | | ‖   with one MDI
    O H   H O   unit)
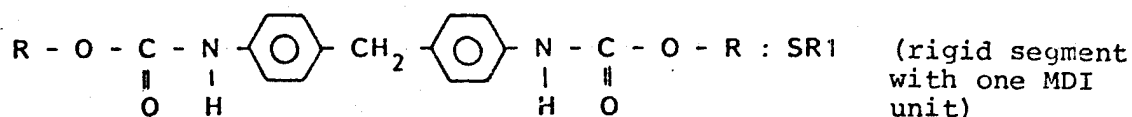
where R is the chain end

The following observations may be made from this examination of the melting temperatures, the melting enthalpy T_f:

-T_f depends both on the segment length and the length of the linear chains attached to its ends.

For segments ending with methyl, ethyl, octyl type short linear chains, T_f increases up to SR3 then decreases for SR4. Conversely, if the chain end is long enough (octadecyl), T_f increases steadily from SR1 to SR4; this indicates the presence of two quite separate phases: one phase containing rigid segments and one phase formed at their ends by long incompatible hydrocarbon chain ends.

Rigid segments of high molecular weight may exhibit an amorphous nature and no second order transition was detected via calorimetry.

b) Following this research, other rigid segments based on MDI and various types of chain extenders [39] as well as the corresponding linear polyurethanes were analyzed. The chain extenders used were the α-ω alkane-diols (from ethane to decane), diaminobutane-1.4, dimethanol benzene-1.4 and methylene 4.4'bis(2-chloroaniiline) or Moca. The following conclusions were drawn from this study:

The α-ω alkane-diols form rigid crystalline segments with MDI, whereas in the case of other chain extenders (aromatics and aliphatic diamines) they are virtually amorphous.

Butanediol has a rigid segment which melts at higher temperatures.

14

The dynamic mechanical properties of the corresponding poly-
urethanes have either amorphous or crystalline rigid segments
with a lower crystallinity ratio than that of the model rigid seg-
ments.

c) Phase Separation Study

The phase separation rate was evaluated quantitatively using
calorimetric measurements (DSC) on polyurethanes and linear polyur-
ethanes [40]. The principle of the method consists of measuring
the variation of the calorific capacity ΔC_p of flexible segments
undergoing the vitreous transition Tg in polyurethanes and then
comparing this value with the variation ΔC_p corresponding to pure
flexible segments. Thus, the flexible segment quantity present in
the rigid ranges may be deduced. This is made possible by the fact that
during the vitreous transition of rigid segments the variations of
the calorific capacity are so small that they are not detectable
in DSC. Thus the presence of these segments as an impurity in the
flexible phase does not influence the determination of ΔC_p.

The following observations may be made from this third part of
the study:

The phase separation rate depends on the nature of the flex-
bile segments present. It decreases from hydrogenated polybutadiene
to polybutadiene to polyether. The highest rate (83%) therefore
corresponds to the urethane polyolefin system where the greatest
incompatibility is observed.

The phase separation rate also depends on the nature of the
rigid segments present. In the case of butane diol-1.4, as chain
extender, the lowest phase separation values are obtained (83%).
Using an aromatic diol HQEE or butane diamine, the value increases
to 90.5%. The highest phase separation is obtained using aromatic
amines as chain extender (93%).

Thus the phase separation rate increases with the degree of interaction between rigid segments: from an aliphatic diol to an aromatic diol, from an aliphatic amine to an aromatic amine.

Conclusion: /19

Polyurethanes underwent numerous studies on the morphology and structure - properties relationships. We tried to show in this bibliographic report the influence of the constituents on the final properties of these polymers. Thus the bibliographic study showed that the properties of elastomer polyurethanes depend enormously on the chemical structure of the components. The most interesting physical properties are obtained using TDI diisocyanante prepolymers (toluene - diisocyanate) and Moca diamine as chain extender. However, the use of MDI prepolymers (Methane Diphenyldiisocyanate) and chain extender diols may give comparable elastomer properties to polyurethanes. The studies now being conducted in our laboratory show the degree of phase separation between flexible segments and rigid segments in polyurethane elastomers as well as on high temperature behavior.

Based on the bibliographic data, we will try to study the polyurethane properties essentially as a function of the nature of the chain extender.

In the first part of this report, we will try to improve our understanding of the structure - property relationships both for polyurethanes prepared commercially and those prepared in the laboratory.

II - PROPERTIES OF LABORATORY-PREPARED FORMULATIONS: IMPACT OF THE /20
     CHAIN EXTENDER

In this part, we present the properties of polyurethanes prepared from diol α-ω oligomers and diisocyanate agents $R(-NCO)_2$.

16

After noting the characteristics of the basic reagents used, we will describe the polyurethane properties as a function of the chain extender.

II-1 Description and Characterization of the Reagents Used

The diol α-ω oligomers are glycol plyoxytetramethylene (POTM) and hydrogenated polybutadiene. Their characteristics are shown in Table XXIX in the experimental part (appendix).

The mean weights in $\overline{Mn}$ number are determined via cyrometry, the polymolecularity index ($\overline{Mw/Mn}$) via chromatography analyses on permeable gel (GPC), the mean functionality in $\overline{Fn}$ number and the microstructure via nuclear magentic resonancy (RMN), and finally, the vitreous transition temperature via calorimetric measurements (CSC) (see experimental part).

The diisocyanate agent used in this part of the study is diphenyl methane diisocyanate (MDI):

$$\text{OCN} - \bigcirc - \text{CH}_2 - \bigcirc - \text{NCO}$$
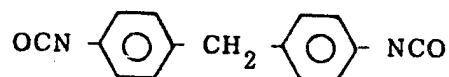
It was preferred over toluene diisocyanate (TDI) because of its linear structure and its high content in aromatic cycles.

The chain extenders are of two types: diol and diamine, aliphatic or aromatic. They are gathered in Table VI.

II-2 Properties of MDI Polyurethanes Prepared in Solution   /21

The materials studied contain one hydrogenated PBHT diol oligomer mole as flexible phase, whereas the rigid phase is made up of MDI diisocyanate (3 moles) and various chain extenders (2 moles).

17

<div align="center">

Table VI

THE CHAIN EXTENDERS USED

</div>

* aliphatic diol

butane diol 1,4	$OH - CH_2 - CH_2 - CH_2 - CH_2 - OH$	Bd
decane diol 1,10	$HO (CH_2)_{10} OH$	Dd

* aromatic diol

xylène diol $HO - CH_2 -\langle O \rangle- CH_2 - OH$ xd

di(β -hydroxyéthyl)hydroquinone

$HO (CH_2)_2 O -\langle O \rangle- O (CH_2)OH$ HQEE

* aliphatic diamine

butane diamine $NH_2 (CH_2)_4 NH_2$ Bda

aromatic diamine

4,4 méthylène bis (2-chloroaniline)

$H_2N -\langle O \rangle- \overset{H}{\underset{H}{C}} -\langle O \rangle- NH_2$ Moca

Figure 3 shows the differential thermal analysis curves for the synthesized polyurethanes.

The vitreous transition temperature of the flexible sequence is independent from the nature of the chain extender (≃ -38°C). In the case of butanediol 1,4 (curve 1), we see two melting endotherms. The endotherm with the highest temperature corresponds to the melting of the corresponding model rigid segment [28], whereas the second endotherm may be associated with the less organized rigid nodules.

Figure 3 - PUR Thermograms Prepared as a function of the Chain Extender
1- butanediol 1,4 2- HQEE 3- decandiol 4- butanediol, Moca or xylenediol
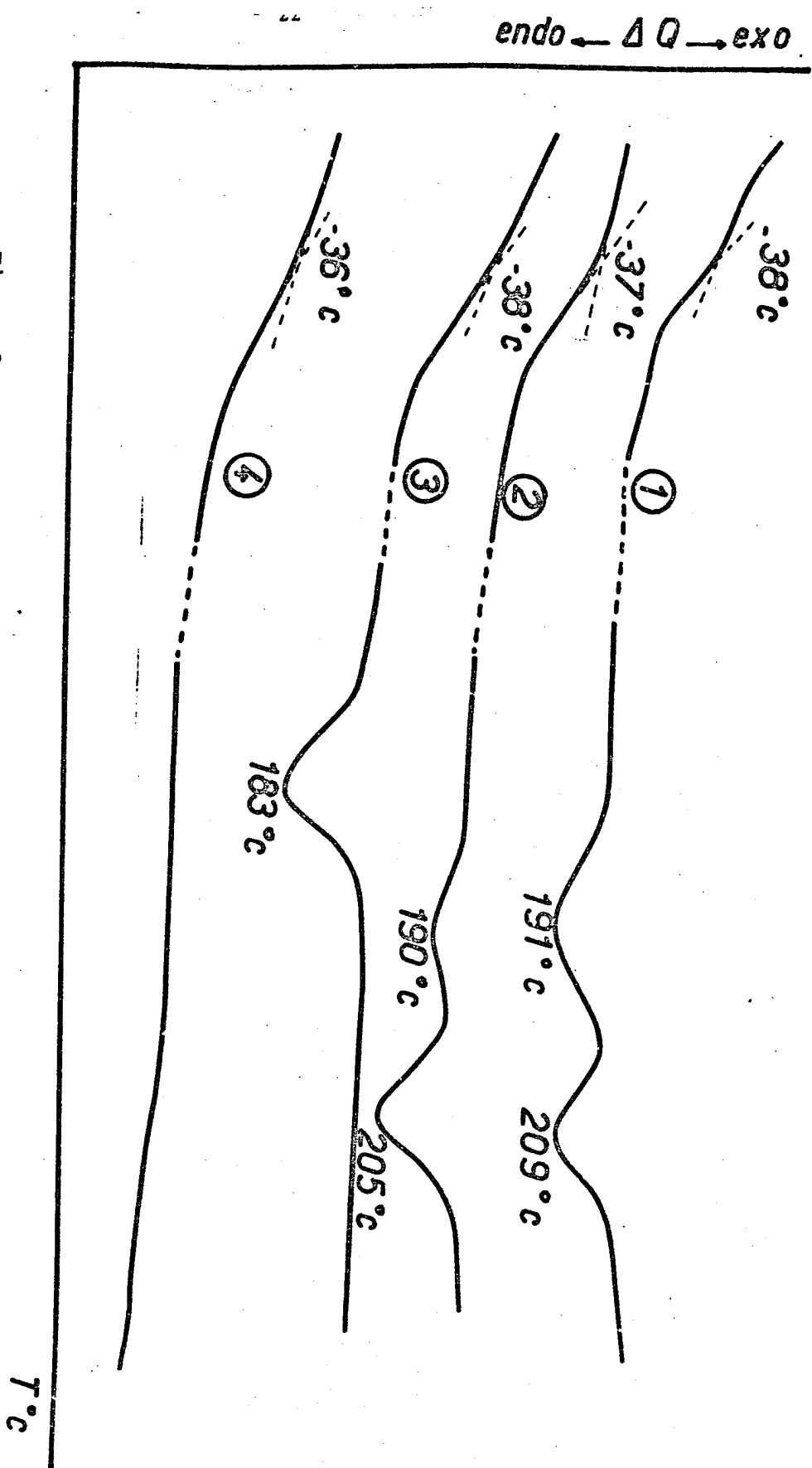
For the aromatic diol HAEE (curve 2), one also observes two melting endotherms very comparable to those in curve 1.

Curve 3 is the polyurethane thermogram prepared with decanediol (Dd). A single melting endotherm is observed, which also corresponds to the melting temperature of the corresponding rigid segment. Curve 4 corresponds to the amine chain extenders (butane diamine and Moca) and to xylenediol (xd). No first or second order transition was detected. This was also true for the corresponding model rigid segments [28].

Furthermore, the very distinct difference between the two aromatic diols is noted: xylene diol is a very rigid molecule, whereas the two oxygens (ethers) of the HQEE molecule give it a certain flexibility.

The dynamic mechanical behavior of these polymers is presented by the curves in Figures 4,5,6 and 7.

Figure 4 gives the variations of the real modulus E' and of the angle of loss tangent (tg δ) in the case of the polyurethanes containing Bd 1,4 chain extenders and decanediol which lead to semi-crystalline rigid segments (with low crystallinity contents), as we have already seen.

The curves are similar in terms of the relaxation of the flexible sequence. At higher temperatures, butane diol has a higher modulus value and we see a delayed onset of creep. This difference may be explained by the role of decanediol which gives the rigid segments less cohesiveness. The most interesting observation is that in both cases, the thermoplastic aspect occurs in the rigid phase at temperatures well below the crystallite melting temperatures. The crystallinity is therefore too low to condition the mechanical behavior of such elastomers.

20

In Figure 5, we compare the polyurethane behavior for the case
of diol chain extenders: Bd-1,4. xd and HQEE of different chemical
structures. The thermoplastic nature of the polymer with Bd occurs
in the vicinity of 110°C, that with HQEE as of 150°C and only near
180°C for that prepared with xylenediol. Although they have perfect-
ly comparable melting points for the rigid segments (200 - 210°C,
Figure 3), the polyurethanes prepared from butanediol and HQEE have
a totally different behavior. This phenomenon is even more flagrant
in the case of xylenediol which does not contain any melting endo-
therm (Figure 3).

The butanediol polymer has a lower modulus value and this is
explained by the presence of aromatic cores in the case of xd and
HQEE which increase the cohesiveness of the rigid segments.

Figure 6 gives the variations of E' and tg δ for the butanediol
and butanediamine chain extenders. Very different behaviors are ob-
served. Whereas the polyurethane extended to Bd exhibits plasticity
in the rigid phase as of 110°C, no similar phenomenon is seen up to
200°C for the polyurethane extended into butane diamine. This very
high cohesiveness was noted by numerous authors [41] and is gener-
ally ascribed in this case to the three-dimensional structure of the
hydrogen bonds which may form urea groupings following the isocyanate -
amine reaction.

In Figure 7 we compare the E' and tg δ curves for the Bd chain
extenders xd and Moca.

Note that the relaxation of the flexible polybutadiene segment
in the Moca polyurethane moves toward the highest temperatures, but
only from 5°C. It is especially interesting to note that the high
temperature behavior of these products is improved when we change
from a linear diol to xylenediol and also when we change from xylen-
ediol to an aromatic amine. We can also see that the rigid sequences
which are capable of crystallizing (case of butanediol) give the

corresponding polyurethanes the worst behavior at high temperatures. This is due to the excessive flexibility which Bd gives in the amorphous part of these rigid segments.

II-3 Properties of MDI Polyurethanes Prepared in Bulk

We used only two diol chain extenders: butanediol 1,4 and HQEE (di(β hydroxyethyl)hydroquinone) ether), with the intention of competing with the (TDI+Moca) system.

The polyurethane formulations studies are presented in Table VII. The flexible phase is POTM polyoxytetramethylene in $\overline{Mn}$ bulk of about 2000.

Table VII
LABORATORY FORMULATION OF POLYURETHANE PREPARED IN BULK

Diol/MDI α-ω oligomers	Chain extender (hardener)	Oligomer/MDI/ hardener formulation in mole	% weight oligomer	burning h/°C
POTM 1	Bd	1/4/3	67.7	24/ 80
POTM 1	HQEE	1/4/3	62.6	16/110
POTM 1	HQEE	1/5/4	56.6	16/110

Note that the HQEE chain extender is added at 110°C and not at 80°C. Actually, HQEE is a very crystalline product with a relatively high melting point (T_f = 105°C) and it has the special property of being soluble in few products. It is therefore possible to cast a polyurethane at 80°C. HQEE therefore tends to recrystallize before it reacts.

Figure 8 shows the ATD curves of the synthesized polyurethanes. The vitreous transition temperature of the flexible sequence (POTM) is again independent from the nature of the extender. Yet, the flexible semi-crystalline POTM 2000 sequences melt near 0°C. Only the high temperature behavior shows differences.

22
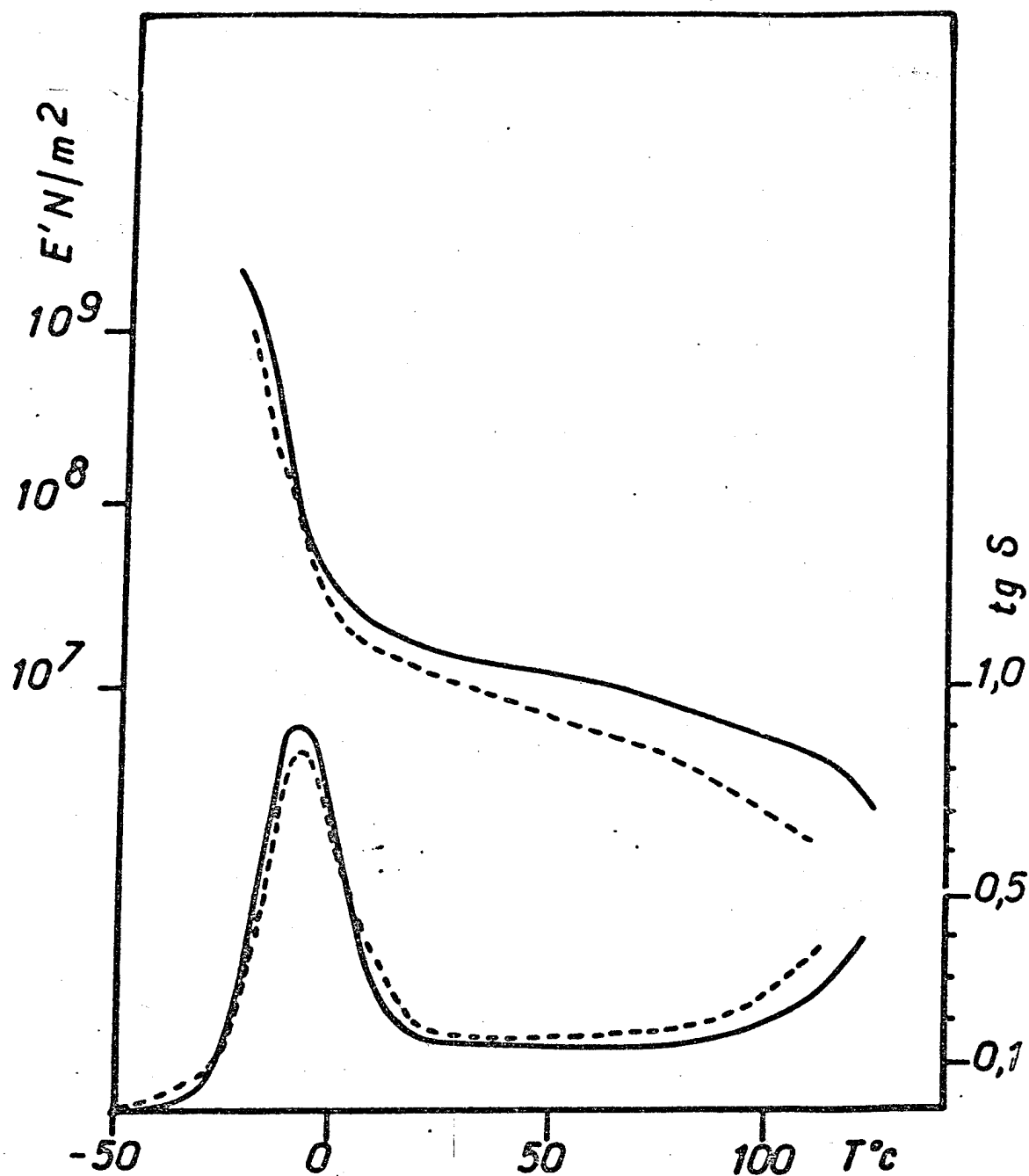
Figure 4 – Variation of the dynamic modulus E'
and tg δ as a function of the temperature
for the PURs containing Bd (-----) and
decanediol (————)
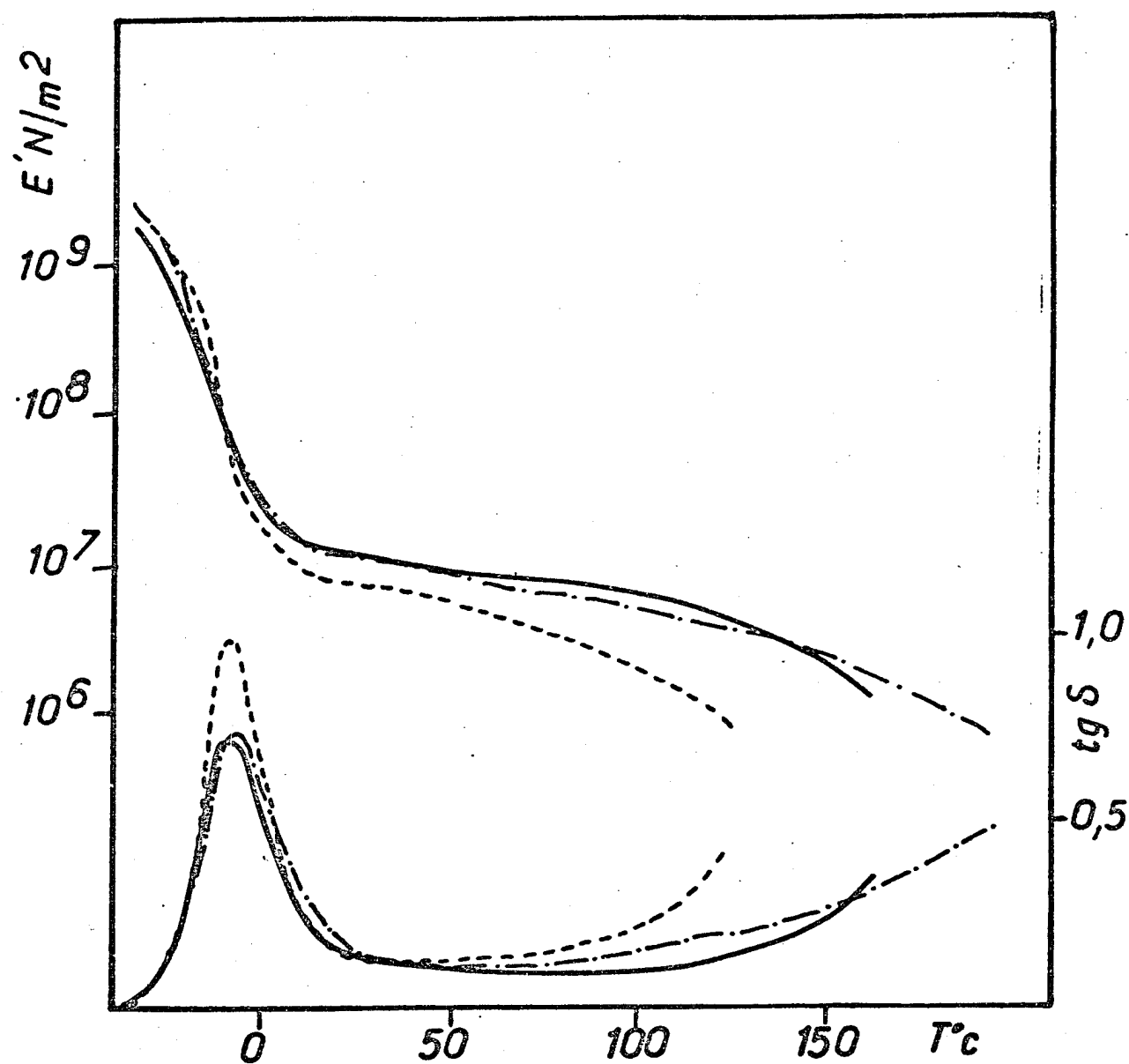
Figure 5 — Variation of E' and tg δ as a function of the temperature for PURs prepared from Bd (-----), from HQEE (————) and xylene diol (-.-.-.).

24
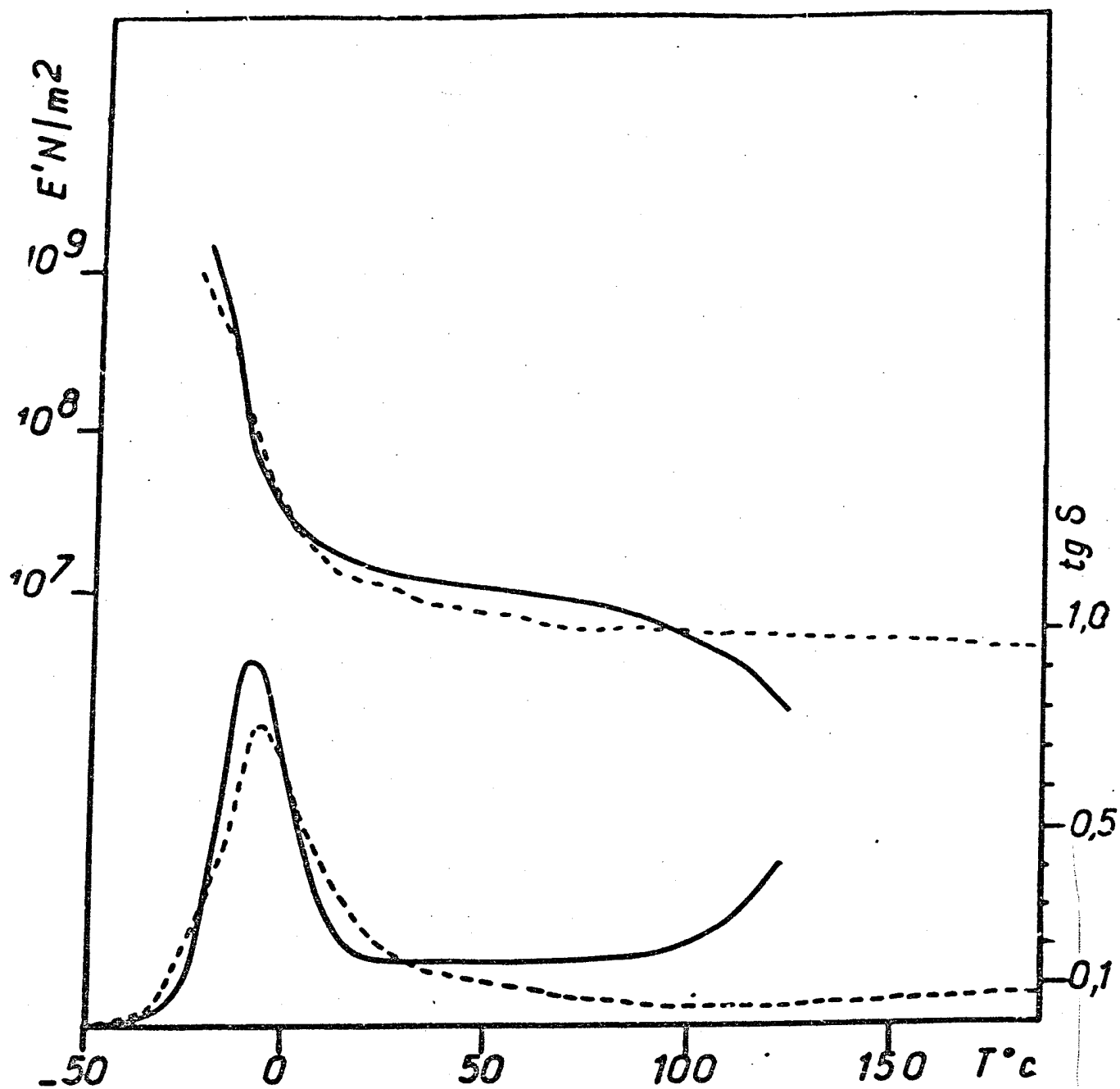
Figure 6 - E' and tg δ curves as a function of the
temperature for the PURs prepared from
Bd (————) and butanediamine (-----)

Figure 7 – E' and tg δ curves of PURs prepared
from Bd (———) from xylenediol (—————)
and from Moca (—·——·——·—)

26

In the case of Bd as chain extender (curve 1), we see a high temperature endotherm which represents the melting of rigid segments. Curve 2 of HQEE shows narrow and well-defined melting peaks. It represents the melting of model rigid segments, whereas those observed at lower temperatures represent the melting of the less organized parts. Nevertheless, an exothermic peak directly follows the first endothermic melting peak. This would represent the cry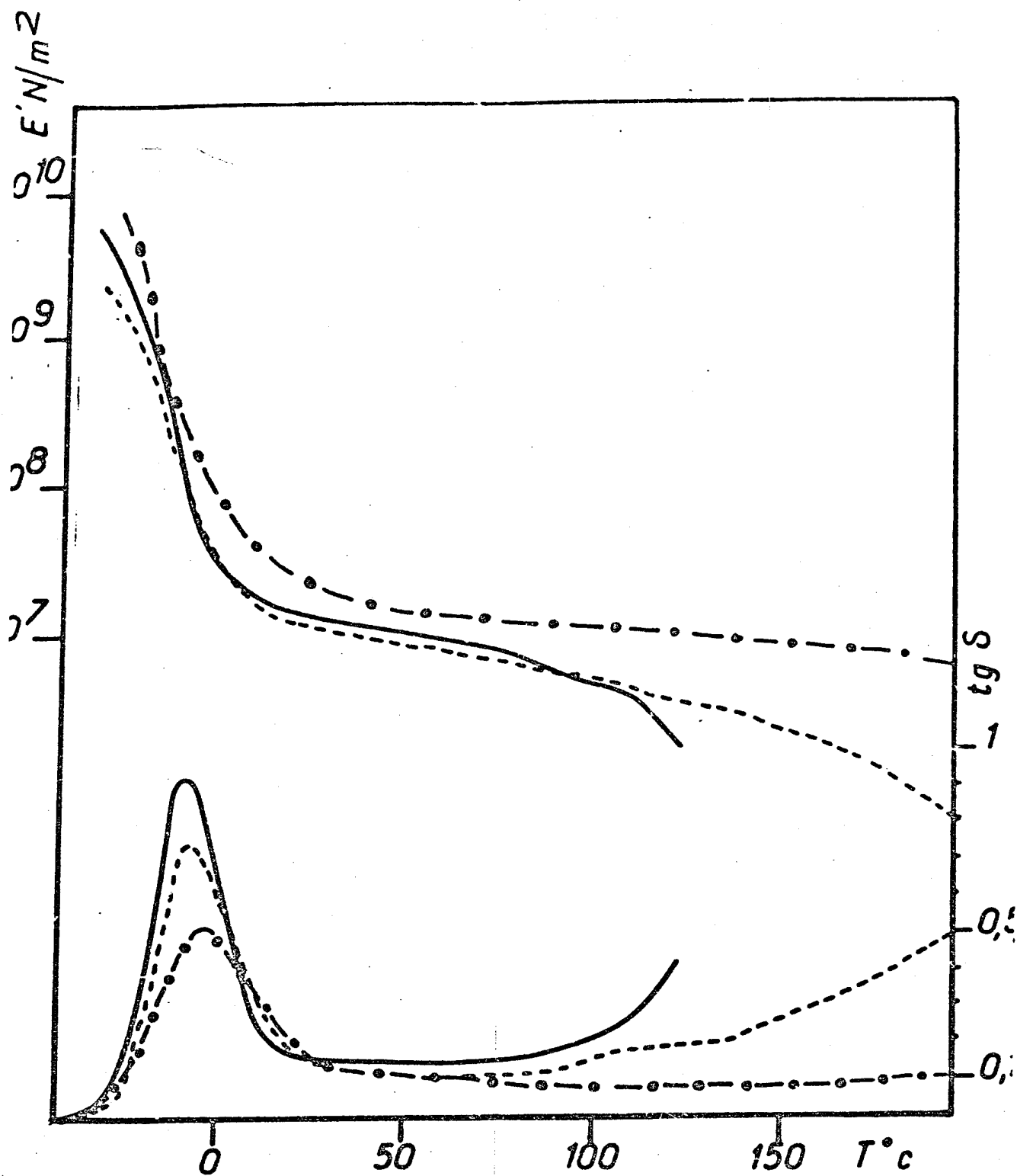st- allization of the rigid segments into very well organized crystals. Due to the symmetry of the HQEE and MDI molecules, it is also possible to have a liquid crystal behavior for these rigid segments, which tends to accentuate with their size.

The dynamic mechanical behavior of these polymers is shown in Figure 9 by the E' and tg δ as a function of the temperature.

The thermoplastic nature of the polymer with Bd as extender occurs near 145°C. That of polyurethanes with HQEE occurs as of 165°C and 175°C respectively. The difference in the module values at the rubber plateau or in the maximum value of tg δ is explained by the fact that the butanediol-based polyurethane contains 32.3 % by weight of rigid segments and the HQEE-based polyurehtane contain a similar percentage of 37.4% for the same formulation: 1,4,3 whereas it is 43.4% for the formulation 1,5,4. The relaxation of the flexible segment (POTM) shifts slightly at the highest temperatures in the case of the HQEEs and it covers a larger temperature range.

Finally, the high temperature behavior of these products is improved when we shift from a linear diol (Bd 1,4) to an aromatic diol HQEE.

Conclusion

1) The first part of the study was performed in solution, due to the excessive reactivity of the amines. Moreover, this synthesis mode makes it possible to obtain linear polymers "a priori" (Table I)
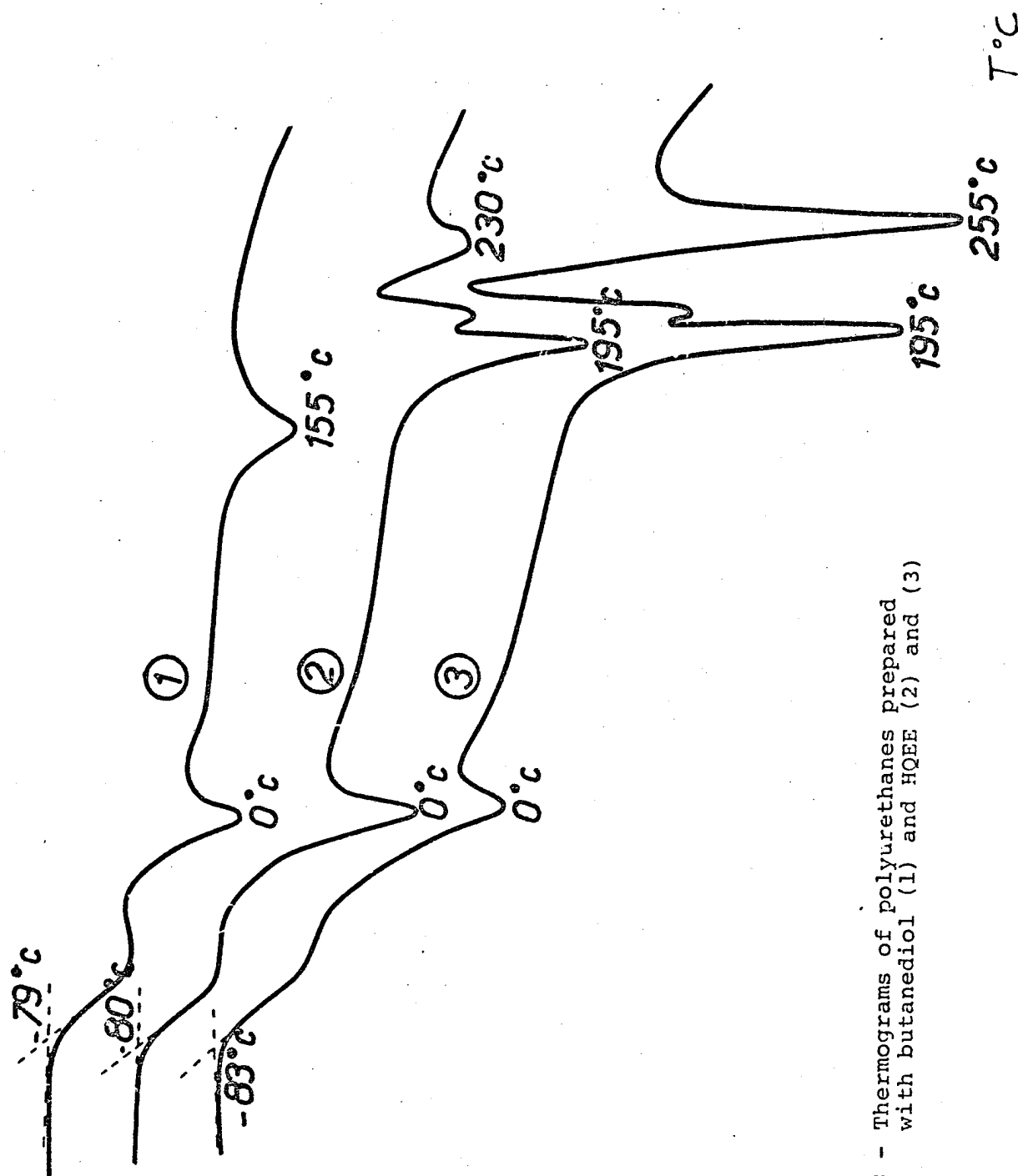
Figure 8 - Thermograms of polyurethanes prepared with butanediol (1) and HQEE (2) and (3)
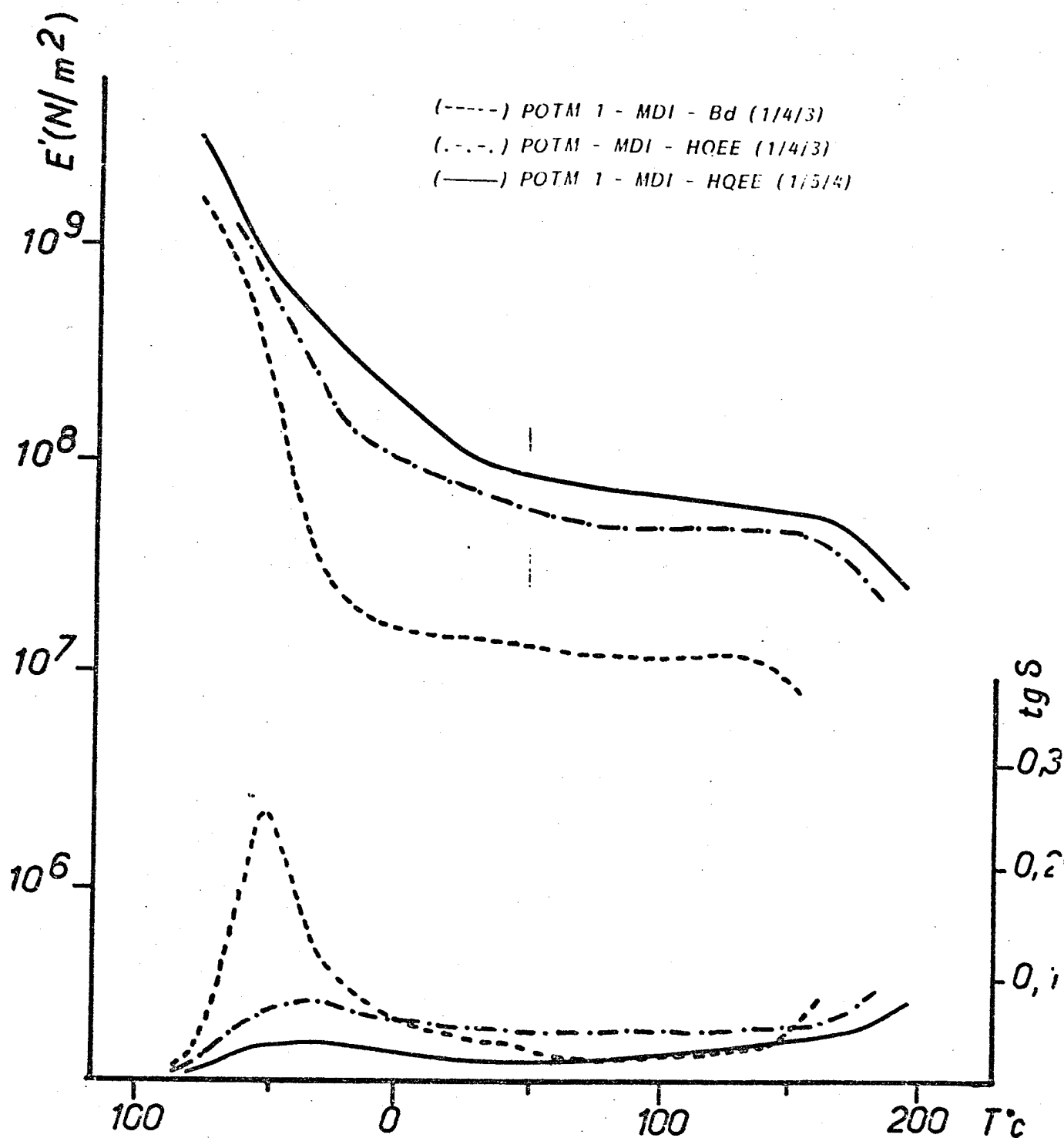
28

Figure 9 — Curve of modulus E' and of tg δ as a
function of the temperature at 11 Hz
for POTM1-based polyurethanes. Compar-
ison bewteen two hardeners: Bd and HQEE.

29

and to limit the formation of secondary products which are always capable of forming because of the high reactivity of the isocyanate functions. We can see from this part of the study that the properties of polyurethane elastomers depend very little on the crystallinity of the rigid phase, but depend a great deal on the nature and the number of interactions between the rigid segments and the possibility of these rigid segments moving into their amorphous state. We may therefore conclude that the properties of linear sequenced polyurethanes will be highly dependent upon the chemical nature of the rigid sequence responsible for the physical reticulation phenomenon. (The presence of aromatic cores in the chain extenders, such as xylenediol (xd) and HQEE give the rigid segments a better cohesiveness). One should still account for the degree of separation of the flexible and rigid phases which varies with their solubility parameters. The rigid phase always occurs with many rigid segments and few flexible segments.

2) If the synthesis cannot be performed in solution, it is necessary to use MDI-based rigid segments such as diisocyanate and diol as chain extender due to the high reactivity of the aliphatic amines on the one hand and the cancerogenic nature and excessive reactivity of aromatic amines on the other hand.

In this case, one should note the improvement in the mechanical properties made by using HQEE diol. It is imperative to use this at high temperatures t, however, because of its relatively high melting temperature ($T_f = 105°C$) and its weak solubility, below its melting temperature, with many common olvents.

III - PROPERTIES OF COMMERCIAL POLYURETHANE FORMULATIONS /34

In conjunction with this study, we tried to characterize a certain number of commercial formulations. This part presents the properties of polyurethanes synthesized from commercial diisocyanate prepolymers.

30

Before studying the polyurethanes made with commercial formulations, we first tried to characterize the basic products (prepolymers) to know the type and chemical structure of the constituents and to have a better understanding of the properties of the final material as a function of this structure.

The products and reagents come essentially from two sources: DuPont and Cyanamid. In the first case, we have various "L" or "M" Adiprene prepolymers. In the second case, "cyanaprenes" are used (Table VIII).

Table VIII
ORIGIN AND CHARACTERISTICS OF COMMERCIAL DIISOCYANATE PREPOLYMERS

Origin	Références	Type (g)	Nature	Viscosities
DuPont "Adiprène L"	L 42	2,8	polyether & toluène diisocyanate (TDI)	1,7 at 30°C
	L 100	4,1		1,8
	L 167	6,3		0,6
	L 315	9,5		1,5
DuPont "Adiprène M"	M 400	7,58	polyether diphénylméthane diisocyanate (MDI)	18,0 at 30°C
	M 467	9,70		8,3
	M 415	10,65		19,0
Cyanamid "Cyanaprènes"	A7QM	2,3	polyester & TDI	1,13 at 100°C
	A 8	1,1		1,14
	A 9	4,2		.16
	A9HT	1,2		.16
	D6	6,0		1,18

The various analysis techniques developed in the experimental part allow us to obtain the results in Table IX.

31

Table IX

MEASURED CHARACTERISTICS OF DIISOCYANATE PREPOLYMERS

Références	% NCO total in g	% NCO TDI in g	% NCO, TDI/total	Chemical Type	$(\overline{Mn})_{PS}$	$\overline{Mn}$	$\overline{Mw}/\overline{Mn}$
Adiprenes							
L 42	2,8	0,09	3,2	POTM + PPG (30 %)	4 520	2 020	2,4
L 100	4,1	0,09	2,2	POTM	2 160	1 300	2,5
L 167	6,3	0,5	9,9	POTM	1 850	1 200	1,9
L 315	9,4	0,6	6,9	POTM	1 450	960	1,9
Cyanaprènes							
A7QM	2,5	< 0,1	4,2	PAEG - Bd	3 910	3 300	2,2
A8	3,1	< 0,2	4,7	PAEG	3 710	3 150	2,0
A9	4,1	< 0,2	5,4	PAEG	2 420	1 900	2,5
A9HT	4,4	< 0,2	5,3	PAEG - Bd	2 430	1 950	3,5
D6	6,0	< 0,3	4,5	PAEG	1 150	950	2,1

POTM (or PTMG): polyoxytetramethylene; PAEG: glycol ethylene polyadipate;

PAEG-Bd: ethylene glycol polyadipate and butane diol 2,3

PPG: propylene polyoxide

a) Products Containing Toluene Diisocyanate TDI

Fiugres 10 and 11 give two examples of the RMN spectrum for an Adiprene and an Cyanaprene. The conclusions which may be drawn are the following:

The Adiprenes contain polyoxytetramethylene glycol (PTOM) and the Cyanaprenes contain ethylene glycol polyadipate (PAEG).

Adiprene L42 is a mixture of the two polyethers POTM and polypropylene glycol (PPG).

The A7QM and A9HT Cyanaprenes are polyesters (PAEG, Bd) prepared from adipic acid and a mixture of ethylene glycol and butanediol 2,3.
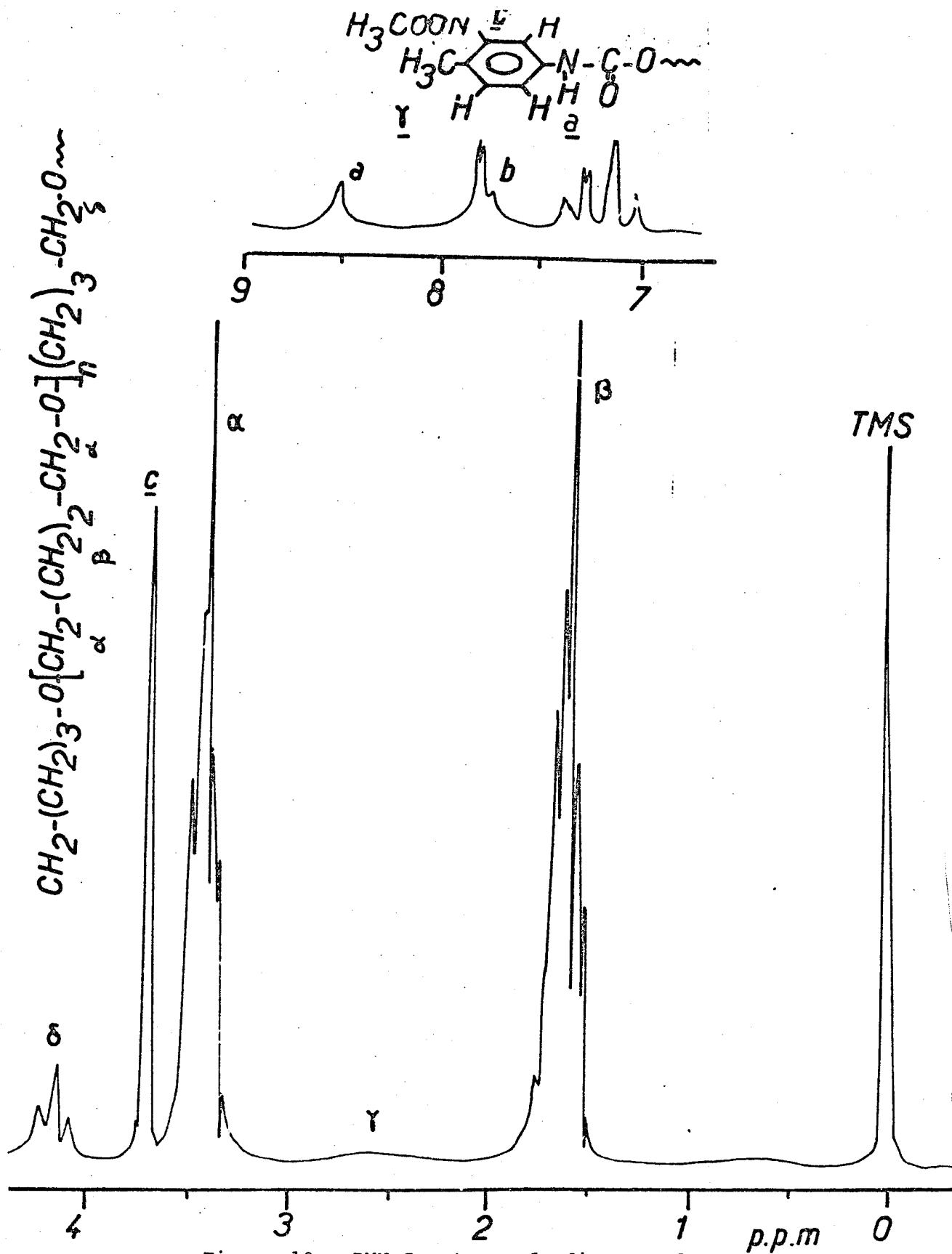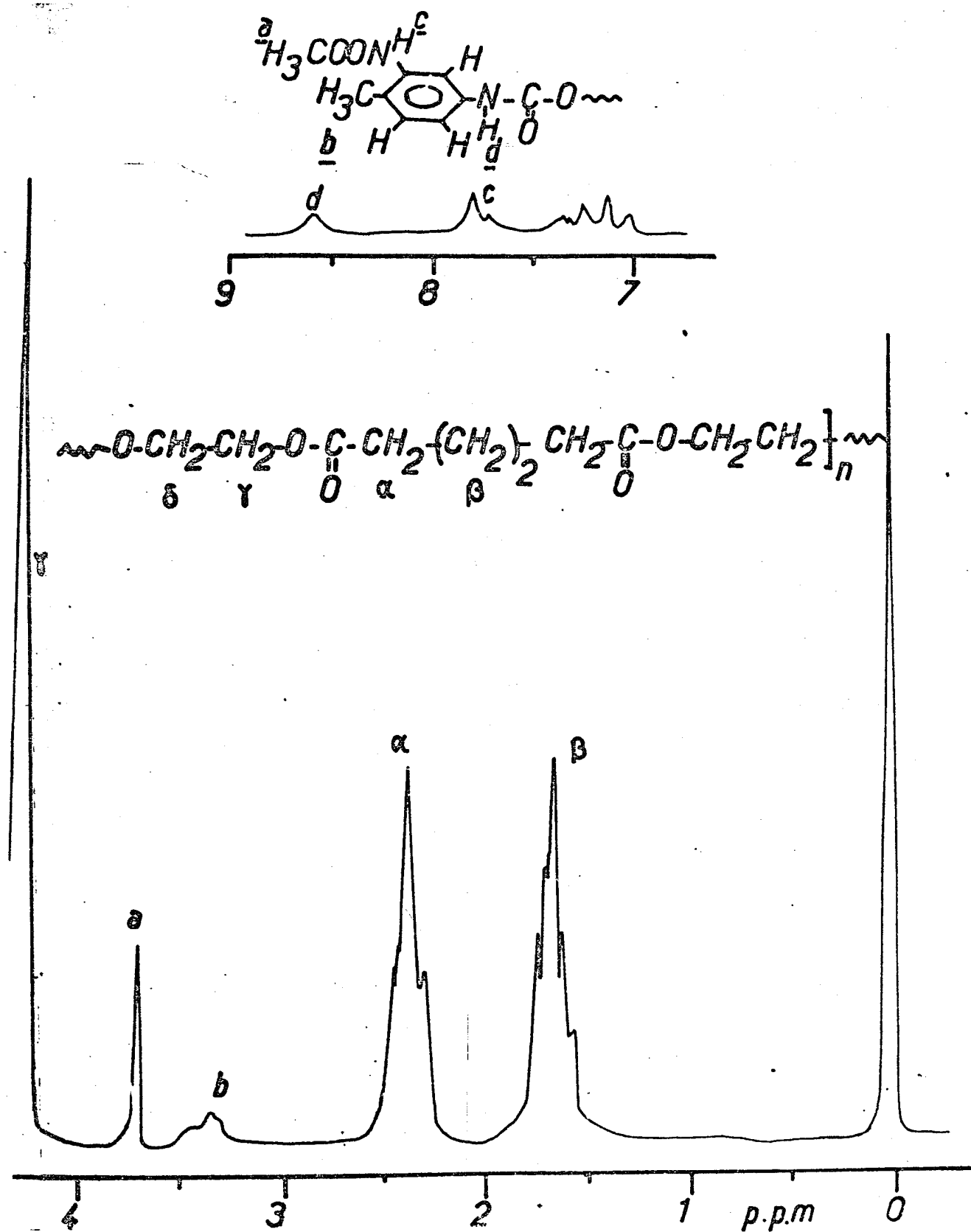
32

Figure 10 - RMN Spectrum of Adiprene L100

Figure 11 - RMN Spectrum of Cyanaprene A9

34

Figures 12 and 13 give the GPC curves of the prepolymers. The following statements can be made:

In all cases, there is a surplus TDI peak. This peak is relatively high. The values are worked out in Table IX. These values were obtained from a preliminary calibration of the TDI response (Figure 14) to the ultraviolet (254 nm) and refractometric detectors of the (GPC).

Adiprene L315 presents an extra and very distinguishable peak in the elution volume 25 (Figure 12). This product has a stonger UV absorption than the rest. We believe this is due to a TDI trimere whose functionality in NCO would be > 2.

b) Products Containing MDI Diphenylmethane Diisocyanate

The MDI-based prepolymers are most recent products. The chromatograms of the three M Adiprenes are shown in Figure 15. Four areas may be differentiated and they are marked I, II, III, IV. Shown in parallel in the same figure are two MDI (from UPJOHN): one is liquid and of functionality $f = 2.2$ and the other is a crystalline solid of functionality $f = 2.0$. From these curves, the following statement may be made:

- area IV corresponds to pure MDI;
- areas I and II belong to polyether $\alpha-\omega$ diisocyanate;
- area III indicates that we are concerned with an MDI whose $f > 2.0$.

Conclusion

The excess in micromolecular diisocyanate is much greater in MDI Adiprenes than in TDI Adiprenes (Figure 16).
The differences between the three M Adiprenes are essentially in proportion with the MDI levels and the fuctionality of these MDI.
It is remarkable that the rates of (NCO) and the MDI percentage
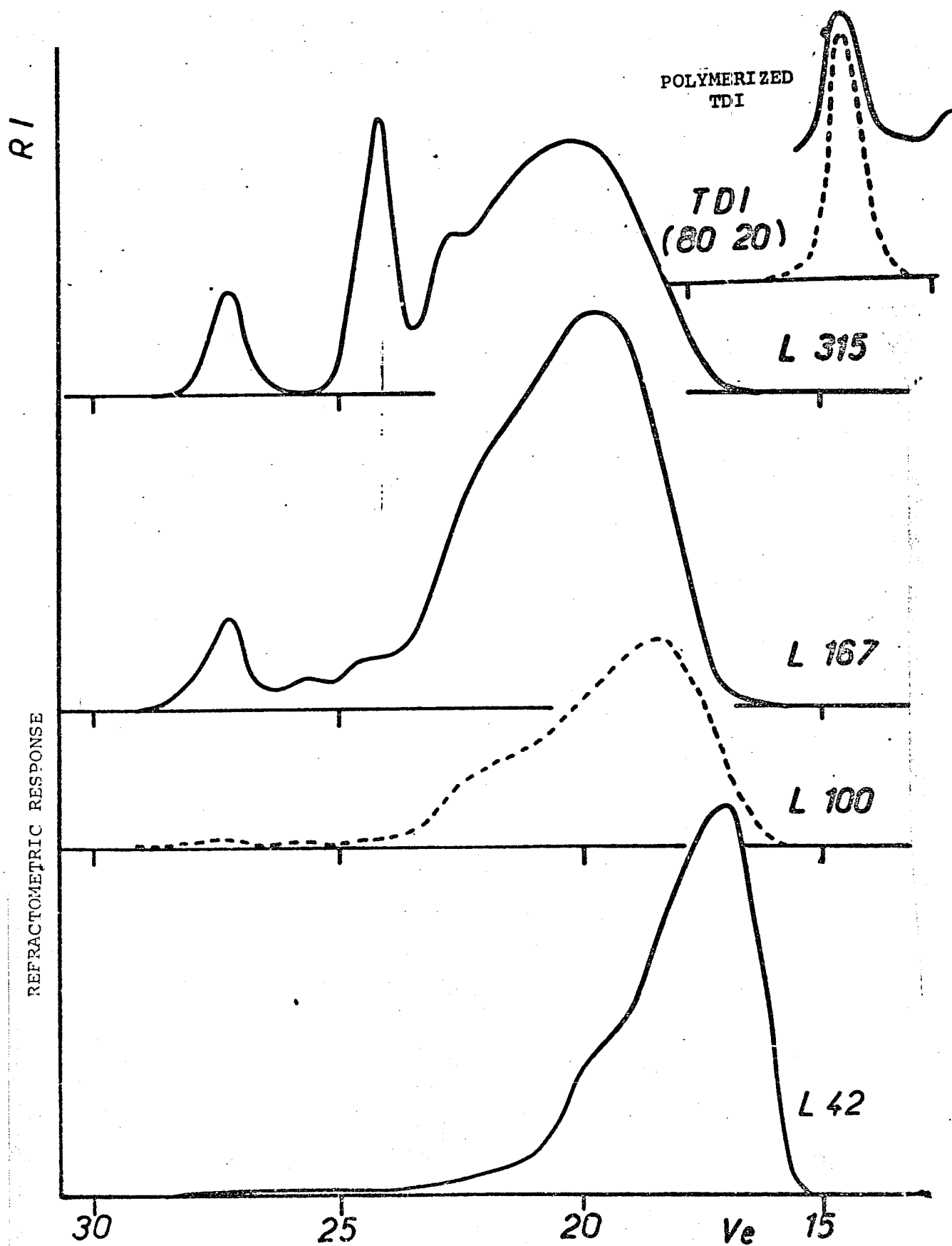
Figure 12 - GPC Analysis of the Adiprenes

Figure 13: GPC analysis of cyanoprenes
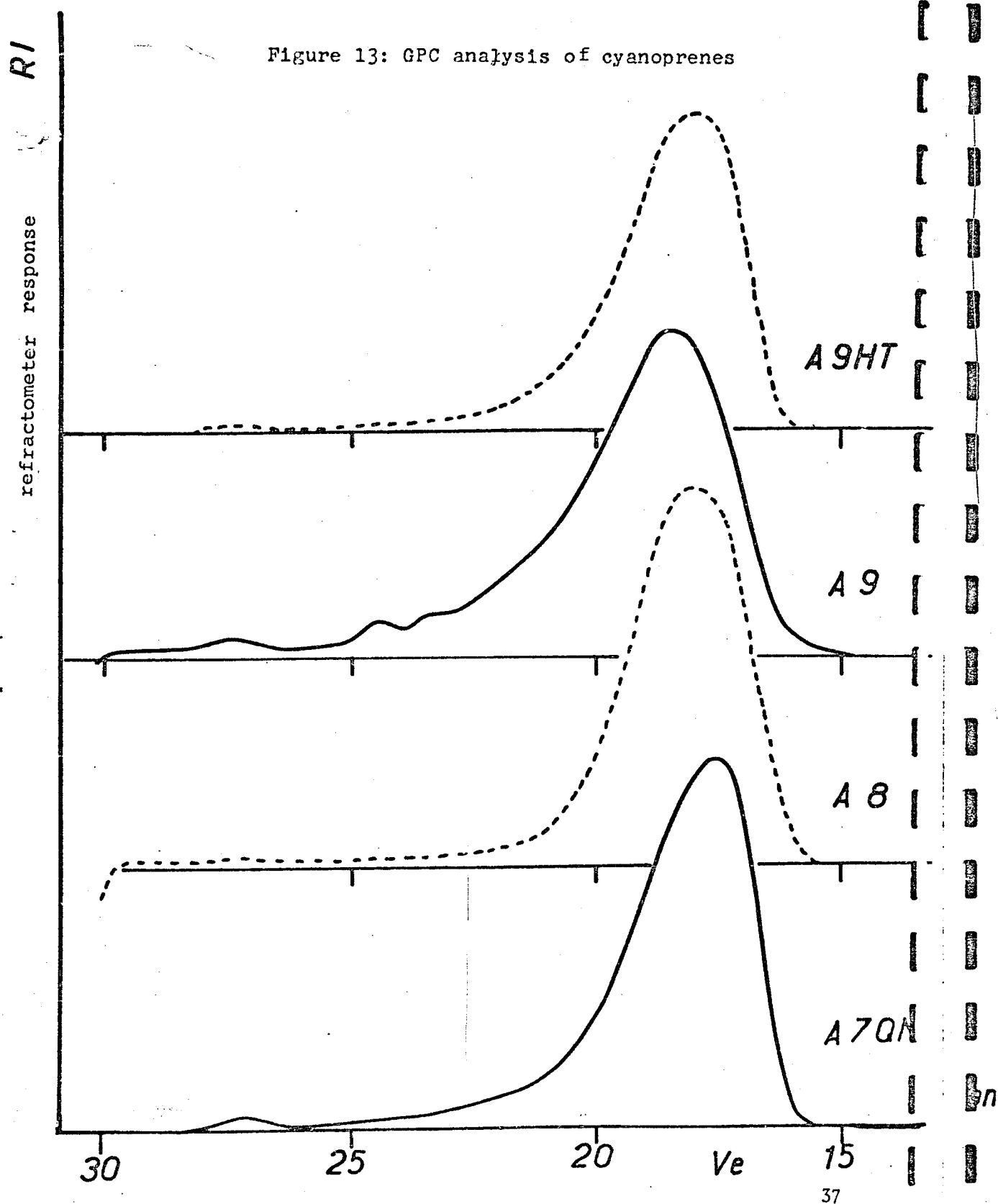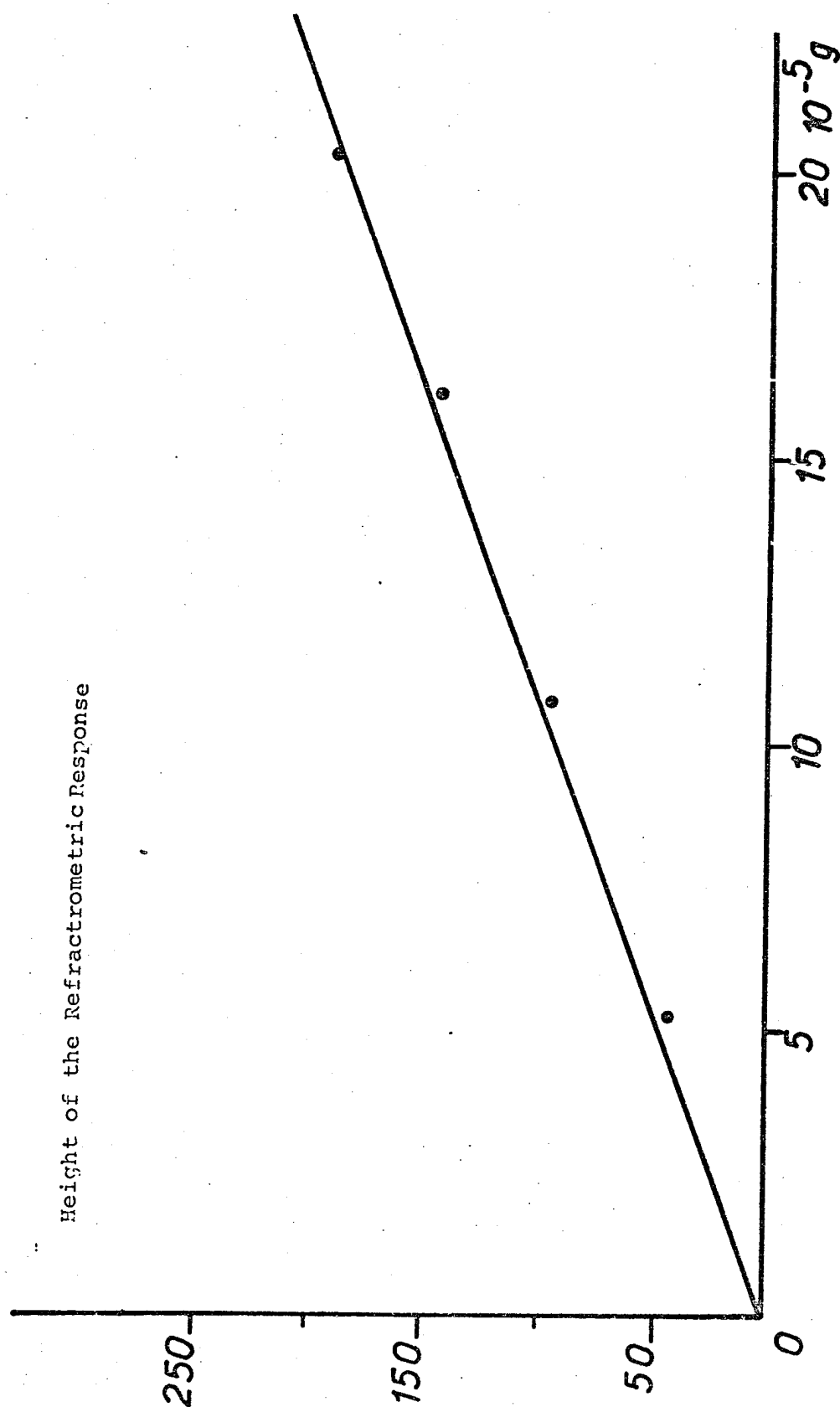
Figure 14 - GPC calibration curve of TDI

38

b)

25 μl

143 L (f=2,2)

15 μl

125M (f=2,0)

a)

MDI Adiprenes

M467

III

M415

II   I

IV

M 400

Ve
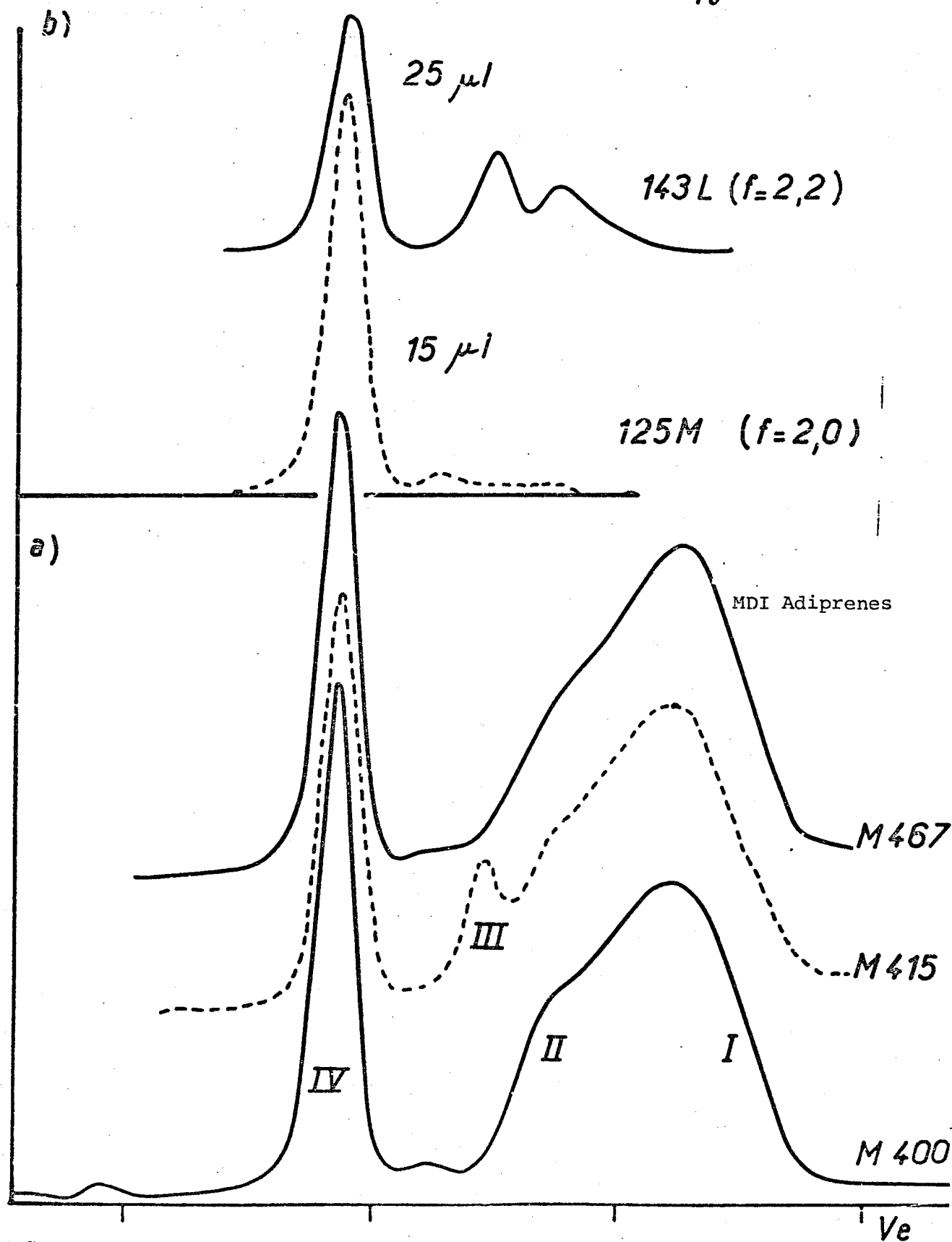
Figure 15 - GPC Analysis of the M Adiprenes
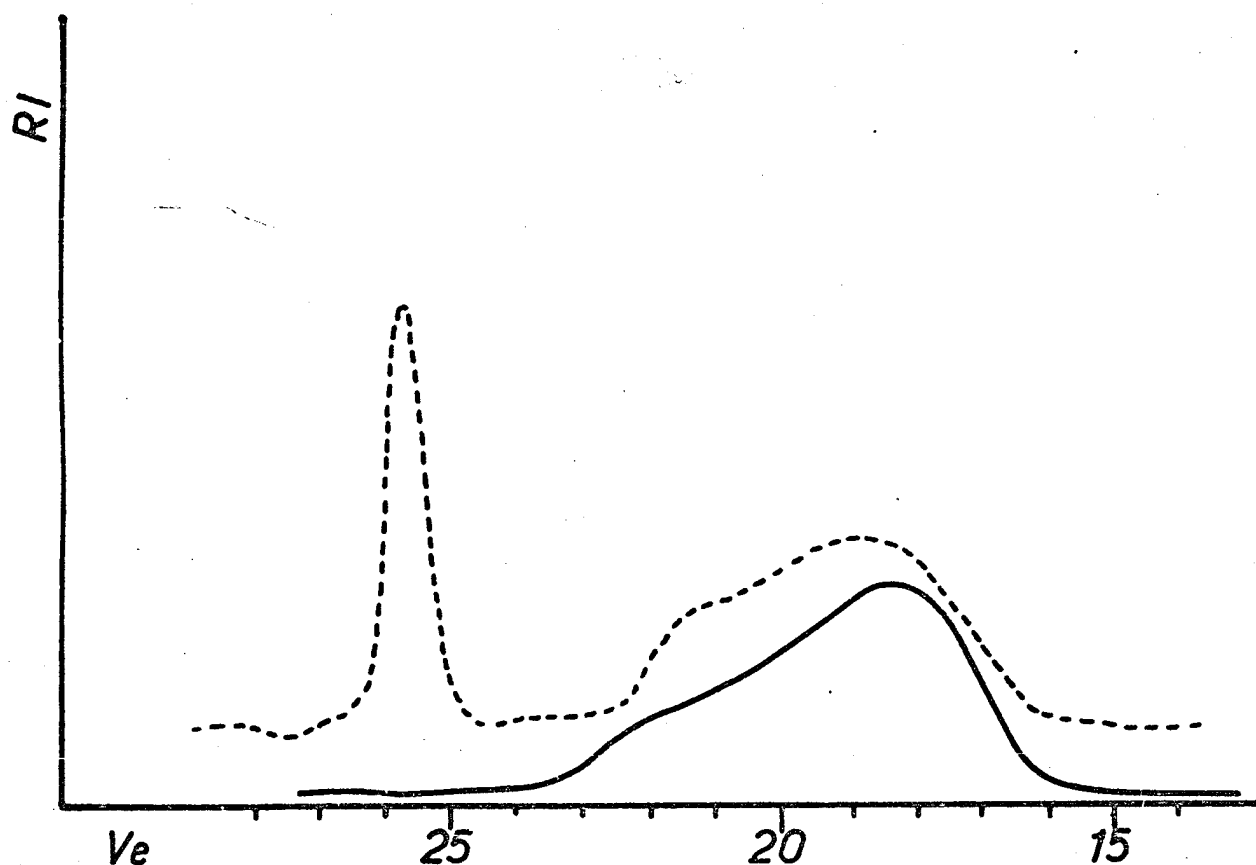
Figure 16 - Comparison of the two Adiprenes (TDI and MDI)
(CPC high pressure)
TDI (L 100) Adiprene (————)
MDI (M400) Adiprene (-----)

does not vary in the same direction when one goes from
MDI 400 to MDI 467. This can only be explained if one
assumes a different functionality and greater than 2 for
M 467. Under these conditions, only M 400 will contain MDI
with f = 2.

Remember that for the L Adiprenes, the main variable was the
molecular weight of the prepolyemrs. The procedure for diversify-
ing the formulations seems different in the two cases and we are
aiming for simplification for the most recent products, i.e. the
M Adiprenes.

We therefore have diisocyanate prepolymers for which the flex-
ible segment is either a polyether (Adiprene) or a polyester (Cyana-
prene).

40

III-2 – Properties of Polyurethanes Synthesized from Prepolymers Containing TDI (Toluene-diisocyanate) and an Amine Chain Extender

The chain extender used is aromatic diamine 4,4 methylene-bis (2 chloro-aniline). Its commercial name is Moca and its melting temperature is 120°C.

In addition to Moca, the CYANAMID Company uses another aromatic diamine for a formulation with the prepolymer A9HT. This is 1,2 bis (2-aminophenylthio)ethane whose melting temperature is Tf = 72°C and whose commercial name is Cyanacure.

The synthesized polyurethanes are shown in Table X. We can see that in general, the life span of the reactional mixing pot (*) decreases when the (NCO) content increases. Accordingly, Adiprene L315 is delicate to use, even at 85°C.(**).

Table X
THE VARIOUS POLYURETHANES PREPARED USING AMINE HARDENERS

Prepolymère 100 g	% NCO (g)	Hardener	Hardener Wt. (g)	Life in pot (min/°C)	Cooking (min/°C)
Adiprene					
L 42	2,8	Moca	8,8	7/100	3/100
L 100	4,1	"	12,5	10/100	3/100
L 167	6,3	"	19,5	5/ 85	1/ 85
L 315	9,5	"	26,6	1/ 85	1/ 85
Cyanaprene					
A7QM	2,3	Moca	6,9	9/100	17/100
A8	3,1	"	9,3	11/100	17/100
A9	4,2	"	12,6	7/100	17/100
D6	6,0	"	18,1	4/100	16/100
A9HT	4,2	Cyanacure	11,7	4/ 90	20/ 90

(*) The time after which the viscosity of the reactional mixture becomes infinite,
(**) The life span in the pot is an important factor in the preparation of polyurethanes, and especially in the preparation of composites reinforced with fibers.

41

Additionally, Moca must melt at a temperature of 120°C /45
approximately, before being added to the mixture at a lower temp-
erature (≈100°C).

a) Moca Chain Extender

The curves for the thermal analysis measurements are shown in
Figure 17 for the L Adiprenes and in Figure 18 for the Cyanaprenes.

We see that the polyethers (L Adiprenes) all exhibit a lower
vitreous transition Tg (about - 70°C) than the polyesters (cyana-
prenes), whose Tg is about - 35°C. The melting of rigid segments
occurs at fairly high temperatures (T > 180°C).

Adiprene L42 is the only compound which exhibits two vitreous
transitions. The first, at about -71°C is ascribable to the POTM
flexible segments and the second at about -5°C corresponds to the
PPG segments. This result definitely confirms the analysis made
of the prepolymer (Table IX).

For Adiprene L315 and Cyanaprene D6, the vitreous transition
is not very definite: it spreads over a wide temperature region.
In regard to high temperatures, an endothermic area followed by
deterioration of the polymer (at about 200°C) is generally observed.

The dynamic mechanical behavior is shown in Figures 19 and 20.
The following observations can be made:

There is always a rubber plateau, but its temperature width
decreases and its value increases as the molar weight of the pre-
polymer decreases (or the NCO content increases, or the Moca per-
centage increases).

Along the same lines of thinking, the tg δ absorption peak
varies with the molar weight of the prepolymer. The maximum absorp-
tion is at lower temperatures and increases as this molar weight
increases.

42
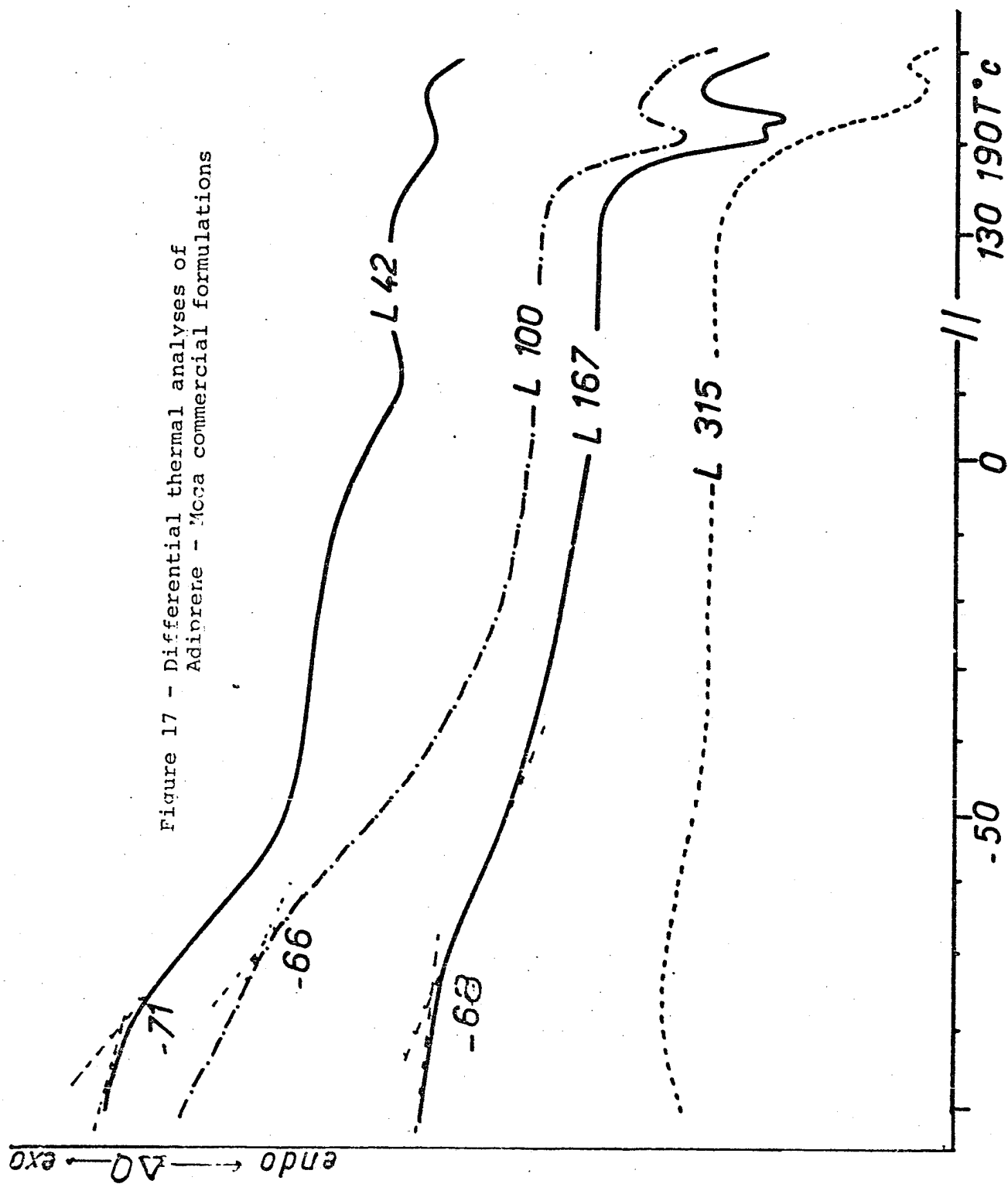
Figure 17 – Differential thermal analyses of
Adiprene – Moca commercial formulations

Figure 18 - Differential analysis of
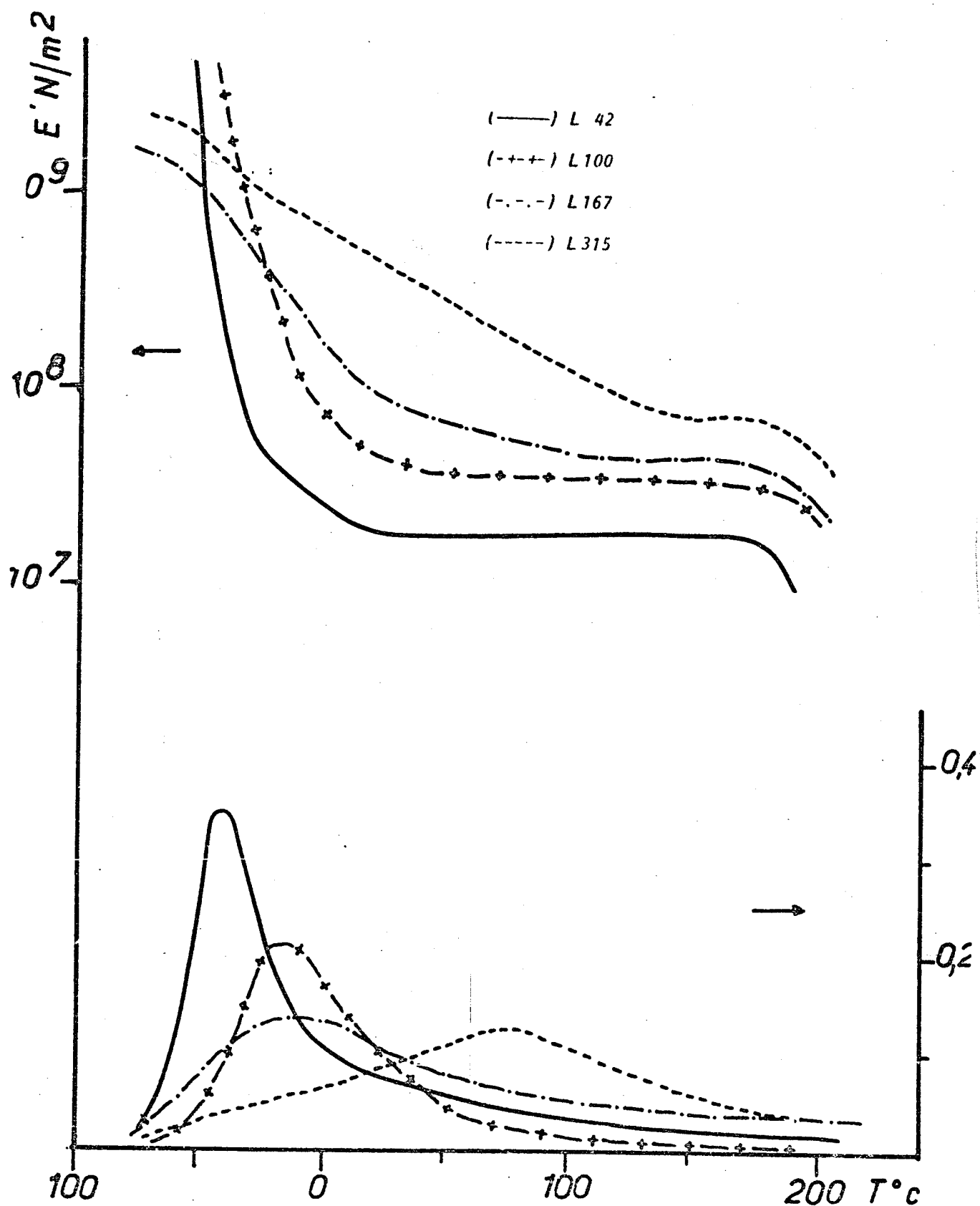commercial formulations for Cyanaprenes - Moca
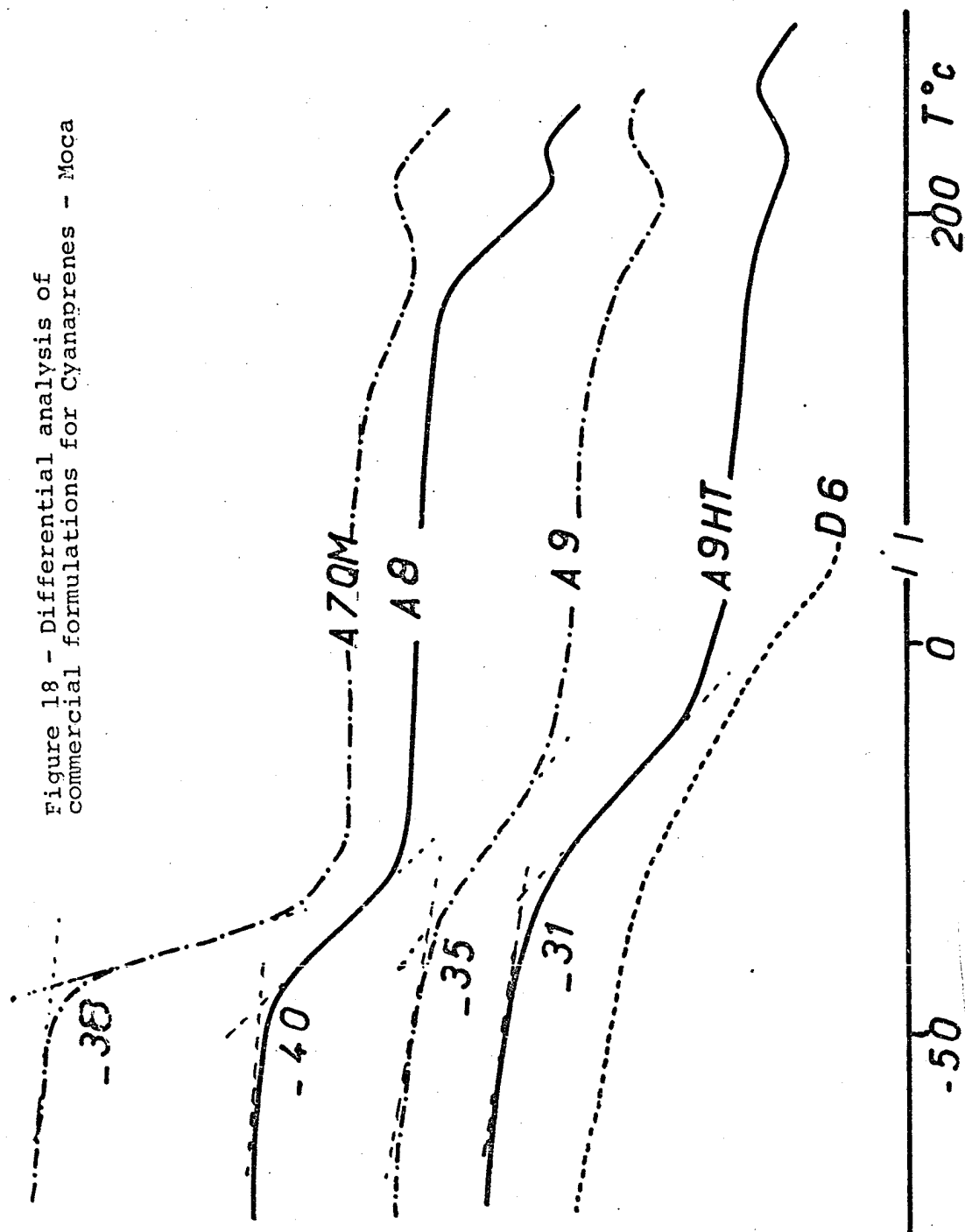
Figure 19 - Dynamic mechanical properties of
commercial formulations for Adiprenes-
Moca

45
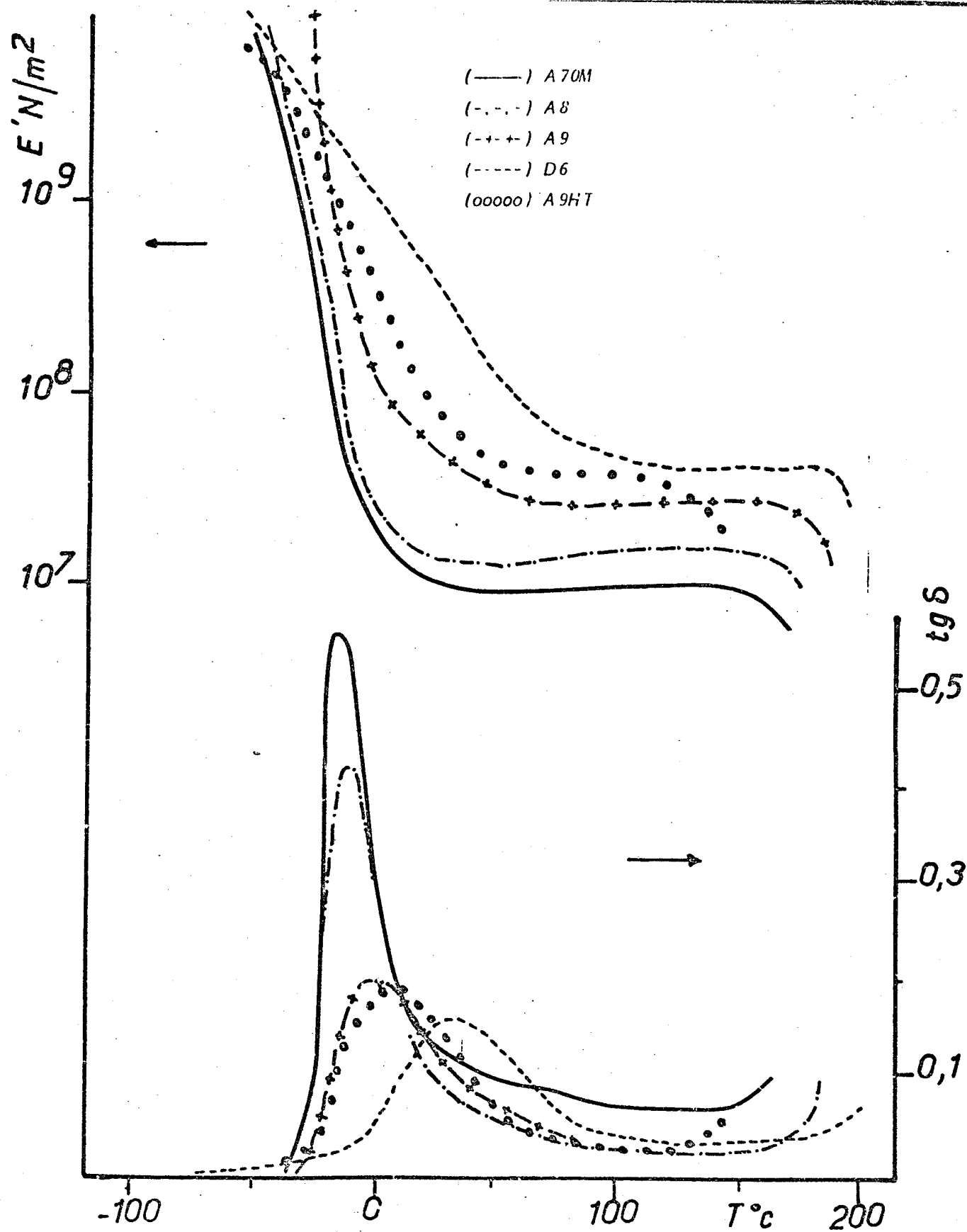
Figure 20 - Dynamic mechanical properties of commercial
formulations for Cyanaprenes - Moca

For L315- or D6-based polyurethanes, the rubber plateau is
truly very limited and occurs only at high temperatures (T > 100°C).
For these materials, the modulus steadily decreases between -40°C
and +100°C. From the practical standpoint, an operating tempera-
ture variation of the material will cause a large modulus varia-
tion.

On the other hand, PURs containing L42, L100 or A7QM and A8
have a very well-defined rubber plateau; the modulus is constant
over more than 100°C. Operating temperature variations will not
modify the value of the real modulus E'.

If we compare two polymer families, modulus E' at 30°C is
situated at about 5.10^8 N/m^2 to 2.10^7 N/m^2 for the Adiprenes and
from 3.10^8 N/m^2 to 9.10^6 N/m^2 for the Cyanaprenes. The absorption
peak of Adiprenes is much lower than for the Cyanaprenes, except
in the case of L42.

The modulus window reduces at 105°C from 7.10^7 to 9.10^6 N/m^2
for the Adiprenes and from 3.10^7 to 9.10^6 N/m^2 for Cyanaprenes.
Finally, Cyanaprenes tend to creep 20°C sooner than Adiprenes.

For L42-based polyurethanes, we had seen that the prepolymer
is a mixture containing 70% POTM and 30% PPG. The fact of having
a mixture will reduce the crystallization capability of the POTM
segments and this explains why the absorption peak of this material
is unusually high.

The static mechanical properties are grouped in Table XI. The
curves giving the stresses as a function of elongation during the
tension tests are shown in Figure 21 (a and b).

If we compare the results obtained with those announced by the
manufacturers, we systematically find lower moduluses and larger
elongations. This is explained by the different preparation conditions

Figure 21 – Static mechanical properties of commercial formulations: a)Adiprenes – Moca; b) Cyanaprenes – Moca

48
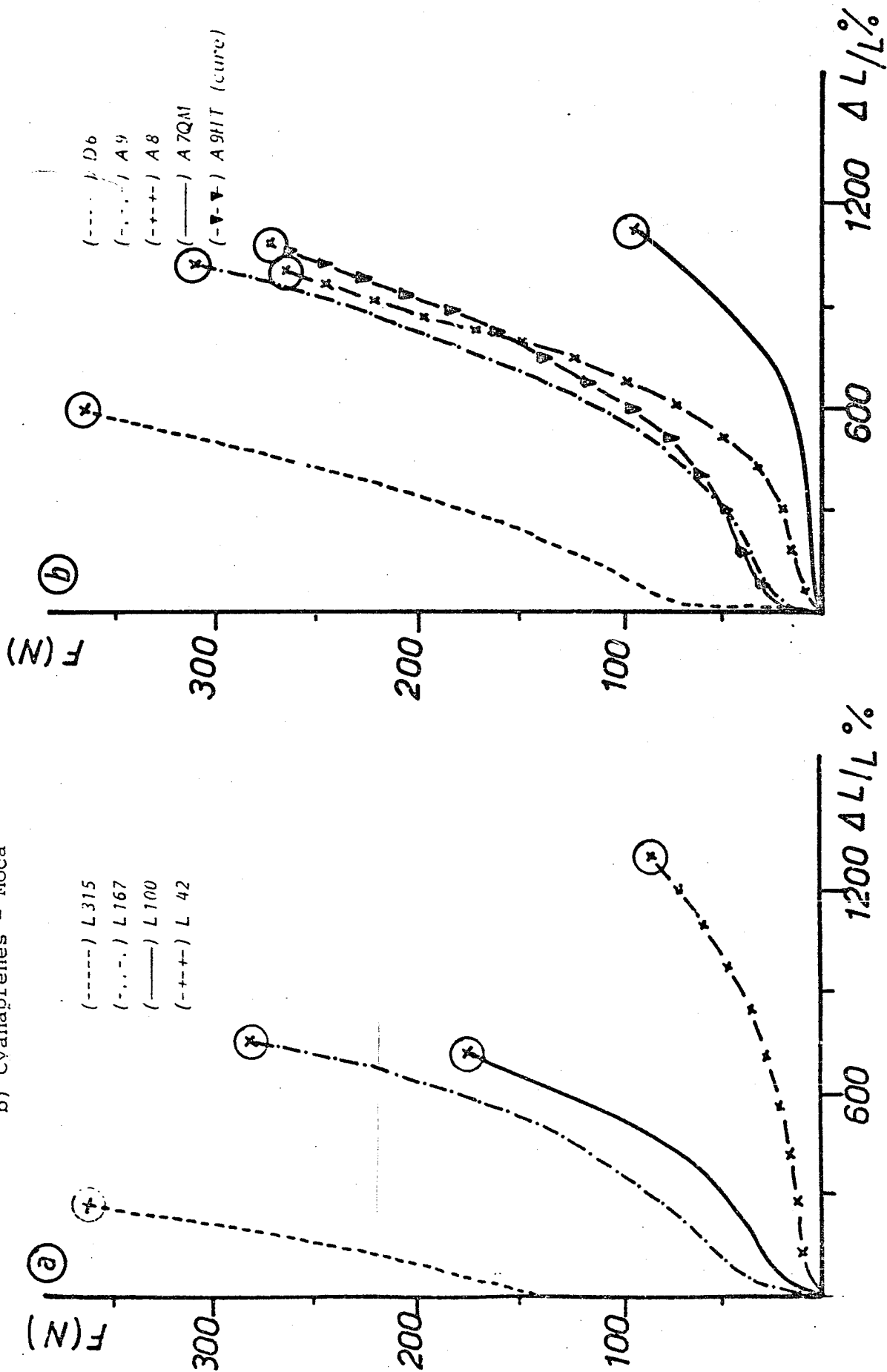
while mixing the chain elongation process with the prepolymer. Yet, the variations occur in the same direction.

The elongation at rupture increases and the residual elongation decreases as the molecular weight $\overline{Mn}$ of the prepolymer increases.

The elastomer nature of the materials is due to the flexible POTM or PAEG sequence, and this quality decreases as the chain extender increases.

b) Diol + Triol Chain Extenders

The chain extenders used are butanediol 1,4 (Bd) and trimethylol propane (TMP).

Table XI
MECHANICAL PROPERTIES OF POLYURETHANES WITH MOCA HARDENER
(THE MANUFACTURER'S FIGURE IS SHOWN BETWEEN PARENTHESES)

Polyure-thane	Shore hardness A D	Modulus (10^6 Pa) 100 %	300 %	Modulus at (10^6 Pa) Rupture	Elongation ϵ_r %	Residual Elongation	Tearing Strength KN/m
L 42	80	1,1(2,8)	2,0(4,3)	17,5(20,7)	1 300 (800)		
L 100	90 43	6,2(7,6)	10,5(14,5)	28,9(31,0)	650 (450)		32 – 78
L 167	95 48	10,5(12,4)	18,2(24,1)	45,6(34,5)	630 (450)	7,5	48 – 82
L 315	78	28,3(29,6)	---	58,7(75,8)	280 (270)	10	80 – 55
						84	104 – 89
A7QM	73	0,9(.2,1)	1,6(2,4)	39,2(33,1)	1 150 (840)		
A8	82	2,7(3,8)	4,5(7,2)	45,9(41,4)	1 040 (630)	5	
A9	91	5,9(7,0)	9,6(13,5)	57,3(45,5)	990 (40)	7,5	
D6	96 60	17,8(18,6)	31,1(29,6)	71 (50,3)	630 (415)	95	
A9HT	93	4,1(6,2)	7,4(9,6)	47,1(40,6)	1 010 (650)	7	

The synthesized polyurethanes are shown in Table XII. The   /54
lifespan in the pot is very reasonable (30 minutes is plenty of
time to prepare a composite) - compared to the very short span of
1 to 5 minutes for the Moca hardener. On the other hand, the cook-
ing time is relatively long.

Table XII
LIST OF POLYURETHANES PREPARED FROM TDI PREPOLYMERS AND POLYOLS (DIOL+TRIOL)

Prepolymer 100 g	Hardener (Molar Ratio) Bd/TMP a)	Hardener Wt. (g)	Cooking (h/°C)	Lifespan in pot (min/C°)
L 100	3,5	4,3	20/100	30/100
L 100	5,3	3,4	20/100	40/100
L 315	3,5	10,0	6/100	45/100
L 315	5,3	9,0	6/100	45/100
L 315	b	9,0	6/100	60/100

$$a)\ Bd = OH\ (CH_2)_4 - OH\ ;\ TMP = CH_3 - CH_2 - C \begin{array}{c} CH_2OH \\ - CH_2OH \\ CH_2OH \end{array}$$
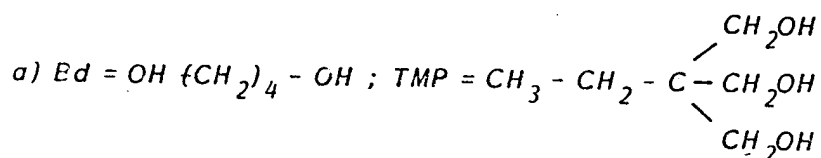
b) Formulation With TMP Alone

The calorimetric measurements are shown in Figure 22. The
most interesting observation is the virtually total absence of
the melting endotherm corresponding to the melting of rigid seg-
ments. A softening and degradation of the polyurethane polymers is
observed. The endotherm area begins at about 150°C for L100 and
after 175°C for L315s. Note also the high temperature performance
of L315/TMP.

The dynamic mechanical behavior is shown in Figure 23. A peak
displacement is observed. This corresponds to the relaxation of the
flexible sequences from PUR-L100 (-20°C) to PUR L315 (+50°C) with
fairly high maximum tg δ peak values (0.55 to 0.85).

50
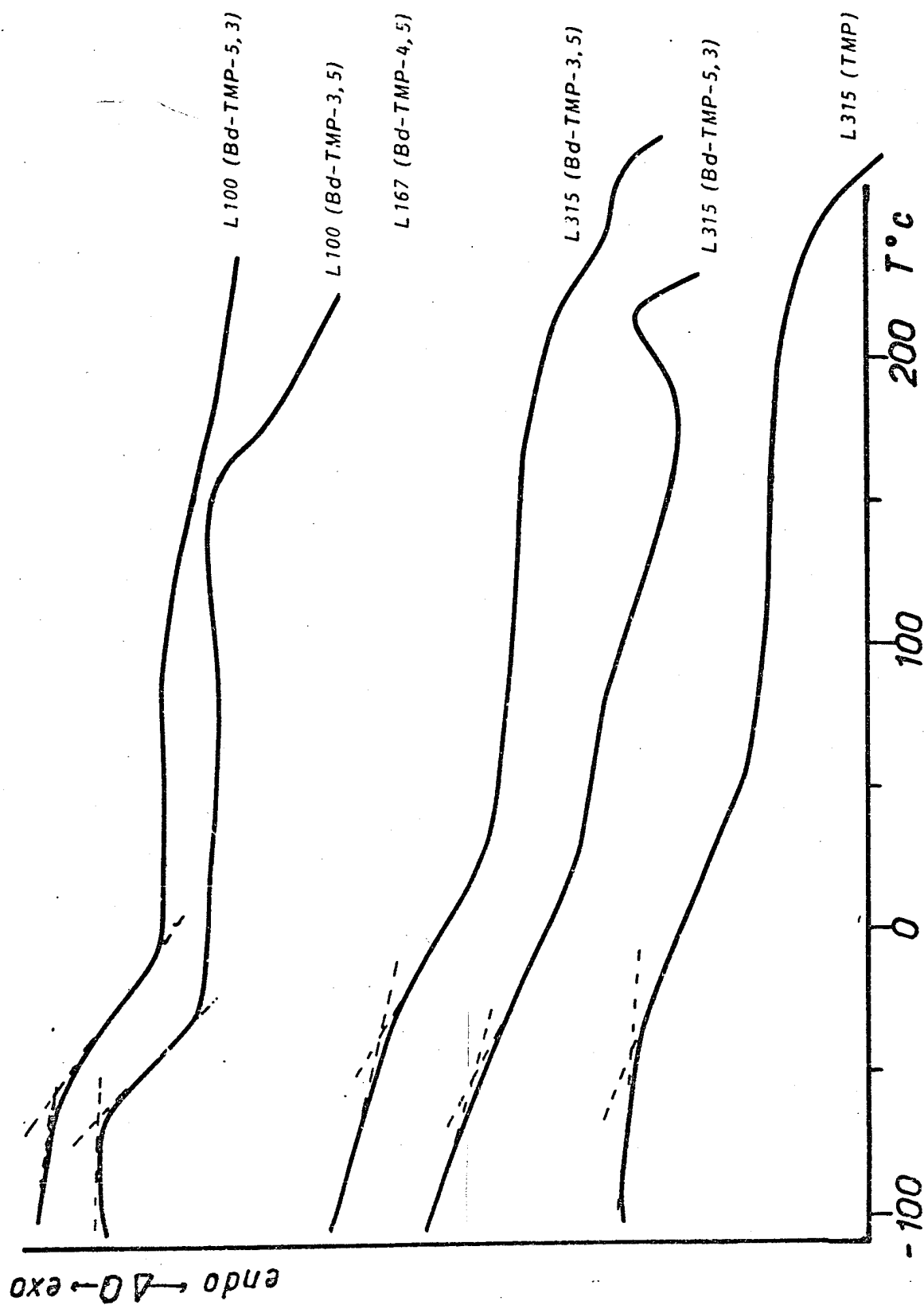
Figure 22 - ATD curves of PUR - alcohols

The curves are labelled (top to bottom):

L100 (Bd-TMP-5,3)
L100 (Bd-TMP-3,5)
L167 (Bd-TMP-4,5)
L315 (Bd-TMP-3,5)
L315 (Bd-TMP-5,3)
L315 (TMP)

Vertical axis: endo ← ΔQ → exo
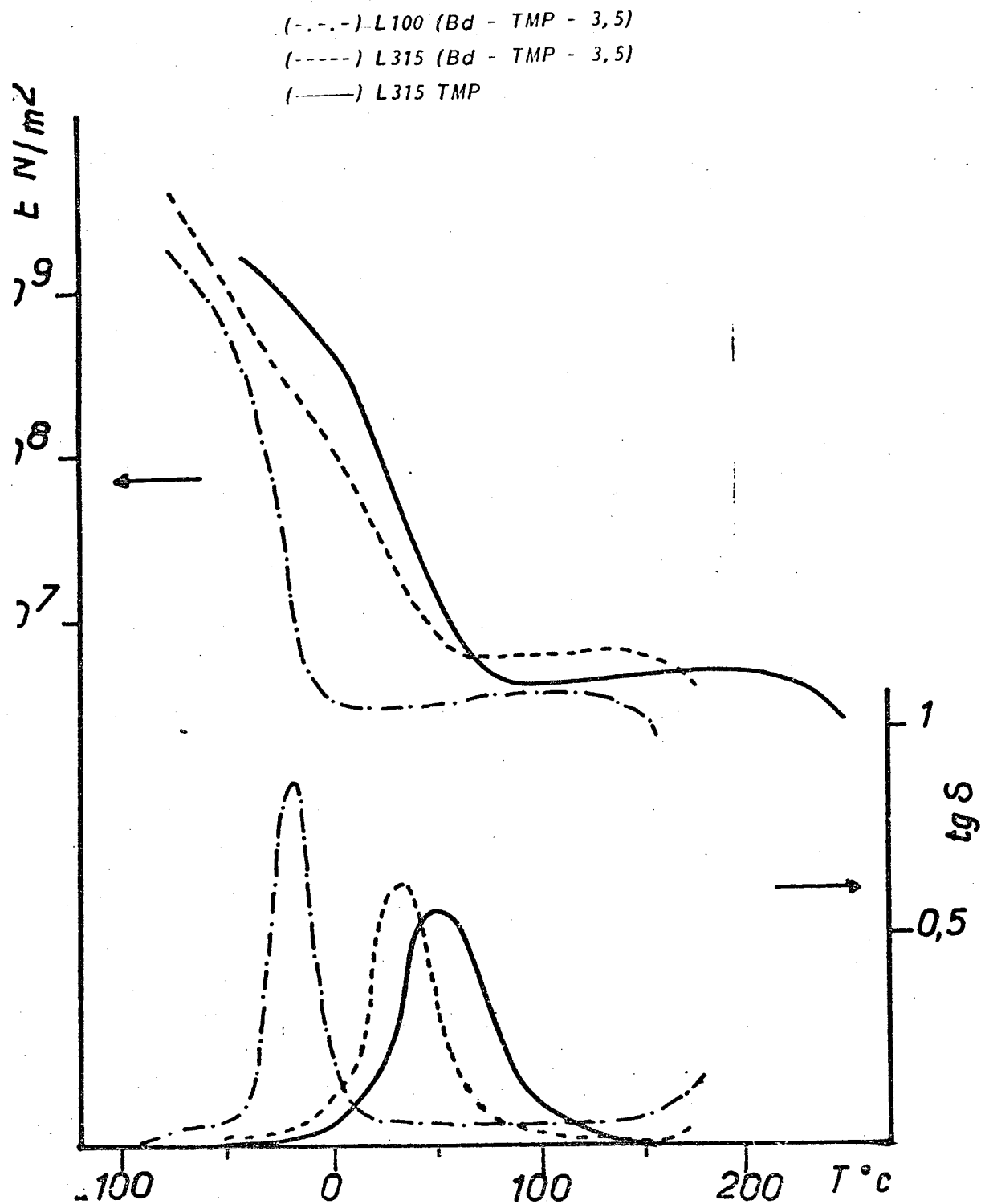
Horizontal axis: $T°c$, with marks at -100, 0, 100, 200

Figure 23 - Dynamic mechanical properties of PUR - alcohols

The rubber plateau shifts to high temperatures with modulus values between 3 and 7.10^7 N/m^2.

A comparison of the dynamic mechanical behavior of the two /57 types of chain extenders seems interesting. Note (Figures 24 and 25) that the E' modulus decreases at the rubber plateau one decade with alcohol hardeners, but spreads over a much broader temperature range. At the same time, the much higher absorption peak with alcohols is more narrow (tg δ_{max} shifts to 0.9 for PUR L100 and 0.65 for L315). These absorption peaks occur at the same temperature in the case of PUR L100s, whereas they occur for different temperatures in the case of PUR L315s.

The high temperature flow area occurs at about 150°C, 160°C for the polymers reticulated by the Bd + TMP mixture. The polymers elongated with Moca have a better temperature behavior.

The PUR L315 reticulated with TMP alone, gives a three-dimensional network without a flow point.

The static mechanical properties are shown in Table XIII and in Figure 26.

Figure XIII
MECHANICAL PROPERTIES OF TDI POLYURETHANES WITH ALCOHOL HARDENERS

Alcohol Poly-urethanes	Bd/TMP	Modulus at 100% (10^6 Pa)	Modulus at Rupture (10^6 Pa)	Elonga-tion ε_r %	Residual Elonga-tion %	Tearing Strength KN/m
L 100	3,5	1,2	13,3	960	8	22,1
L 100	5,3	1,8	19,2	850	1	
L 315	3,5	2,3	14,5	700	10	24,7
L 315	5,3	2,9	39,4	490	3	
L 315	(TMP)	4,5	28,3	390	10	40,4

We can see lower values for the rupture force and higher values for the elongation at rupture for polyurethane reticulated with polyols compared to those elongaged with Moca (diamine).

We can also see low residual elongation values of about 10%   /61
for PUR L315 - polyol compared to 80% for PUR L315 Moca. Also, when the proportion of the triol reticulating agent (TMP) increases, the values of the rupture force increase and those of the elongations at rupture and residual elongations decrease.

III-3- Properties of Polyurethanes Synthesized From MDI-Based Prepolymers As A Function of the Type of Diol Chain Extender

The prepolymers used, containing MDI diisocyanate, are M Adiprenes. The diol extender recommended by the manufacturer is butanediol 1,4. We used HQEE diol for comparison with the M400 Adiprene-based formulation.

The list of polyurethanes prepared is shown in Table XIV.

Table XIV
POLYURETHANES PREPARED FROM MDI-BASED PREPOLYMERS AND DIOL EXTENDERS

Prepolymer 100 g	Butane diol 1,4 (g)	HQEE (g)	% NCO (g)	Lifespan in Pot (min/°C)	Cooking (h/°C)
M 400	7.7	--	7.58	6/ 80	16/110
M 400	-	16.9	7.58	3/110	16/110
M 467	9.9	--	9.70	4/ 80	16/110
M 415	10.8	--	10.65	4/ 80	16/110

The calorimetric measurements are in Figure 27 and in Table XV a). The vitreous transition of the flexible sequences occurs at temperatures between -50°C and -60°C.
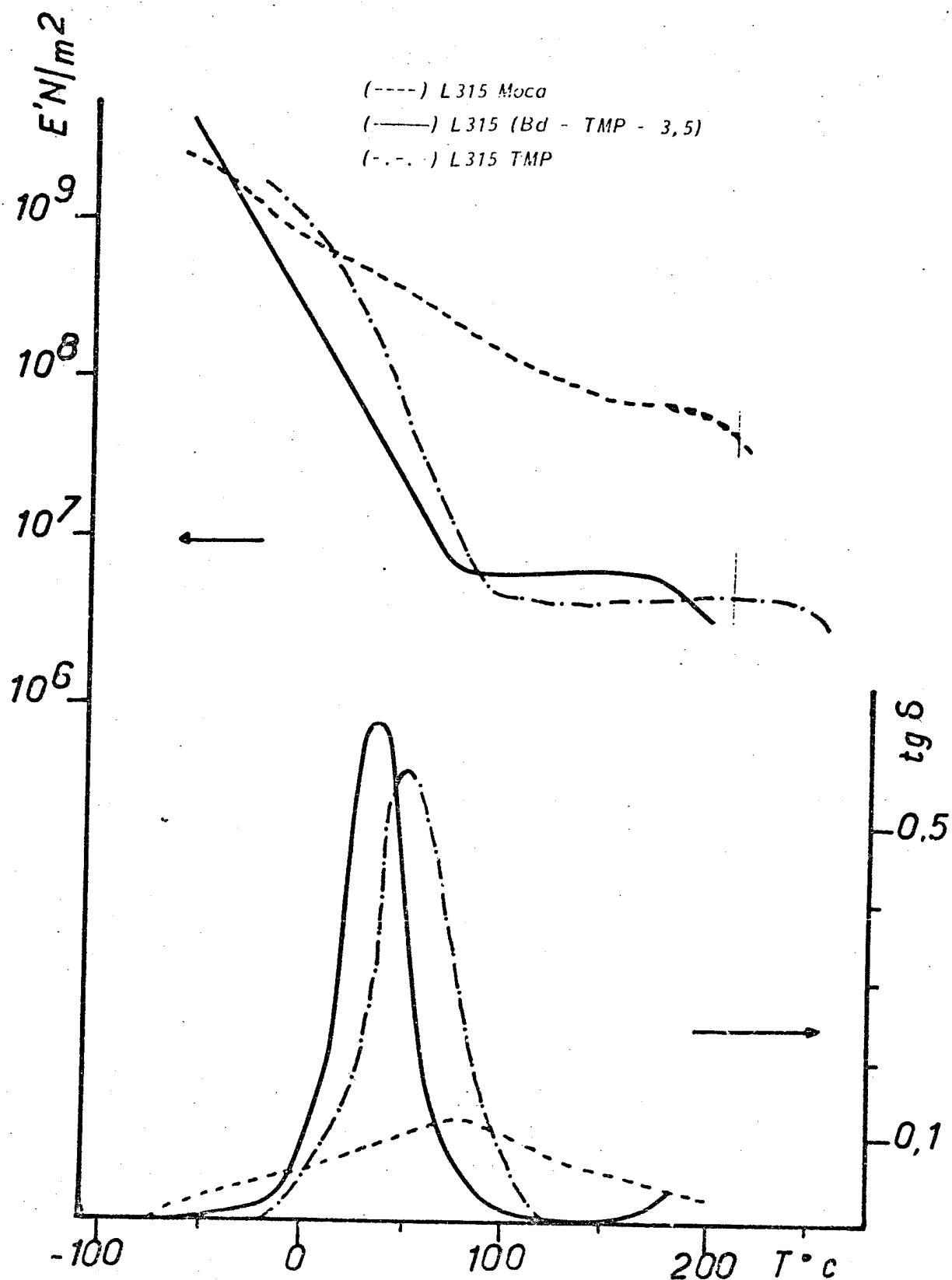
Figure 24 — Comparison of the dynamic mechanical behavior
of the two types of chain extenders, (-----)
diamine; (-·-·-·-·-) triol and (————) (diol + triol).

55
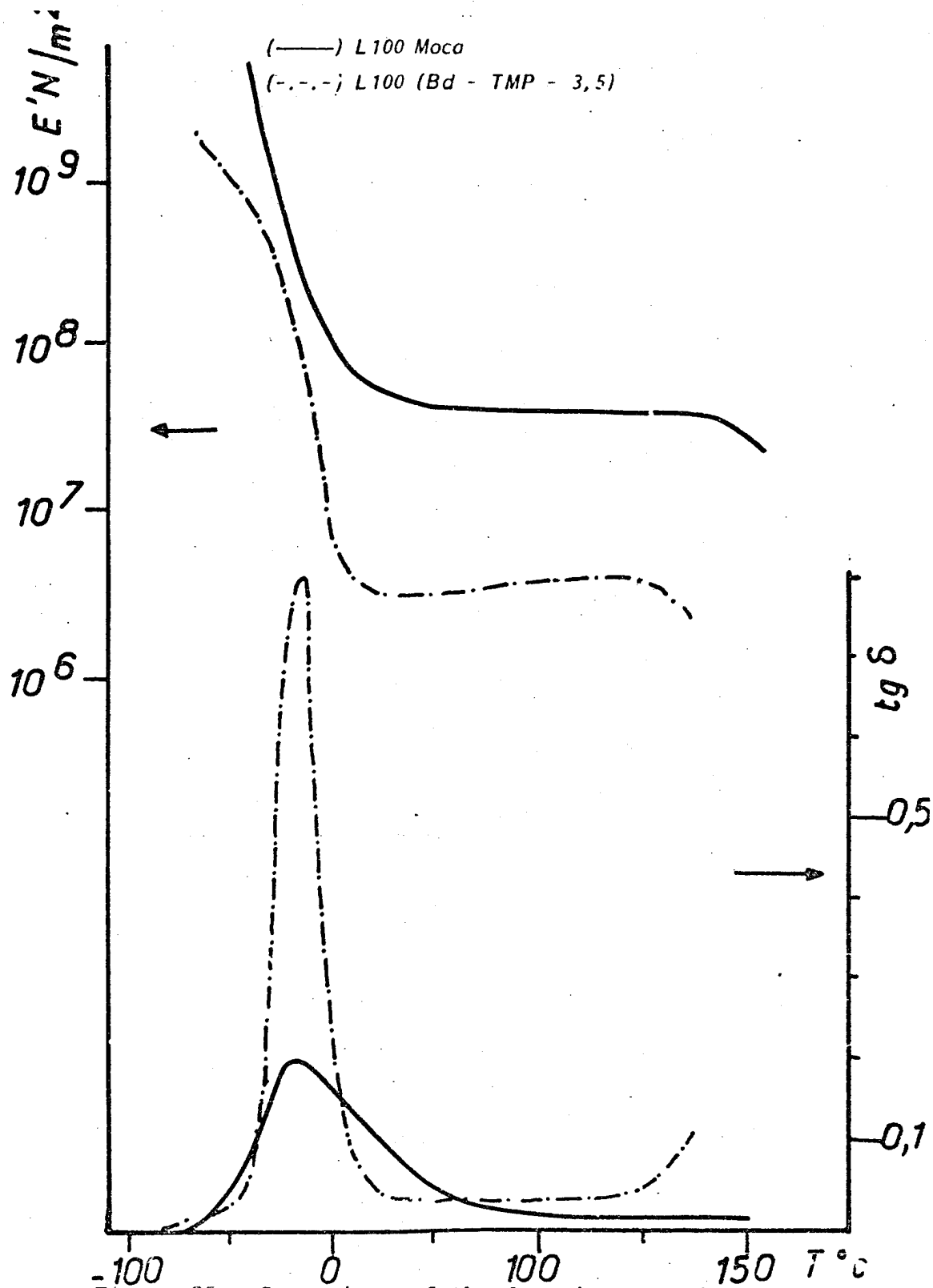
Figure 25 – Comparison of the dynamic mechanical behavior of
two types of chain extenders (————) diamine and
(–·–··–··–) polyol.
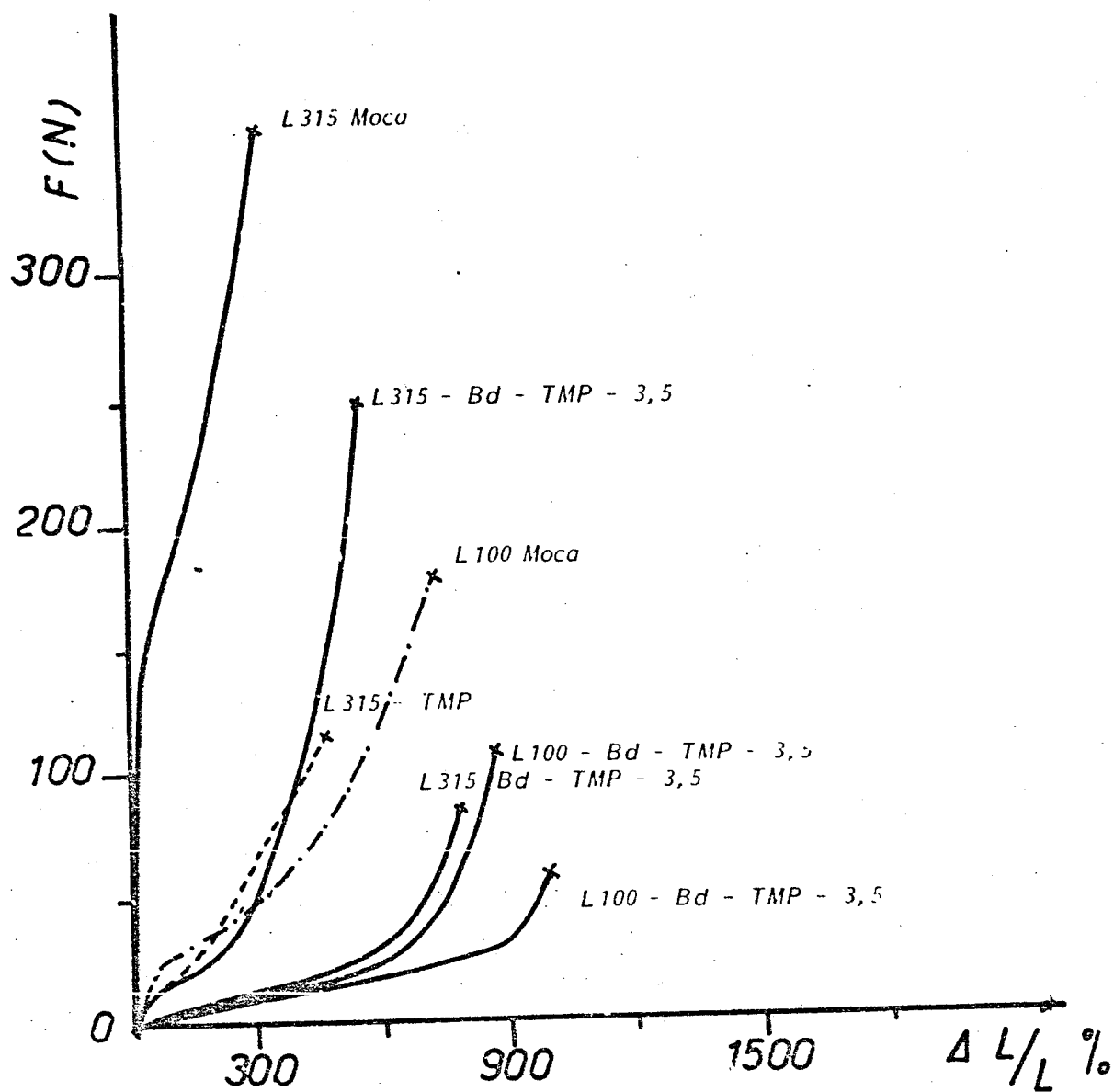
Figure 26 – Curves along the static mechanical properties
        for PUR –alcohols

57
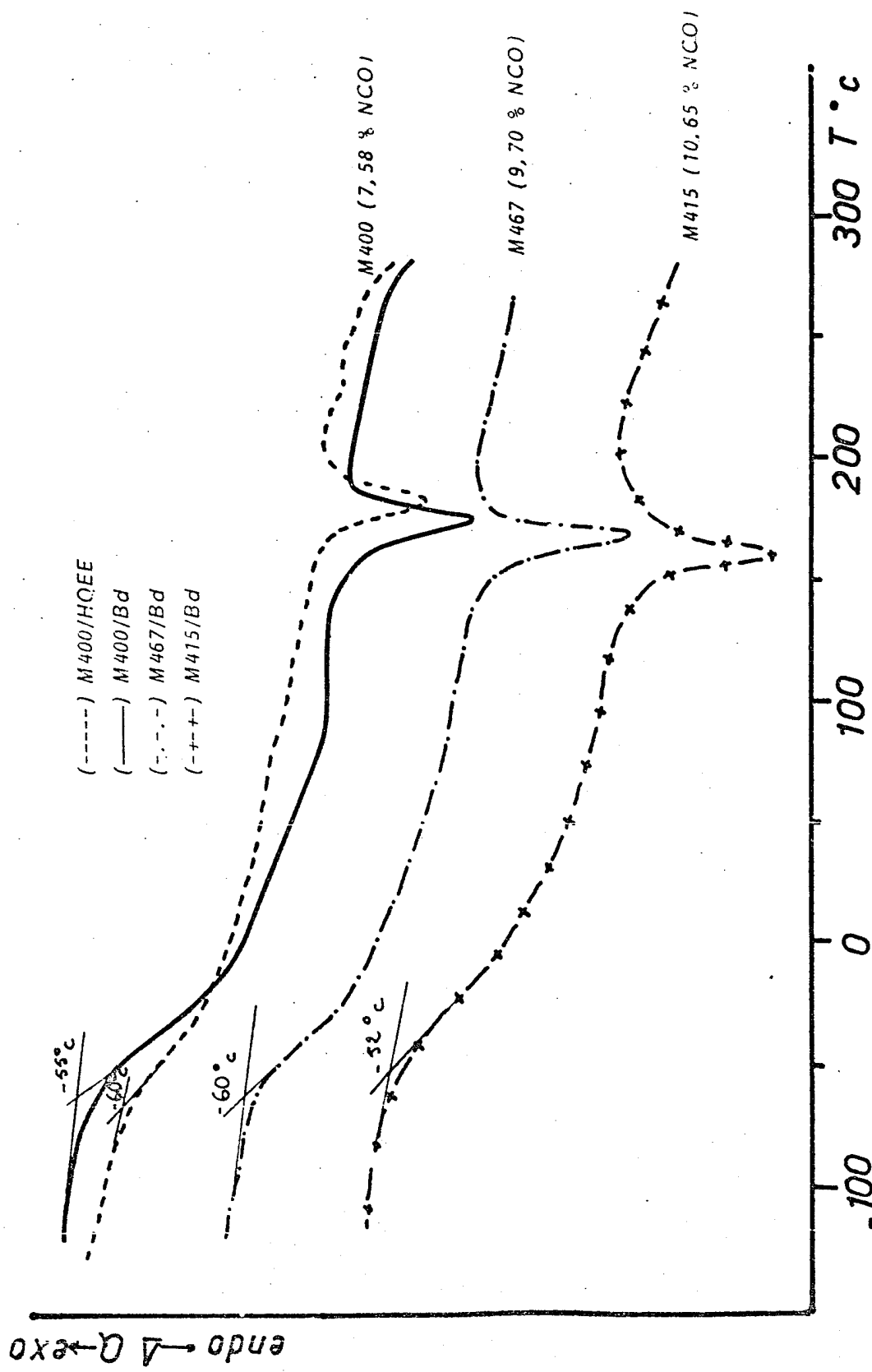
Figure 27 - Calorimetric measurements of polyurethanes prepared from MDI prepolymers and diol chain extenders

Legend (inset):
(------) M400/HQEE
(——) M400/Bd
(-·-·-) M467/Bd
(-+-+-) M415/Bd

Curve labels: M400 (7,58 % NCO), M467 (9,70 % NCO), M415 (10,65 % NCO)

Transition temperatures: -55°C, -60°C, -60°C, -52°C

Y-axis: endo ←ΔQ→ exo

X-axis: -100 0 100 200 300 T °c

58

Table XVa

CALORIMETRIC MEASUREMENT OF VARIOUS PURs ELONGATED USING DIOL BUTANE OR HQEE

Prépolymère	% NCO (g/100)	Hardener	Tg (°C)	Tf(°C)	ΔH$_f$ (J/g)
M 400	7,58	Bd	− 55	153	7,2
M 400	7,58	HQEE	− 60	180	24,3
M 467	9 70	Bd	− 60	164	14,6
M 415	10,65	Bd	− 52	156	16,3

At higher temperatures (T > 100°C) the rigid sequences melt (156°C for PUR-M415; 164°C for PUR-M467; 173°C for PUR M400). Also, the melting heat increases with the percentage of the (NCO) functions of the prepolymer.

Use of HQEE diol increases the rigidity and produces a higher melting heat ΔH$_f$ in rigid segments than for the Bd-1,4 formulation.

The dynamic mechanical behavior is shown on the curves in Figure 28. We see absorption peaks corresponding to the relaxation of flexible sequences at about 0° and 50°C, which is 50° to 80°C above the vitreous transition Tg measured by ATD. The basic product M400, which has the lowest NCO content (7.6%) and a difunctional MDI, has the highest absorption peak (tg δ_{max} = 0.3), the largest rubber plateau, and the lowest plateau modulus (1.510^7 N/m^2).

For M415-based polyurethane, whose NCO content is the highest (10.7%) and for which the MDI surplus has a functionality > 2, the absorption peak is high with a value at the maximum point of 0.15 (lowest value). The E' modulus steadily decreases between −10C and 80°C and its value at 100°C is 5.10^7 N/m^2. For M467-based polyurethane whose NCO% is 9.7%, intermediary properties are observed.

The same Figure 28 shows the behavior of the polyurethane obtained using HQEE as diol extender. We see higher modulus values at the rubber plateau ($1.6.10^8$ N/m^2). The relaxation of the flexible sequences occurs in the same temperature range, but with a lower maximum peak value (0.11 compared to about 0.3).

The polymer flows at about 10° earlier than when butanediol is used as chain extender.

The results of the static mechanical measurements are shown in Figure 29 and in Table XV b).

<div align="center">

Table XV b

STATIC MECHANICAL PROPERTIES OF THE SAME POLYURETHANES

</div>

Prepoly-mer	Hard-ener	%NCO (g)	$E_o (10^7 N/m^2)$ Young's Modulus	Rupture Tension σ_r %(MPa)	Elongation at Rupture ε_r %	Residual Elongation T_A %
M 400	Bd	7.58	1.8	45.2	570	10
M 400	HQEE	7.58	6.6	38.4	700	70
M 467	Bd	9.70	3.0	49.2	590	40
M 415	Bd	10.65	5.7	49.6	520	95

Young's modulus E_o increases as the NCO content increases. Likewise, the residual elongation increases with the percentage of the NCO functions present in the polymer. The rupture behavior (elongation and stress) is comparable for the three formulations.

The use of HQEE increases the E_o modulus of the PUR - M400 formulations as well as the elongation at rupture. Conversely, the residual elongation also increases considerably (from 10% to 70% on the average). This is due to more rigid structure of the HQEE molecule which gives the materials more cohesiveness.
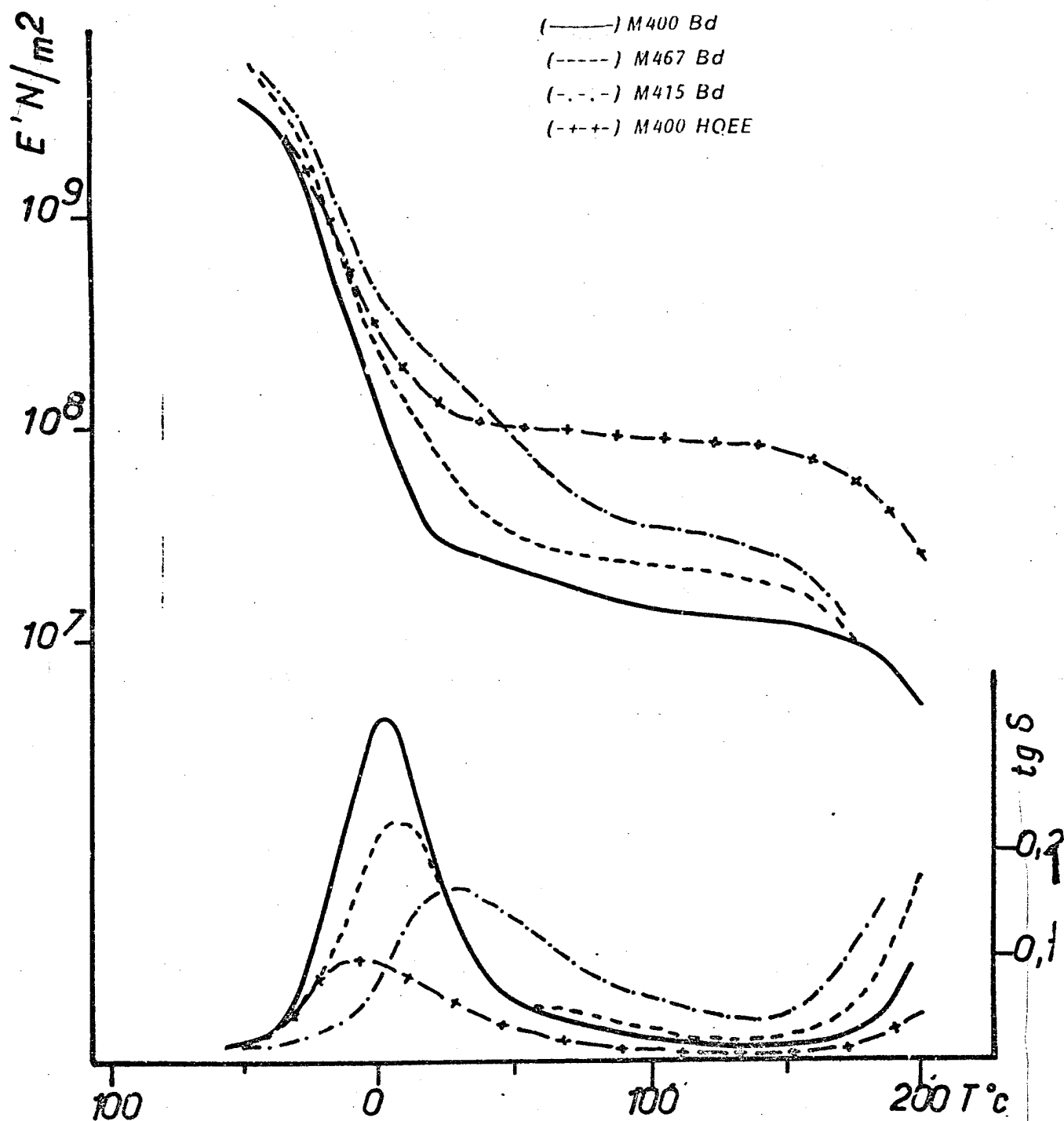
60

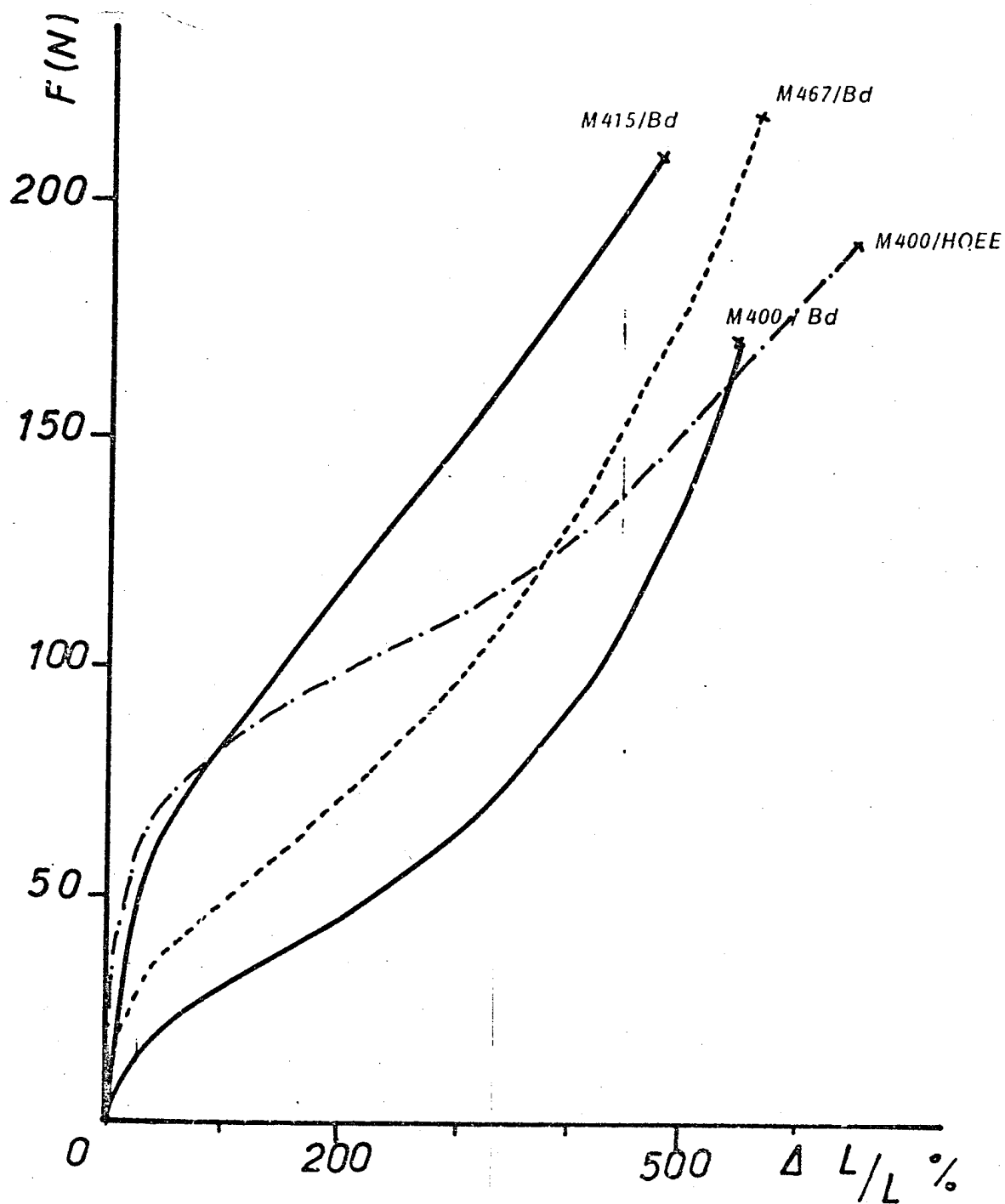Figure 28 – Dynamic mechanical properties of polyurethanes prepared from M Adiprenes and diol chain extenders

Figure 29 - Curves giving static mechanical properties
of polyurethanes prepared with M Adiprenes
and diol chain extenders.

Conclusion

1) In M Adiprene-based polyurethanes, the rigid segments
formed by MDI diisocyanate and butanediol have a semi-crystalline
nature which results in well-defined melting endotherms at high
temperatures ($T \sim 150 - 170°C$). The increased concentration of the
rigid sequences (from the NCO function content which increases
from one prepolymer to another) causes a shift in the maximum re-
laxation peak of the flexible phase to higher temperatures.

When butanediol is replaced by HAEE as chain extender, the
length and number of aromatic cores increase within the rigid se-
quences. This increases the interchain interactions and the co-
hesiveness of the rigid phase.

2) For L Adiprene-based polyurethanes and Cyanaprenes, the
rigid segments melt at much higher temperatures. The diisocyanate
in this case is TDI toluene diisocyanate which is a dissymetric
molecule compared to that of MDI. In this type of polyurethane,
the hydrogen bonds are numerous owing to the presence of urea func-
tions in addition to the urethane functions.

To this one must add the very rigid chemical structure of the
diamine used (Moca) due to the presence of two aromatic and polar
cores and and two chlorine atoms.

This phenomenon is more pronounced for polyurethanes pre-
pared from Cyanaprenes whose flexible sequences are made up of
polyesters. In this case, the supplementary interchain hydrogen
bonds are sandwiched beween flexible and rigid segments so that
the phase separation phenomenon is more complex. This results in
flexible segments which spread over a wide temperature area, and in
a dynamic modulus which decreases as a function of the temperature
(especially if the concentration of the rigid segments is increased).

3) Utilization of the diol chain extenders in the L Adiprene formulations substantially modifies the corresponding elastomer properties. The dynamic modulus E' decreases rapidly in the area /68 corresponding to the vitreous transition with high relaxation peaks, and covering a narrow temperature region. To explain this, we can state that the dissymetric molecule of TDI and the smaller number of hydrogen bonds than previously do not favor the association of rigid patterns. The phase separation is therefore not as good.

However, the presence of a triol proportion (TMP) allows a certain reticulation of the chains, while preserving the elastomer nature. The formulation using triol alone leads to a three-dimensional polyurethane network whose high temperature performance does not result in any first or second order endotherm up to 200°C.

GENERAL CONCLUSIONS ON THIS FIRST PART /69

In summary, this first study gives us the following information:

The study performed on "laboratory" formulations shows that the polyurethane elastomer properties are highly dependent upon the type and chemical structure of the basic products. This helps us to understand the commercial formulations.

We essentially note that the high temperature behavior depends solely on the interaction forces of the rigid segments in the amorphous state. Accordingly, the aromatic diamine (Moca) used as chain extender exhibits rigid segments which flow at higher temperatures.

Likewise, use of the rigid molecule of diol (HQEE) gives the corresponding polyurethanes a better temperature performance and increases the modulus value at the rubber plateau.

In practice, certain formulations will be preferred to others

64

depending on their applications.

a) If we want to have an elastomer die with low vitreous
transition, several L Adiprenes hardened with Moca may be used
(L42, L100). The L315 formulation risks being too rigid with a
modulus which varies substantially with the temperature.

Moca has the disadvantage of being cancerogenic, the other
amines currently proposed are much less efficient and the L or M
Adiprenes hardened with alcohols have a much too high Tg.

Conversely, the formulations based on the POTM oligomers of
$\overline{Mn}$ > 2000, MDI or Bd are totally interesting. Use of the hardener
HQEE instead of Bd can produce more efficient products, provided
that the operating temperature (110°C) rather than 80°C is not
rehibitory.

b) If we want to have an absorbent die with a Tg between -20°C /70
and ambient temperatures, all L or M Adiprenes hardened with al-
cohols are perfectly suitable.

The L100 Adiprene hardened with the Bd + TMP mixture has a
very high absorption peak, but over a very narrow temperature range.

The M Adiprenes hardened with Bd or L315 Adiprene hardened
with the diol + triol mixture are also suitable for a lower absorp-
tion peak, but over a broader temperature range.

c) Cyanaprene-based polyurethanes have intermediary properties.

We summarized these remarks in Table XVI. It is evident that
this is a general scheme and that within each product class, the
formulation can be modified to alter the:

value of the modulus at the rubber plateau;

65

"shore" hardness;

the rate of elongation at rupture;

the operating conditions (temperature and time in pot before casting).

Table XVI

PRACTICAL CONCLUSION ON THE VARIOUS POLYURETHANE FORMULATIONS

Vitreous Transition Tg of final material	Prepolymer Diisocyanate		Chain Extender
Tg < - 50°C	Commercial products:	(L 100 (TDI) (L 42 (TDI) (	Moca
	Laboratory:	POTM 2000+MDI	Bd 1,4 or HQEE
-50°C < Tg < -20°C	Commercial Products	(Cyanaprenes ((TDI)	Moca + cyanacure
Tg > - 20°C		{ L Adiprenes ((TDI) (M Adiprenes ((MDI)	Bd 1,4/TMP Bd 1,4 or HQEE

In order to approach the second part of our study and the   /71
synthesis of polyurethane composites, we selected Adiprene L100/
Moca formulations as well as Adiprene M400/Bd 1,4.

A laboratory formulation based on $\alpha-\omega$ diol oligomer (POTM)
of MDI diisocyanate and on the chain extender 1,4 is also tested
for comparison.

66

PART TWO: REINFORCED UNIDIRECTIONAL POLYURETHANES

I - GENERAL

I-1 - Introduction

Broadly speaking, any heterogeneous material could be qualified as a composite material. Moreover, the term "composite" could also mean "a composition of two or more distinct parts". Thus, any material made up of two or more components, two or more phases, could be considered a composite material.

Plastics reinforced by glass or other fibers represent the prototype of the composite material defined above, due to the remarkable difference in the properties of its components.

In the study below we will use the term composite in a more limited sense. The materials we are interested in are made of two constituents having different properties and different mechanical functions: one binder or die and one reinforcement in the form of unidirectional fibers.

Figure 30 presents a general classification scheme of composite materials with reinforcements [42].

Two types of composite materials have been developed in recent years:

structural composites (resins and glass, carbon fibers) whose low density makes it possible to lighten the structural weight;

thermostructural refactory fiber composites - refactory matrices such as carbon-carbon whose resistance to thermal and mechanical shocks is excellent.

The aeronautics industry has already used these materials widely, especially because of their light weight.

I-2 The Material, Reinforced Plastic

Generally speaking, reinforced plastics are two-phased materials:

a rigid and resistant reinforcement in filamentary form.;
an organic die serving as an interfiber binder.

The mechanical properties of these composites depend on numerous parameters associated with the type of component, the presentation of the reinforcement and the preparation method, on the one hand, the heterogeneity and anisotropy, on the other hand.

This paragraph groups various types of material compositions and characterization. We suggest a general qualitative approach, plus a synthesis of current, rapidly developing knowledge.

I-2-1 Components

a) Reinforcements [43,44]

The list of the main reinforcement fibers, as well as their mechanical characteristics is given in Table XVII.

For the study below, we essentially used unidirectional R glass cloths, as well as high-strength carbon cloths (HT). The Kevlar K49 cloth was used for comparison.

b) Function of the Matrix

The matrix has multiple functions.   It links and protects the fibers and transmits stresses between the fibers.

This role stresses the importance of a good adhesion

Composite Materials

composites reinforced by fibers (fibrous composites)

composites reinforced by mineral fillers

single layer composites

multiple-layer composites

with sheets

hybrid

composites reinforced with continuous fibers (fibers, cloths)

composites reinforced with discontinuous fibers

unidirectional reinforcement

two-directional reinforcement

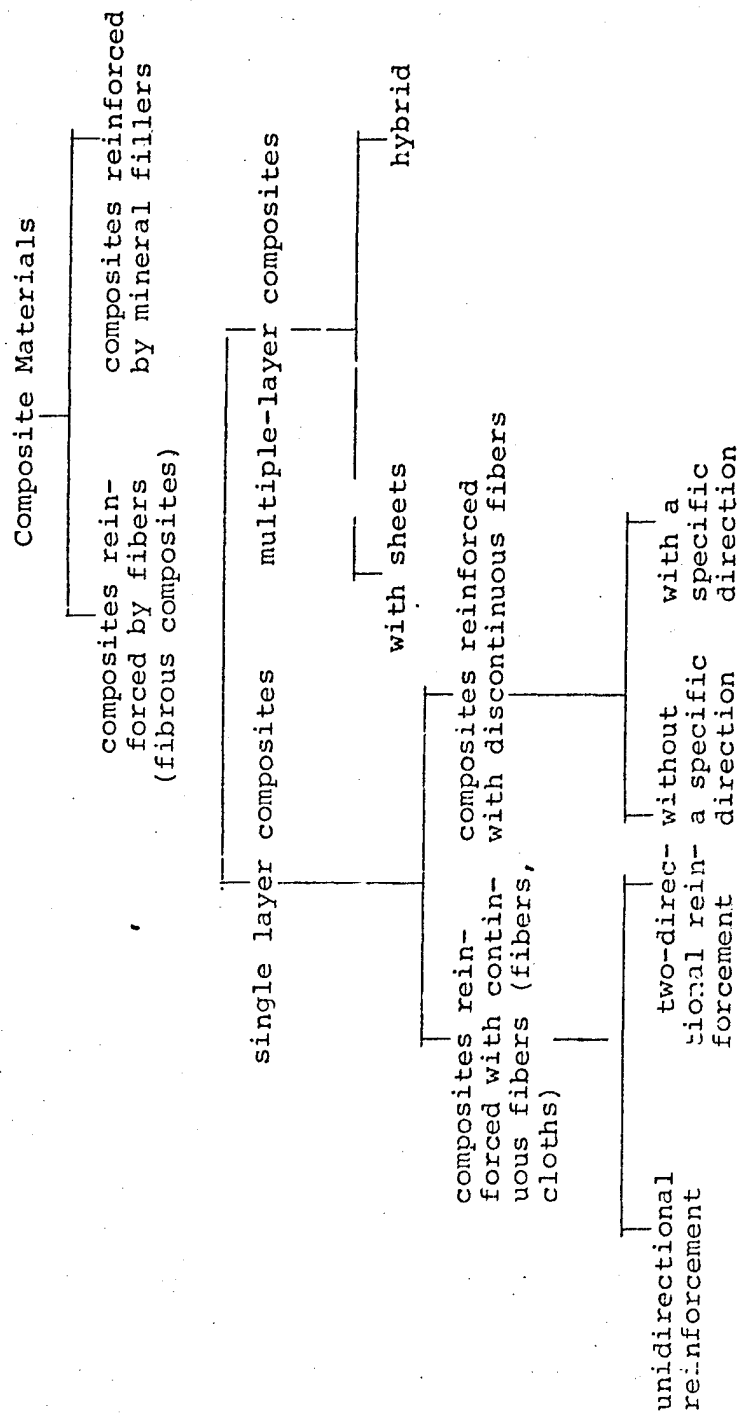without a specific direction

with a specific direction

Figure 30 – Classification of Composite Materials

Table XVII

MAIN REINFORCEMENT FIBERS

Type of Fiber		Dia-meter	Density	Young's Modulus (GPa)	Rupture Strength (MPa)
Glass	-E	5 - 20	2,54	79	3 400
	-R or S	5 - 20	2,50	87	5 500
Boron		100	2.65	420	3 000
Graphite	-High strength (HT)	8	1,75	250	2 800
	-High modulus (HM)	8	1.92	350	2 000
Aramides	High strength (HT)	12	1.45	84	3 000
	High modulus (HM)	12	1,45	130	2 700

between the reinforcement and the matrix. This is made possible
by carefully selecting the constituents and by proper treatments
when the composite is prepared (oiling for glass, surface oxidation
for carbon). Additionally, the matrix protects the outside from
shocks (the reinforcements are often fragile materials highly sen-
sitive to impacts) or from the mechanical environment: chemicals,
humidity, etc. [45].

Finally, the color, transparency or opacity generally depend
on the die.

A certain number of impregnation resins are used to obtain
polymer dies. The most common ones are polyesters (especially
with glass fibers) and polyepoxydes (or "epoxyde resins").

For certain appplications, on also uses phenols, silicons and
formol-melamines. Polyimides have good mechanical properties as-
sociated with excellent temperature behavior (thermoregulated dies).
However, they have the disadvantage of being delicate to prepare
and often require special manufacturing facilities, owing to their
toxicity.

70

In regard to polyurethanes, to our knowledge, there are no published studies on the behavior and mechanical character-istics of a unidirectional composite with a polyurethane matrix. On the other hand, numerous communications and patents (46,49] on polyurethanes obtained by the RIM process (Reaction-Injection-Molding) or R-RIM (Reinforcement-Reaction-Injection-Molding) de-scribe in detail the research done on adding ground fibers to one or several of the polyurethane components. This addition is gen-erally done to the polyol component prior to reaction and implemen-tation. Other studies [50] pertain to polyurethane foams, also reinforced with cut glass fibers.

For the second part of our study, we therefore used polyure-thane elastomer matrix selected previously on the basis of the follow-ing criteria:

a low vitreous transition $(Tg \leq 50\,°C)$
a rubber plateau above Tg, large and constant over about $100\,°C$.

I-3 Behavior of Unidirectional Composite Materials

I-3-1) Introduction

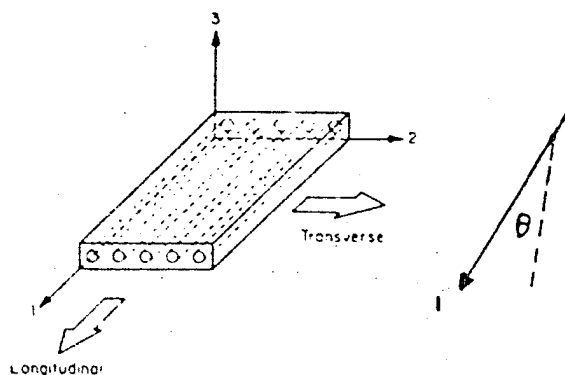Figure 31 shows the diagram of a unidirectional composite material.

Figure 31 - Illustration of an unidirectional composite. Definition of the θ angle with respect to the fiber direction.

71

Several unidirectional layers may be stacked in a certain direction to each other to obtain a composite of which each layer is considered elementary. The material is orthotropic and the symmetry identification axes fall along three planes which coincide with the axes 1, 2, 3 in Figure 31. We define an orientation angle (θ) which we will use for the rest of the report.

The direction of axis 1 (parallel to fibers) is called the longitudinal direction ($\theta = 0$). The direction perpendicular to the fibers is called the transverse direction (any direction along the 2-3 plane): ($\theta = 90°$). The most important properties, Young's /80 modulus* in particular, are in a longitudinal direction.

Yet, the unidirectional fabric should be elicited. The longitudinal direction is called the chain. However, there is a fiber proportion in the cross-direction, the weft, used to hold the fabric. "A priori", the properties of the elementary layer should be a function of the fiber "proportions" in each direction, and of the fabric frame. This is the type of reinforcement found in the fabrics we used (glass, carbon or Kevlar).

I-3-2) <u>Mechanical Characteristics of a Unidirectional Composite</u>

One of the most important factors in defining composite properties is the relative proportion of the die and reinforcement. This proportion may be expressed according to mass W or volume θ fractions defined thus:

$$\text{fiber volume fraction } \theta_f = \frac{\text{volume occupied by fibers } v_f}{\text{composite volume } v_c}$$

$$\text{matrix volume fraction } \theta_m = \frac{v_m}{v_c}$$

$$\text{fiber mass fraction } W_f = \frac{\text{fiber weight } W_f}{\text{composite weight } W_c}$$

$$\text{matrix mass fraction } W_m = \frac{W_m}{W_c}$$

---

72   *i.e.   modulus of elasticity.

with $v_c = v_f + v_m$ (as long as porosity can be disregarded)

and $W_c = W_f + W_m$

The indices f, m and c correspond to the fiber, the matrix, and the composite respectively.

The mass fractions, for glass fiber based composites, are easily /81 obtained via gravimetry by heating the material at high temperatures (in the vicinity of 500°C).

The volume fractions may be deduced from the mass fractions if we know the respective densities of fibers (ρ_f) and of the matrix (ρ_m) using the following equation:

$$\phi_f = \frac{1}{1 + \frac{\rho_f}{\rho_m}\left(\frac{1}{W_f} - 1\right)}$$

If we take into account these parameters as well as the fiber & matrix moduluses. we can determine the longitudinal modulus of the composite ($E_{\theta=0}$) using the mixing law.   We are assuming that the fiber and matrix contents are proportional to their volume fractions.

$$E_{\theta=0} = E_f \phi_f + E_m (1-\phi_f)$$

If the longitudinal modulus $E_{\theta=0}$ may be theoretically predicted so easily, it is hard to have theoretical predictions or semi-empirical equations simple enough to be applied to the transverse moduluse $E_{\theta=90°}$.

73

The equations then become more complex, but all depend on the parameters: moduluses, Poisson's factor, volume fraction of the constituents. To this, one must add factors pertaining to fiber alignment, the row-weft balancing factor in the case of fabrics, the fiber arrangement or "packing", the presence of "empty spaces" in the die, etc.

We have at our disposal several means for determining the static mechanical properties of a composite material: tensile, bending, torsion and shearing tests.

Although the bending tests stress the material in a more complex manner, we gave preference to the tensile test for several reasons:

A break in a unidirectional reinforcement material during a /82 tensile test does not occur in a section perpendicular to the stress. It is always associated with numerous longitudinal ruptures which cross the sample from one end to the other [51,52], as we can see on the photos in Figure 32.

For this type of composite material, tensile stresses should be transmitted via jaws which hold the ends of the samples in a compressive state. As the stress applied is very strong, the longitudinal ruptures parallel to the fibers very often initiate in the jaws.

The sample portion in the jaws should be very large and reinforced in thickness. This requires special molds to machine the samples in a special shape and this often very hard to do [53] (Figure 33).

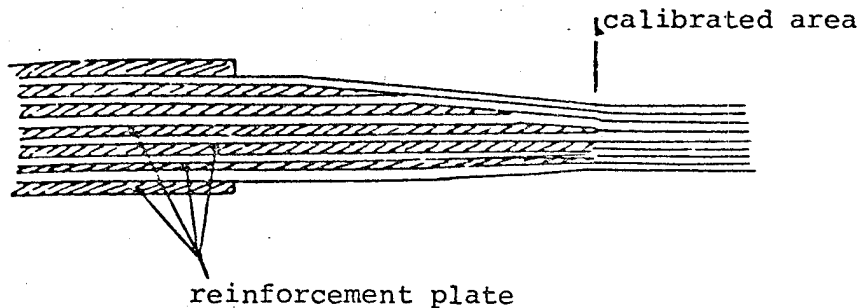We sent samples to be tested at SNIAS Marignane and the same phenomena were observed.

74

Figure 33 - Type of sample used for tensile tests on composites

We therefore adopted a 3-point bending test, which is much simpler to implement, but which complicates the predictional calculation.

I-3·3) Predictional calculation methods

The methods of evaluating mechanical properties and proposed in literature are very numerous. They develop mathematical equations, which are most often fairly complex, and semi-empirical equations.

The purpose of these calculation methods is to predict the elastic or viscoelastic constants of composite materials. We are not going to give details and review all of the existing methods and models (moreover, this is not the purpose of our work). However, we did retain GREZCZUK's [54], PUCKS's [55] and TSAI's [56] [57] results, which seem to be the most frequently used in the laminated plastics industry [44]. We did not test more complex models for which one accounts for the fiber - matrix adhesion, the number of layers used, etec. The selected models supposedly have a perfect adhesion betwen the fibrous reinforcements and the matrix.

The elastic behavior of a unidirectional composite material is characterized by three moduluses: longitudinal $E_{\theta=0}$ (E_1), transversal $E_{\theta=90}$ (E_2) and shearing modulus G_{12}, on the one hand; and

75

by the corresponding Poisson factors (υ). These modulii are accessible to experiments and the theoretical approach is possible via micromechanical analysis of the fiber-matrix system.

The notations 1 and 2 in the equations given by the various models correspond to the fiber direction ($\theta=0$) and to the transverse direction ($\theta=90°$).

a) PUCK's Model

The author adopts the mixing law for E_1; the calculation of E_2 is conducted with the resistance of materials using an elementary volume to represent the rectangular contour:

$$E_1 = E_f \phi_f + (1 - \phi_f) E_m$$

$$E_2 = E_m^o \frac{1 + 0,85\ \phi_{vf}^2}{(1 - \phi_{vf})^{1,25} + \dfrac{\phi_f E_m^o}{E_f}}$$

where f = fiber, m = die

ϕ_f = volume fraction of the reinforcement

with $E_m^o = \dfrac{E_m}{1 - \upsilon_m^2}$ where υ_m = Poisson factor of the die

b) GRESZCZUK's Model

GRESZCZUK includes in his calculations the influence of empty spaces in the die and uses the disturbed die concept introduced earlier by EKWALL [58] which assumes that the matrix deformations in the fiber direction are nil, for a transverse stress (perpendicular to the fiber direction).
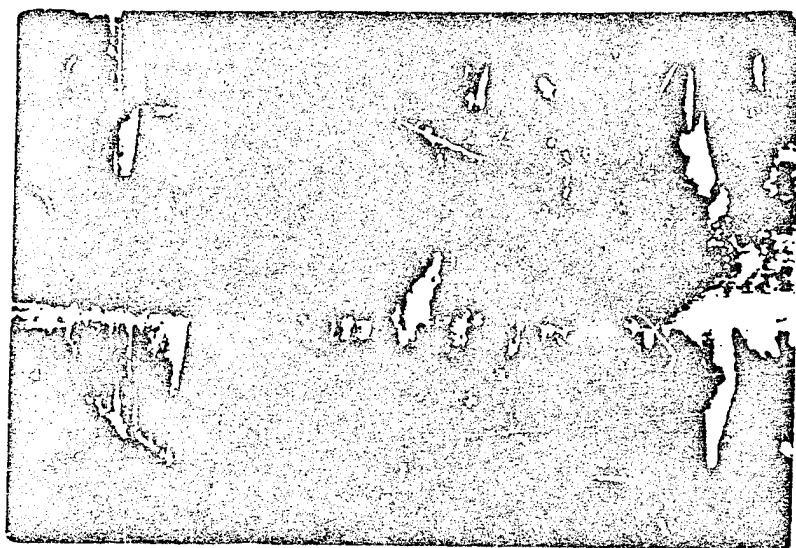
From this assumption and a three-dimensional strain – deformation law, he obtains the modulus of the disturbed matrix. For the longitudinal modulus, the mixing law still applies:

76

a) rupture of sample along fibers begins in jaws.

b) the break in sample is produced in area within jaws.

c) the area on the sample where the break should occur (note weft fibers in unidirectional fabric used).

Figure 32 - V-400 composite under tensile stress

$$E_1 = \phi_f \, E_f + (1 - \phi_f) \, E_m$$

$$E_2 = E_o \, \beta + E^*_m \, (1 - \beta) \qquad \text{where } \beta = \sqrt{\frac{\phi_f}{\pi}}$$

with

$$E_o = \cfrac{E^*_m + 2\,\beta\,(E_f - E^*_m)}{1 + \cfrac{2\,\beta\,(1 - 2\,\beta)}{E^*_m \, E_f} \left\{ (E_f - E^*_m)^2 - (\nu_m E_f - \nu_f E^*_m)^2 \right\}}$$

where

$$E^*_m = \frac{E_m}{1 - \nu_m^2}$$

c) TSAI Model

TSAI studies the problem of cylindrical inclusion (fibers) in the elastic die. He begins with six assumptions and calculates the upper and lower boundaries for E_2, G_{12} and ν considering that:

the fibers and matrix are isotropic,
the fibers and matrix are linearly elastic,
the fibers are uniformly distributed in the matrix,
the fibers and the matrix do not have empty spaces,
there is perfect adhesion between the fibers and matrix i.e.,
there is no intermediate area between the fibers and matrix,
the interfacial thickness is nil.

The boundaries are evaluated by interchanging the role of the fibers and the matrix. The upper and lower boundaries are too far to be processable. TSAI therefore assumes that the elastic behavior of a unidirectional layer is found somewhere between the two boundaries and may be illustrated using a linear association of these two boundaries. He introduces the adjacency factor concept C. The meaning of this factor is the following:

78

C = 0: the matrix is contiguous → all fibers are separated by the matrix

C = 1: the fibers are contiguous

0   0 < C < 1 represents all other possible combinations.

The value C = 0.2 gives a good correlation between theory and experiment for the glass - epoxy systems.

$$E_1 = k\{\phi_f E_f + (1 - \phi_f) E_m\}$$

with K: factor of incorrect fiber alignment $0.9 < k < 1$

$$E_2 = 2\left[1 - \nu_m - \phi_f(\nu_f - \nu_m)\right]\left[(1 - C) \times \frac{K_m (2 K_f + G_m) - \phi_f \times G_m (K_m - K_f)}{(2 K_f + G_m) + 2\phi_f (K_m - K_f)}\right.$$

$$\left. + C \times \frac{K_m (2 K_f + G_f) - \phi_f \times G_f (K_m - K_f)}{(2 K_f + G_f) + 2\phi_f (K_m - K_f)}\right]$$

with $K_f = \dfrac{E_f}{2(1 - \nu_f)}$ $K_m = \dfrac{E_m}{2(1 - \nu_m)}$

$G_f = \dfrac{E_f}{2(1 + \nu_f)}$ $G_m = \dfrac{E_m}{2(1 + \nu_m)}$

I 4 - Preparation and Methods of Analyzing Composites With Polyurethane Matrix

I-4-1) Description of Reinforcements Used

a) In Table XVIII we showed the characteristics of various fibrous reinforcements used. Note that it is useful to know the calculated thickness of a layer to prepare a composite plate. This allows us to determine the number of folds needed for a

plate with a set and known thickness (e). Additionally, the % weight of the various wefts is shown, according to the fabric used.

TABLE XVIII

CHARACTERISTICS OF FABRICS USED AS REINFORCEMENTS
a) REF. VETROTEX; b GAMMA AMINOPROPYL TRIETHOXYSILANE γ
c) BROCHIER TERM; d) VALUE OBTAINED BY DIVIDING THE
WEIGHT PER UNIT OF SURFACE BY THE DENSITY

Fabrics	V-P109 [a] V-A1100 [b]	G 827 [c]	E 1950 [c]
fiber	glass R	carbon T300	Aramide K49
% wt. weft	6.5	1.5	5
type of weft	glass E	glass E	polyester
surface wt (g/m^2)	0.340	0 160	0.100
density (g/cm^3)	2.55	1.74	1.45
calculated thickness of a fold (mm)	0.13	0.09	0.07

b) In the case of glass fibers R, we used two types of oiling*, P109 and A1100. An analysis via infrared spectrometry gave us information on the nature of these oilings. P109 is a Vetrotex reference, whereas A1100 is an aminosilicone treated on the same glass fabric R and while removing the oils first at high temperatures.
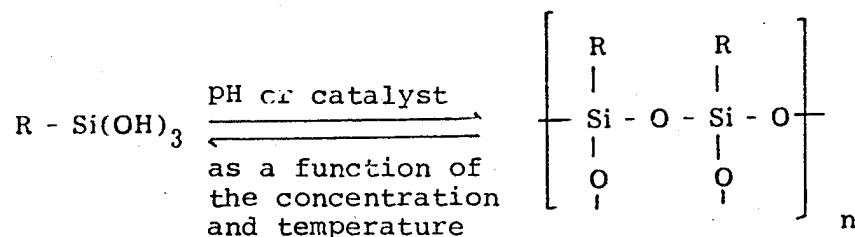
The mechanism by which silicone interacts with glass was studied in literature [59,60]. The surface of glass has reactive sites of silanols ⟩SiOH, oxides or adsorbed water. We assumed that the   /88 interaction mechanism is the following [61]. In the initial phase, silicone is hydrolyzed and deposited on the glass surface:

$$R - SiX_3 + 3 H_2O \xrightarrow[\text{catalyst}]{\text{pH}} R - Si(OH)_3 + 3 HX$$
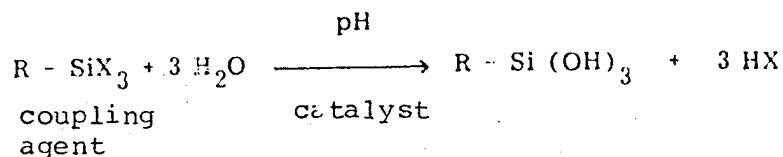
coupling
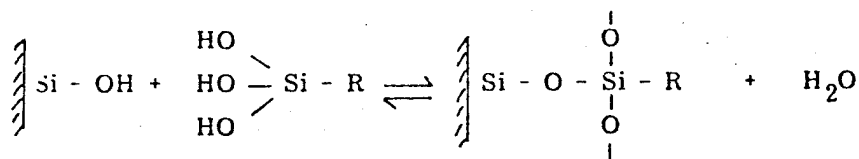agent

*Translator's note: i.e. a coupling agent.

80

HX is most often an alcohol.

This first phase is quick. The silanol function of silicone is not stable ! it tends to autopolymerize to form a siloxane homo-polymer

$$R - Si(OH)_3 \quad \underset{\substack{\text{as a function of} \\ \text{the concentration} \\ \text{and temperature}}}{\overset{\text{pH or catalyst}}{\rightleftarrows}} \quad \begin{bmatrix} R & & R \\ | & & | \\ Si - O - Si - O \\ | & & | \\ O & & O \\ | & & | \end{bmatrix}_n$$

The equilibrium depends on the pH, the temperature and the concentration. For example a pH of 4 or 5 is favorable for high monomer concentrations which preserves the functionality of the coupling agent.

The desired reaction should lead in the second phase to a bond between the hydrolyzed silicone and the glass surface:

$$Si - OH + \begin{matrix} HO \\ HO - Si - R \\ HO \end{matrix} \rightleftharpoons \begin{matrix} O \\ | \\ Si - O - Si - R \\ | \\ O \\ | \end{matrix} + H_2O$$

Since this reaction is reversible, the bonds may form and loosen. It does not use the three silanol groupings of the hydrol-yzed silcone molecule. These surplus functions may therefore con-dense with other silicones to form another three-dimensional polymer which favors silicone retention at the interface are available.

c) For an IR analysis, the fibers are ground into powder and /89 are mixed with potassium bromide KBr. This was possible with glass fibers and carbon. Conversely, the Kevlon fibers are hard to grind and the corresponding spectrum could not be made.

81

Figure 34 shows the spectra of three types of oiling for glass fibers. These spectra were obtained by comparing two spectra: one with oil-removed glass fiber R and the other with oiled fiber R. In this way we can have an idea of the functions provided by the coupling agent on the reinforcement surface. We also showed the spectrum of A187 which is a coupling agent whose chemical composition is known: γ:glycidoxy-propyl-trimeth-oxysilicone which is an epoxy-silicone. The characteristic bands will serve as a comparison with the other coupling agents. In the absorption area of the Si-O-Si bond, we see a wide band spreading over 500 cm^{-1} approximately. This is due to the high polymerization rate of silicone and the magnitude of the deposited layers. There is a small absorption band, about 3300 cm^{-1} which corresponds to the presence of the amine functions. Furthermore, not knowing the exact chemical nature of reference P109, we can affirm the presence of the epoxyde functions in addition to the amine functions. This assumption is possible due to a comparison with oiling reference A187, where we are certain of the epoxyde presence.
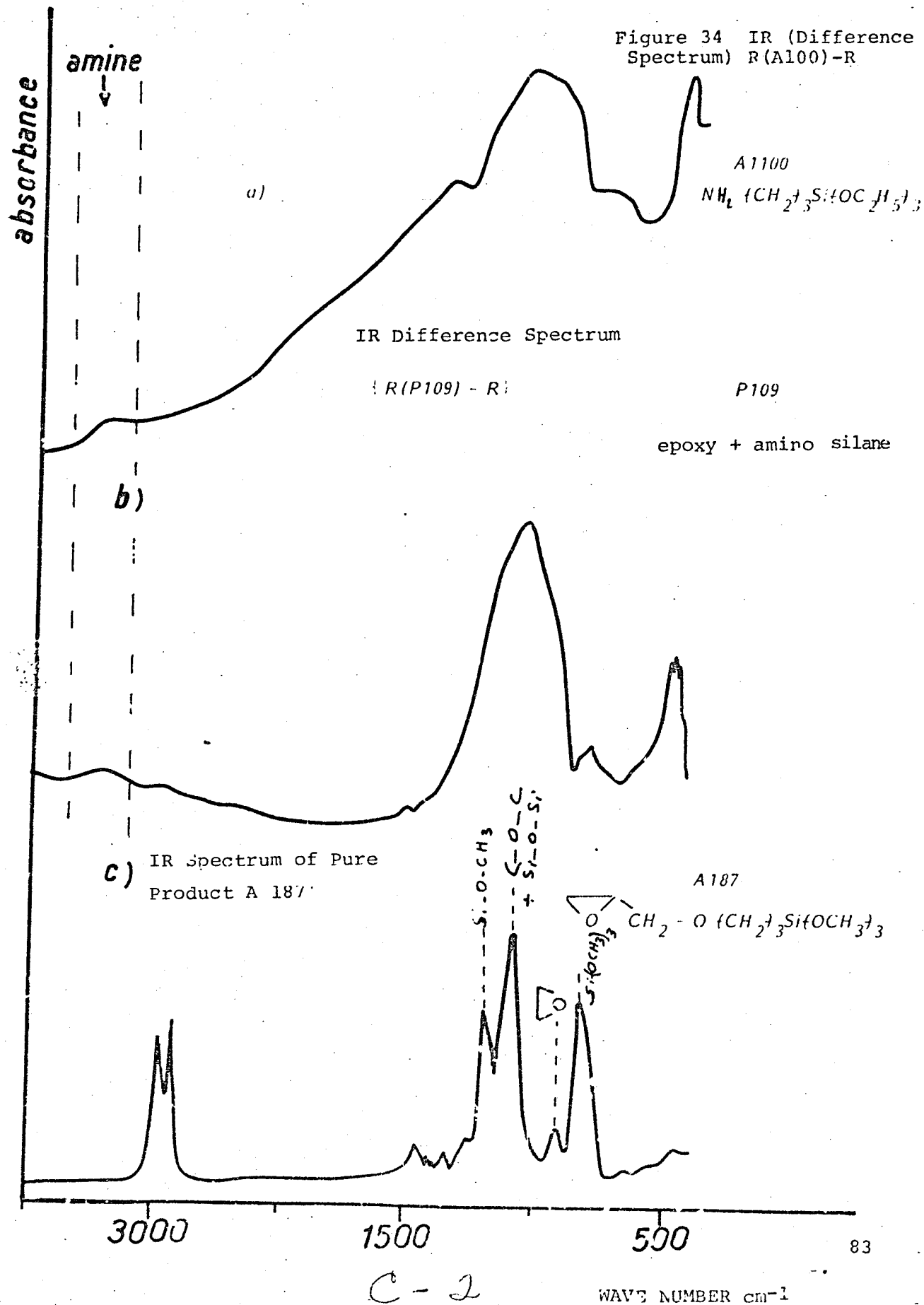
In the case of carbon fibers, the corresponding spectrum accumulates in 10 minutes, but spreads considerably and is hard to analyze.

I-4-2) Summary of Matrices Selected

Three types of formulations were selected to study the corresponding composites.

Two commercial formulations for preparing polyurethanes (PUR) from L100 and M400 diisocyanate prepolymers.

In the first case, the chain extender is the aromatic diamine, Moca. The reaction temperature is 100°C for 3 hours mold time (at 100°C). In the rest of the report, we will call it the PUR-L00 matrix.

82

Figure 34   IR (Difference Spectrum) R(A100)-R

a)

amine

absorbance

A 1100

$NH_2 \ (CH_2)_3 Si(OC_2H_5)_3$

IR Difference Spectrum

$R(P109) - R$

P 109

epoxy + amino silane

b)

c) IR Spectrum of Pure
Product A 187

$Si-O-CH_3$

$-C-O-C-$
$+$
$Si-O-Si$

A 187

$O \quad CH_2 - O \ (CH_2)_3 Si(OCH_3)_3$

$Si(OCH_3)_3$

O

3000   1500   500

83

$C - 2$

WAVE NUMBER cm^{-1}

In the second case, the extender used is butanediol 1,4.
The reaction temperature is 85°C for 17 hours mold time (at 110°C);
this will be the PUR-M400 matrix.

The laboratory formulation begins with diol oligomers and
diisocyanate which reacts at 80°C for 2 hours, to obtain a diiso-
cyanate prepolymer. This prepolymer is extended in the second
phase by butanediol, at a temperature of 80°C for 24 hours mold
time (at 80PC). These will be our CP_1 matrices (with POTM 2000 oli-
gomer) and CP_2 (with POTM 1000 oligomer).

I-4-3)   Preparation of the Composite Plates

Most often a mold has to be made to fabricate composite plates.
In our case, one must consider the "pot life" of the die to allow
the reinforcement fibers to impregnate. It is generally fairly
short for the formulations used (on the order of a few minutes).
The casting must therefore be carried out quickly to avoid an
excessive increase in the viscosity of the reactive system.

The implementation and fabrication conditions of a composite
material are among the determining factors for the fiber-die ad-
hesion. This point is specified in the work accomplished in the
"Interfacial Physicochemistry Laboratory of the National Superior
School of Chemistry of Mulhouse"; M. BOMO [62] studied the adhes-
ion between filamentary reinforcements and a polyurethane die
using a method based on the observation of the length of fiber
fragments broken inside a composite sample subjected to tensile
testing to its breaking point.

These tests showed that there is a correlation between the
adhesion thus measured and the time separating the preparation
of the reactional mixture for placing in contact with the fiber.
However, if it was necessary to coat the reinforcement as
quickly as possible, it was also indispensable to homogenize the
reactional system as perfectly as possible. A compromise should

84

be made to obtain both a homogeneous matrix and maximum adhesion.

Figure 35 shows a diagram of the cast we used in our syn-
theses. A quantity of resin is cast in the bottom of the mold,
the folds of previously cut unidirectional fabrics are then de-
posited and a generous resin quantity is poured over it. The
system is plated so that the resin surplus rises around the piston.
The composite plate is obtained with the desired thickness and
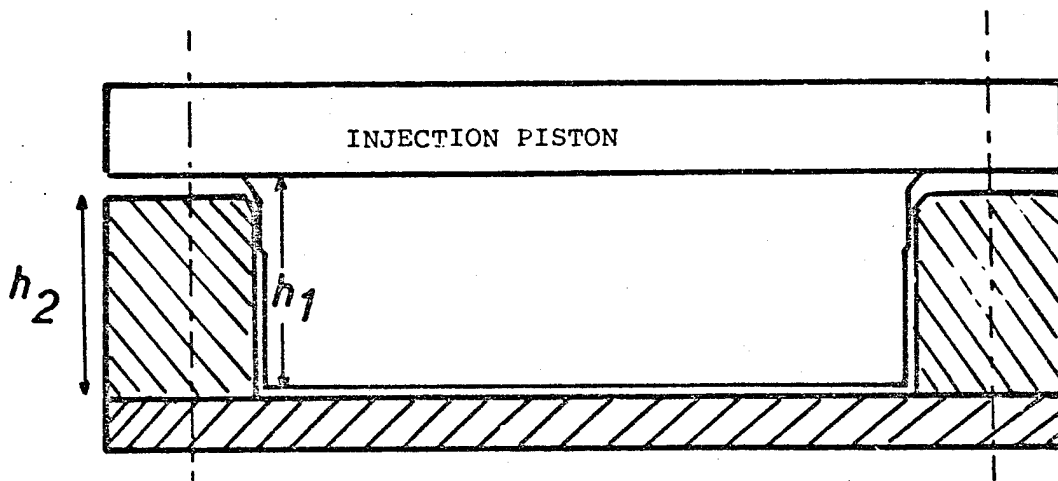this is adjusted in advance by $h_2 - h_1$.

Figure 35 - Composite Plate Modulus - Elastomer - Reinforce-
ment. Schematic Diagram.
$e = h_2 - h_1 = $ thickness of cast plate

The prepared polyurethane composites (Table XIX) are in
the form of a plate about 1 mm thick.

We established a fraction of reinforcement per unit of volume
in the vicinity of 50%. Knowing the theoretical thickness of a
fold, we can therefore determine the number of folds required
which varies from one composite to another, depending on the type
of fabric used. Here, we will define the name we adopted for
our composites. The reference used is (X-die) where (X) may be
V in the case of glass fibers; C in the case of carbon fibers;
K in the case of Kevlar fibers. The matrix may be either L100.
M400.CP_1 or CP_2. For example, a glass composite prepared with the
PUR L100 die is represented by V-100.

C - 2

TABLE XIX

PROPERTIES OF PREPARED POLYURETHANE COMPOSITES

Composite	V(glass)[a]	C(carbon)[b]		K(aramide)[b]
Number of layers	4	6	8[b]	8
% reinforcement per unit of volume (mean) with a matrix				
L100	56	54	55	49
M400	52	--	56	48
CP1	53	--	--	--
CP2	54	--	--	--

(a) measurements performed by burning the matrix at 600° C

(b) obtained by calculating the theoretical thickness of a fabric layer

I-4-4) Methods of Analysis

The analysis techniques are presented in the experimental part (appendix). We review here the methodology followed in the study of composites:

Differential thermal analysis (ATD) allows us to measure the transitions of polyurethane composites (Tg and Tf measurements).

Characaterization of the die and the potential differences caused during the course of the synthesis of the material due to the presence of fibers are studied by extraction testing using an organic solvent so as to compare the possible soluble fractions of our materials. We did not conduct a systematic study to detect the best solvent or the optimal experimental conditions. We simply took tetrahydrofurane (THF), because this is our solvent for chromatography analysis on permeable gel (GPC). This method allows us to analyze the extracted polyurethane fractions. The

infrared (IR) spectrometry is then applied to complete this part of our analysis.

The IR technique also allows us to analyze and obtain information on the quality of the fiber-die interface.

The static mechanical characteristics are performed via /94 bending tests as a function of the temperature to allow us to have access to the longitudinal $E_{\theta=0}(E_1)$ and transverse $E_{\theta=90°}(E_2)$ modulus.

Measurements of absorption tg δ as well as of the conservation modulus E' as a function of the temperature are performed on the viscoelasticimeter rheovibron and allow us to characterize the dynamic mechanical properties of our composites. The samples in this case are subjected to tensile stresses; the frequency of the excitations is 11 Hz. Still we measured tg δ at much higher frequencies (up to 10 KHz) via dielectric measurements.

II - STUDY OF COMPOSITES WITH A POLYURETHANE DIE /95

II-1 - Matrix Quality

II-1-1) Differential Thermal Analysis

The results obtained on the various composites are grouped in Tables XX. The corresponding thermograms are shown in Figures 36, 37, 38 and 39.

In low temperature areas, the second order transitions cor- /100 respond to the vitreous transition of flexible matrix segments. The endothermic peaks observed near the highest temperatures (T > 100°C) correspond to the melting levels of the various rigid segments (TDI + Moca) or (MDI + butanediol).

THERMAL ANALYSIS OF THE VARIOUS PURs PREPARED AS WELL
AS OF THE CORRESPONDING COMPONENTS

matrix & composites	Polyurethane % wt.	Flexible Segments % wt.	T_g (°C)	T_f (°C) [a]	T_f (°C) [b]
L 100 matrix	100	83,2	– 65		190
V(P109)-L100	24	19,9	– 68		190
C-100	38	31,6	– 65		185
K-100	44	36,6	– 65		*
M400 matrix	100	75,4	– 55		170
V(P109)-M400	31	23,3	– 53		162
C-M400	31	24,8	– 52		145
K-M400	45	33,9	– 55		*
CP1 matrix	100	67,7	– 80	8	145
V(P109)-CP1	27	18,3	– 79	10	155
CP2 matrix	100	58,8	– 70		130 – 150 *
V(P109)-CP2	29	17,0	– 68		130 – 150

*see Figures 37, 38, 39

a) melting point of flexible segments; b) melting point of rigid
   segments. The two melting peaks correspond to rigid segments
   of different lengths.

The introduction of fibers into the polyurethane matrices allows /100
us to make the following observations:

The vitreous transition of the composite (on the thermogram)
is delicate. These second order transitions are less clear than
for the matrix alone, because they "lead" to high temperatures and
the quantity of matrix present is on the average 23% by weight, in
a glass composite containing about 55% reinforcement by volume.
Nevertheless, the values of these transitions do not vary signif-
icantly.
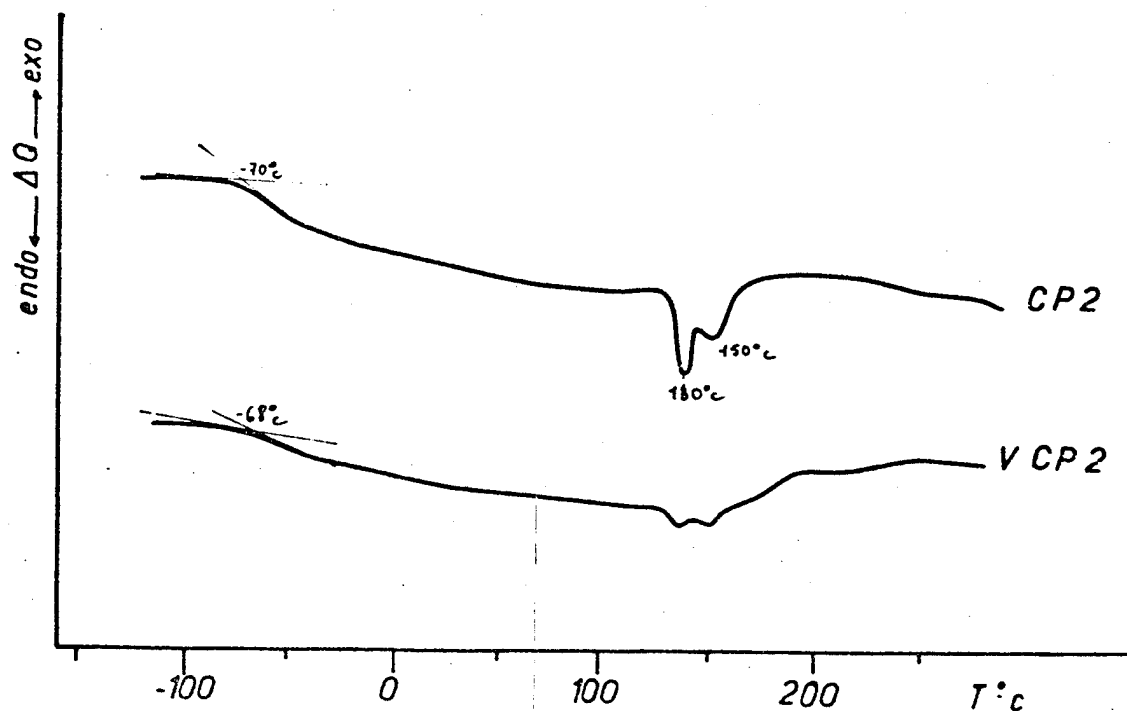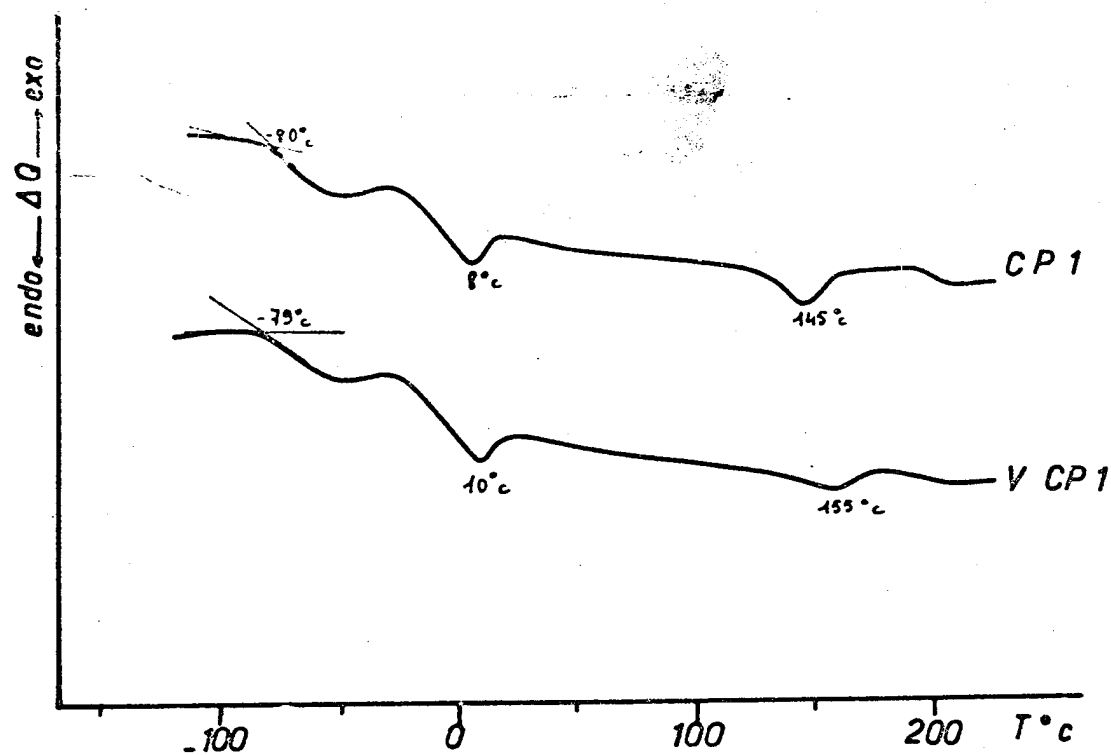
Figure 36 - Differential Thermal Analysis of Composites V-CP1
and V-CP2
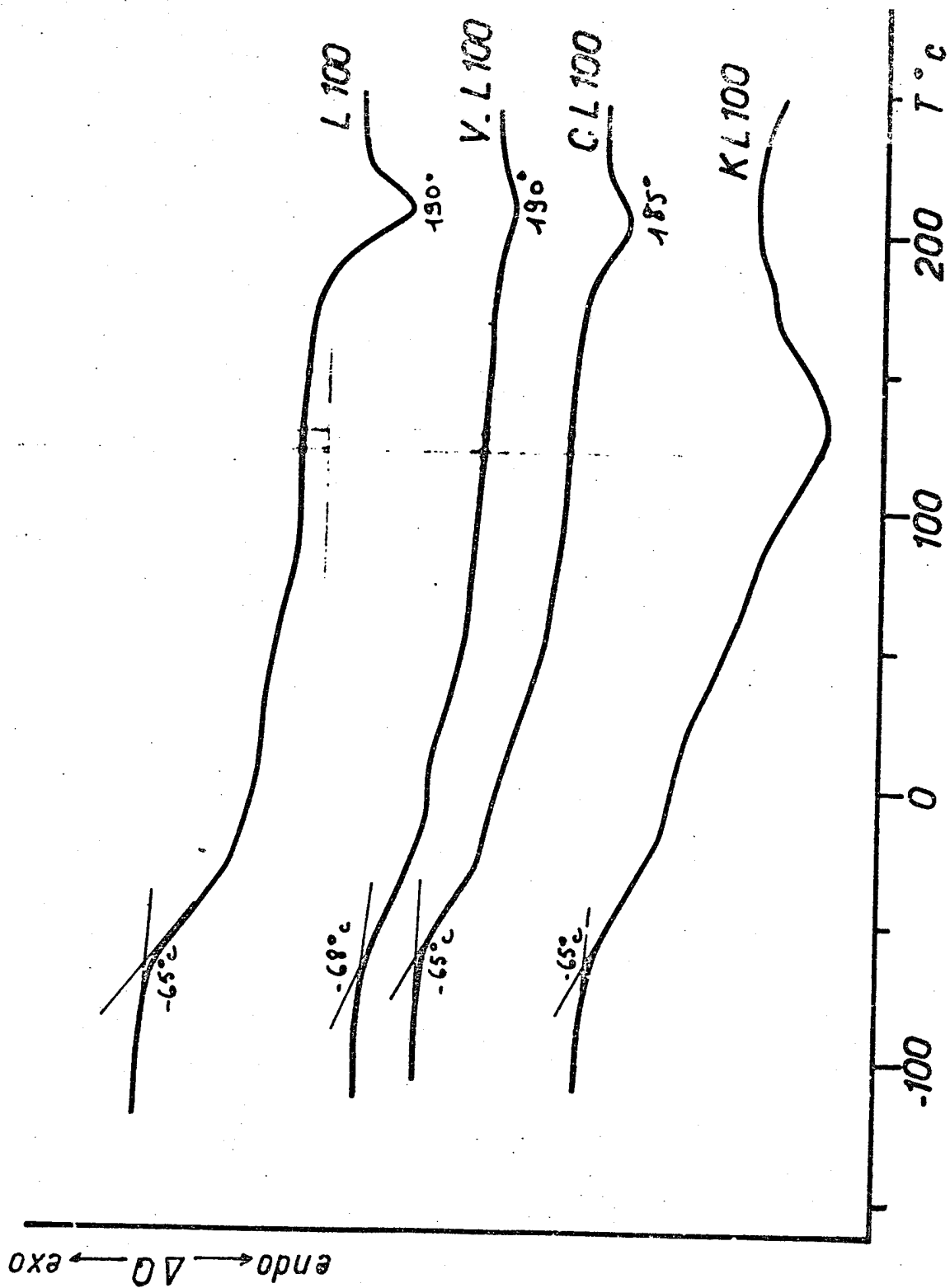
Figure 37 – Differential Thermal Analysis of the Various Components With PUR-L100 Matrix
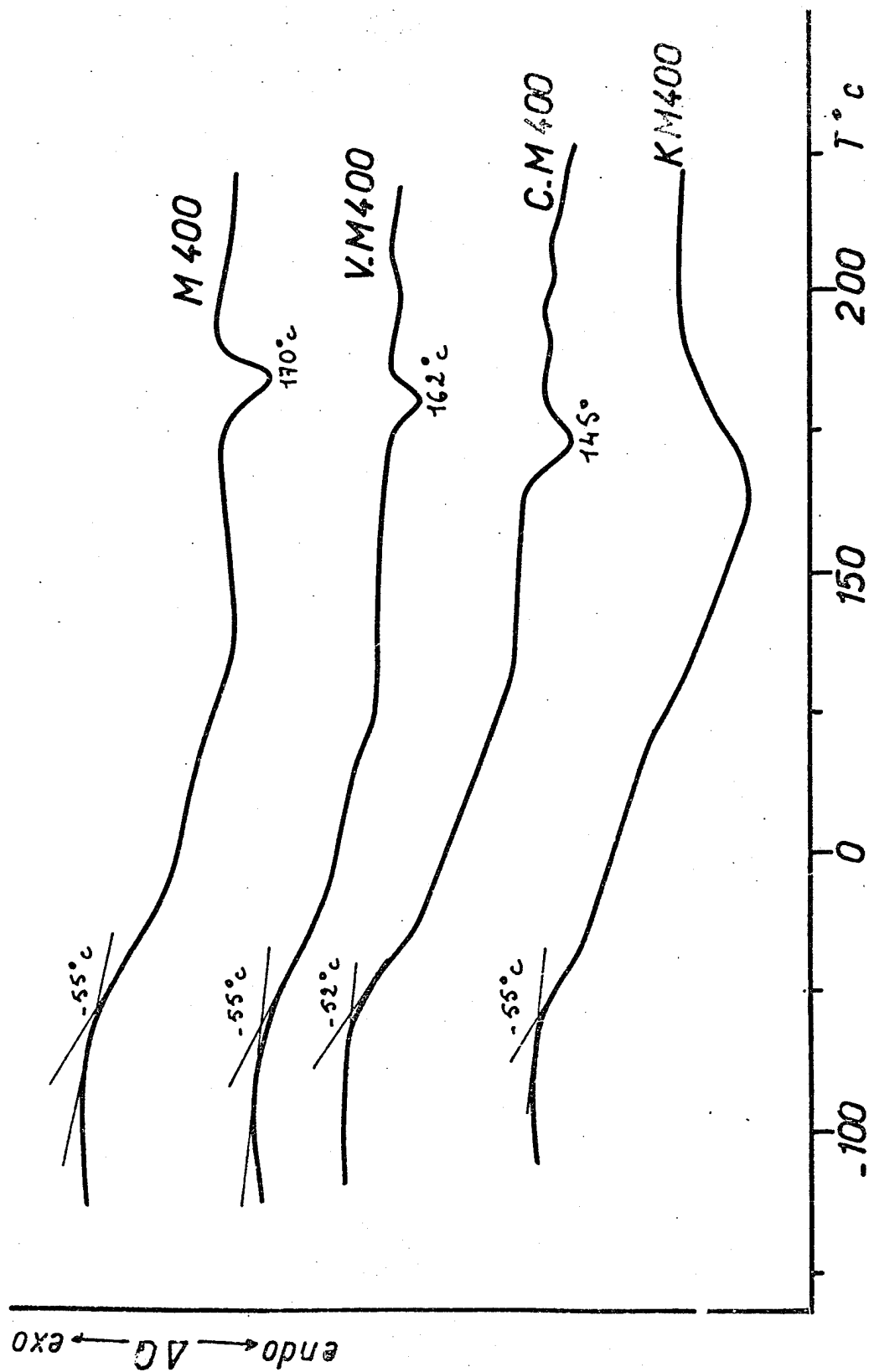
Figure 38 – Differential Thermal Analysis of the Various Composites
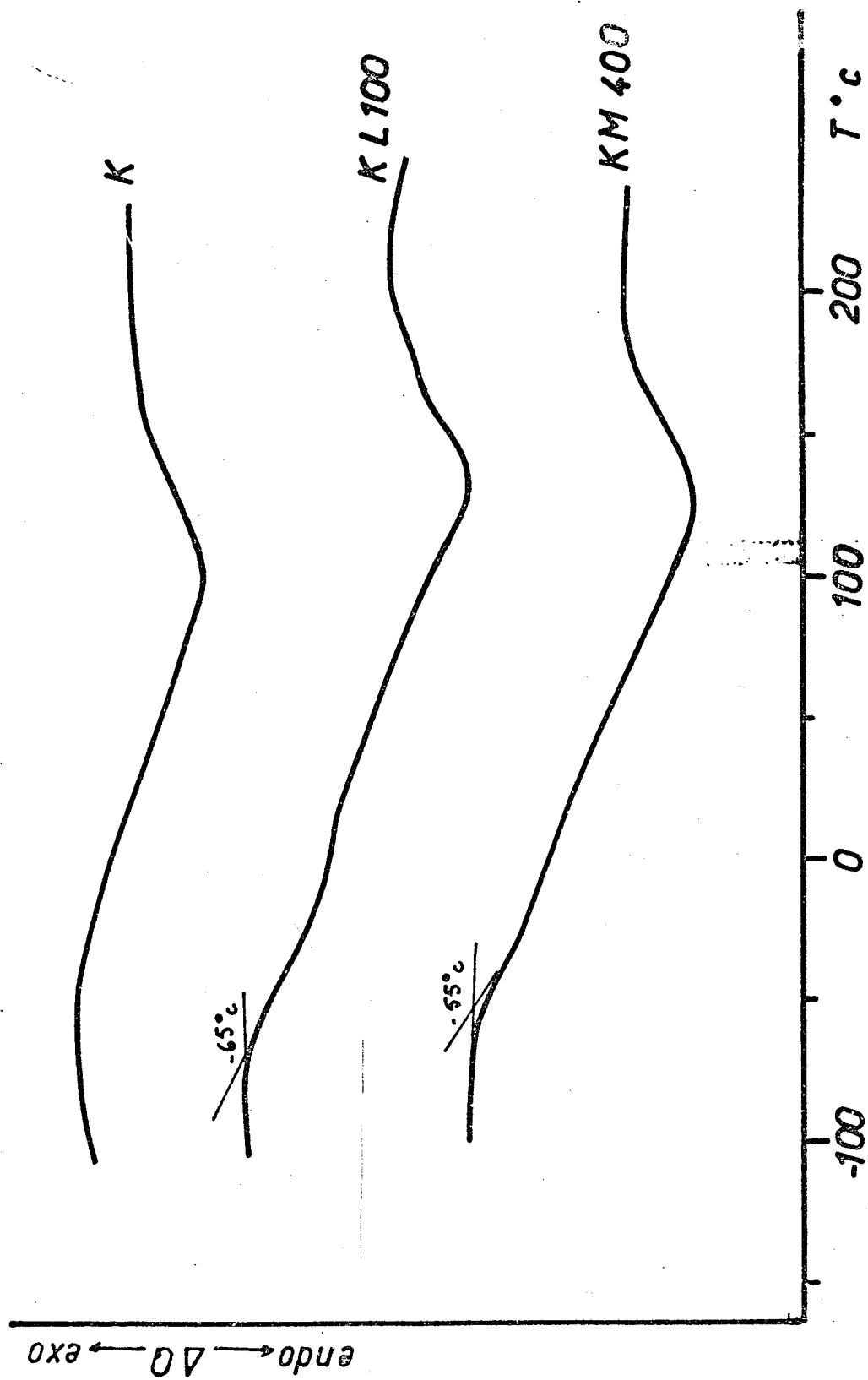with PUR-M400 Matrix

Fig 39 Comparison of the Thermograms For Aramide Fibers
(K49) and Various Composites

Figure 40 shows a comparison of the thermogram patterns for the M400 and L100 dies and the corresponding glass and carbon composites in the vitreous transition range. We see (especially for glass fibers) a less distinct transition which accentuates with higher temperatures. We may assume that this phenomenon is directly related to the type of structure on the reinforcement surface. Actually, in a study conducted in our laboratory, J.P. BAOYOUX [63] examined the influence of the filler/polymer interface on the viscoelastic properties of composite materials (epoxydes filled with glass balls). The author tried to bring to evidence the impact of the reinforcement surface on the dynamic properties and his conclusion was that the relaxation times are modified as a function of the filler treatments. In figure 41, BAYOUX observed that the chain movements are favored when the fillers are covered with silicone and are more disturbed when the ball surface exhibits a greater affinity for the matrix (oiled and nontreated glass).

The chain relaxation may be disturbed by the fillers [64] when these allow attachment points. We actually think that the reinforcement type affects the chain movement so that for a better adhesion, the chains will relax for a longer period of time and the Tg phenomenon will spread over a broader temperature range.

A comparable phenomenon also exists for the melting temperatures of rigid segments. There is a Tf variation for the various composites with the PUR-M400 die. The temperature values decrease in the following manner:

$$T_{PUR-M400} > T_{V-M400} > T_{C-M400} > T_{K-M400}$$

For composites with Kevlar fibers, it is impossible to determine the melting temperatures, owing to the appearance of the thermograms (Figures 37 and 38). The curves show an endothermic zone beginning at about -20°C and spreading to 150°C.

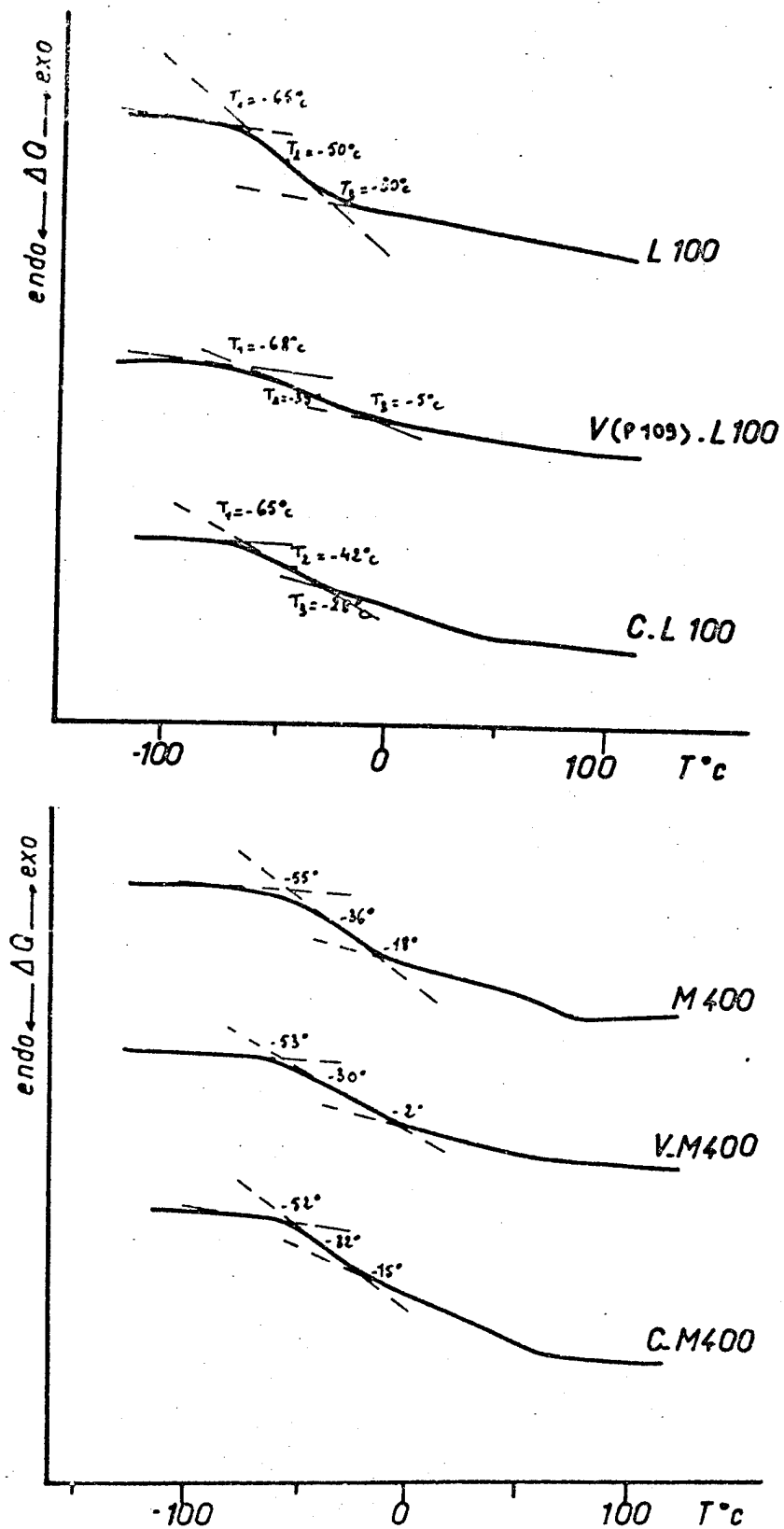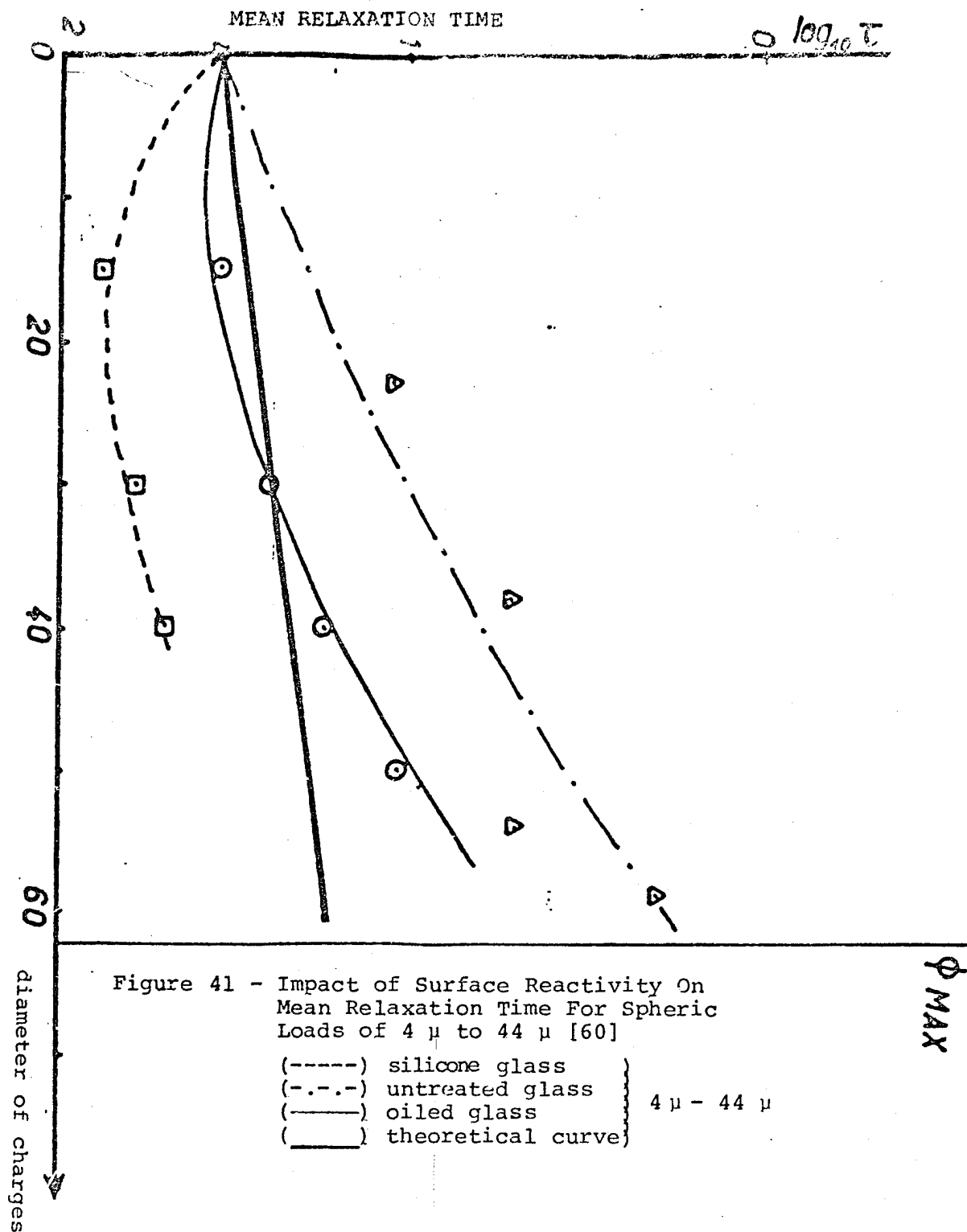We analyzed the fiber used and the corresponding thermogram

93

Figure 40 – Comparison of the Thermograms of Matrices
PUR L100 (a) and PUR M400 (b) With the
Various Corresponding Composites

Figure 41 - Impact of Surface Reactivity On
Mean Relaxation Time For Spheric
Loads of 4 μ to 44 μ [60]

(-----) silicone glass)
(-.-.-) untreated glass)
(———) oiled glass   ) 4 μ - 44 μ
(____) theoretical curve)

MEAN RELAXATION TIME

$log_{10} \tau$

ϕ_{MAX}

diameter of charges

(Figure 39) presents the same endothermic zone that we are not able to explain, and that to our knowledge, is not mentioned in literature.

The CP1 laboratory formulation presents two melting peaks on the thermogram in Figure 36. The first located at about 8-10°C corresponds to the melting of the flexible segmetns of molar weight 2000 (POTM 1), the second located at about 100° (145-155) again corresponds to the melting of the rigid segmetns. Conversely, for the CP2 formulation prepared from POTM2 (see Table 29) with a molar weight $\overline{Mn} \cong 1000$, the melting peak for 10°C does not exist, the flexible phase is completely amorphous which correspond to T >100°C presents two well-defined peaks and which correspond to the melting of the rigid segments of various lengths. This formulation allows us to measure the phase separation rate in the polyurethane die, given the quantities of the basic products. To accomplish this, we used the variation of the calorific capacity Cp at the transition of Tg, perfected in our laboratory by Y. CAMBERLIN [40]. The principle for this was developed in the bibliographic introduction on the PURs. We obtained a phase separation rate of the same order of magnitude, (65% for the die alone and the composite), but with a major error of 20% in the measurement on the composite (the second order transition (figure 42) not being clear in the case of composites).

II-1-2) Results of the Extraction Tests

Before presenting the results, let us mention that each measurement is repeated three times and we give the mean value. The extracted parts are then injected into GPC.

The weight losses of the die part of the composites, after THF extracts part of the polyurethane die, are grouped in Table XXI. We see slight differences according to the type of polyurethane or according to the number of fabric layers (6 or 8 in the case of carbon fabrics). However, the essential differences come from the fiber type. The product losses with glass fabric are about three

times greater than the matrix alone. For carbon fabrics, they are much greater and with Kevlars they reach 90% to 95%. The GPC analysis of soluble fractions virtually always gives the same molar weight distributions corresponding to the polyurethane solubility limit in THF (Figure 43). Further, the distribution curves do not show fractions of low molar weights. The extracts contain neither prepolymers nor diisocyanate or a chain extender which would not have reacted.

TABLE XXI

POLYURETHANE WEIGHT LOSSES IN COMPOSITES AGITATED
DRASTICALLY 48 H IN THF

Reinforcement % by wt. a)	Matrix Without Reinforcement	$V-P109_{(4)}$	$V-A110_{(4)}$	$C_{(6)}$	$C_{(8)}$	$K_{(8)}$
PU-L100 extract	2.2	6.9	4.9	17.4	24.4	96.4
PU-M400 extract	2.3	5.6	/	/	34.4	97.1

a) the figures are calculated in terms of the polyurethane weight present in the composite,

b) the figure in parenthesis denotes the number of fabric layers.

The appearance of the composite samples after extraction leads to the same conclusions. The following statements can be made:

For Kevlar fibers, the fiber folds initially deposited to prepare the composite are found intact,

For carbon composites, the fibers are detached on a few points of the sample,

For glass fibers, the composite keeps its general appearance.
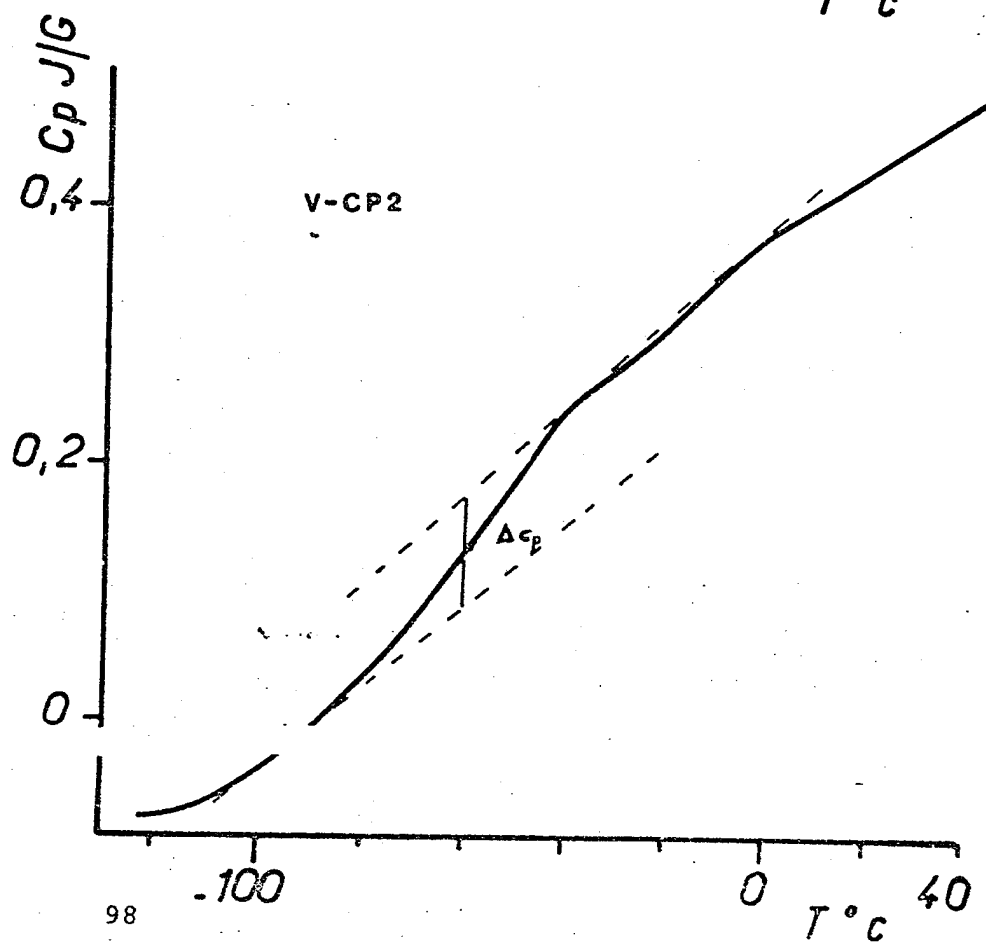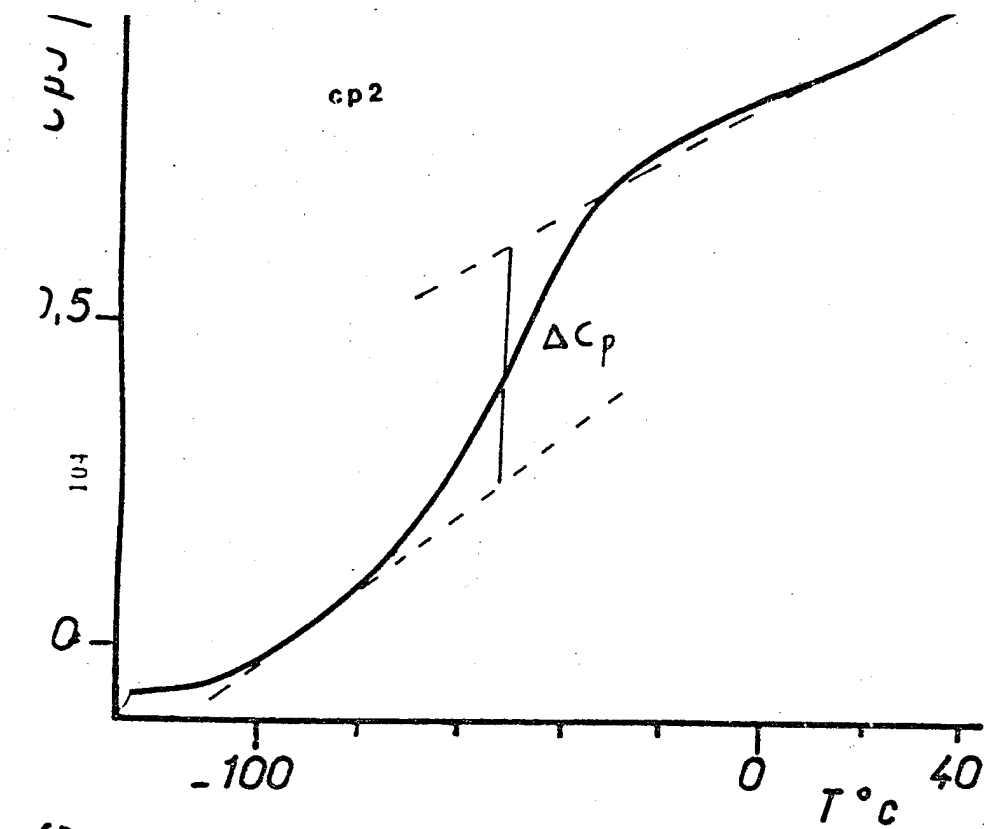
Figure 42 Measurements of ΔC_p for the Polyurethane Matrix, CP2, and the Corresponding Glass Composite, V-CP2
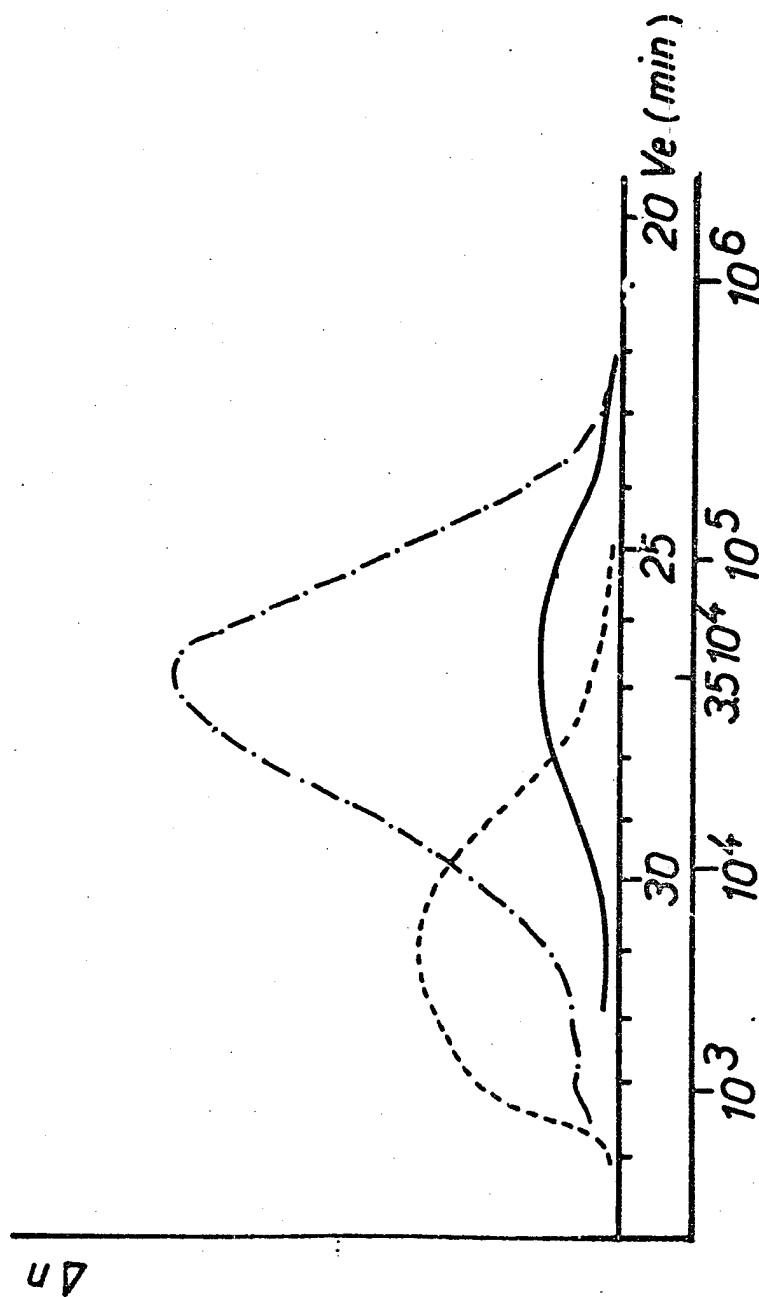
98

Figure 43 – Chromatograms of Polyurethane Matrix Fractions Soluble
In the Solvent, THF: (————) C[6] L100 and; .-.-.)
C[8] M400; (------) basic prepolymer, L100 by comparison.

For each composite, two types of measurements were made:
the first was made on a sample taken from the core of the mater-
ial, and the second on a sample obtained by scratching the fiber
surface. We then analyzed the entire matrix and any modifications
on the fiber surface.

a)   Polyurethane Dies (L100; M400)

Figures 44 and 45 give the IR spectra of the polyurethanes,
L100 and M400. The characteristic bands may be distinguished in
Table XXII.

b)   PUR Composites   /110

We mainly focused our attention on the range between 2000 cm^{-1}
and 1200 cm^{-1} and in particular on the cluster of carbonyl bands
$>C = O$: 1732 cm^{-1} for C = O free urethane, 1705 - 1695 cm^{-1} for $\overset{C}{\underset{O}{\vee}}$
bound urethane and 1650 - 1660 cm^{-1} for C = O urea.

In figure 46, we compare the IR spectra of the composite
V(P109) - M400 taken from the core of the polyurethane die, or
from the glass surface. The a) spectrum of the sample taken in
the composite die essentially differs from that of M400 alone by
a greater percentage of bound urethane $>C = 0$, with respect to
free $>C = 0$, and especially due to the presence of urea $>C = 0$
at 1650 cm^{-1}.

The b) spectrum of the sample taken from the glass surface is
very different from the preceding one. Again, one notes the rela-
tively substantial presence of urea and the total absence of free
urethane $>C = 0$, the band of 1706^{-1} becoming very intense. The
remarkable fact is the very clear appearance of a band of 1395 cm^{-1}
which we ascribed to the isocyanurate cycles [69], and which also
explains the large increase in the 1706 cm^{-1} band; this being due

TABLE XXII

TYPICAL IR ABSORPTION BANDS FOR PUR-L100 AND PUR M-400 POLYURETHANES

Wave Number cm^{-1}	Band Absorption
PUR L100	
3300	Bound N-H
1730	Free C = 0 → urethane
1719	Bound C = 0 → urethane
1638	C = 0 → urea
1602 1574 1534	C = C → aromatic core
1224	$\underset{O}{C} - O - C$ → urethane
1100	C - O - C → POTM
PUR M400	
3350	Free N-H
3325	Bound N-H
1732	Free C=0 → urethane
1700	Bound C=0 → urethane
1596 1547 1511	C = C → aromatic core
1223	$\underset{O}{C} - O - C$ → urethane
1112	C - O - C → POTM

to the superposition of bound urethane $\geq C = 0$ and ioscyanurate $\geq C = 0$. Finally, note that the bands of the (POTM) segments are fine if we compare them to the same bands shown in the die alone (i.e. of 1080 cm^{-1} and 1110 cm^{-1}) and of low intensity. This would lead one to believe that there is a degree of order in the polyether chain segments and a lack of these segments on the fiber surface.
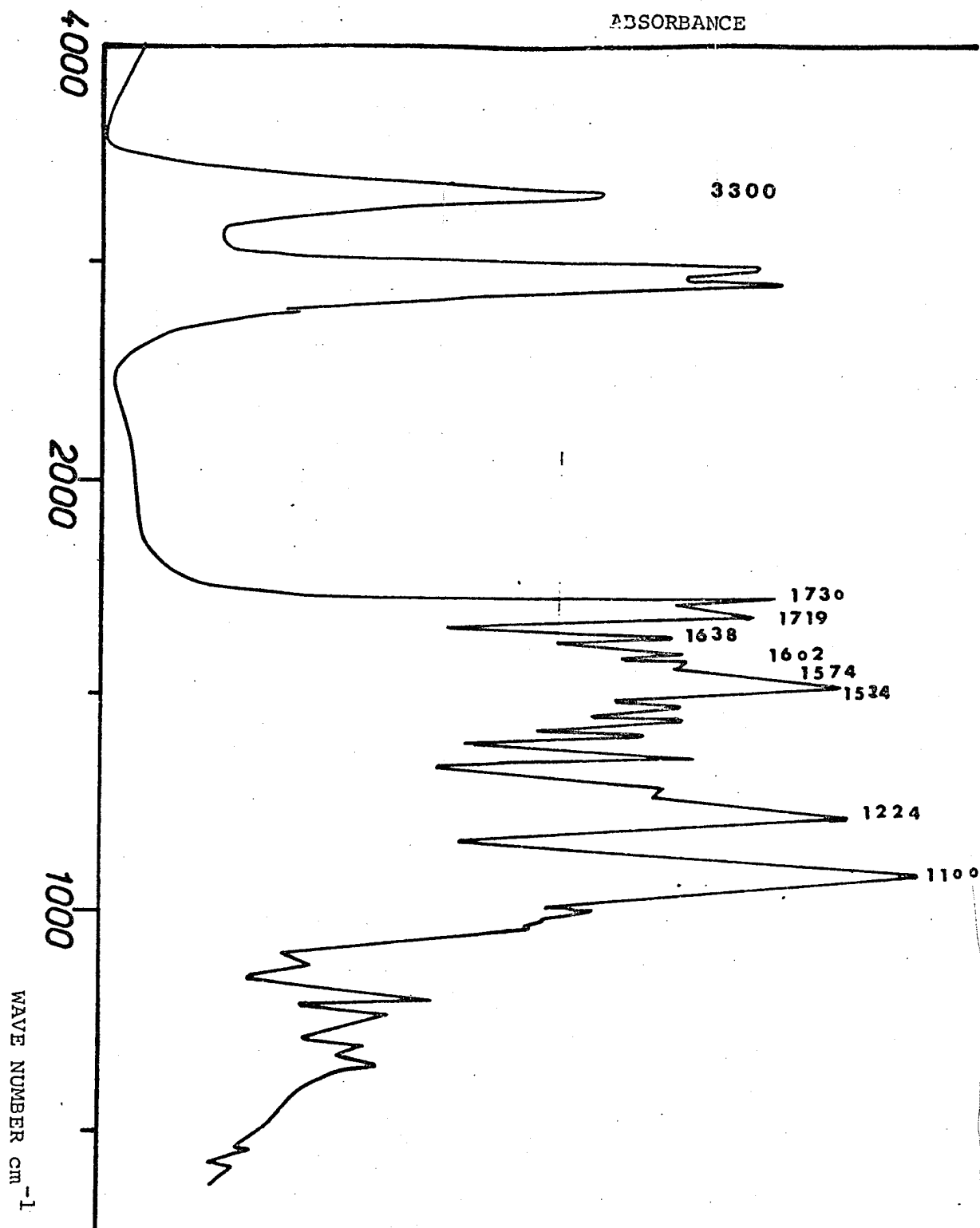
Figure 44 - IR Spectrum of the Polyurethane Matrix
L100 Alone (Accumulation)

102
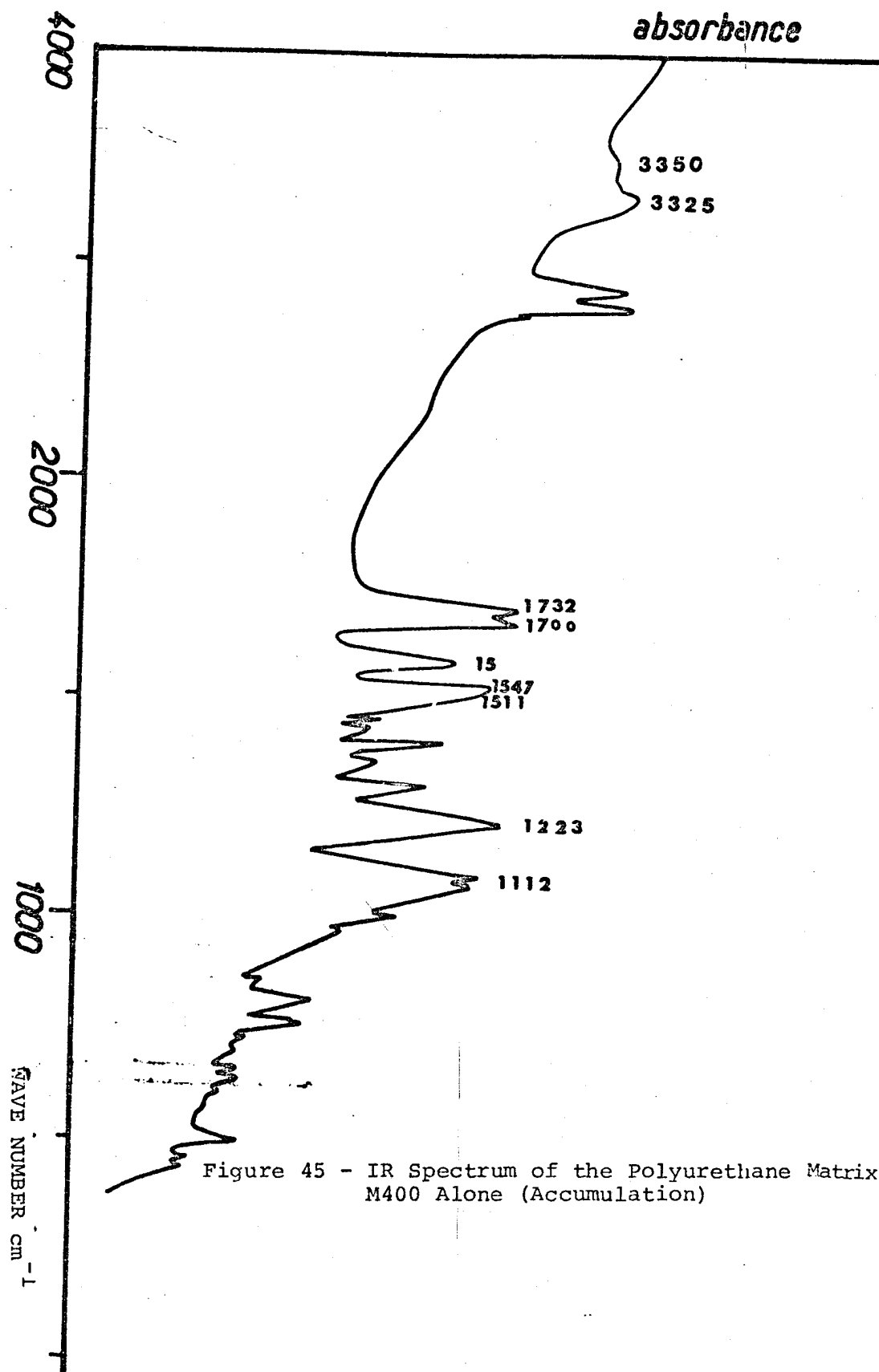
Figure 45 - IR Spectrum of the Polyurethane Matrix
M400 Alone (Accumulation)

On the spectra in Figure 48 for composite C-L100, the bands due to urea $\geq C = 0$ at about 1650 cm^{-1} seem much smaller than in the V-L100 composite if we compare them respectively to the urethane bands $\geq C = 0$.

The bound and free urethane $\geq C = 0$ bands are inadequately /114 separated in C-L100 (Figure 48) as if there were a wide range in the forces of the hydrogen bond: they separated better for V-L100 (Figure 49), the bound band being displaced to 1690 cm^{-1}. The N-H band at 3330 cm^{-1} is the same size in both cases (V-L100 and C-L100), but the maximum is more pointed for V-L100 (3330 cm^{-1}) whereas it is flatter (wider band) for C-L100 passing from 3320 to 3420 cm^{-1}.

Finally, to conclude this description of results, the extracts of fractions soluble in THF were generally analyzed. The IR spectra are comparable to those obtained for the matrix.

DISCUSSION AND CONCLUSION

/116

1 - Extractions using the solvent, THF, show that the polyurethane dies of composites with carbon fabrics or Kevlar fabrics are made up of an unusually high percentage of soluble macromolecules of very high molar weight ($\overline{Mn} > 30,000$).

This is confirmed by the IR spectra. In the case of C-L100, for example, we may distinguish on the IR spectrum of the polymer, urea bonds due to the elongation of the macromolecular chains of the urethane bonds of the basic prepolymer. Further, these urea bonds are in lower percentages than for a urea polyurethane L100 prepared in the absence of fabrics. Conversely, the band (N-H) is large and complex, certainly because of the presence of NH$_2$ chain endings:
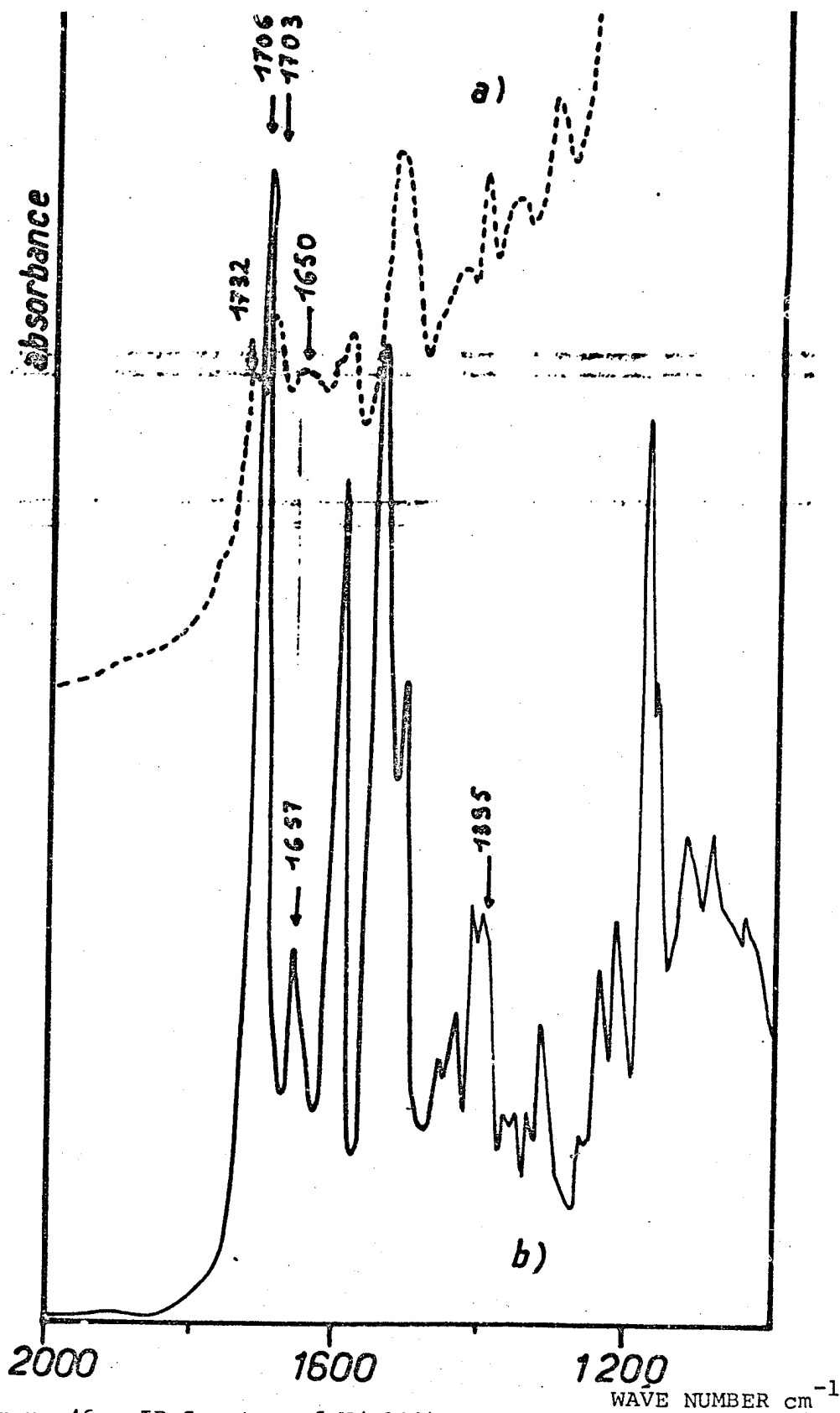

104
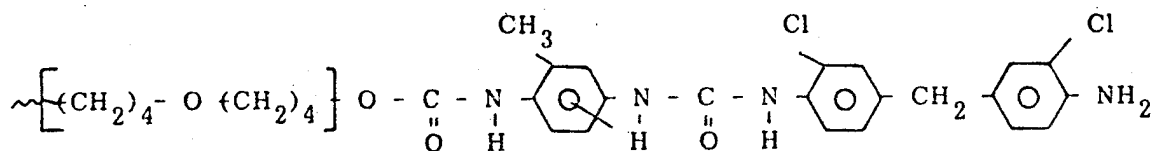
Figure 46 - IR Spectra of V(P109)-M400 Composite
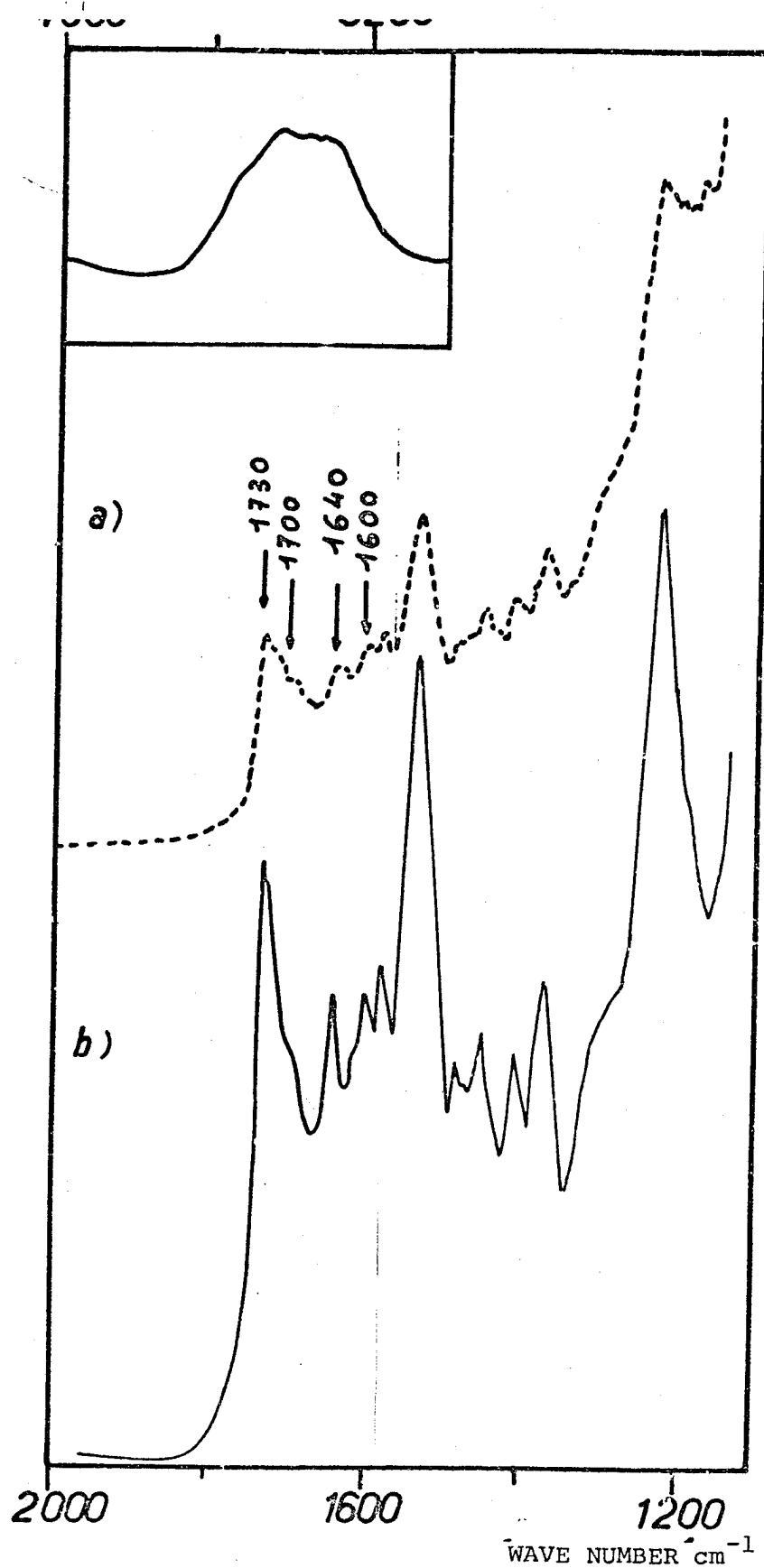a) At Core; b) On Fiber Surface

Figure 48 —IR SPectra of C-L100 Composites
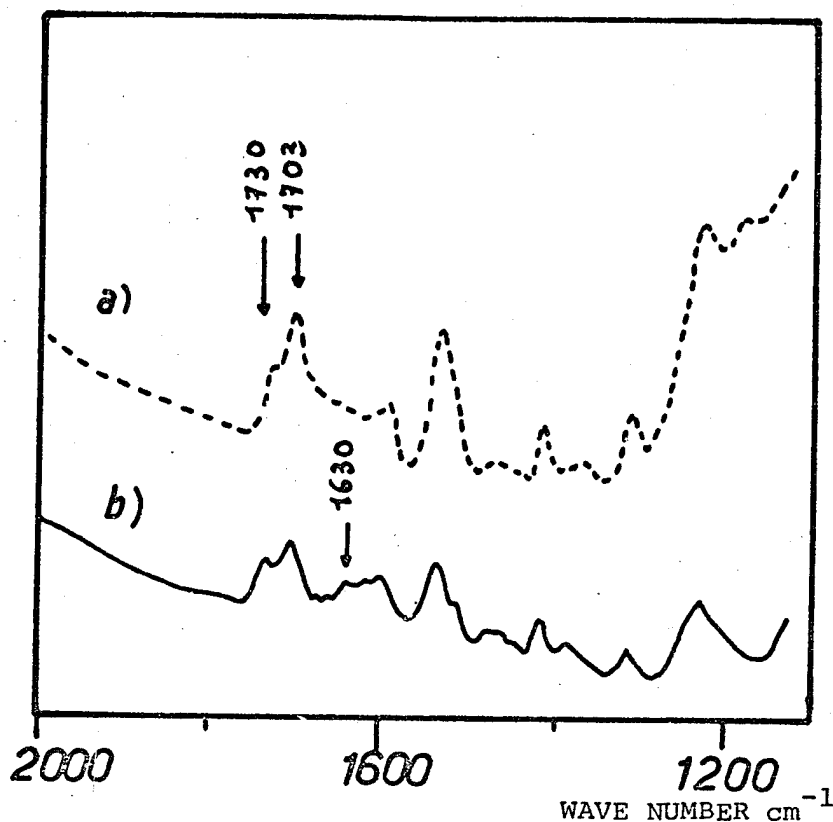a) At Core; b) On Fiber Surface

Figure 47 - IR Spectra of C-M400 Composite
a) At Core; b) On Fiber Surface

The macromolecule functions have difficulty in reacting at the end of the reaction due to the presence of fabric layers. This would explain: the lower molar weight distributions, the absence of urea functions and the persistance of amine functions when the chain extender is Moca. For carbon fabrics, the extract concentration increases when there is an increase from 6 to 8 layers. However, one does not observe any noticeable difference between the structure of the die at its core or on the fiber surface.

2 - The presence of a Kevlar fiber fabric has a catastrophic effect on the advancement of the polycondensation reaction. In addition to the steric and dilution obstacle of the reactive functions, due to the presence of fabrics, we may elicit to explain this result, the polar nature of the Kevlar molecule capable of complexing the alcohol and isocyanate functions and thus blocking the chemical reaction.
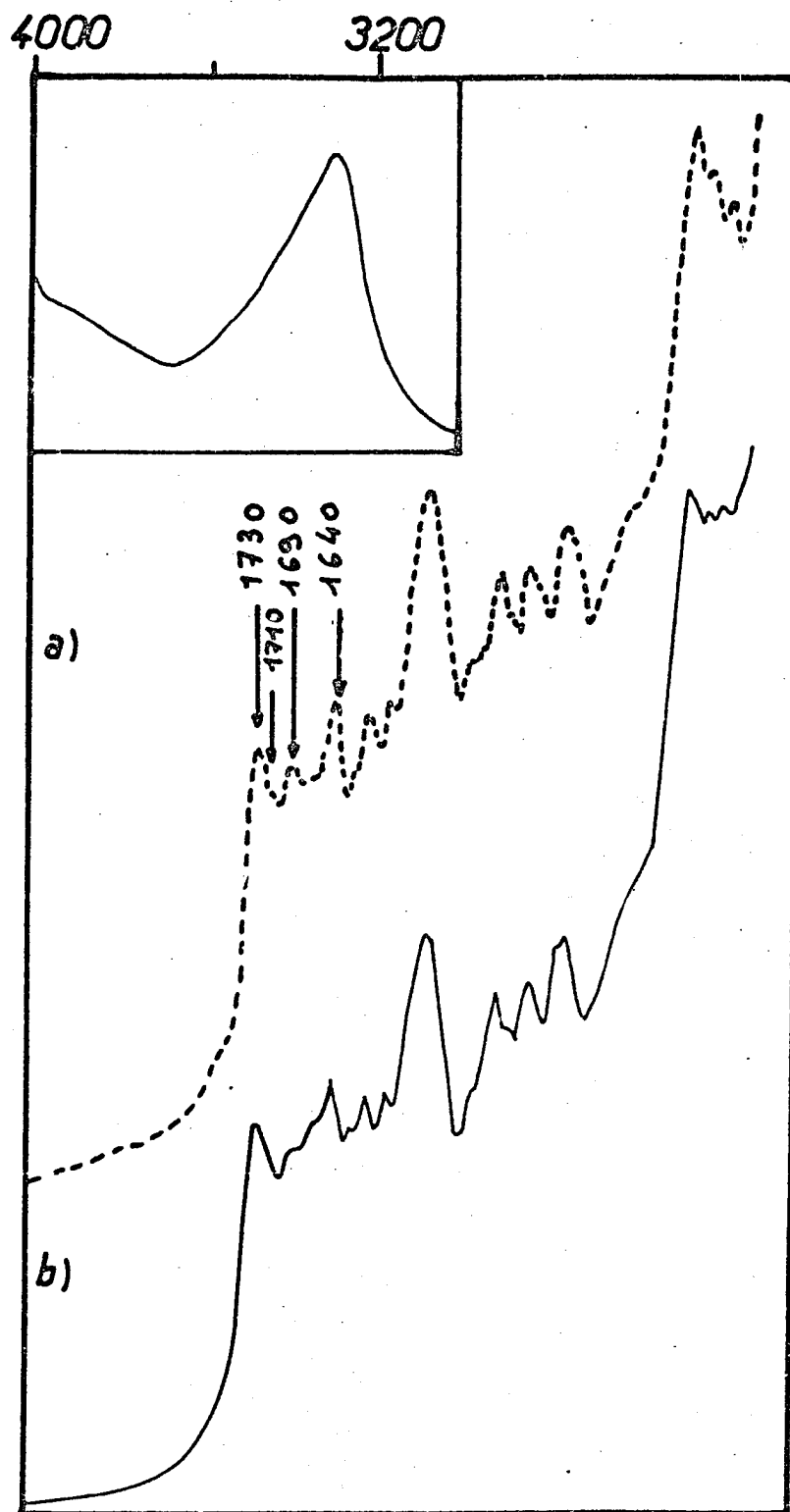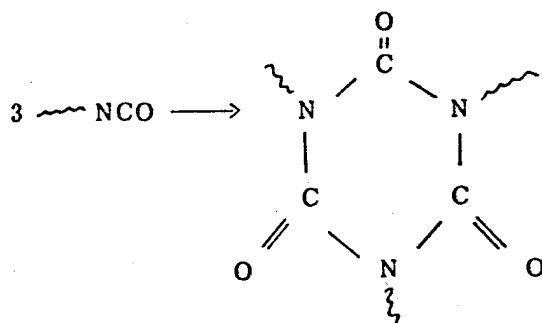
106

Figure 49 - IR Spectra of V(P109)-L100 Composite
a) At Core; b) On Fiber Surface

3 - Glass fibers give a completely different result. It is
well-known that the water molecules are always on the surface of
glass [66]. These molecules are not inert with respect to the
isocyanate functions. They react, thus producing amine functions /117
capable of reacting in turn to produce urea bonds (these bonds may
be obtained by reaction with a higher number of urea bonds in
V-L100 than in C-100). This mechanism may also explain the presence
of urea bonds in V-M400 which logically should only have urethane
bonds. These urea bonds are also found on the reinforcement surface
at the matrix core. The reactivity of the glass surface would elimin-
at the negative effects caused by the presence of fabric layers,
as we have already seen.

The V-M400 composite also has another special feature of having
very different polyurethane molecules on the fiber surface than the
rest of the matrix. The basic nature of glass may explain the forma-
tion of isocyanurate cycles:

$$
3 \; \text{---NCO} \longrightarrow
\begin{array}{c}
O \\
\| \\
C \\
N \quad\quad N \\
| \quad\quad\quad | \\
C \quad\quad C \\
O \quad\quad N \quad\quad O
\end{array}
$$

In the presence of a basic catalyst, these cycles are easier
to obtain with MID than with TDI [67]. They reinforce the poly-
urethane matrix on the fiber surface.

Finally, the lack of polyoxytetramethylene (POTM) segments
may be explained by the segregation of MDI-Bd 1,4 segments on the
fiber surface as this was observed on the cold walls of a mold
when using this type of polyurethane via the RIM process [68].
The (-NCO) + amine reaction is much quicker than the (-NCO) +
alcohol reaction and this will not be observed with the L100 formu-
lation.

4 - The differential thermal analysis curves show only one second order transition corresponding to the relaxation of the flexible segments. There is virtually no change with the introduction of fibers. However, for glass fibers, this transition increased the temperature. From this, we could conclude that in the presence of glass fibers, the polyurethane matrix has a great affinity for the reinforcement, whereas in the case of carbon or /118 Kevlar, the melting temperature Tf of the rigid segments decreases. This may be due to the difficulty of the molecules to elongate and form rigid segments of corresponding length.

Further, the calorimetric measurements indicate the degree of phase separation between the flexible segments and the rigid segments, which would not be modified in the composite. Yet, this measurement is not very accurate in the case of the composite and it is an overall value. This method cannot be used to measure what is happening on the reinforcement surface.

5 - Before going on to the next chapter, let us mention within the same context the results of the adhesion measurements performed by BOMO on the elastomer-fiber composites [62], essentially, the PUR-100 matrix in the presence of glass fibers, R(P109) and A1100) and carbon fibers, T300 (HT) (Table XXIII).

TABLE XXIII

RESULTS OF THE FIBER-MATRIX ADHESION [62]

Polyurethane Composite With L100 Matrix	Pure R Glass	R-A1100 Glass	RP109 Glass	T300 Carbon
:(Pa) Rupture Strength of Fiber	$3.16.10^9$	$3.16.10^9$	$3.4.10^9$	$1.48 - 2.27.10^9$
T (Pa) Shearing Strength of Fiber	$3.3.10^7$	$4.1.10^7$	$7.0.10^7$	$2.19 - 2.25.10^7$

*If the carbon fiber is brittle, the two values given pertain to the low and high part respectively.

The concave part is subjected to a compressive stress (C), whereas the convex part is subjected to a tensile stress (T). The tensile and compressive forces occur on either side of a neutral axis in the middle of the sample, so that they create a bending moment (M) at the curvature radius R. We thus determine the bending rigidity by $M \cdot = (\frac{I}{R}) = MR$. The moment M is associated with the modulus of elasticity of the material by the following equation:

MR = EI where E: modulus of elasticity

I: moment of inertia with respect to the section.

For a material with rectangular section, I is defined by:

$$I = \frac{bh^3}{12}$$ where b and h are the width and thickness of the sample, which allow us to express the bending rigidity:

$$EI = \frac{Ebh^3}{12}$$

The bending rigidity is often determined by deflection measurements (δ) on a material using the formula giving the bending of the material with a load applied to the center:

$$\delta = \frac{F}{48\ EI} I^3$$ where F: charge

I: distance between supports

δ: deflection

The bending rigidity becomes:

$$EI = \frac{F}{48\ \delta} I^3$$ which gives for the E modulus the following value (by replacing I with its value):

$$EI = \frac{F}{4bh^3\ \delta} I^3$$ where the ratio ($\frac{I}{h}$) denoted (ε) as well as

112

deflection δ are the main factors used in determining E.

We also find in literature the equation giving the total deflection δ_T as a function of the longitidunal modules E_1, of the interlaminary shearing modulus G_{12} and the ratio $\frac{I}{h} = \epsilon$.

$$\delta_T = \frac{F}{4\,b\,E_1}\,\epsilon^3 \left[1 + (\frac{3}{2})(\frac{E_1}{G_{12}})(\frac{1}{\epsilon^2})\right] \quad \text{(73)} \qquad (1)$$

By rearranging this equation, the following equation is ob-   /122
tained for the longitudinal modulus determined for bending:

$$E_1 = \frac{F}{4\,b\,\delta_T}\,\epsilon^3 \left[1 + (\frac{3}{2})(\frac{E_1}{G_{12}})(\frac{1}{\epsilon^2})\right] \qquad (2)$$

Generally, the first term of the equation (2) is used to calculate the bending modulus E_1, while disregarding the inter-laminary shear which results in an apparent value of the modulus: E_{app}.

This may be justified if for a given $\frac{E_1}{G_{12}}$ value the ratio ($\frac{I}{h} = \epsilon$) is high enough. In this case, we may express for the equation

$$E \neq \frac{F\,\epsilon^3}{4\,b\,\delta_T} \qquad (3)$$

CHAMBERS and McGARRY [71] tested three types of polyester composites on 3 bending points varying ϵ from 7 to 70. Their results (Figure 51) show the considerable influence of the shearing modulus for the various values of ϵ. On the other hand, for high ϵ values ($\epsilon \geq 30$) the effect of G_{12} may be negligible.
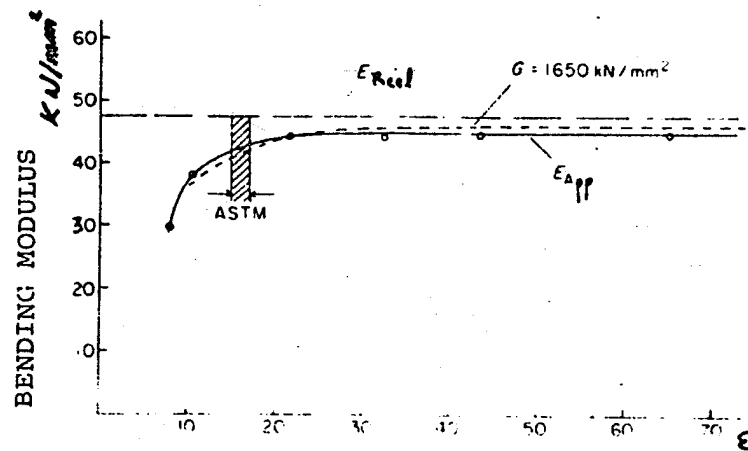
113

Figure 51 - Apparent Bending Modulus E_{app}
on 3 points as a function of ε for glass
fiber polyesters. For a better agreement
with the experimental values, modulus G
has a value of 1650 KN/mm^2 (broken-line curve).

Furthermore, FISHCER et al [70] tested several types of comp- /123
osite materials and plotted the variations of the ratio $\frac{E_{app}}{E_1}$ as a
function of ε and of the ratio $\frac{E_1}{G_{12}}$. Their results shown in Figure
52 indicate that for a fairly high ε value, the real modulus
E_1 can be determined using equation (3) in which the interlaminary
shearing effect may be disregarded.
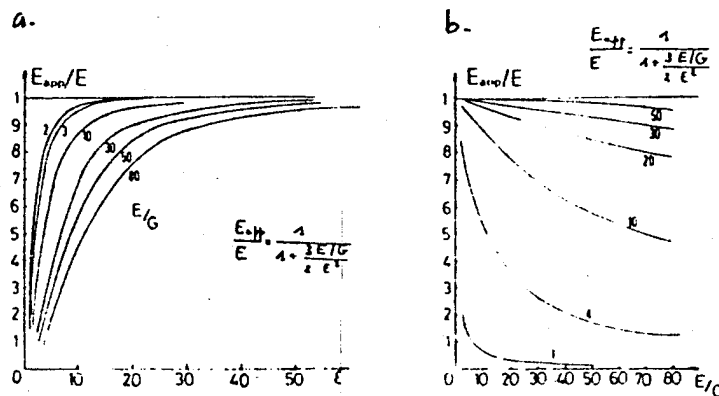
Figure 52 - a) Apparent Modulus E_{app}. as a function of ε.
b) Apparent Modulus E_{app}. as a function of
the ratio $\frac{E}{G}$.

In regard to our composites, the 3-point bending tests are conducted with a high ε value ($l = 50$ mm, $h \cong 1$ mm $\rightarrow \varepsilon = \frac{l}{h} \cong 50$). Consequently, our measurements can give us serious information on the moduluses of the composites we prepared.

II-2-2) Experimental Values of Moduluses As a Function of the Temperature

Figure 53 shows a comparison of the moduluses obtained for the various composites. A few experimental points are shown in Table XXIV. Measurements $E_{\theta=0°}$ were not performed for Kevlar for technical reasons. Actually, it is very hard to cut out composite samples along the fiber direction ($\theta=0$). In all cases we have threads which stick out and deform the sample we want to measure. In Figure 54, we compare the glass composites (P109) /124 for various dies (L00, M400 and CP2). A few experimental points are grouped in Table XXV. Figure 55 shows a comparison of two types of oiling for the composite V-100.

TABLE XXIV

COMPARISON OF THE BENDING MECHANICAL PROPERTIES FOR V*-L100 COMPOSITES: C-L100 AND K-L100

Température (°C±2)	Bending Moduluses				
	$E_1(\theta = 0°)$ (Pa)		$E_2(\theta = 90°)$ (Pa)		
	V*-L100		C-L100		K-L100
- 70	$4.2.10^{10}$	$6.4.10^9$	$8.6.10^{10}$	$5.7.10^9$	$5.0.10^9$
- 42	3.1	3.3	6.8	1.8	$5.3.10^8$
- 22	3.0	2.1	6.5	1.0	3.9
+ 20	2.1	1.9	4.4	$9.9.10^8$	2.1
38	2.6	2.0	3.2	8.1	2.6
67	2.6	1.6	4.5	6.3	2.5
92	2.4	1.6	3.8	4.7	2.0
112	2.0	2.3	5.6	7.9	1.3
128	2.1	2.0	4.7	6.7	1.1
135	2.2	1.9	4.2	6.4	
142	2.0	2.0	3.3	6.3	
152	1.5	1.9	4.0	5.4	

*P109 oil is used.

115

TABLE XXV

MECHANICAL PROPERTIES UNDER BENDING STRESSES FOR VARIOUS PUR-P109 GLASS FIBER COMPOSITES - A FEW EXPERIMENTAL POINTS

Temperature ($^{\circ}$C ± 2)	Bending Moduluses					
	E_1 (Pa)				E_2 (Pa)	
	V-L100		V-M400		V-CP2	
- 70	$4.2.10^{10}$	$6.4.10^{9}$	$3.2.10^{10}$	$9.0.10^{9}$	$7.3.10^{10}$	$1.1.10^{10}$
- 42	3.1	3.3	3.1	5.3	6.8	$5.0.10^{9}$
- 22	3.0	2.1	2.6	3.4	6.5	3.6
20	2.1	1.9	2.1	1.4	4.3	2.6
38	2.6	2.0	1.6	1.8	3.2	2.5
67	2.4	1.6	1.3	1.7	3.4	2.0
92	2.4	1.6	1.3	$9.3.10^{8}$	3.6	2.0
112	2.0	2.3	1.4	$1.3.10^{9}$	3.5	1.6
128	2.1	2.0	1.3	1.0	3.1	1.7
135	2.2	1.9	1.1	1.1	3.1	1.1
142	2.0	2.0	1.0	1.2	1.0	$5.1.10^{8}$
152	1.5	1.9	$8.7.10^{9}$	1.0		

The following observations may be made:

The first drop in modulus (E), in terms of low temperatures, corresponds to the vitreous transition of the die,

A relatively large rubber plateau, followed by the second drop in the modulus which corresponds to the flow of the polyurethane matrix,

The modulus values which vary as follows:

$$E_{PUR\ matrix} < E_{\theta=90^{\circ}} < E_{\theta=0^{\circ}}$$

Further, they are slightly higher for (A1100) oiling than for (P109) oiling (Figure 55).

The temperature behavior for the V(P109)-CP2 composite is not as

116
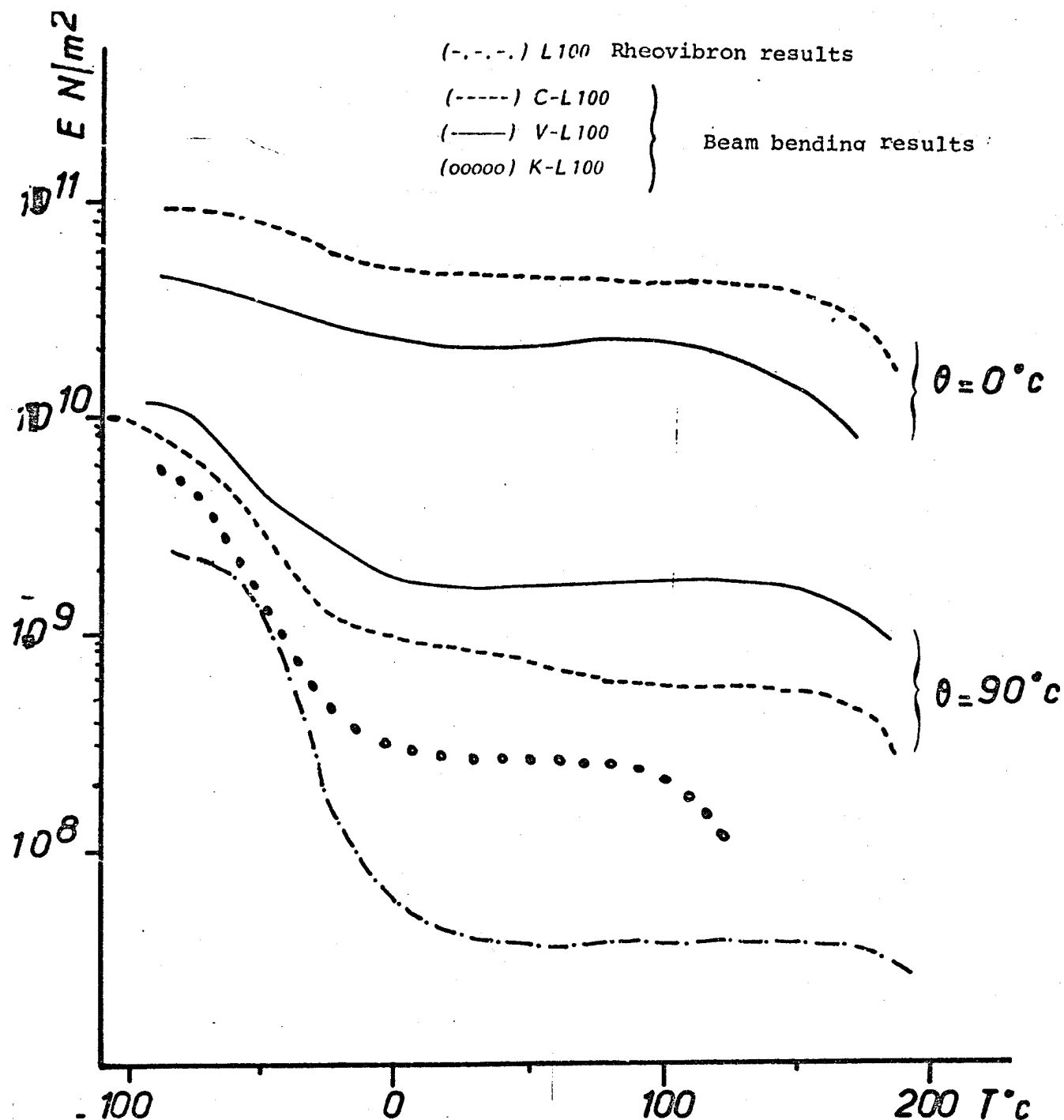
Figure 53 - Variation of the E_1 and E_2 moduluses as a function of the temperature determined by beam bending on 3 points for the composites V-L100, C-L100 and K-L100 as well as the E modulus of the matrix determined with Rheovibron.
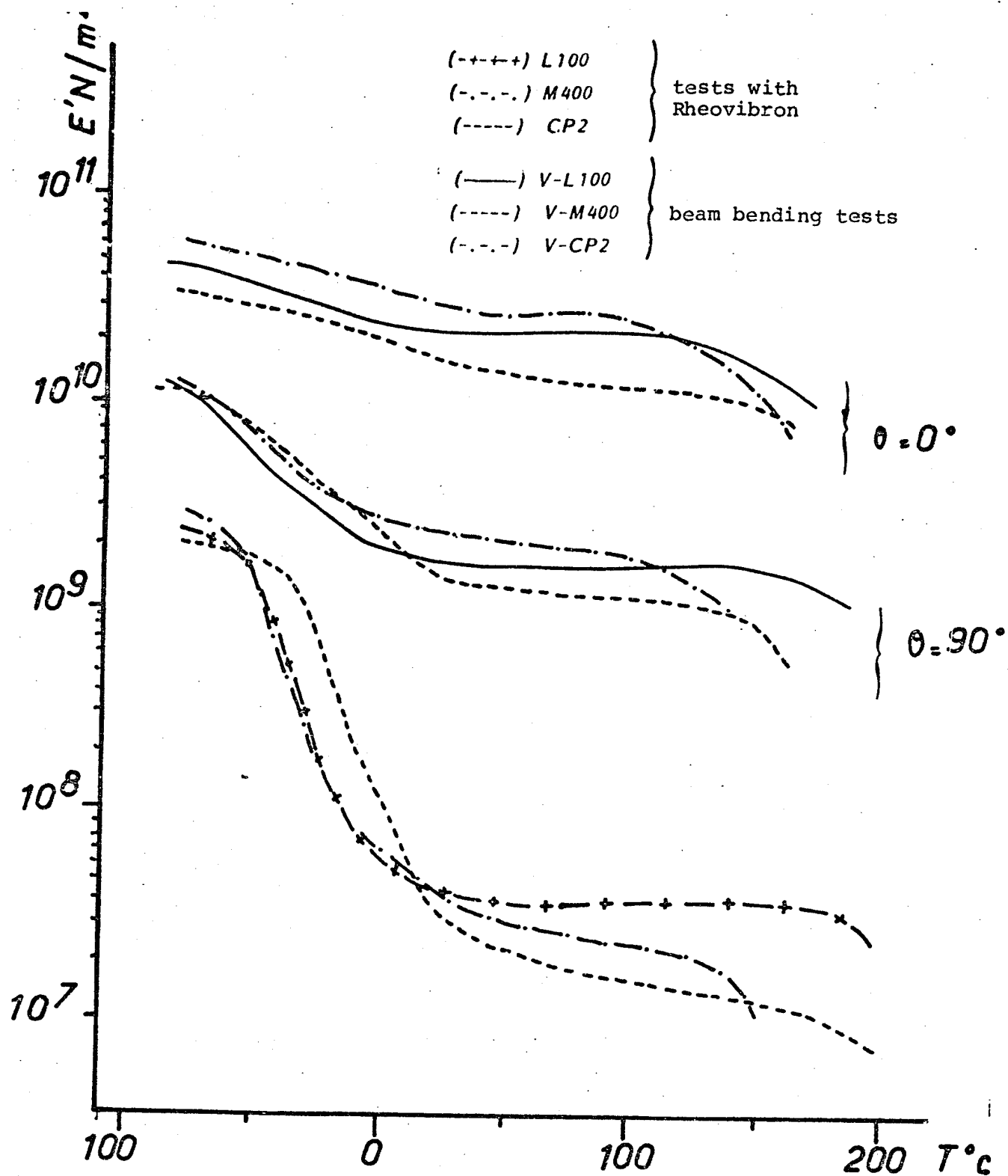
Figure 54 - Variation of the E_1 and E_2 moduluses as a function of the temperature of composites V-L100 and V-M400 and V-CP2 (P109 oiling) under beam bending on 3 points, as well as the corresponding matrix, measured with Rheovibron.
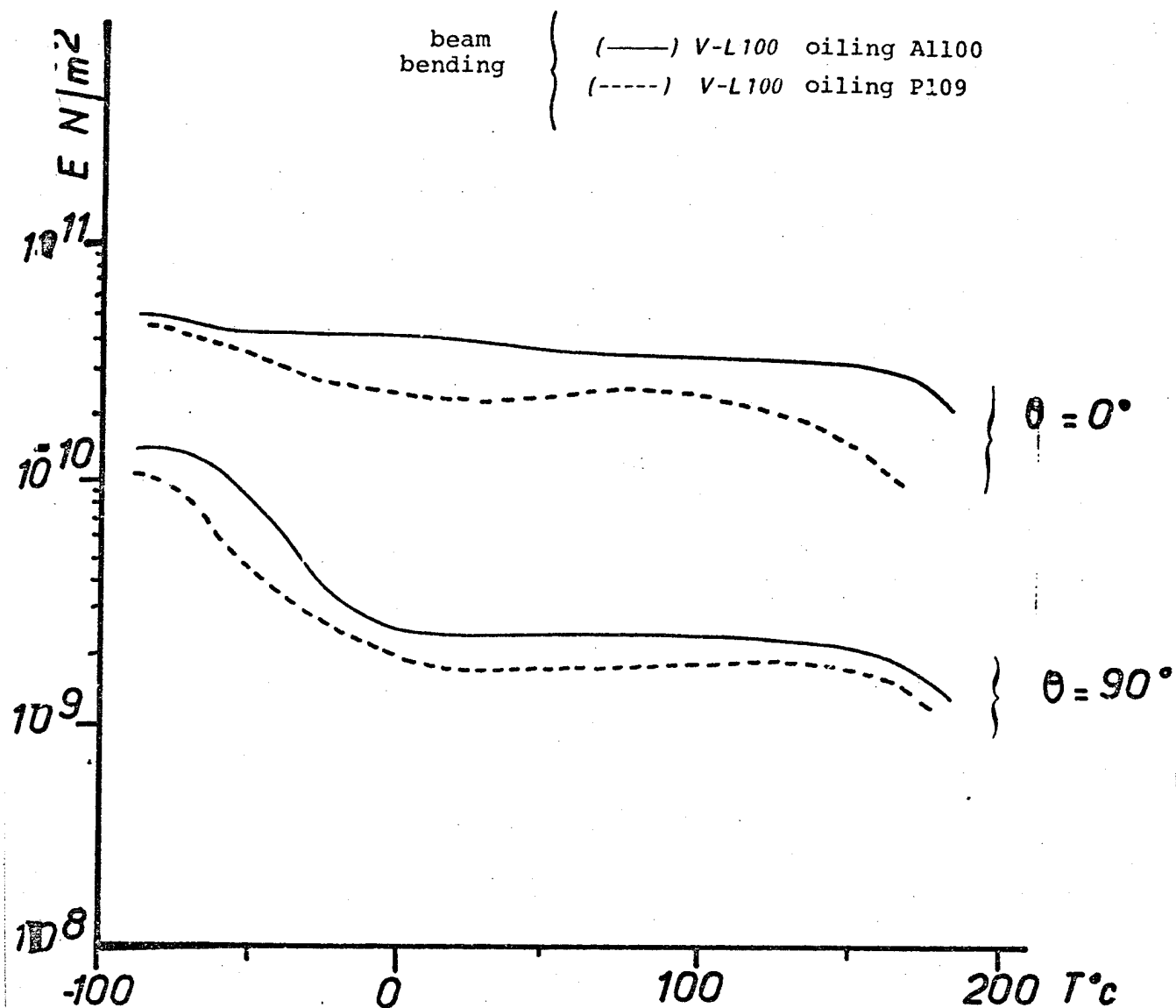
118

Figure 55 - Variation of the E_1 and E_2 moduluses as a function of the temperature for the composite V-L100. Comparison between the two types of oiling.

good as for other glass composites (P109) (Figure 54). The creep temperature of the die, CP2, ($\cong$ 120°C) is quite a bit lower than for the V-M400 formulations ($\cong$150°C) or V-L100 ($\cong$160°C). Further, the vitreous transition temperature is the lowest in composite V-L100.

In conclusion, we may essentially point out the influence of the reinforcement type on the static mechanical properties of the composite.

For samples cut out in the fiber direction (θ= 0°), the bending test stresses mainly the fibers. The modulus values obtained in the C-L100 composites are higher than the moduluses of composite V-L100. This comes from the fact that carbon fibers have a higher longitudinal modulus of elasticity than glass fibers (Table XXIV).

In contrast, for samples cut out perpendicularly to the fibers   /129 (θ=90°), it is the die which is essentially stressed by the bending test. In this case the modulus values decrease from the glass composite to the Kevlar composite (Table XXIV).

$$E_{\theta=90°}(K-L100) < E_{\theta=90°}(C-L100) < E_{\theta=90°}(V-L100)$$

This results, as well as the behavioral difference at high temperatures observed in this case, makes us conclude that the polyurethane L100 matrix preserves its elastomer properties more in the presence of glass fibers than in the presence of carbon or aramide fibers.

Furthermore, the bending tests give us information on the die-fiber adhesion and we will refer to this information in the following chapters.

120

II-2-3 - Recorded Curves

Figure 56 shows the appearance of the curves recorded during a 3-point bending test. They provide information on the behavior of composite materials. We may therefore determine the modulus, stress and defelction measurements, which are therefore the characteristics specific to the tested material (see experimental part in the appendix).
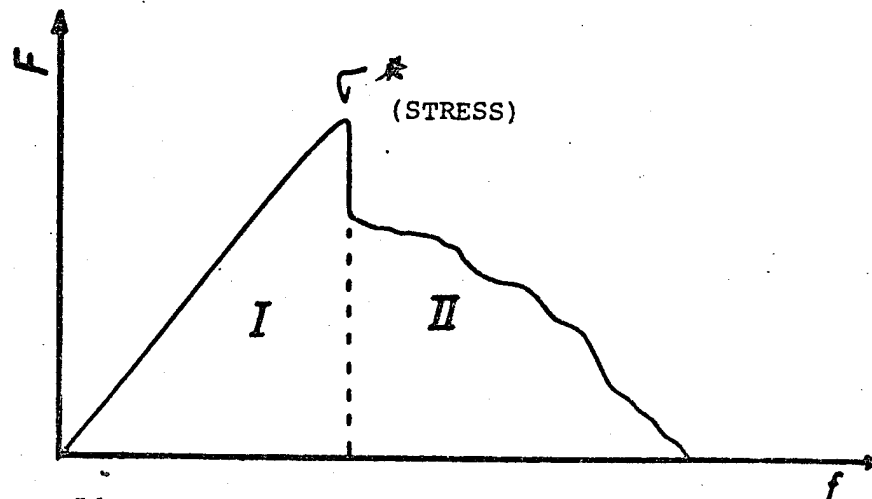

Figure 56 - Appearance of the curves recorded during the
3-point bending tests.
I - rupture or main decohesion area,
II - rupture propagation area
*this is either a rupture stress (in the case of a total rupture of the material) or a maximum stress for a given deflection.

Figures 56 and 57 show the curves recorded at temperatures /130 below the vitreous transition temperature of the die for the composites, V-L100 and C-L100. We were thus able to calculate these various properties at a temperature of -75°C, for samples cut out according to the angle θ = 90°, or θ = 0°. The results are shown in Table XXVI. The values for the composite, K-L100, are determined alone in the case where θ = 90°.

121

TABLE XXVI

MECHANICAL PROPERTIES DETERMINED UNDER BENDING CONDITIONS AT A TEMPERATURE OF −75°C FOR VARIOUS COMPOSITES WITH MATRIX L100

Composite	samples cut along 90° angle		samples cut along 0° angle	
	σ_m (Pa)[a]	δ (mm)	σ_r (Pa)	δ (mm)
V(RP109)-L100	$1.8 \cdot 10^8$	12.5	$1.0 \cdot 10^9$	17.5
V(A1100)-L100	$1.6 \cdot 10^8$	11.0	$9.9 \cdot 10^8$	16.4
C-L100	$1.2 \cdot 10^8$	10.3	$1.3 \cdot 10^9$	6.6
K-L100	$5.0 \cdot 10^7$	9.1	--	-

a) α_m = maximum stress

Case where the matrix is essentially stressed ($\theta=90°$). There is a decrease in the maximum stress σ_m by switching from glass fibers to Kevlar fibers, as well as a corresponding deflection decrease. In the curve recorded (Figure 56) there is a sudden and clean break, for C-L100, whereas in the case of V-L100 there are successive delaminations without sudden break.

Case where the fibers are essentially stressed ($\theta=0°$). The results show a better rupture stress in the case of carbon composites than for glass composites, whereas the deflection recorded is lower. The corresponding curves (Figure 56) show a total break in the sample in the presence of carbon fibers, whereas in the presence of glass fibers the rupture is not complete.

Examination of the rupture surface in the microscope becomes interesting at this point, because one can observe the nature of the rupture observed at the fiber-die interface. Actually, the fiber-matrix interface plays a fundamental role in transferring the stress. The bond between the fiber and the matrix must therefore be perfect or at least as close as possible to a perfect bond to obtain optimal composite properties [72]. To study the interfacial bond between the matrix and the fiber, the composite is subjected to

Figure 56 - Curves recorded under bending conditions at T = - 75°C (Tg = -65°C for the matrix with L100) giving the transverse modulus E_2 (θ=90°)
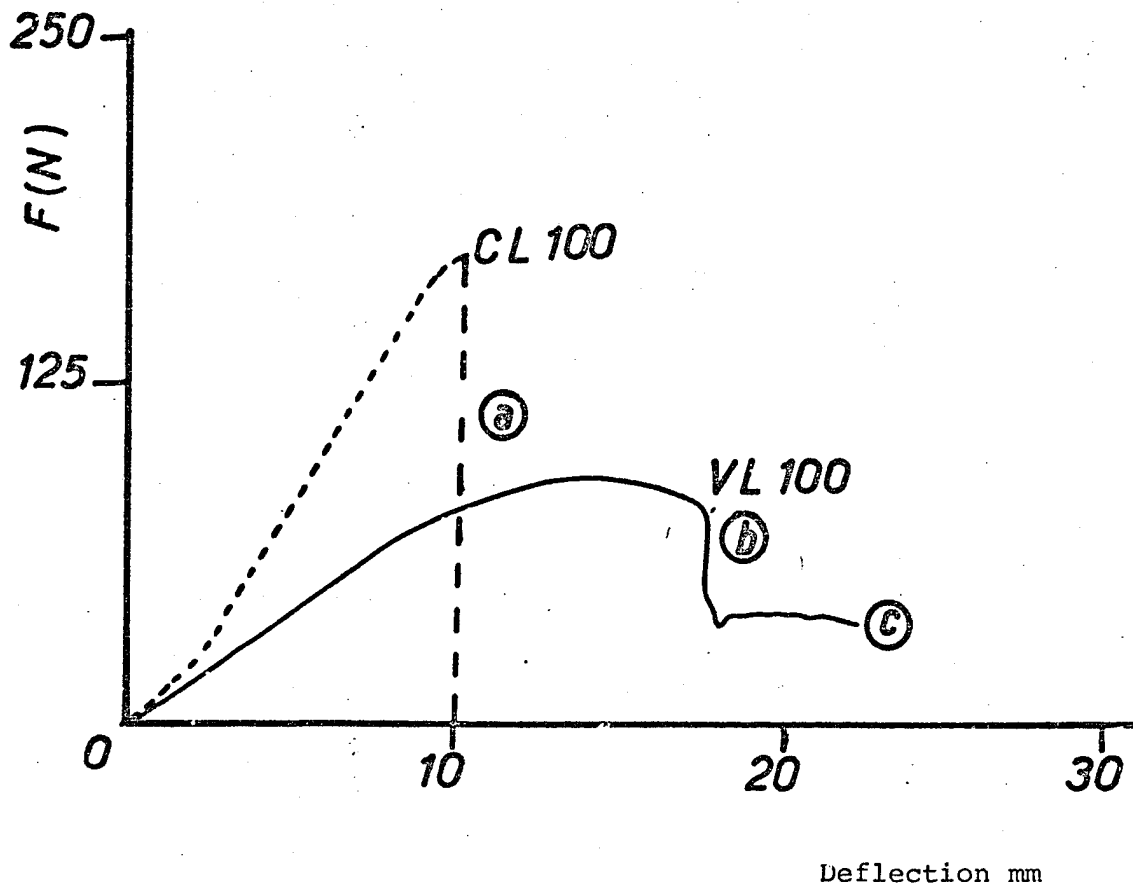
a) virtually total break in sample,
b) sample leaves jaws.
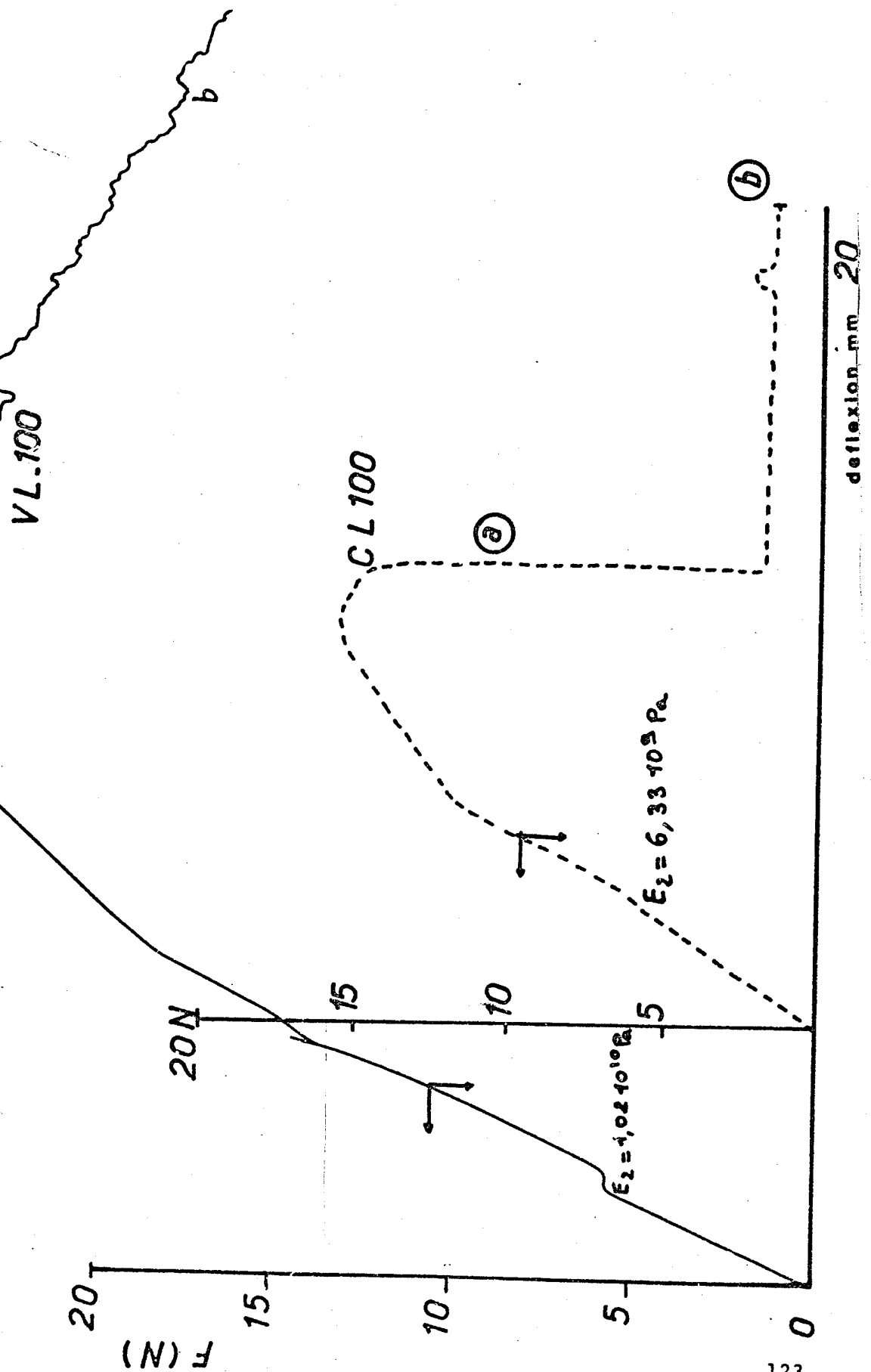
Figure 57 - Curves recorded under bending conditions
at T = - 75°C (Tg = -65°C for the matrix), giving
the longitudinal modulus E_1 (θ = 0)

a) rupture of sample
b) fiber-die decohesion (sample not broken)
c) sample leaves jaws.

outside shearing stresses and its rupture mode is observed. Two
extreme cases may be presented:

The interfacial bond is weak: in this case the composite
breaks after delamination. As the fibers have no bond with the
matrix, they slide into their seating and the load can no longer be
transferred.

The interfacial bond is good: in this case the die transmits
the load to the fibers until they reach their rupture limit and
suddenly give: the composite breaks under tensile stress.

124

II-2-4 - Observations in an Electronic Scanning Microscope

The electronic scanning microscope makes it possible to directly observe the appearance of the fracture after the composite breaks completely.

We made microphotos on the C-L100 and V-L100 composites tested at a temperature of -75°C. For samples where $\theta = 90°$, only the composite, C-L100, which is broken, is observed in the microscope.

In the case of carbon fibers (($\theta=0°$) (Figure 58, micrography a,b,c)), we observed two types of clear breaks corresponding to compression (c micrography) and to tensile stress (b micrography).

On part c) the fracture is quite irregular, the fibers leave their seating, and this is typical of the delamination process.

On part b) the fracture has a totally different appearance: its surface is relatively even and smooth, and this indicates good fiber-resin adhesion.

The same types of ruptures are seen for glass fibers (($\theta=0°$)   /135
(Figure 59 micrographies a,b and c)), except for carbon fibers.
In the area where the fracture is even and smooth (micrography b), it is greater than that where a separation is observed between the fiber and the die. This leads us to the conclusion that the adhesion between the two components of the composite is better in the presence of glass fibers.

Thus, the direct observation of the fracture appearance in the electronic scanning microscope makes it possible to characterize the rupture mode of the material.

Figure 60 shows the micrography of the composite, C-L100 ($\theta = 90°$). Irregular fractures are particularly noticeable.

Figure 58 - Examination in
an electronic scanning
microscope of rupture
surface (at T = -75°C) of
sample C-100 where θ=0°C

a) microphoto of entire
rupture surface (tensile
stress break) (break under
tensile stress (T) and
buckling compression (C)).

b) microphoto of
area where rupture
is due to tensile
stress (even rup-
ture surface)

c) microphoto of
area where rupture
is due to compres-
sive stress (the
fibers leave their
seating): uneven
rupture surface.

126
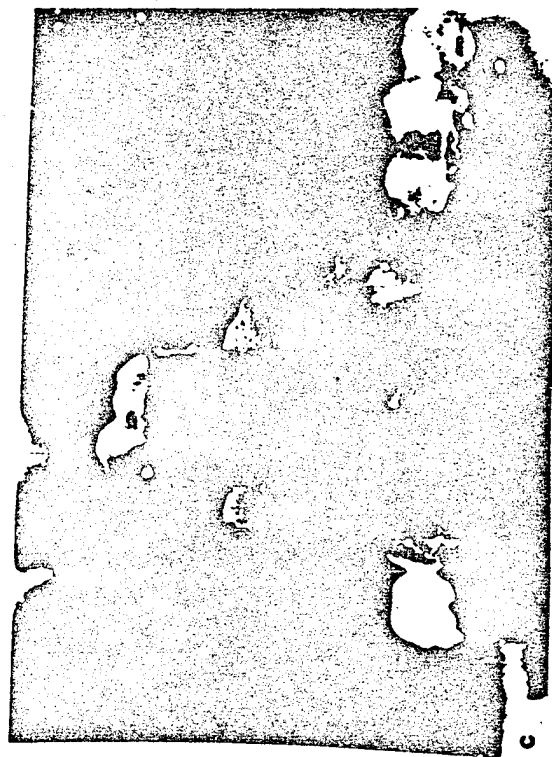
Weft fiber ruptures are also seen in the sample.

II-2-5 – Comparison of the Experimental Values of Moduluses $E_1 (\theta=0°)$ and $E_2 (\theta=90°C)$ With The Values Calculated For Each Model.

In this part, we compare the properties of the composite with L100 die reinforced with glass carbon. The comparison is made for two values, in the vitreous area (T $\cong$ -70°C) and for the rubber plateau (T $\cong$ 100°C).

Knowing the moduluses of the die and the reinforcement, the respective Poisson factors (υ) as well as the reinforcement density, we may calculate the values of the moduluses E_1 and E_2 (longitudinal and transversal) according to the models selected. These values are compared to those obtained under bending conditions.

The value of the matrix modulus alone is determined using a rheovibron viscoelastometer. The Poisson factors υ_{matrix}, υ_{glass} and υ_{carbon} are not measured. The values used are 0.45; 0.22 and 0.2, respectively.

a) Comparison of the Longitudinal Modulus E_1

The results are shown in Table XXVII. The following observations can be made.

At a temperature of -70°C in the vitreous area of the die, the experimental values coincide with the models for glass-composites. The deviation is, however, 8 to 12% for the two types of oiling. In the presence of carbon fibers, the deviation is greater, on the order of 30%.

At a temperature of 100°C (rubber plateau), the difference between the experimental values and the calculated values is greater. However, a difference of about 55% for carbon composites and of 3)% for glass composites may be noted.

Figure 59 - Examination in the electronic scanning microscope of the rupture surface (at T = -75°C) of the sample V-100 where θ=0°C.

a) microphoto of entire rupture surface (tensile stress fracture (T) and by buckling compression (C)).
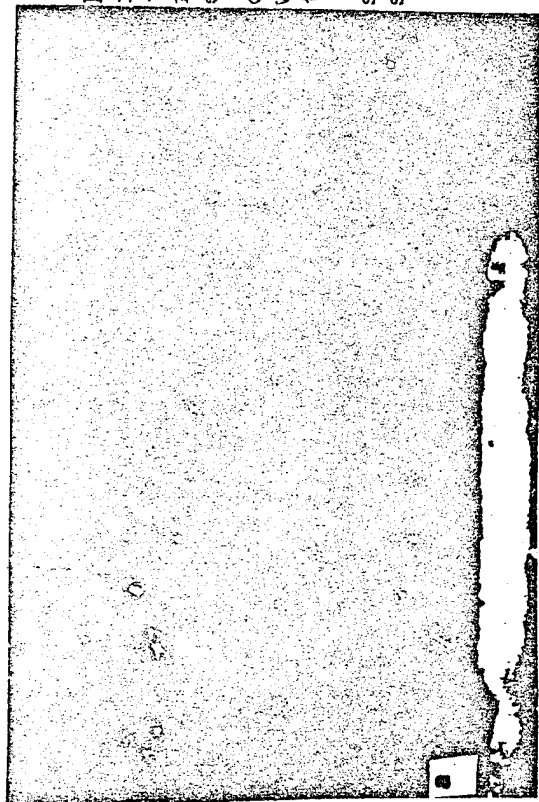
b) microphoto where rupture is due to tensile stress (the rupture surface is even).

c) microphoto of area where rupture is due to compressive stress (fibers leave their seating): uneven ruptur surface.

128
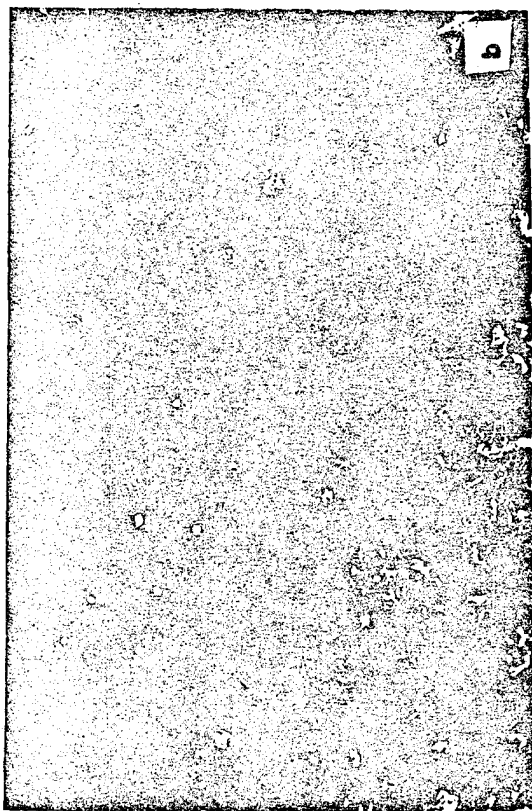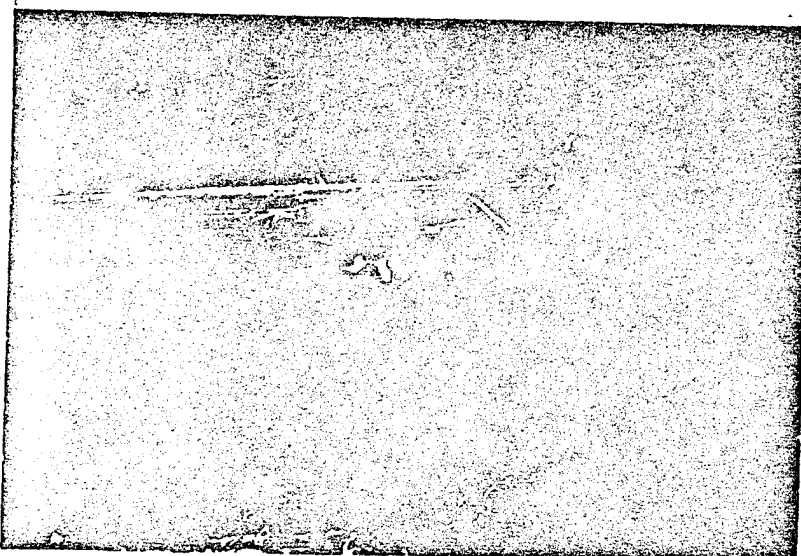
Figure 60 - Microphoto of rupture surface at - 75°C corresponding to C-L100 sample where $\theta=90°$

We therefore detect a greater deviation from the caculated /138 values in the case of a composite reinforced with carbon fibers. Furthermore, in the presence of glass fibers, the deviation is smaller when aminosilicone (A1100) is used for oiling.

b) Comparison of the Transverse Modulus E_2 ($\theta=90°C$)

The results are shown in Table XXVII. The following observations may be made.

The TSAI model gives modulus values which are close to the experimental values (at -70°C and at +100°C). However, there is always a greater difference between the two modulus values for the composite C-L100 (of 40 to 60%) than for the composite, V-L100 (of 6 to 13%).

The modulus values calculated according to the TSAI model are obtained with a contiguity factor C = 0.1. This corresponds to a composite where the fibers are virtually separated by the matrix (let us recall that for C = 1.*, the fibers are contiguous and the alignment is not perfect).

_____

*Illegible.

TABLE XXVIII

COMPARISON OF THE TRANSVERSE MODULUS E_2 ($\theta=90°$)

Composites	Température (°C)	Matrix (Pa) Modulus	Experim.Modulus (Pa)	Calculated Transverse Modul. GRESZCZUK	PUCK	TSAI [a]
V(P109)-L100	-70	$2.1.10^9$	$6.4.10^9$	$8.5.10^9$	$8.6.10^9$	$7.4.10^9$
C-L100			$5.7.10^9$	$9.3.10^9$	$9.0.10^9$	$9.8.10^9$
V(P109)-1100	+100	$3.8.10^7$	$1.9.10^9$	$1.8.10^8$	$1.6.10^8$	$1.8.10^9$
C-L100						
C-L100			$6.1.10^8$	$1.75.10^8$	$1.7.10^8$	$4.7.10^9$

a) given value corresponding to a contiguity factor C = 0.1 in the TSAI model.

In conclusion, the comparison of the experimental measurements /139 of E_1 and E_2 with the values given by the various models allows us to make the following remarks.

1) As already mentioned at the beginning of this chapter (I-3-3)), the models proposed in literature do not account for the adhesion factor in composites in general, since it is considered to be perfect. A comparison between the two types of oiling in the presence of glass fibers (Table XXVII) gives us different experimental values for the E_1 modulus, whereas in the models, the calculation predicts only one.

TABLE XXVII

COMPARISON OF THE LONGITUDINAL MODULUS E_1 ($\theta=0°$)

Composites	T(°C)	Matrix (Pa) Modulus	Experim. Modulus$_1$ (Pa)	Mixing Law s	Alignment Factor (TSAI)
V(P109)-L100	-70	$2.1.10^9$	$4.2.10^{10}$	$4.8.10^{10}$	$4.3.10^{10}$
V(A1100)-L100			$4.5.10^{10}$	$4.8.10^{10}$	$4.3.10^{10}$
C-L100			$8.6.10^{10}$	$1.3.10^{11}$	$1.1.10^{11}$
V(P109)-L100	+100	$3.8.10^7$	$2.4.10^{10}$	$4.7.10^{10}$	$4.2.10^{10}$
V(A1100)-L100			$3.4.10^{10}$	$4.7.10^{10}$	$4.2.10^{10}$
C-L100			$5.2.10^{10}$	$1.2.10^{11}$	$1.1.10^{11}$

a) alignment factor used by TSAI
   k = 0.9.

2) The comparison of the two types of reinforcement (carbon
and glass) shows for carbon composites a greater difference (30-50%)
between the measured moduluses and the models. We believe that the
fiber-die adhesion (better in the presence of glass fibers) may be
the reason for this difference. Yet, the L100 polyurethane matrix
does not have the same properties in the presence of carbon fibers
or glass fibers (results observed by extraction tests and infra-
red measurements). Consequently, the matrix modulus is not constant.

Conclusion: /140

During the various tests performed, we found different behav-
iors in our composite materials, as a function of the reinforcement
and the formulation.

Reinforcement Impact

Various authors [73,74] showed that the surface condition of
the reinforcement material could modify the polymerization reaction
of the resin causing a change in the mechanical properties of the
resin at the interface, along a relatively high gradient.

. The magnitude of the gradient in the mechanical properties of
the resin caused a modification in the stress propagation. This
explains the various rupture profiles observed for V-L100 and
C-L100 composites, indicating a better stress transmission from
the matrix to the fibers, in the case of glass fibers.

Further, the high temperature performance as well as the value
of composite moduluses are relatively high, depending on the type
of reinforcement used.

The Kevlar case is surprising. We showed its catastrophic
impact on the rate of advancement of the reaction where we were

able to extract about 90% of the soluble fractions so that the composite material produced exhibited a very poor temperature performance with a rubber plateau whose modulus does not exceed $2.6 \cdot 10^8$ N/m^2 (pure E_2) whereas the die alone has a modulus of $3.8 \cdot 10^7$ N/m^2 and the fiber a modulus of elasticity of $8.5 \cdot 10^{10}$ N/m^2.

The carbon fibers, although they have a much higher longitudinal modulus, give the corresponding composite material a fragile behavior, especially in the vitreous area of the matrix.

An examination in the electronic microscope of the rupture surface shows weak adhesion at the fiber-die interface, where one sees a major portion of the fibers which leave their seating.

Generally speaking, the glass fibers seem to be the most suit- /141 able for the polyurethane formulations studied. There is a fairly good temperature performance with the rubber plateau which has a constant modulus up to about 160°C for V-L100. It seems that the polycondensation reaction is not "disturbed" in the presence of the reinforcement. The soluble extracts are in small quantities. The observation in the electronic microscope of rupture surfaces shows a good interfacial bond. An even rupture surface is noted. The adhesion is therefore better, and in differential thermal analysis, one notes a relaxation of the flexible sequences which rise in temperature.

Formulation Impact

Although the laboratory formulation CP2 has somewhat higher modulus values, the temperature behavior is not as good. Indeed, polyurethane flows at high temperatures much sooner than commercial formulations. We believe that PUR-L100 polyurethane has better properties than the other dies. The curves for the transverse modulus as a function of the temperature shows a better temperature behavior with a rubber plate having a constant modulus over about 100°C. However, we stressed in the first part the disadvantages

of the aromatic diamine chain extender (Moca).

The PUR-M400 formulation is not to be totally discarded, because the percentage of the various reagents can be modified, especially if the "consumption" of the isocyanate functions (NCO) leads to the formulation for isocyanurates in the presence of glass fibers.

II-3 – Viscoelastic Measurements of Composites With Polyurethane Matrix /142

II-3-1) Introduction

The mechanical properties of a polymer always depend on possible chain segment movements. These movements depend on the interactions within and between molecules and overlapping phenomena.

The viscoelastic study of composite materials is important, because it helps us to know and understand part of this phenomenon. As composites are heterogeneous mixtures of at least two phases, from the microscopic standpoint, the properties are determined by those of components, and the responses of the material may be complex.

The most widely used instrument for studying dynamic properties is measuring the deformation of a material in response to vibration forces. Using these measurements, one may then determine the elasticity modulus and the mechanical absorption which gives the dissipated energy in the form of heat while the deformation is occurring. The mechanical absorption or the internal friction factor is important not only as a property which characterizes the materials, but its industrial applications as well. In addition to the dynamic mechanical tests, dielectric tests may be used. Here, materials are subjected to alternative electric fields of variable frequency.

The study of the dynamic mechanical properties of composites

pertains essentially to materials reinforced with fillers. Composite materials with fibrous reinforcements were studied much less.

The studies performed by K. REED [75] on unidirectional epoxy-glass fiber composites and those performed in our laboratory by YONG-SOK O [76] on epoxydes reinforced with carbon fibers should be mentioned.

a) K. REED studies the dynamic mechanical properties of his composites using samples cut out along an angle (θ) to the fiber direction, varying from 0 to 90°, per 15° pitch. The mechanical measurements are performed on a DuPont instrument, the schematic diagram of which is shown in Figure 61. The sample is tightened /143 at its two ends between parallel arms which can undergo bending stresses. One of the two arms is mobile with low frequency movements, the other remains passive. The frequency of this system is thus variable and is less than 3 Hz. A frequency is imposed which induces a resonancy frequency into the sample as a function of the recorded temperature. The rate of temperature rise is 5°C/mn.
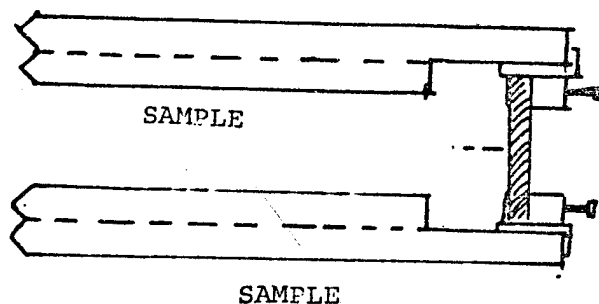
SAMPLE

SAMPLE

Figure 61 - Diagram of DuPont Dynamic Mechanical Analyzer

The author notes the existence of a second absorption peak on the tg δ curves and especially for samples at $\theta = 15°$ and $\theta = 0°$ (Figures 62, 63).

The thermomechanical analysis measurements (Figure 62) present a second peak observed for tg δ, beyond Tg.

134

Furthermore, the annealing impact as well as the thickness variation of the sample were studied. The same appearances are obtained for tg δ curves (Figure 63). The second peak is always present; however, it increases as the sample becomes thinner.

In concluding his study, K. REED ascribed this effect to an interphase between the fibers and die which would exhibit different properties than those of the pure matrix. We may conclude that these interfacial differences may have several causes:

.chemical: bond with fibers, interfacial phase segregation of /146 macromolecules of different structures,

.physical: direction of macromolecules at interface, very strong physical interactions, etc.

b) The viscoelastic measuremetns of YONG SOK O [76] pertain to epoxyde unidirectional composites of industrial reference BSL 914, reinforced with T30C carbon fibers whose fraction per unit of volume is 60% approximately. The dynamic measurements are performed using the METRAVIB viscoelastimeter for 3-point bending tests as a function of the temperature and for frequencies ranging from 15.6 Ha to 500 Hz. The measuring cell used is shown in Figure 64.
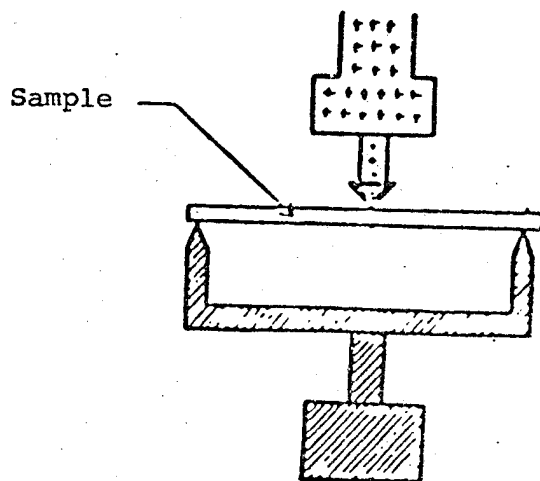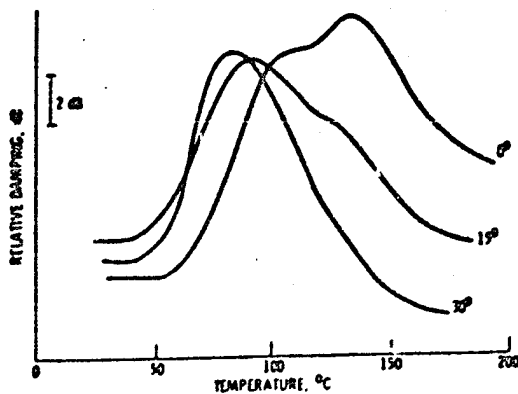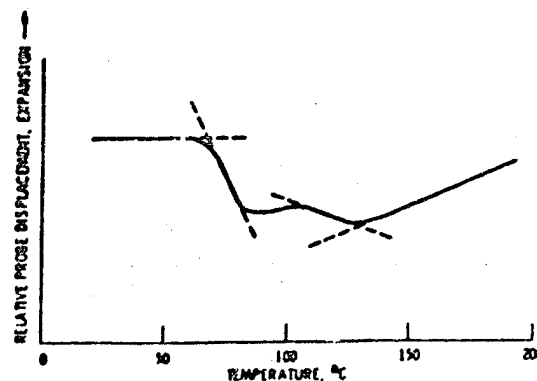

Figure 64 - Dynamic mechanical properties under beam bending forces.
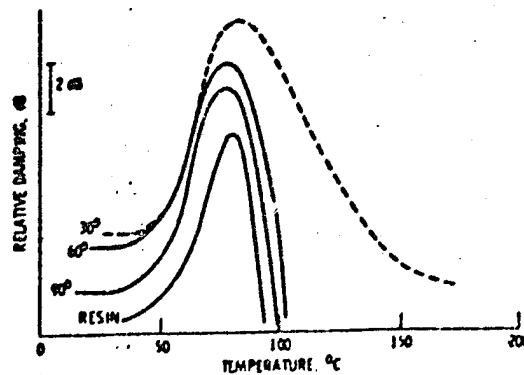
a) absorption curves for pure resin and samples where θ=30,60,90°

b) absorption curves as a function of the temperature for θ = 0, 15, 30°

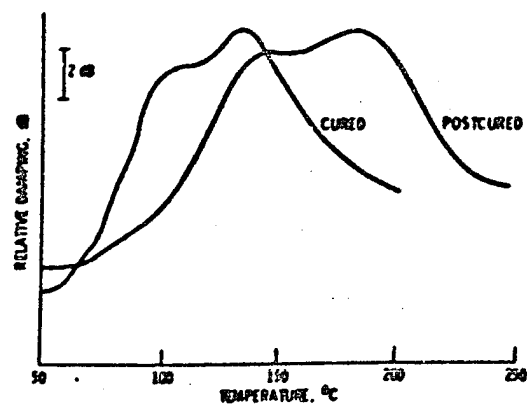c) thermomechanical analysis curve of a unidirectional epoxyde/glass E composite.

Figure 10
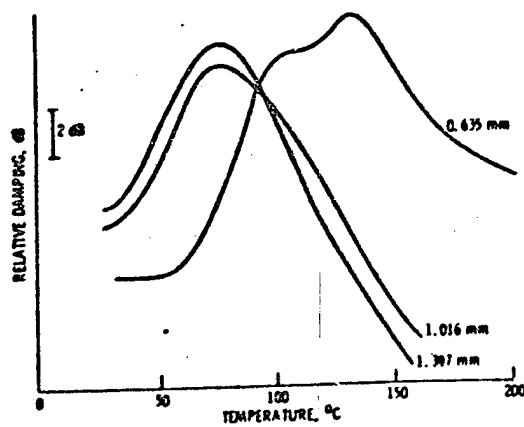
System: DGEBA (DER 332)   100 g
        reactive diluent (RD2)   20 g
        DDM + mPDA (Tonox 6040)   22.8 g
        M roving glass
        (filamentary winding: 5 braids of 2.54 over a width of
        14.9 cm; silicone finish)

        5 hours at 82°C under 100 psi pressure
        ~22% resin in the composite (by weight)
        Tg - 76 - 78°C

a) Impact of post-curing   (θ=0°) - 4 h at 204°C

b) Impact of thickness on measured sample (DMA DuPont)

Figure 60

137

Metravib is a viscoelasticimeter which measures by applying a stress or periodic deformation to a sample placed between a force sensor and a dyanmic displacement sensor. The mechanical stiffness of the apparatus provides direct access to the real stresses. This apparatus prepares the stiffness modulus and measures the phase shift angle between the force and the displacement as a function of the temperature and the frequency.

The measurements were performed on samples cut out along an angle (θ) to the fiber direction. The results show a single relaxation peak (in the tg δ curves) which may be associated with the vitreous transition of the die. Figures 65 and 66 show the results for angles θ = 45°, 0° at 15.6 Hz frequency. In this case, the die formulation is complex (epoxyde network plus polysulfone thermoplastic) and the vitreous transition (Tg) occurs at higher temperatures, which complicates measurements beyond Tg. /149

c) In conclusion, is there a second relaxation beyond the vitreous transition in composites with fibrous reinforcements? The answer is not clear-cut and the viscoelastic measurements of polyurethane composites will have a two-fold interest: we will characterize the behavior of our composites and we will try to introduce an additional experimental element to this second relaxation presented by K. REED.

We began by using the Metravib and the 3-point bending measuring test which we abandoned for technical reasons. Actually, polyurethane composite materials are relatively flexible, and too flexible to perform reliable measurements as a function of the angle (θ), because the sample comes off while excitation forces are applied, as soon as ambient temperatures are reached. Accordingly, the measurements are no longer meaningful.

We finally used the Rheovibron viscoelasticimeter which has the advantage of having been used already for testing
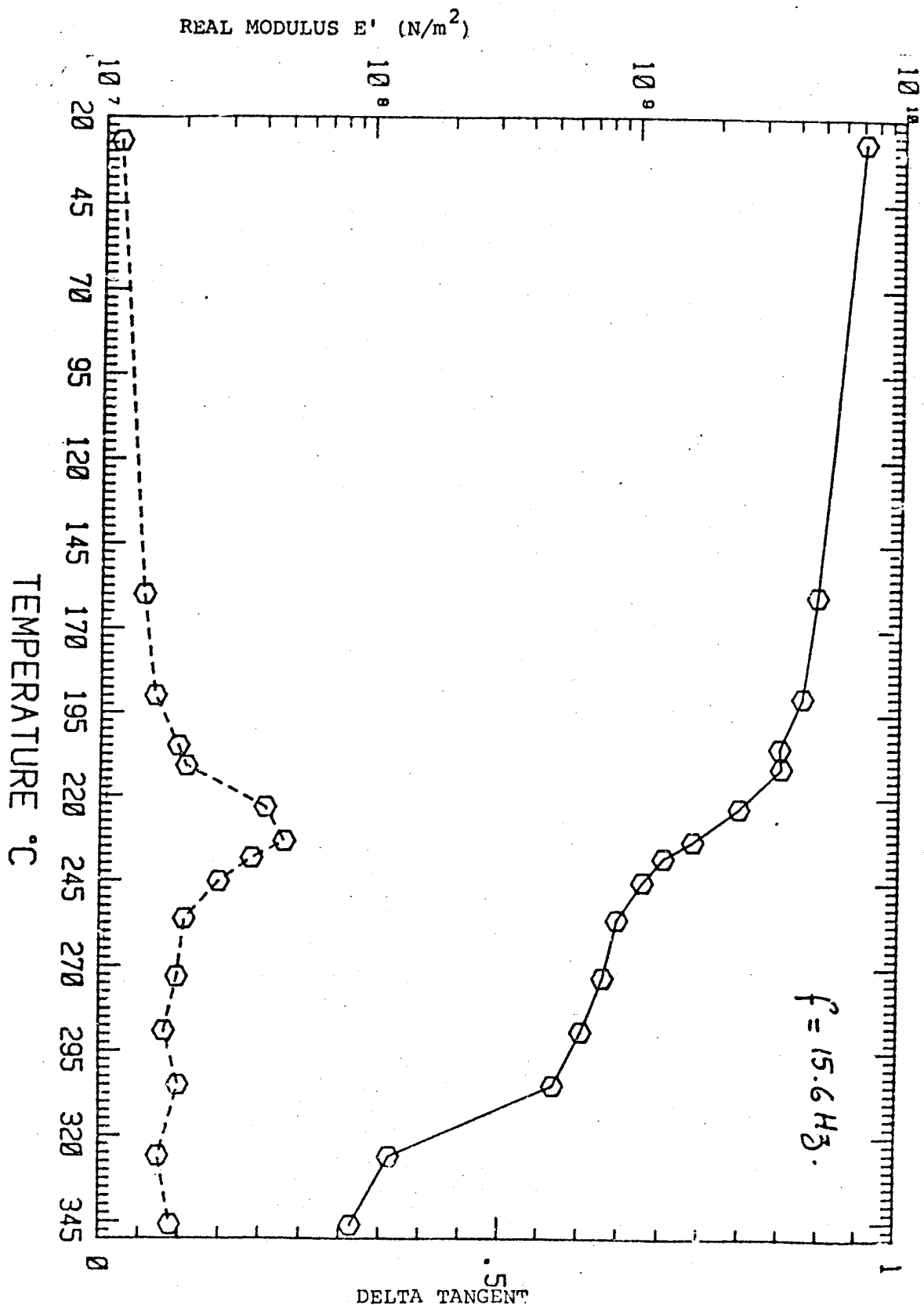
138

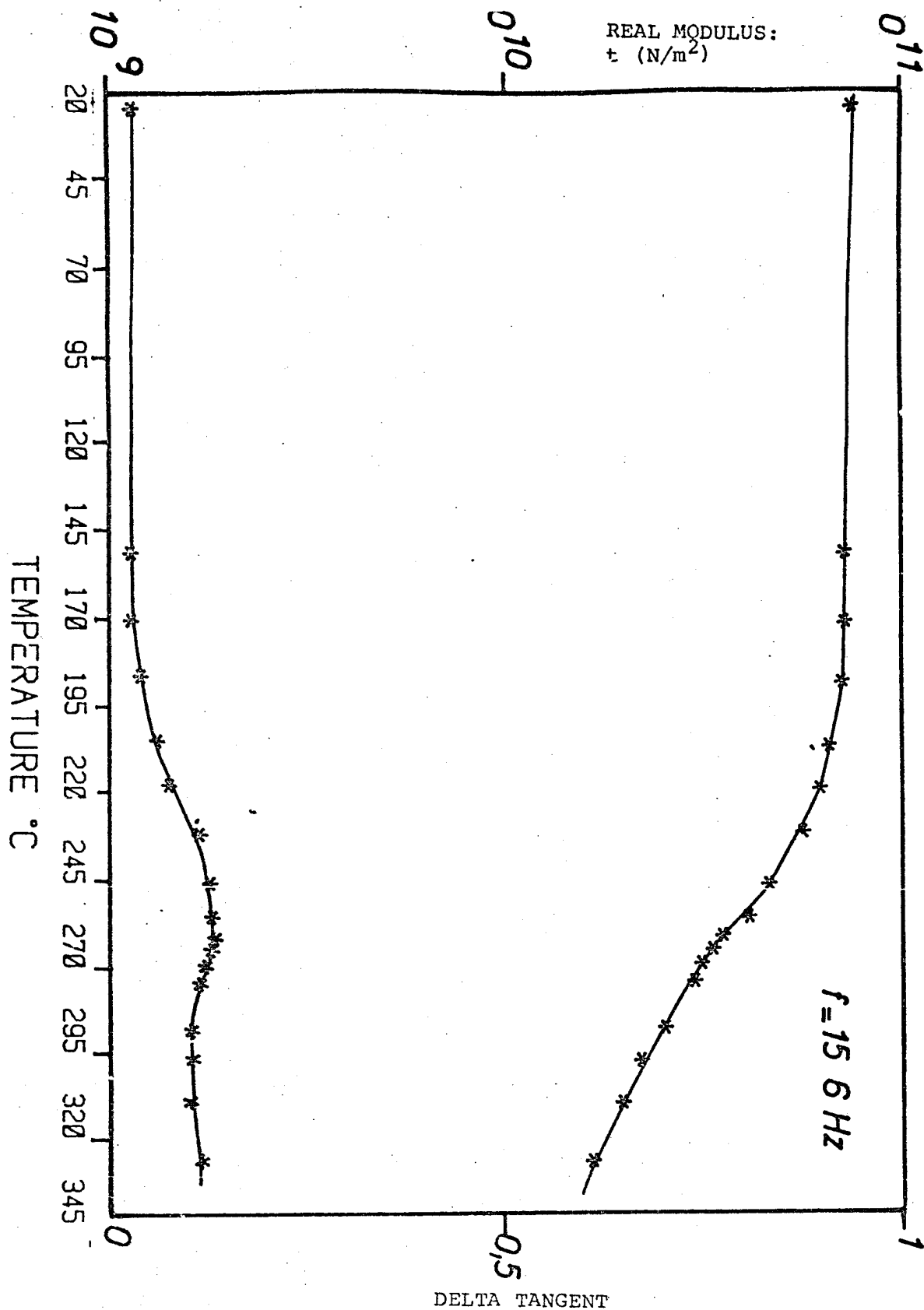Figure 65 - Dynamic measurements of viscoelasticity for epoxide/
carbon composites

Figure 66 – Dynamic measurements of viscoelasticity for epoxide/
carbon composites θ = 0

140

polyurethane dies. It has the disadvantage of being limited for high modulus measurements.

The samples are on the average 3 cm long, 4 mm wide and 1.2 mm thick. The number of fiber layers is 4 for glass composite and 8 for carbon composites. Our measurements were essentially made on V-L100 and V-M400 composites. C-L100 and C-M400 composites were studied for comparison.

II-3-2) Results For Glass Composites

a) The absorption (tg δ) and the preservation modulus E' were measured as a function of the temperature (Figures 67-70) on samples cut along an angle (θ) to the fiber direction. The following observations may be made:

The maximum peak tg δ decreases considerably in the change /150 from 0.2 (L100) and 0.3 (M400) to about 0.05 (V-L100) and 0.07 (V-M400) (Figures 67,69). As for the matrix alone we may state that this relaxation peak is associated with the vitreous transition Tg of polyurethane.

The begninning of the absorption peak moves toward higher temperatures when the angle (θ) approaches 0, the fiber direction.

The beginning of the rubber plateau (Figure 68, 70) giving E' as a function of the temperature moves toward higher temperatures when the fiber direction is approached.

Figure 71 shows the variation of the modulus E' as a function of the angle (θ). A minimum level is observed at $\delta = 45°$ and a modulus rise is observed between 45° and 90°. This rise may be explained by the presence of weft in the fabric used. The poor quality of the measurements for high moduluses with rheovibron do not allow us to plot these same curves with the vitreous modulus values.

141

To clarify the weft effect, we made V-L100 composite plates completely unidirectional while depilating the weft. The variation of E' (100°C) decreases with the angle (θ) (Figure 71).

After all these remarks, however, the most striking observation was the very distinct onset of a second absorption area beyond the first one (FIgures 67, 69) which is not very apparent at θ = 90° and θ = 75°, but becomes very distinguishable as of θ = 60°. This observation, which is comparable to K. REED's results, will be discussed later. However, before jumping into assumptions and to have a more clear idea of the problem we first repeated our measurements on various samples by varying the form factor and the annealing time.

b) Impact of form factor. In Figure 72 A and B, we showed the variation of tg δ as a function of the temperature by varying the form factor (A, θ = 45°); B, θ = 60°C). We observe the same curve form and a second absorption area in the same temperature range. The variations of tg δ with the form factor are small.

c) The annealing impact. Figure 73 A and B shows the tg δ /157 curves for the first two samples where θ = 60°. The second change occurred right after the first one. We can see the near disappearance of the two peaks which now form only one, but in the same total temperature range. Another measurement is performed on the same sample one month after the first two transitions. Figure 73 B shows the total absence of the second absorption area, and a Gaussian form curve with a single absorption peak.

d) To complete our study, we prepared a V-L100 composite plate where the fabric layers are staggered by 90°. The sample in this case is cut out to have an angle θ = ±45°C.
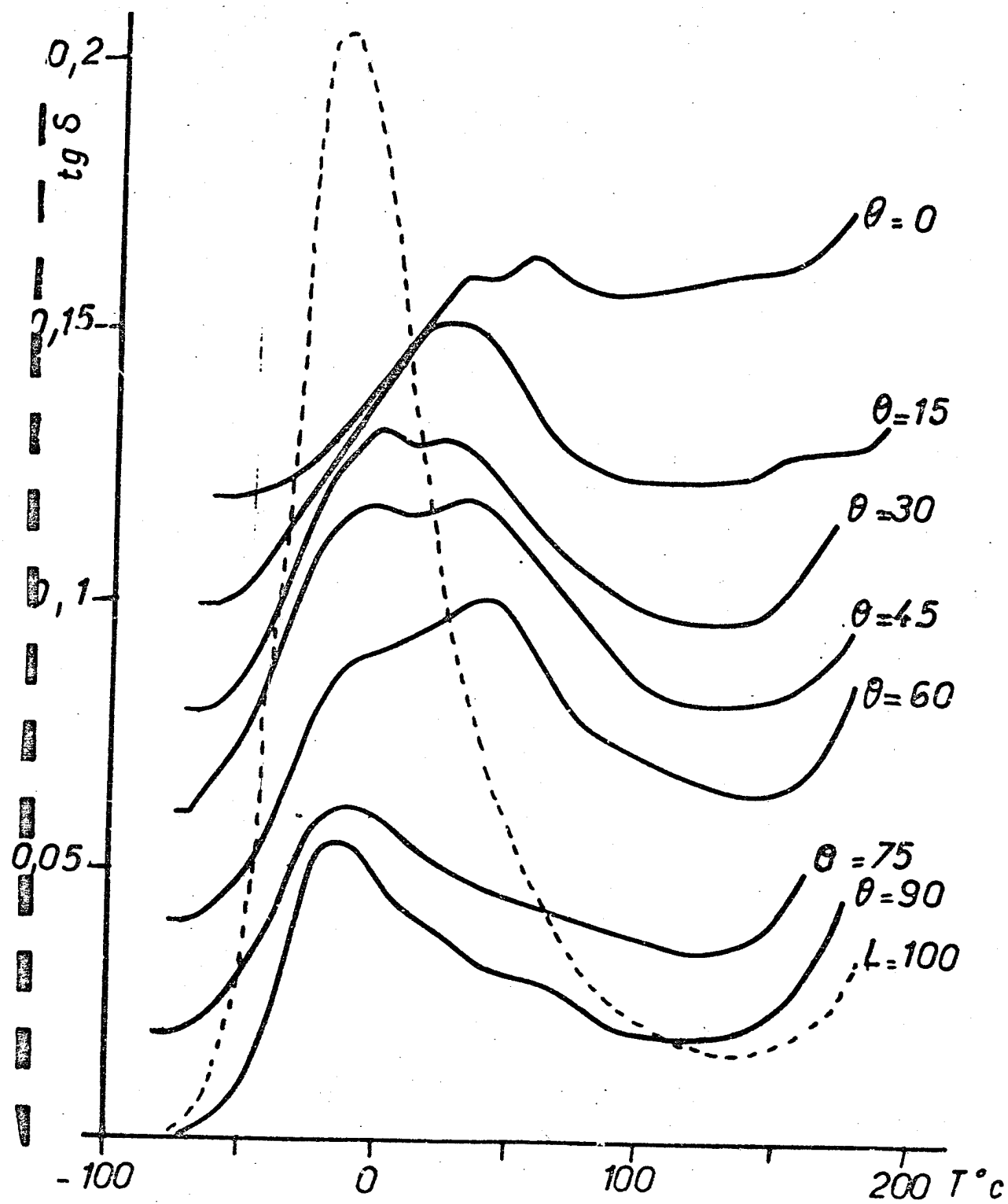
Figure 67 – Curves giving tg δ as a function of the temperature
for PU-L100 Adiprenes (-----) and for V-L100 composite
for various angles θ.
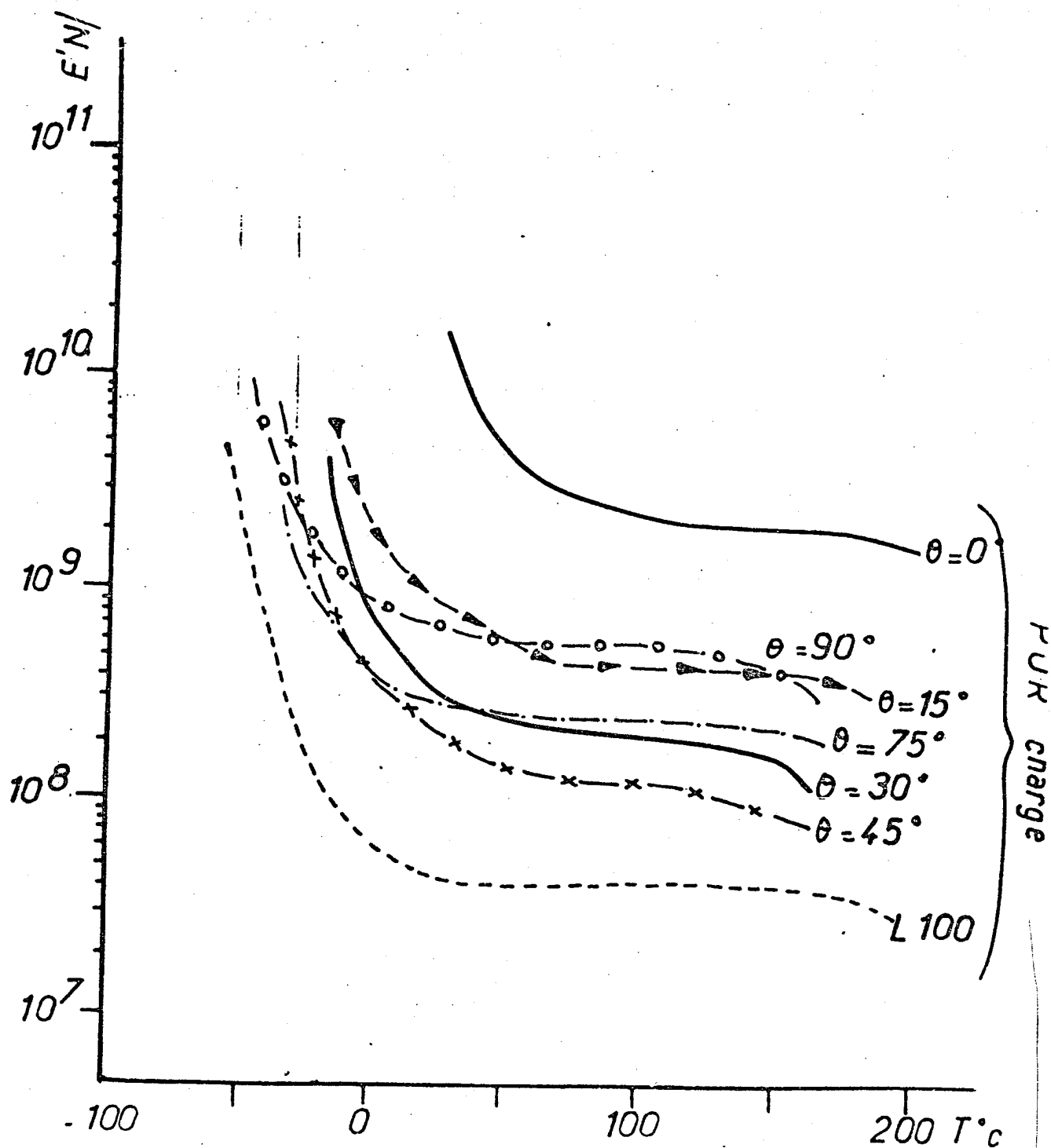
Figure 68 - Curves giving the modulus E' as a function of the temperature for PU-L100 (-----) and for the composite VL100 along different angles θ.
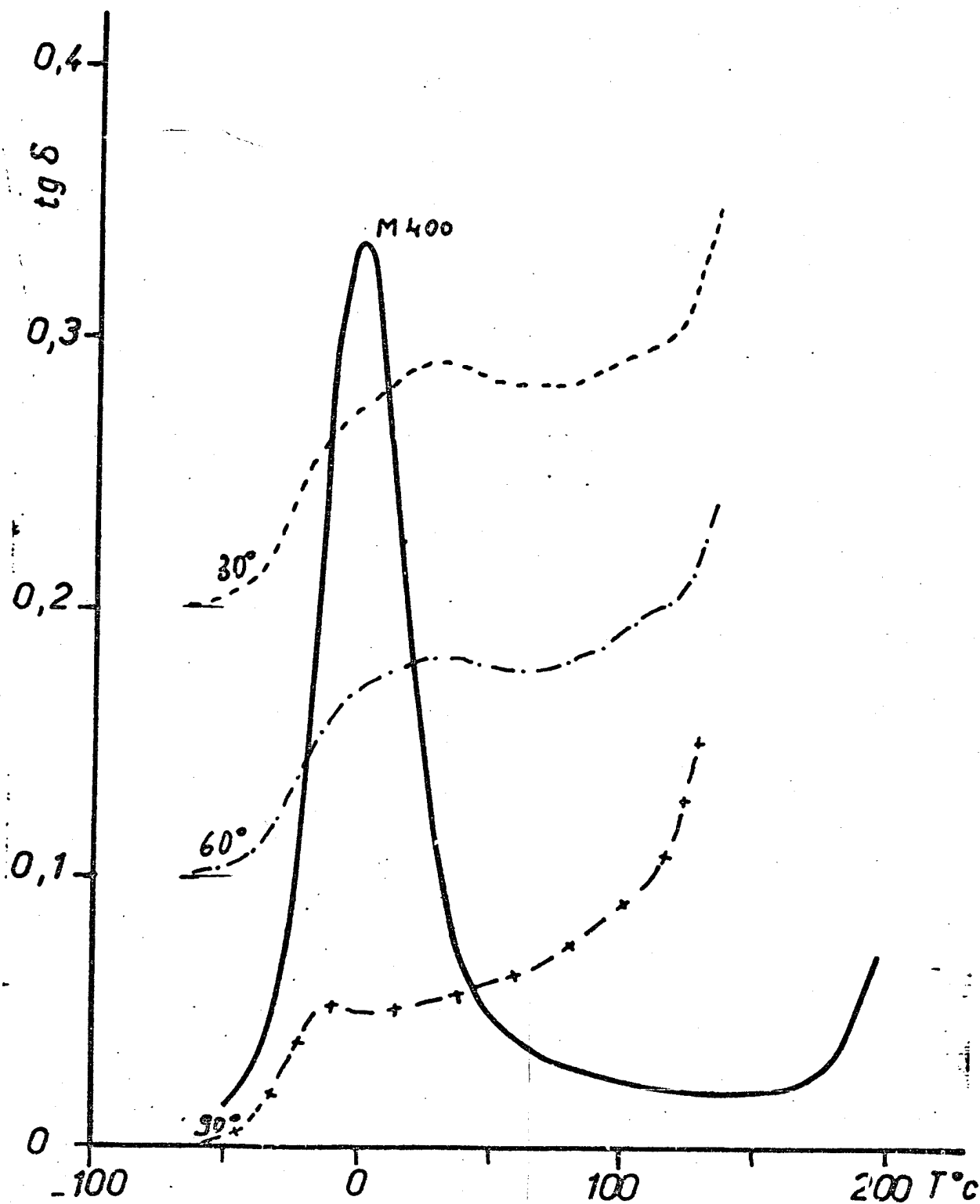
Figure 69 - Curves giving tg δ as a function of the temperature for
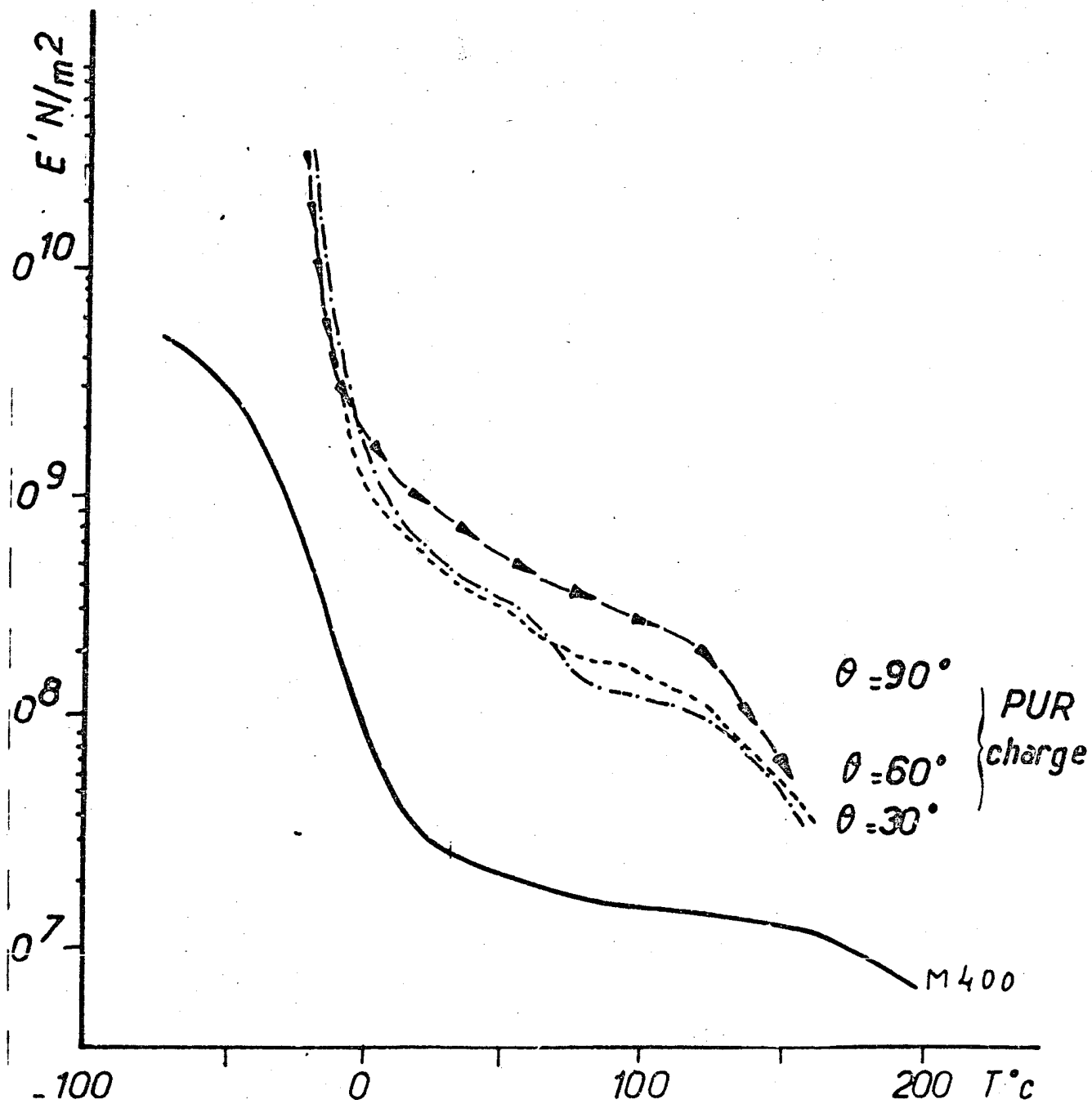PU - Adiprene M400 (———) and for V-M400 composite according to
different θ values.

Figure 7C - Curves giving the modulus E' as a function of the temperature for PU-M400 and the V-M400 composite according to various angles θ.
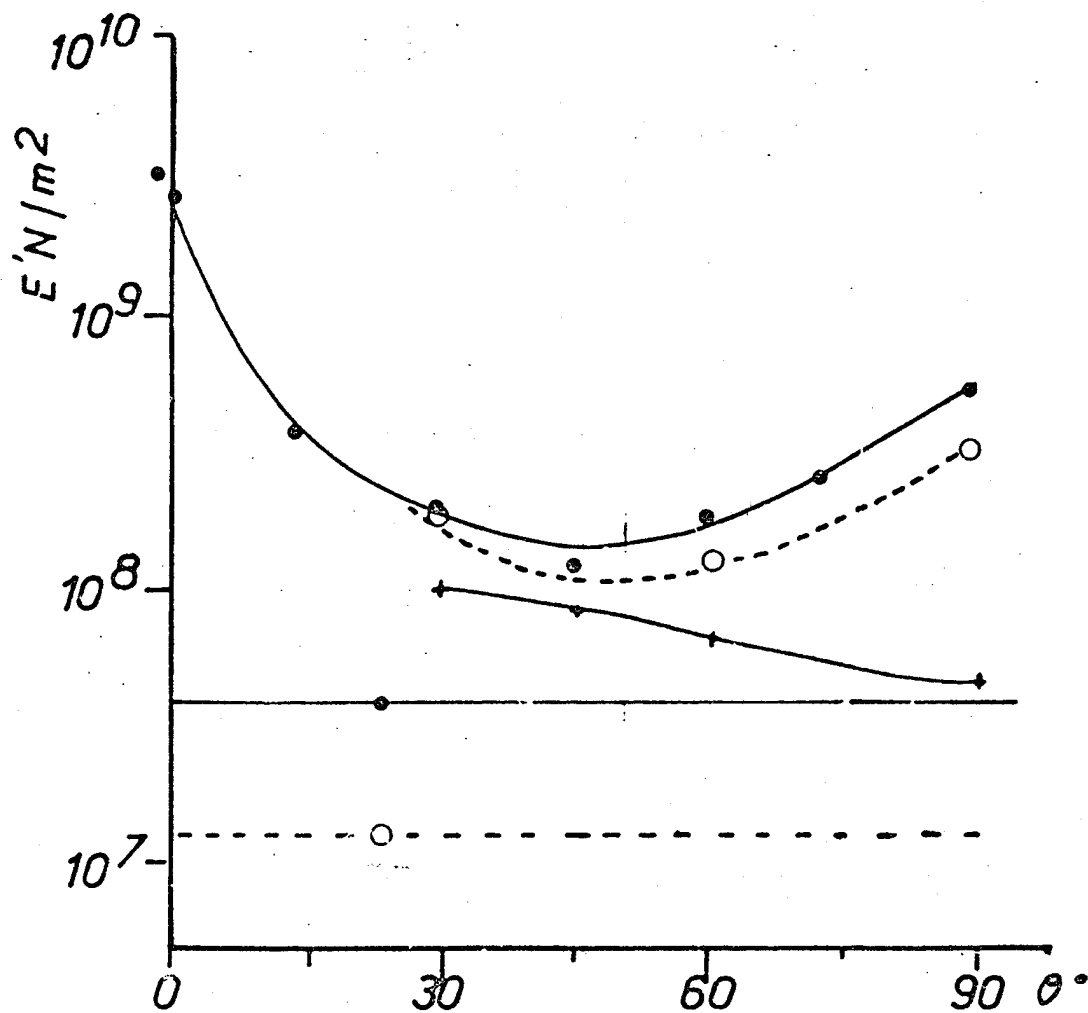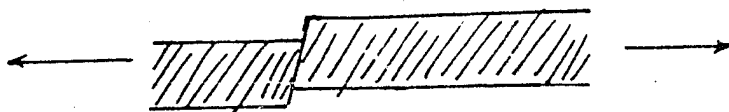
Figure 71 - Variations of the modulus E' at T >> Tg as a function of the cutting angle. This V-L100 composite was prepared with the same V-P109 glass fabric, while depilating the weft.

The purpose of this operation is to be able to eliminate any phenomena of matrix slipping along the fibers while the measurements are done.
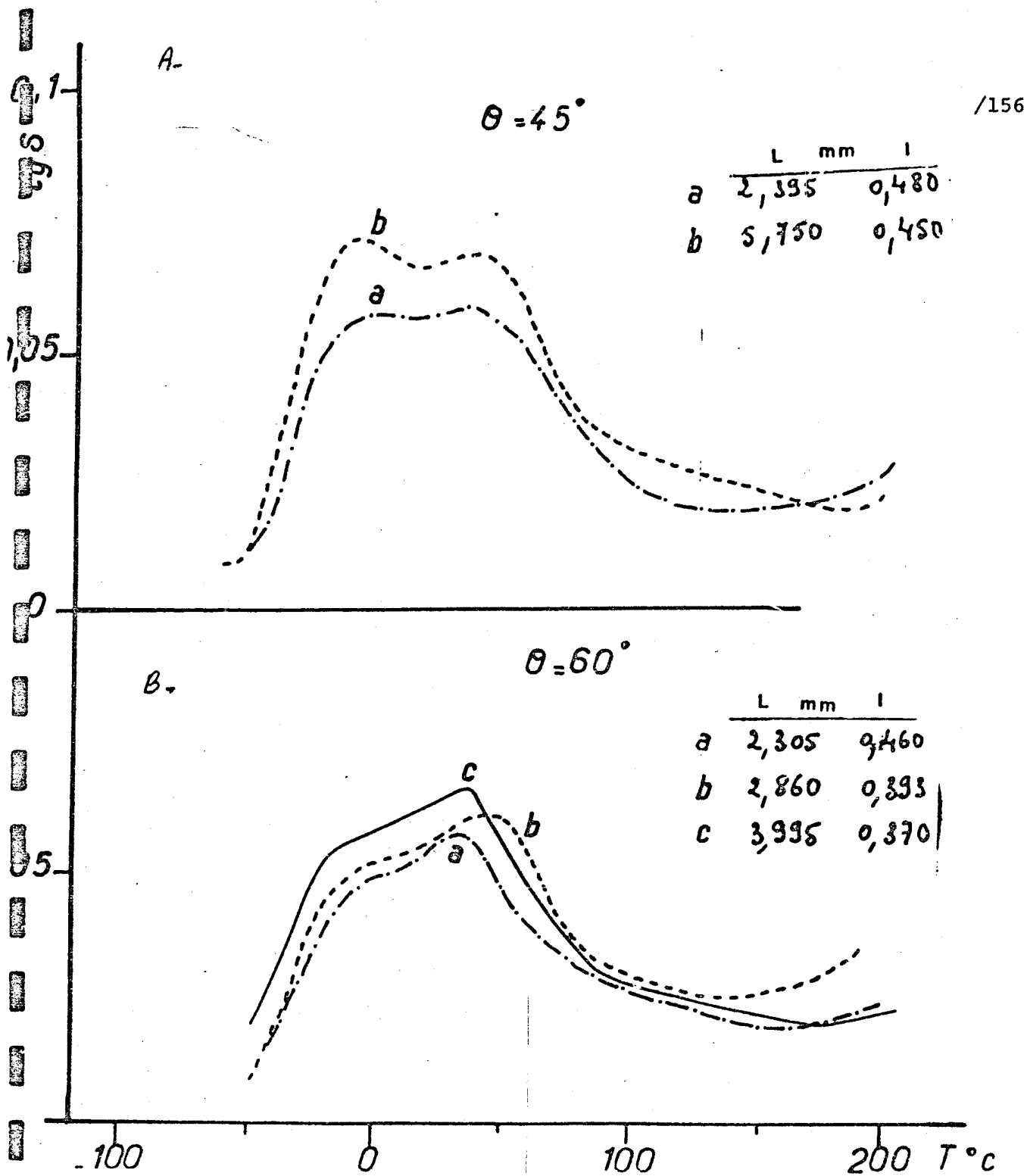
Figure 72 - Impact of form factor on tg.

The results are shown in Figure 74. One can see considerable /157
differences between the composite with unidirectional fabric layers
(θ = 45°) and the composite with a layer of crossed fabrics (θ=±45°).
In particular:

The second relaxation disappears completely for the composite
(θ=±45°). The main relaxation is found in the same range as for
the pure matrix.

The rubber plateau is found at a slightly higher level, and
it is perfectly constant in temperature.

As with the previous cases, we studied the impact of the form /160
factor and of annealing. Figure 75 a and b shows that the tg δ
curves are independent from these two parameters.

e) In addition to the rheovibron measurements, we performed
dielectric measurements on the L100 matrix and the corresponding V-L100
composite where the sample is stressed without regard to the fiber
direction.

Figures 76 and 77 show the results obtained.

We see a single relaxation peak for the tg δ curve, for both
the L100 matrix and the corresonding composite.

We calculated the activation energy using the following equation:

$$f = f_o \ \exp \ (- \frac{Ea}{RT} \ )$$

where f: frequency
    Ea: activation energy
    R: perfect gas constant (2 cal.mole^{-1})
    T: temperature (+273°C)

149
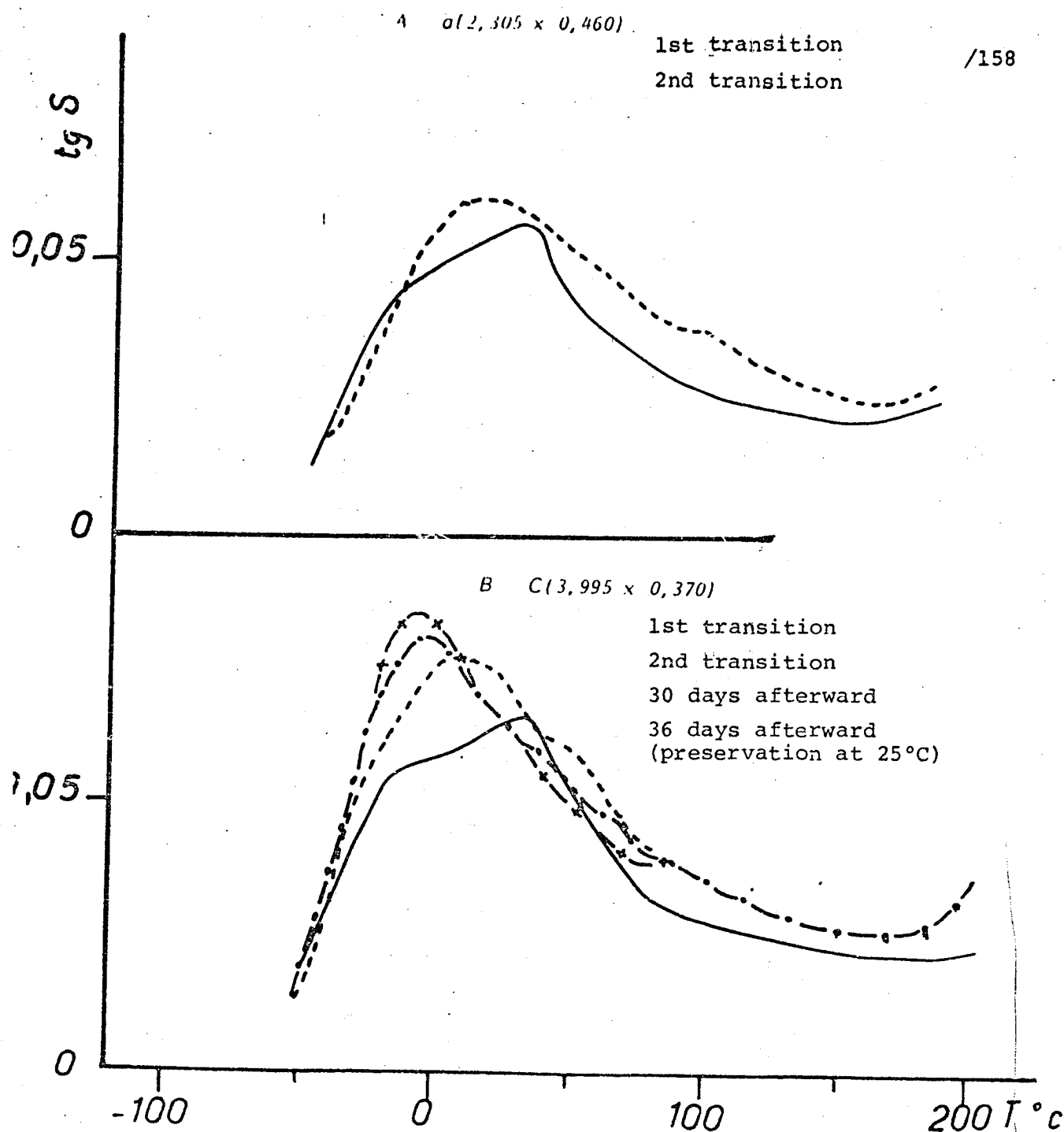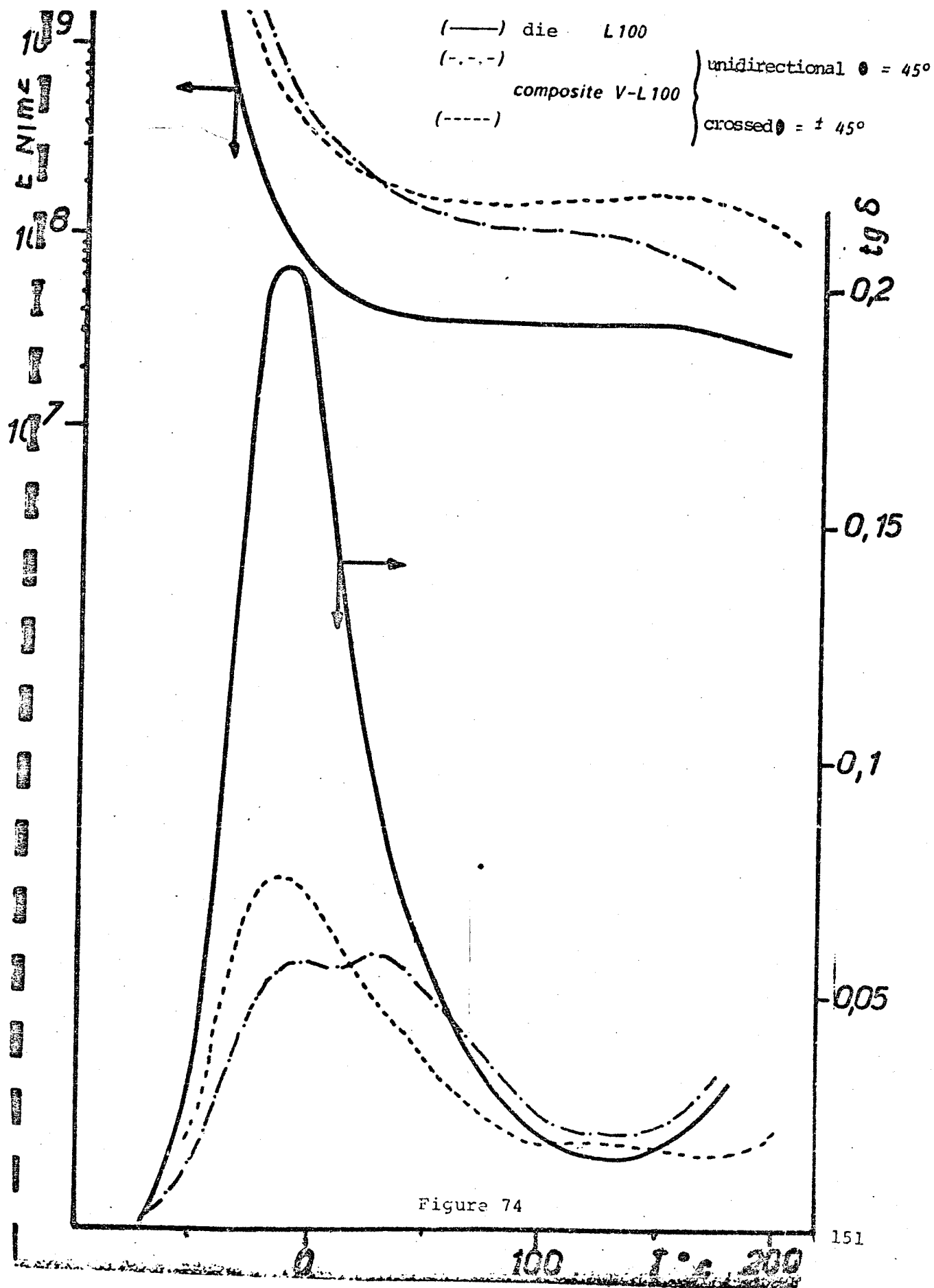
A   a(2,305 x 0,460)

1st transition

2nd transition

B   C(3,995 x 0,370)

1st transition

2nd transition

30 days afterward

36 days afterward
(preservation at 25°C)

Figure 73: Annealing impact on samples
cut out at 60°

150

Figure 74

$$\text{Ln } f = \text{Ln } f_o - \frac{Ea}{RT}$$

$$\log_{10} f = \log_{10} f_o - \frac{Ea}{2.3 \text{ R}} \cdot \left(\frac{1}{T}\right)$$

By plotting the straight line $\log_{10} f = f\left(\frac{1}{T}\right)$, the activation energy Ea is obtained, if we know the slope value α:

$$\alpha = - \frac{Ea}{2.3 \text{ R}} \rightarrow Ea = -2.3 \text{ R}$$

(with a negative slope, we obtain a positive value for Ea).

The results shown in Figure 78 indicate virtually the same   /165
activation energy value ($\simeq$ 23 kcal/mole) in both cases (matrix alone
and composite).

We tried to extrapolate what temperature the 11 Hz frequency
used in the case of Rheovibron corresponds to. To do this, we
used the straight line $\log_{10} f = f\left(\frac{1}{T}\right)$ concerning the composite.
The extrapolation to 11 Hz shows a temperature equal to about - 33°C,
which corresponds to the first relaxation observed with rheovibron
(Figure 67) and associated with the vitreous transition of the matrix.

II-3-3_   Results For Carbon and Kevlar Composites

For comparison, we showed in Figures 79-82 the curves giving
tg δ and E' respectively as a function of the temperature for poly-
urethane-carbon composites. On the whole, the same observations
are made in regard to the second relaxation beyond the first cor-
responding to the vitreous transition.

We did not do viscoelastic measurements on kevlar composites
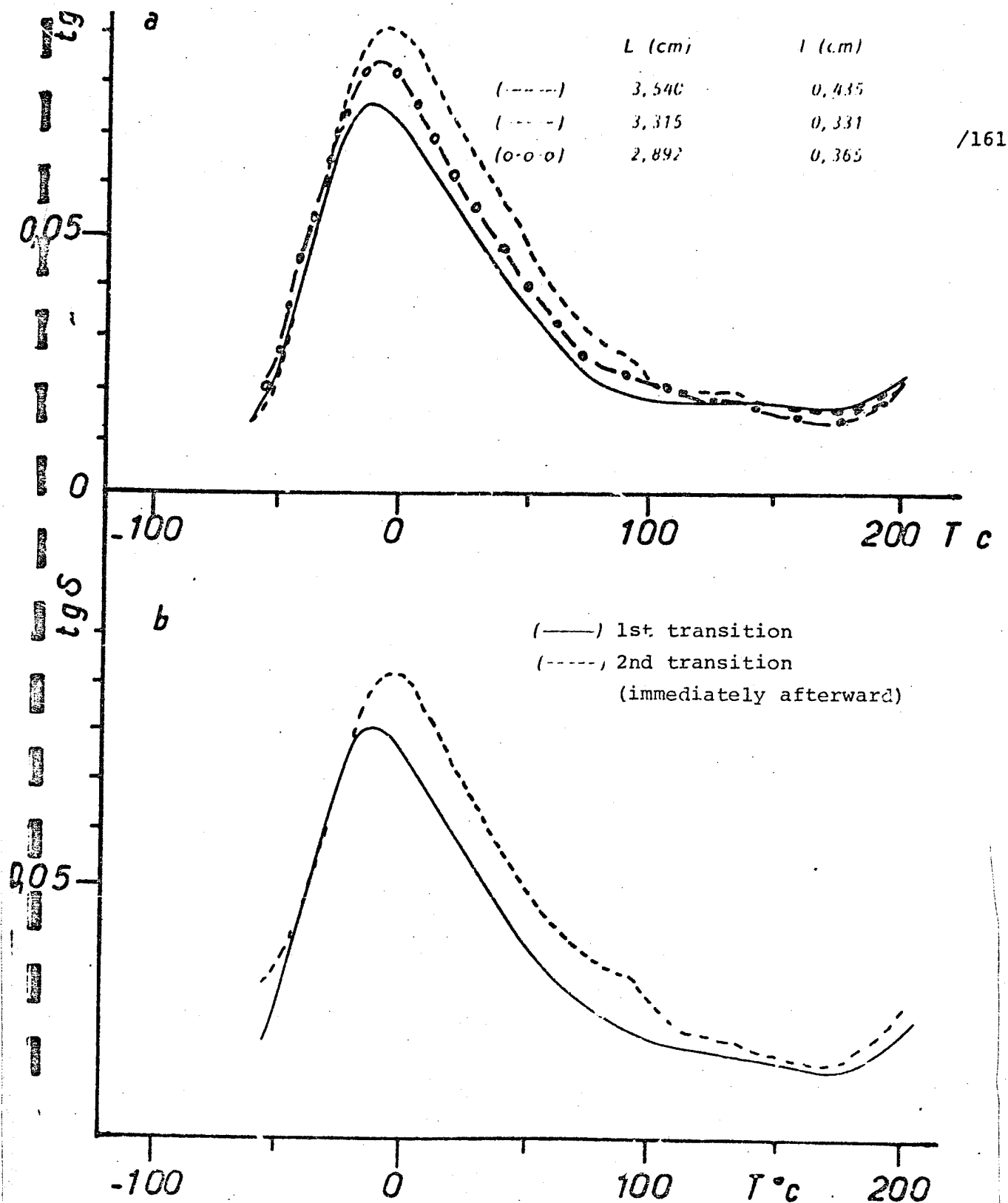because the samples are hard to cut out along angles (θ) between
90° and 0° (0° < θ < 90°).

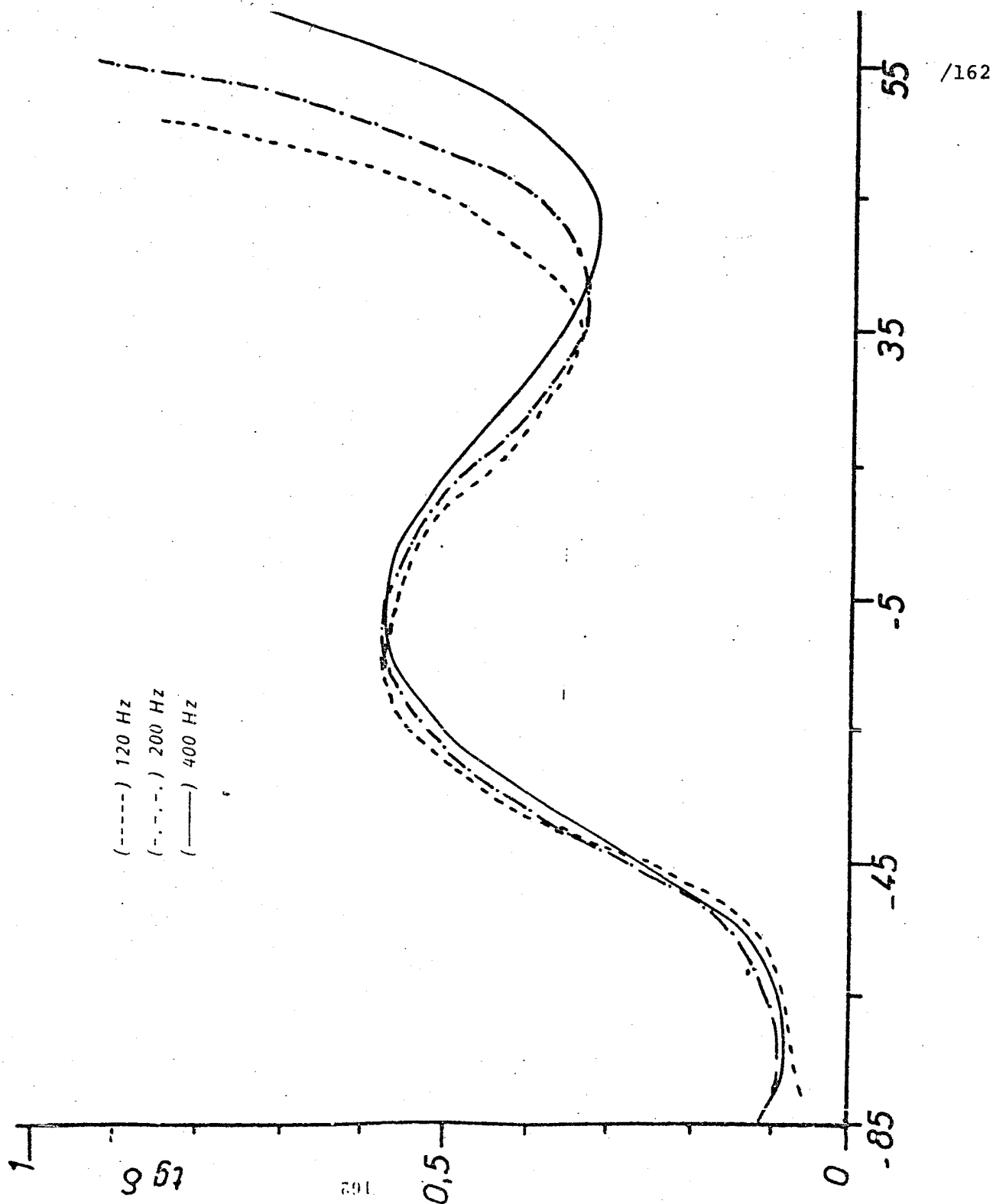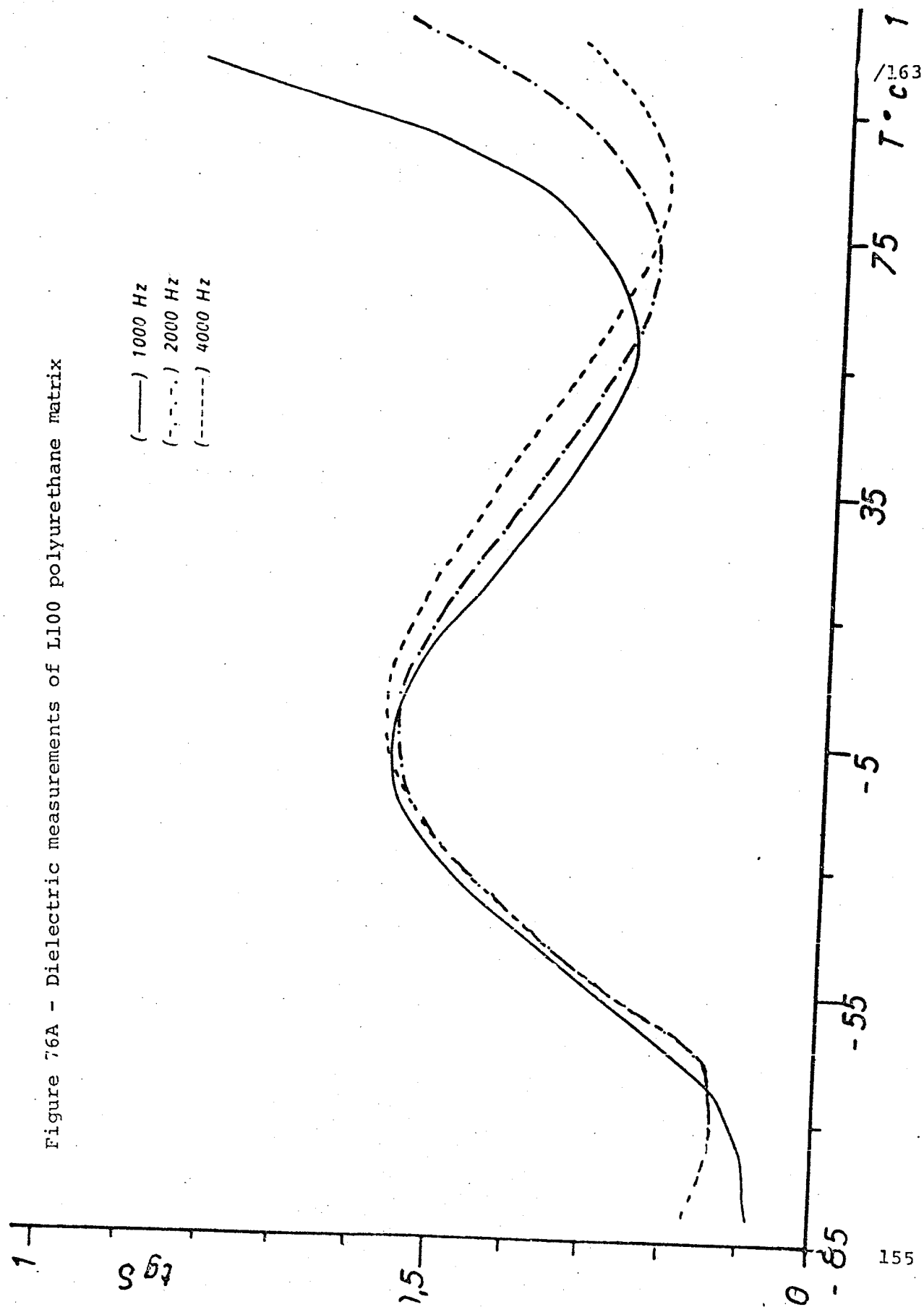Figure 75 - Behavior of V-L100 composite with layers of fabrics crossed at 90° (= ± 45°)

Figure 76 - Dielectric measurements of L100 polyurethane matrix

154

Figure 76A – Dielectric measurements of L100 polyurethane matrix

(———) 1000 Hz
(—·—·—) 2000 Hz
(————) 4000 Hz

$tg \, \delta$

/163

155

Figure 77 – Dielectric measurements of V-100 composite
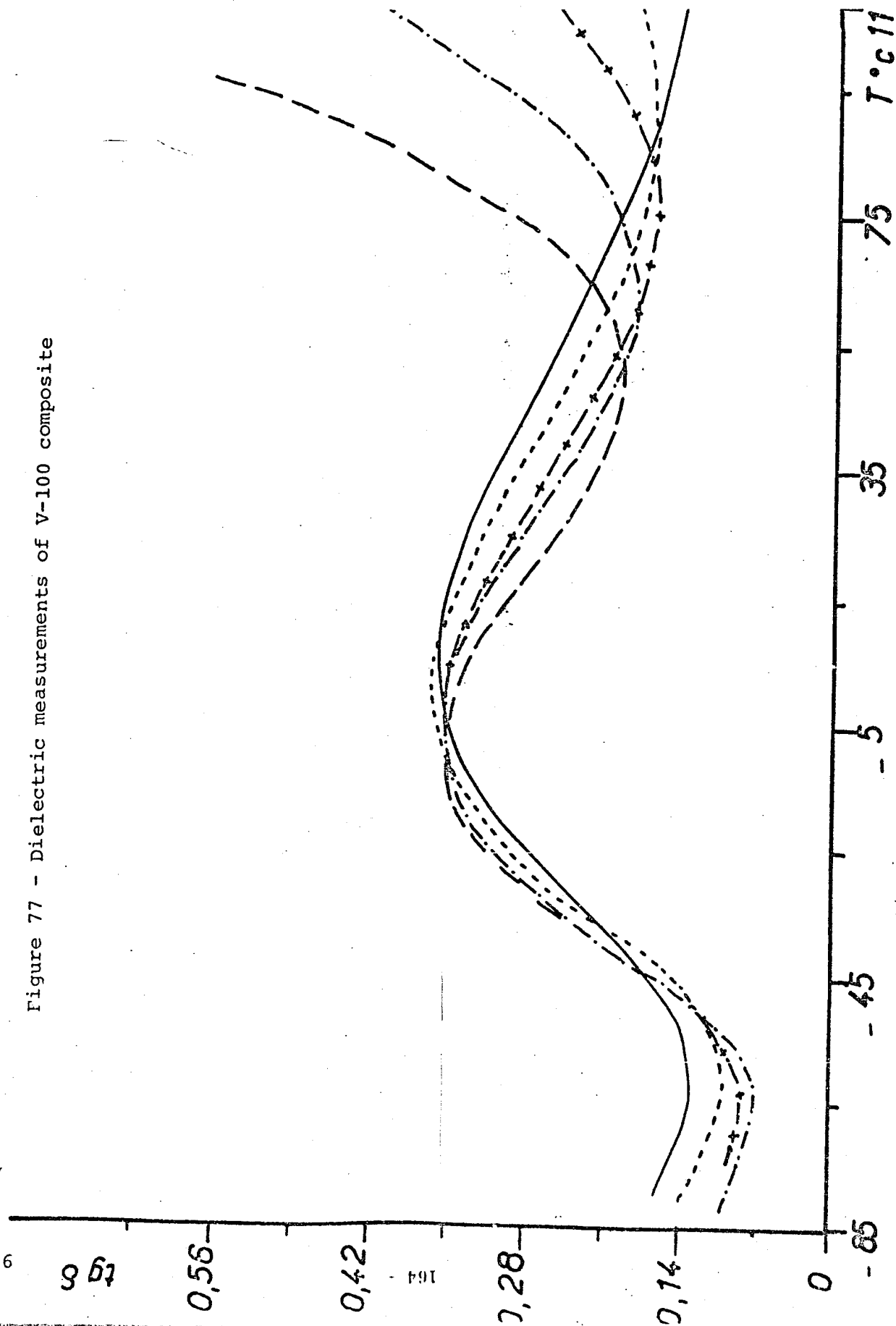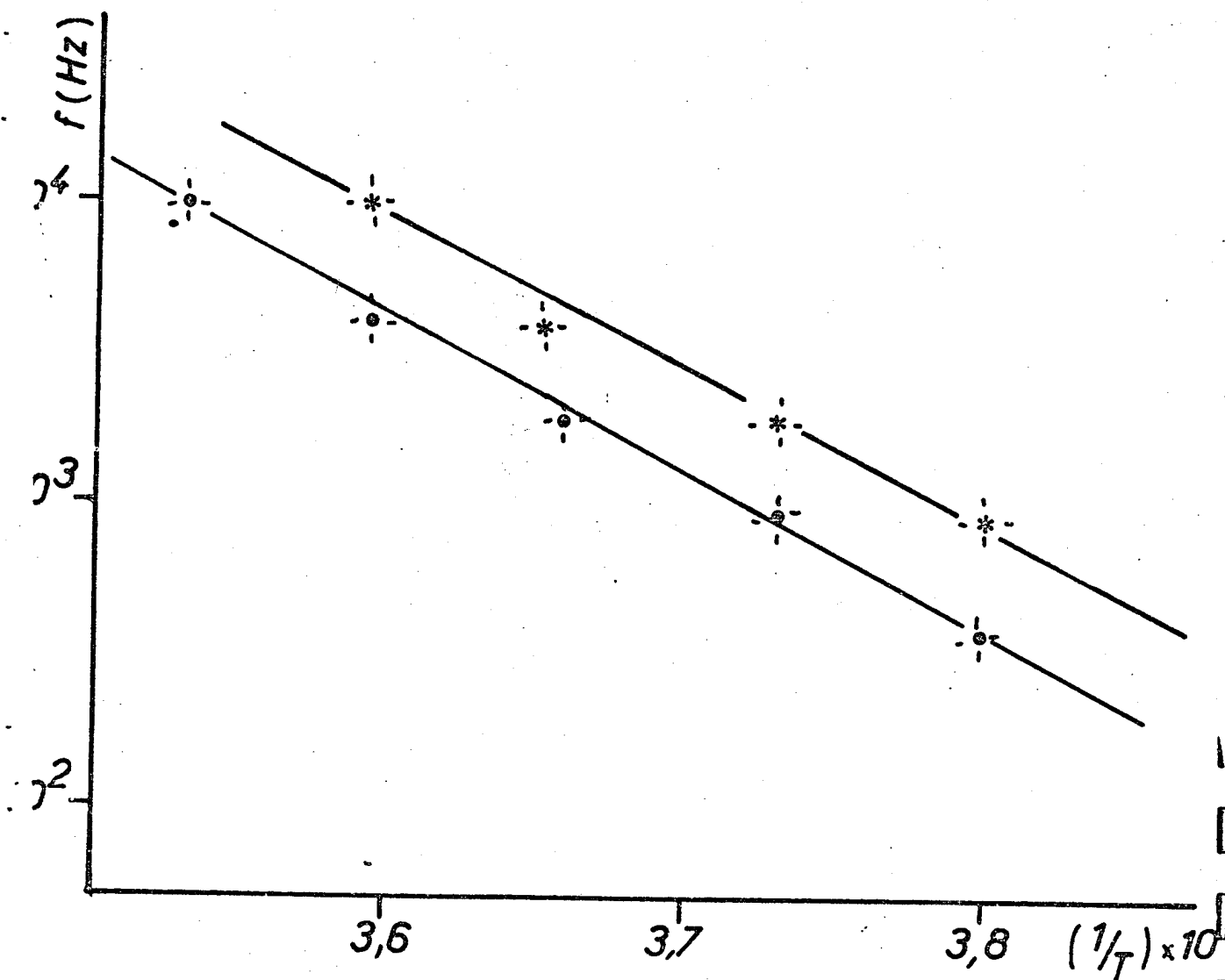
Figure 78 - Calculation of the activation energy for PUR-L100
and for V-L100
straight lines giving frequency as a function of $\frac{1}{T}$.

II-3-4)   Discussion and Conclusion

a) Our discussion will pertain to the presence of a second relaxation beyond the vitreous transition. Remember that the differential thermal analysis performed on our composites showed the absence of a second transition and that the only transition observed corresponded to the relaxation of the flexible sequences present in polyurethane.

157
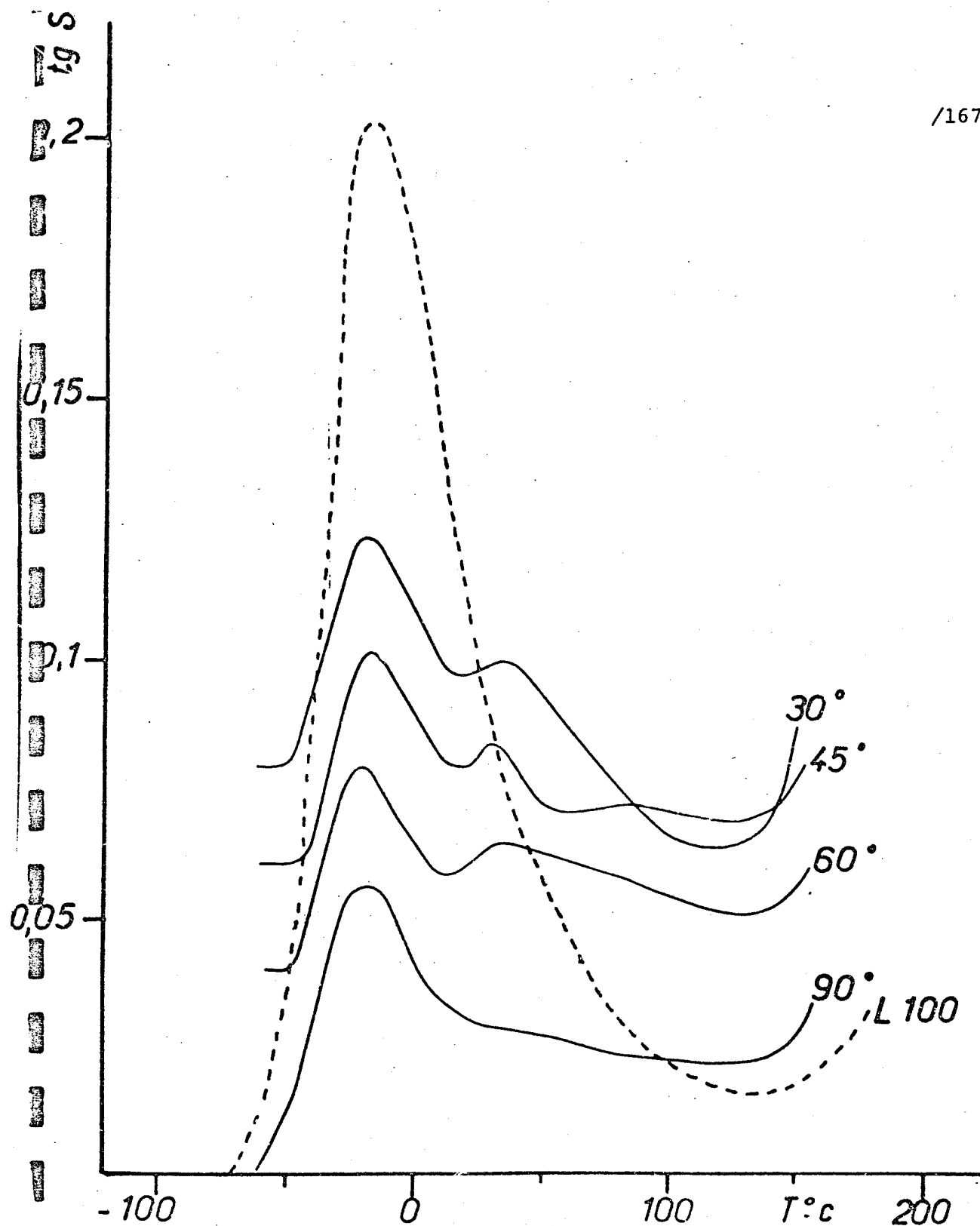
Figure 79 - Curves giving tg as a function of the temperature for L100 polyurethanes (-----) and for C-L100 composite according to the various values of angle θ.

158

Figure 80 - Curves giving E' modulus as a function of the temperature for PUR-L100 (-----) and C-L100 composite according to the various angles θ.

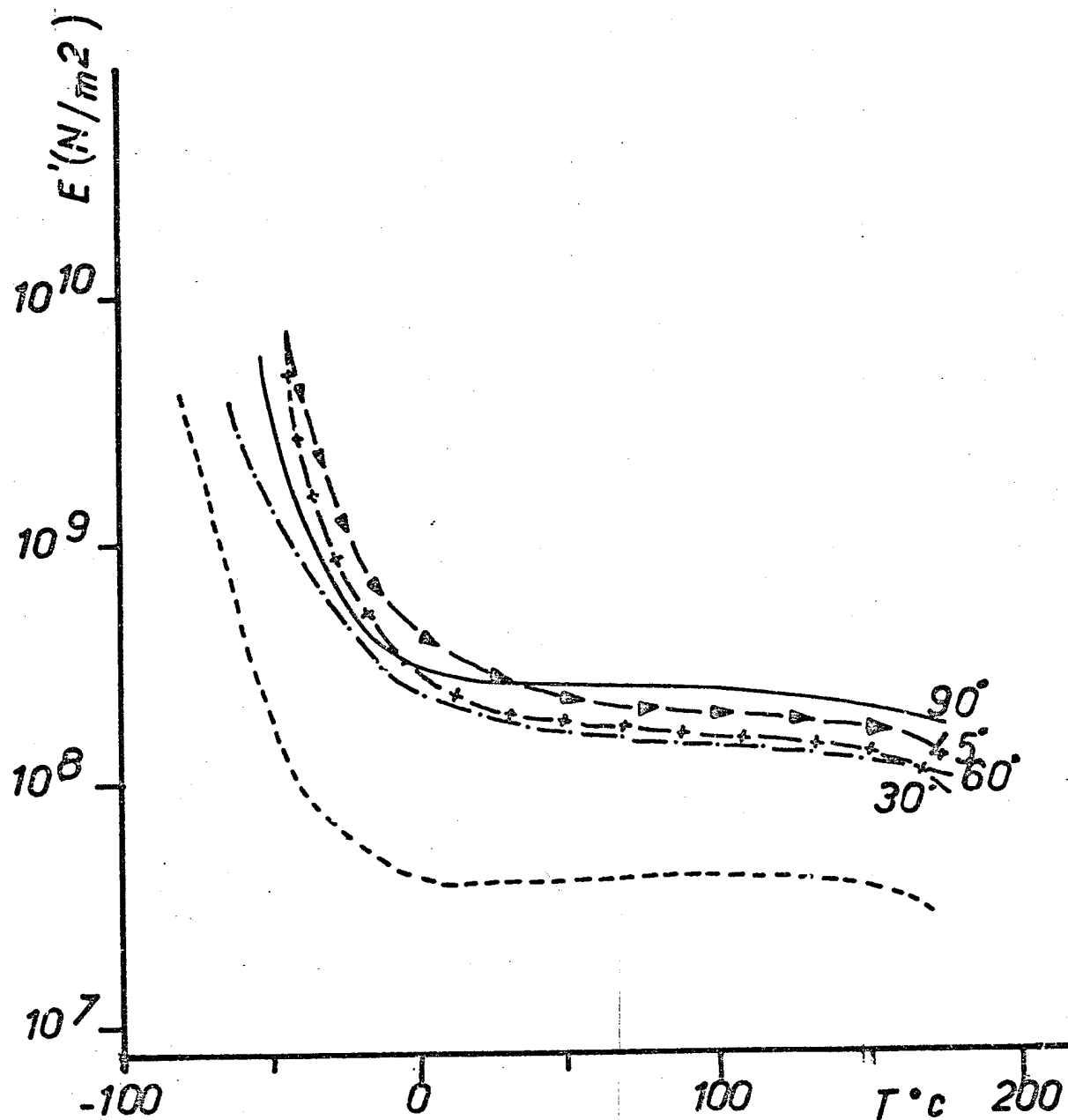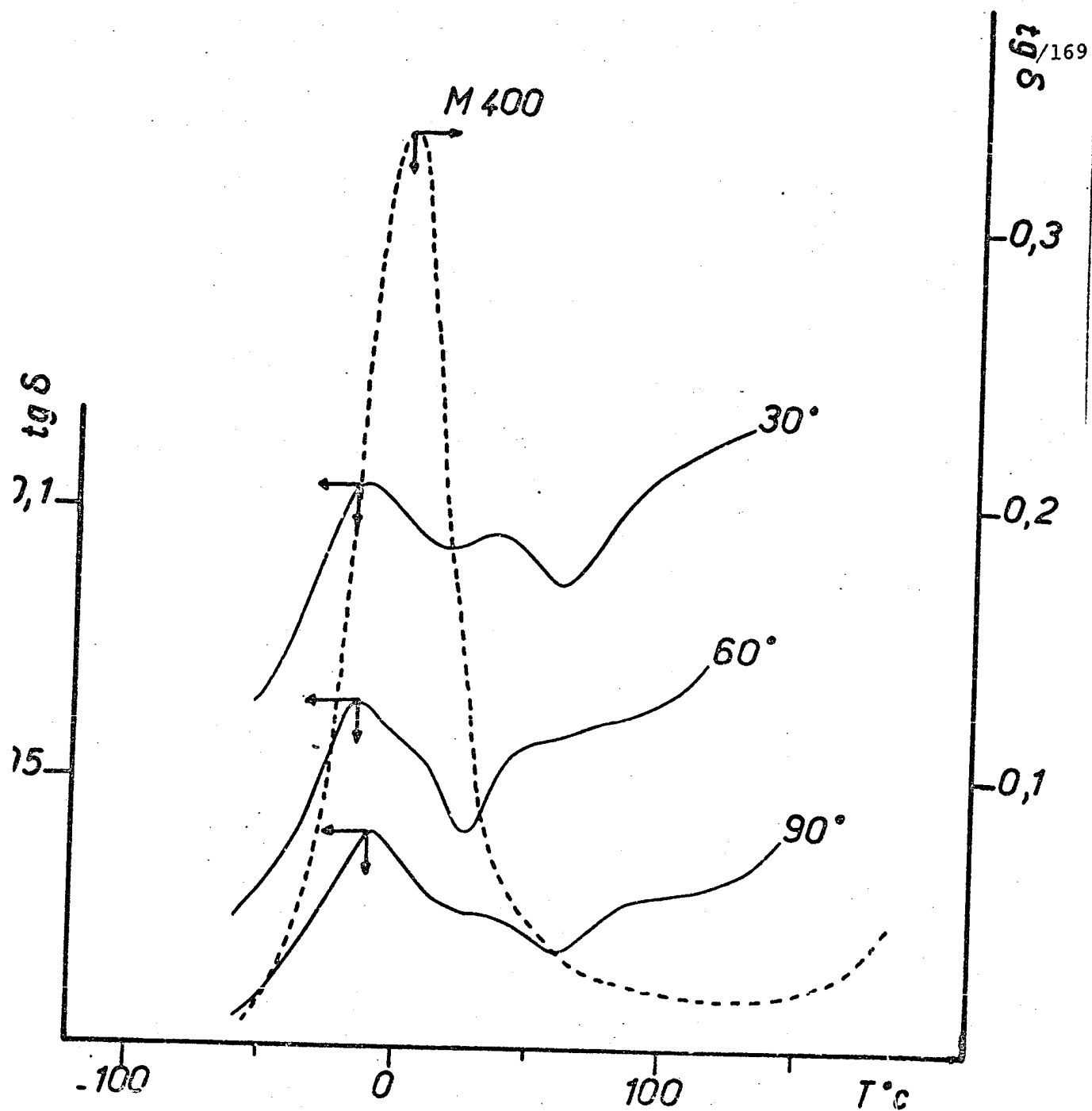Figure 81 - Curves giving tg δ as a function of the temperature for PUR-M400 (-----) and C-M400 composite according to the various angles θ.
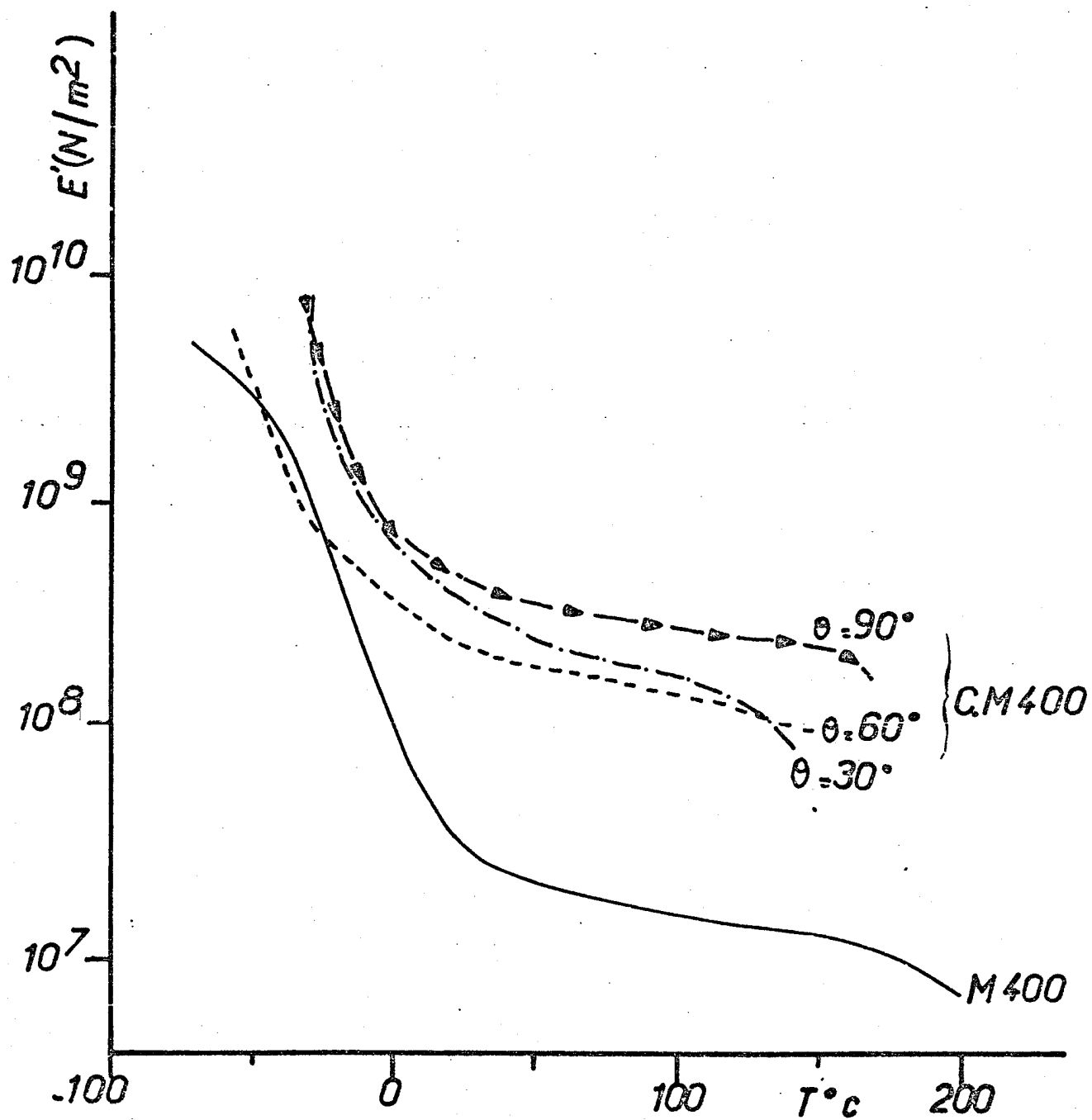
160

Figure 82 - Curves giving E' as a function of the temperature for PUR-M400 (————) and C-M400 composite according to various angles θ.

The second relaxation of molar origin would imply a double
fiber-interphase, interphase-die discontinuity. If a fiber-die
discontinuity is totally understandable, a discontinuity betwen
an interphase (of what thickness?) and the matrix is much harder to
accept. We therefore considered the possibility of being in a
measuring error.

b) Certain authors (BOYER, GILHAM et coll.; mainly, [77])
described for very numerous polymers a liquid-liquid transition
T_{11} above their vitreous transition Tg. According to these, the
liquid would be in a "fixed" state for temperature areas $Tg < T < T_{11}$,
for which beyond $T > T_{11}$ the set of macromolecules is involved in
a deformation. To show the existence of this transition, BOYER
and GILHAM developed a "Torsional Braid Analysis" (TBA) technique
which consists of a pendulum with free oscillations whose torsion
is given by a composite element which is an impregnated braid. The
braid is generally made up of glass fibers and the impregnator is
the polymer material whose mechanical responses were studied.

The concept of liquid-liquid transition T_{11} has been the sub-
ject of many controversies over the past few years. McKNIGHT and
NIELSEN esepcially [78] denied the molecular origin of this transi-
tion. We think that this controversy on the transition T_{11} may
concern our measurements because the measuring technique we used
implicates tensile stresses on the fibers, analyzed particularly
within a polymer.

Recently, D.J. PIAZEK et coll. [79] devoted a series of 4
articles on "A few proofs against the existence of a liquid-
liquid transition" to disprove its existence.

These authors showed that the second mechanical loss peak
which occurs after the first Tg-related one and which BOYER and
GILHAM ascribed to T_{11}, is a measuring error. It reflects the

162

behavior of the system and not the property of the material: the material which impregnates the braid is sheared by moving threads.

For this demonstration, PLAZEK built a "TBA" apparatus to study its behavior, especially its response as a function of the oscillation amplitude, the nature of the braid, its torsion, its oscillation frequency and the nature of the impregnator. The results show the presence of a second absorption peak during the peak temperature scanning tests. The peak is directly related to the interaction between the impregnator properties and the nonlinear response of the glass fiber braid (bare braids all have a nonlinear response).

Figure 83 (a and b) shows the results obtained on the behavior of a "glass braid - polystyrene" composite. One sees a second peak beyond Tg for a polystyrene of $\overline{Mw}$ = 20,400 and a glass fiber braid. The same curve appearance is observed for the same polymer, but with two different braids. Figure 84 shows the curves corresponding to the resporse obtained by varying the oscillation amplitude.

According to these two experiments the two maximum levels are related to Tg for tne first and to the "braid" effect for the second. This would therefore correspond to friction phenemona in the braid fibers, which increase with t.. amplitude of the frequency applied.

Thus, any composite sample made up of an elastic support coupled to the viscous liquid must necessarily produce such a "relaxation" whose origin is in no case molecular. This relaxation may be calculated from viscous components of the impregnator and braid characteristics. PLAZEK calculated the values of tg θ for a system where the material which impregnates the braid is sheared by the moving fibers. The calculated curves (Figure 85) have a second relaxtion peak beyond the vitreous transition (Tg).

163
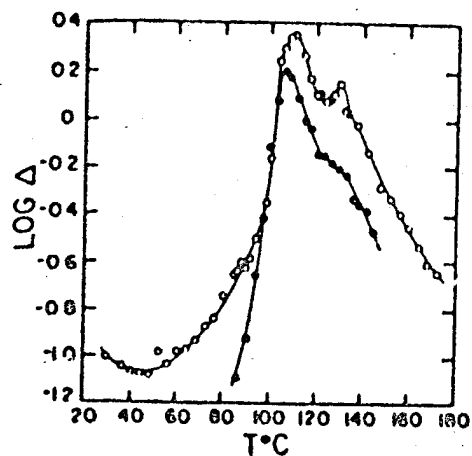
Figure 83 g - Logarithm of decrement for polystyrene (Mw = 20,400) in the case of two different braids (( ) → braid length # 6 cm; (●) → # 2) as a function of the temperature. The braid torsion is kept constant in both cases.

Figure 83 b (right) - Variation of Log v^2 and Log Δ as a function of the temperature for polystyrene (Ms = 20,400) using a braid # 5 cm long (v = frequency; Δ = decrement)
(-----) curves obtained during temperature rise
(———) curves obtained during temperature decline.
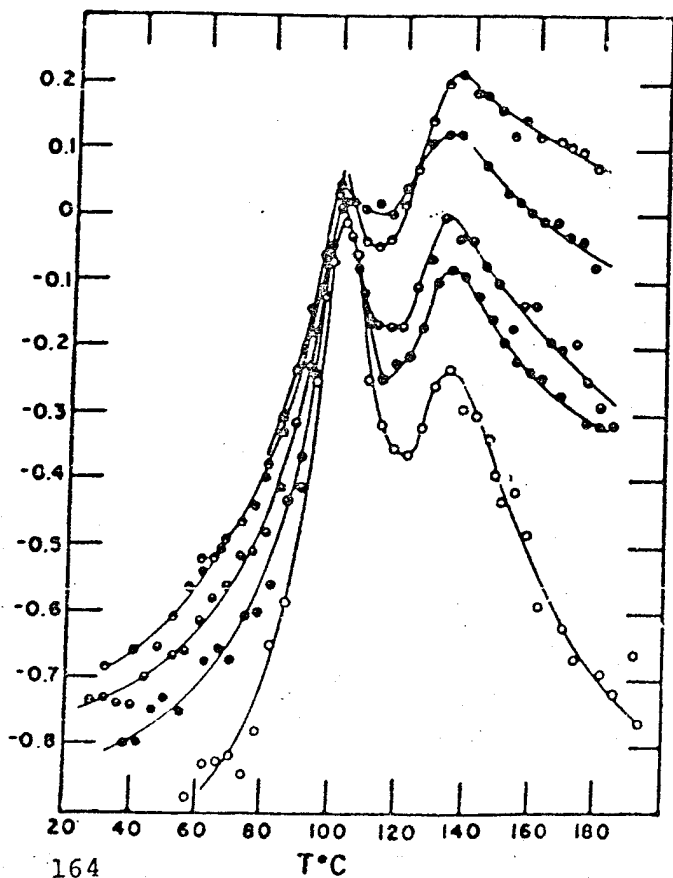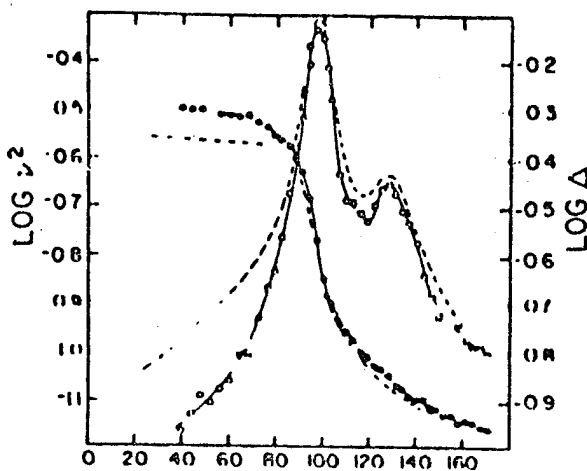
Figure 84 (left) - Variation of Log Δ for polystyrene (Mw = 20,400) using braid #4 cm long as a function of the temperature. Behavior recorded at various oscillation amplitudes.

(●) 40° ; (●) 15° ; (●) 8° ; (●) 4° et (O) 1,2°

164
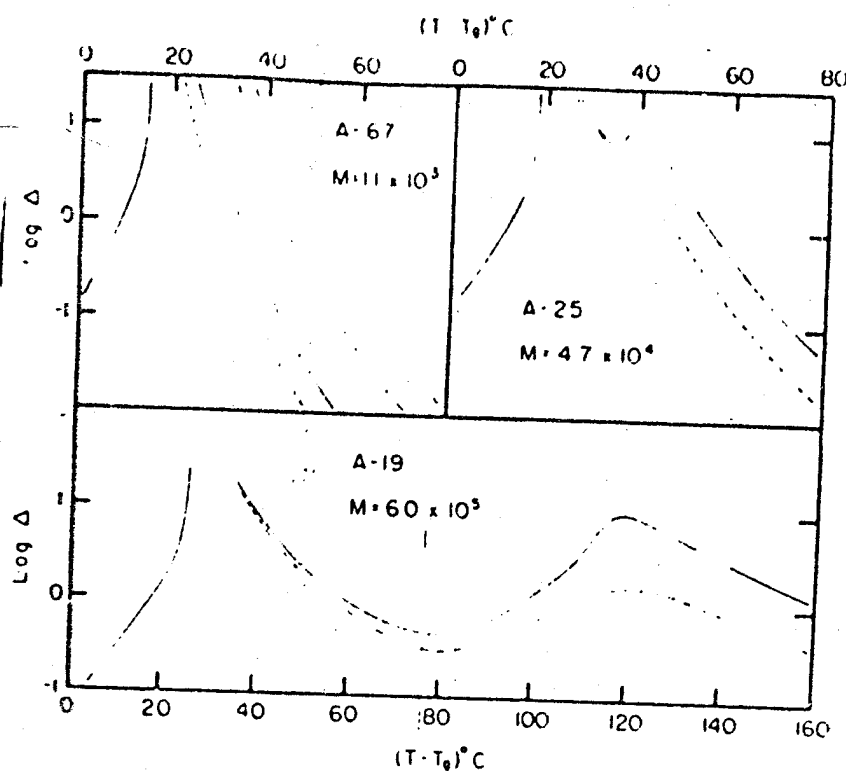
Figure 85 - Variation of log of decrement as a function of (T - Tg)°C. Results obtained by calculation, for anion polystyrenes with oscillation system whose moment of inertia is 1000 g/cm^2. The various peaks obtained beyond Tg result from fibers which support the polymer. They have the following k constants:
k = 0.10 (-..-..-..); 1.0 (-.-.-); 10 (....);
100 (———) and 1000 dynes,cm (-----).

c) In concluding this study, by analogy with what we have just presented, we believe that the second relaxation observed during our viscoelastic tests and K. REED's tests does not have a molecular origin, but comes from the system used. This may therefore be related to the stresses of the fibers present in our samples tested with rheovibron where they were under tensile forces which could cause slipping phenomena of the die in the fiber direction. This analogy helps us to explain the following points:

The appearance of the second peak obtained on the tg δ = f(T°C) curves is increasingly distinguishable for samples where the angle θ approaches the fiber direction, because slipping does exist for θ ≠ 90° and it is nil for θ = 90°.

The variations (small, it is true , but not completely negligible) which exist with the form factor.

The disappearance of the second relaxation peak for crossed fabrics when $\theta = \pm 45°$.

The fact that this second relaxation does not occur when dielectric measurements are performed on a nondirectional sample.

It would be interesting if we could build a model of the viscoelastic measurements with rheovibron and perform theoretical calculations comparable to those of PLAZEK for "TBA". Qualitatively-speaking, one could conclude that the response of our composite depends on the system used and involves several elements, such as the fiber modulus, their distribution in the polymer, the type of die and above all the fiber-die adhesion.

It would seem that the die slipping along the fibers during measurements with rheovibron reaches a limit fairly quickly, as the adhesive forces play the role of retraction forces. (This would explain the absence of the second relaxation after three successive measurements on rheovibron).

In the case of carbon composites where the soluble die extracts are high ($\cong 25\%$) and where the fiber-die adhesion seems weak, the peak of the second relaxation is sharper and more distinct (Figures 79, 81). In this case, we do not see a shouldering of the peak associated with the vitreous transition, but relatively well-defined peaks.

APPENDIX

EXPERIMENTAL PART

1) <u>INTRODUCTION</u>   /179

This part describes the various experimental techniques used in this study:

166

.Characterization of the basic diol oligomers,

.Characterization of the commercial diisocyanate prepolymers,

.Synthesis of polyurethanes and corresponding composites,

.Analysis of die quality in composites,

.Static mechanical measurements,

.Dynamic mechanical measurements,

.Dielectric measurements,

.Examination in microscope.

2) METHODS OF PHYSICO-CHEMICAL ANALYSIS

2) 1 - Chromatography Via Gel Permeation (GPC)

CPS consists of separating all products contained in a mixture as a function of the hydrodynamic volume. For example, small organic molecules are separated from macromolecules.

Use of the GPC technique enabled us to:

.measure the properties of the reactive prepolymers such as mean weight in $\overline{Mn}$ number and the polymolecularity index $\overline{Mw}/\overline{Mn}$,

.analyze the soluble parts after extraction testing on the polyurethane die alone or in the composite.

2) 2) Cryometry

The mean molecular weights in $\overline{Mn}$ number of diol oligomers, are determined via cryometry in benzene, using an apparatus which provides an accuracy of $\pm 5\%$ for $\overline{Mn} < 4000$. However, one of the main sources of systematic errors is the presence of low molecular weights (traces of solvents, water, secondary reaction products, etc.) which may be eliminated by purifying the oligomers under dynamic vacuum before measuring $\overline{Mn}$.

2) 3 - <u>Nuclear Magnetic Resonance RMN</u> [1]H

We used this method to dose the oligomer chain endings to determine their mean functionality $\overline{Fn}$, and to "chemically" characterize the commercial reactive prepolymers.

Actually, the dosage of hydroxyl chain endings is a delicate problem. The phtalilation method [80] allows us to find the number of hydroxyls in diol aliphatic polymers. It is applicable to gycol polyethers containing a mixture of primary and secondary groups.

The functionalities of diol oligomers may also be determined in certain cases, such as for hydroxytelechelic polybutadienes (PBHT), via direct RMN ^{1}H analysis [81,82] or more often by indirect dosage, acetylation [83] or silylation [84], for example.

For our study, we used a simple dosage method perfected in our laboratory [85] which calls on a chemical reaction between alcohol functions and a monoisocyanate surplus, then a GPC or RMN ^{1}H analysis. The diol $\alpha-\omega$ polyether oligomers (POTM) modified with n-propyl isocyanate (n - C_3H_7 - NCO) are analyzed in RMN ^{1}H, for example, (Figure 86) and the $\overline{Fn}$ dosage occurs via a simple planimetry of the CH_3 in $+ \underline{C}H_3 - Ch_2 - CH_2 - NH +$ and in the $\beta-CH_2-$ groups of the chain.

$$\overline{Fn} = \frac{(\underline{C}H_3 - CH_2 - CH_2 - NH -) : 3}{(CH_2 - C\underline{H}_2 - C\underline{H}_2 - CH_2 - O) : 4} \times \overline{DPn}$$

or via planimetry of the peaks at 4.18 ppm and 1.69 ppm:

$$\overline{Fn} = \frac{(- C\underline{H}_2 - O - CO -) : 2}{(- CH_2 - C\underline{H}_2 - C\underline{H}_2 - CH_2 - O) : 4} \times \overline{DPn}$$
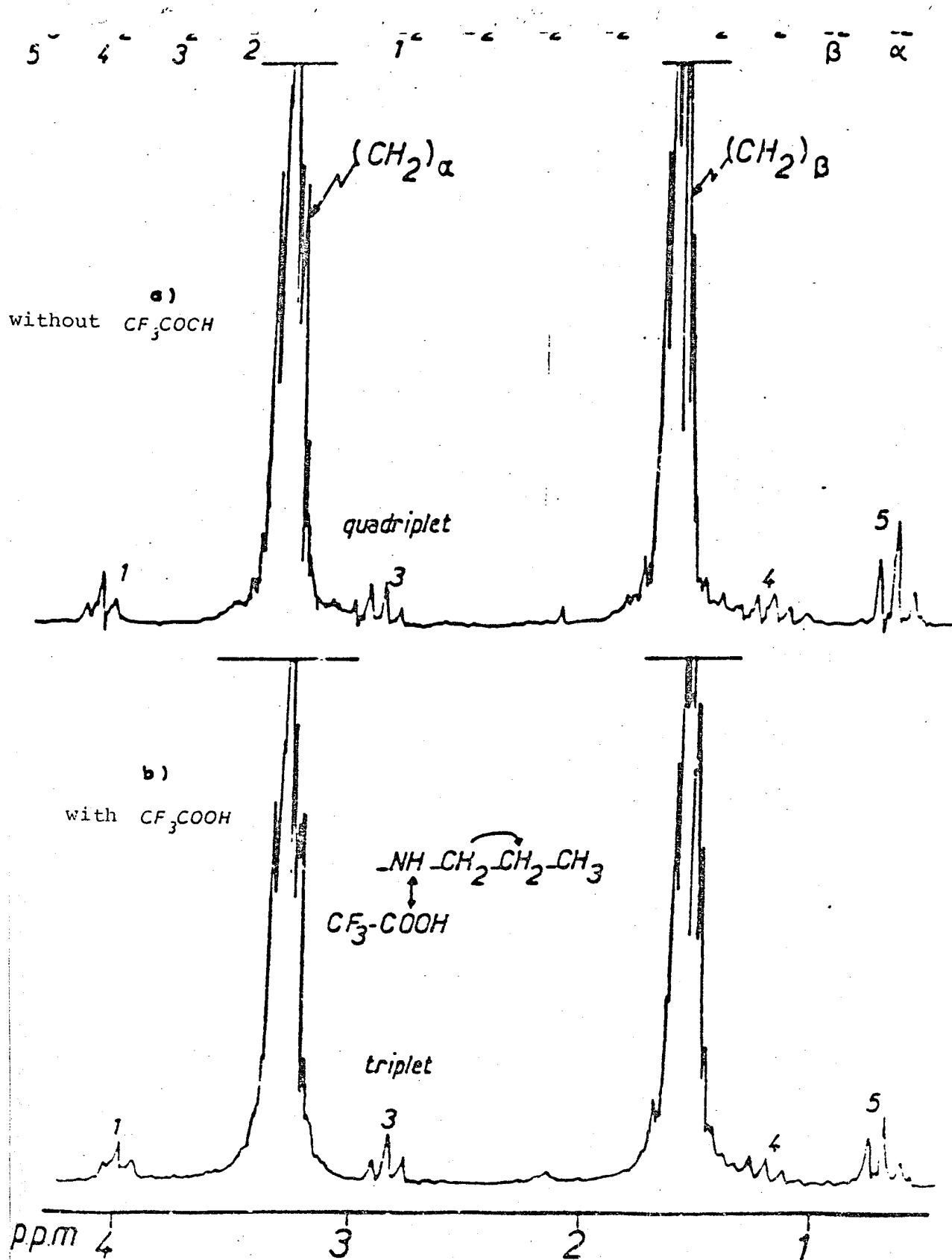
168

Figure 86 – RMN ^{1}H spectrum of a glycol plyoxytetramethylene after reaction with n-propylisocyanate.

We preferred the first method. In all cases, the calculation of $\overline{Fn}$ requires a very correct measurement of $\overline{Mn}$.

The addition of a few drops of CH_3COOH (trifluoracetic acid) into the RMN tube makes it possible to identify the coupling between ($-CH_2-$) of the $nCH_3-CH_2-CH_2$ - NH group with adjacent protons (Figure 86 b).

The RMN ^1H analyses are performed on a Brucker spectrometer at 80 Hz.

The spectra are made using 5% solutions (weight/volume) of the products to be analyzed in deuterium acetone and for certain products in deuterium benzene. In all cases, the internal reference is tetramethylsilicone (TMS).

2) 4 - Infrared Spectrometry (IR)

The infrared spectrometry technique was used in the analysis of the polyurethane die quality in various corresponding composites.

The IR analysis was performed on a spectrometer using the Fourier Transform (IRTF) Nicloet MX1. The number of accumulations varied from 32 to 128 according to the spectra (transition time 1 minute to 4 minutes). The samples (ground) were mixed and formed into pellets with potassium bromide kBR used specially for IR spectrometry.

2) 5 - Chemical Reversion Dosage of the NCO Isocyanate Functions

Excess dibutylamine (DBA) reacts to the isocyanate (NCO) functions of prepolymers. The reversion dosage of excess DBA using hydrochloric acid makes it possible to obtain the NCO content.

The reactions involved are the following:

170

$$R - N = C = O + H - N \diagup^{C_4H_9}_{\diagdown C_4H_9} \quad \rightarrow R----N - C - N \diagup^{C_4H_9}_{\diagdown C_4H_9}$$

DBA

$$H - N \diagup^{C_4H_9}_{\diagdown C_4H_9} \quad + HCl \quad \rightarrow \quad HCl, \ H - N \diagup^{C_4H_9}_{\diagdown C_4H_9}$$
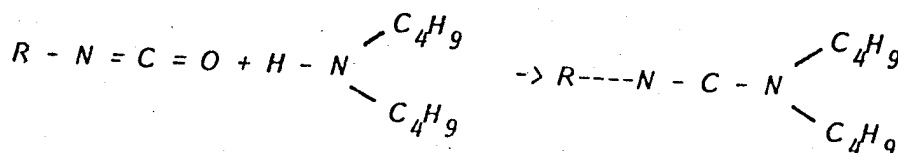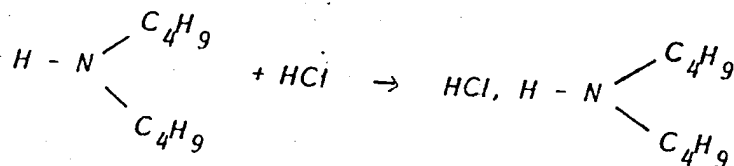
excess DBA

The reagents are:

.N/10 dibutylamine in THF
.green from bromocresol (1% solution in THF),
.N/10 hydrochloric acid in water solution.

about 1 g prepolymer reacts with 20 ml DBA (N/10) for about 30 minutes. The excess DBA is titrated with the HCl N/10 solution in the presence of a few drops of "bromocresol green". At the equivalent point, the solution changes from a dark blue color to an orangish yellow.

2) 6 - Differential Thermal Analysis

The thermograms are performed on two types of analyzers: DuPont 990 and Mettler Ta 3000, in sealed capsules with a temperature rise of 10°C/mn. The temperature range studied varied from -150°C to +300°C and for the melting enthalpy measurements ΔHf, the apparatus was calibrated with indium.

Table XXIX shows diol $\alpha-\omega$ oligomers used, as well as their properties and various construction patterns.

3) EXTRACTION TESTS

We used tetrahydrofurane (THF) as extraction solvent, because it is our GPC analysis solvent.

The products were agitated vigorously in THF at ambient temperatures for 48 hours.

The remaining polymer is filtered, then dried under vacuum until it reaches constant weight.

4) SYNTHESIS OF POLYURETHANES AND CORRESPONDING COMPOSITES /185

We used two methods of synthesis for polyurethanes formulated in the laboratory, in solution and in mass. For polyurethanes pre-pared from commercial prepolymers, as well as for various compos-ites, the synthesis was performed in mass.

Figure 87 shows the general diagram for obtaining polyurethane. The synthesis is conducted in two phases:

4) 1 - Laboratory Formulation; Synthesis in Solution

All of our syntheses were performed in solution under argon atomosphere and in anhydrous toluene as argon solvent.

The first phase (Figure 87) lasted 2 hours and the second 48 hours. At the end of the reaction, the polymer was precipitated in methanol, dried under vacuum at 60°C for 24 hours, then pressed in the form of plates at a temperature which depends on the type of chain extender used.

172

TABLE XXIV

PROPERTIES AND CONSTRUCTION PATTERNS OF α,ω DIHYDROXYLIC OLIGOMERS

Oligomer	origin	$\overline{Mn}$ ± 10 %	$\overline{Mw}/\overline{Mn}$	Fn ± 0,1	1,4 mole (%)	Tg (°C)
PBHT-9	Nippon Soda "G 2000"	2 200	1,3	2,1	12	– 20
PBHT-9-100	Nippon Soda "G 2000" hydrogenated 100 %	2 290	1,3	1,8	10	– 45
POTM 1	Du Pont Téracol 2000	2 400	2,1	1,8	--	– 93
POTM 2	BASF "PTHF" 1000	1 210	1,7	2,7	--	

Polyoxytetra-methylene (POTM)

$$\{CH_2 - CH_2 - CH_2 - CH_2 - O\}$$

Polybutadiene 1,2
    PBHT

$$\{CH - CH_2\}$$
$$|$$
$$CH$$
$$\|$$
$$CH_2$$

Polybutadiene 1,2

PBHT-H

$$\{CH - CH_2\}$$
$$|$$
$$CH_2$$
$$|$$
$$CH_3$$

4)2 - Laboratory Formulation; Synthesis in Mass

In this case, the first phase (obtaining the diisocyanate prepolymer) is performed for 2 hours at 80°C. At the end of reaction, the reactional mixture obtained is degasified under vacuum (on the order of 5 mm Hg) with a vigorous agitation.

Once the mixture is degasified, we proceed with the second phase which consists of adding the desired chain extender to the reactional mixture while agitating vigorously for about 1 to 15 min.

The final mixture is then poured into a teflon mold and subjected to cooking for 24 hours at 80°C (otherwise, the experimental conditions will be redefined) to complete the reaction.

4)3 - Commercial Formulation; Synthesis in Mass

For polyurethanes prepared from commercial diisocyanate prepolymers, the second phase, that which consists of adding the chain extender, is the only one remaining to be accomplished. This consists of heating the diisocyanate to the desired temperature and degasifying it under vacuum. The chain extender is then added and the total mixture is heated after pouring it in a teflon mold.

In the synthetic reactions in mass, an important factor is used: the lifetime in the pot. It varies according to the chain extender - diisocyanate molecule couple. In general, the lifespan is short for diamine chain extenders, whereas it is longer for diols of low molecular weights.

The experimental conditions are defined in the presentation of the results.

4)4 - Synthesis of the Polyurethane Composites

In all cases (laboratory or commercial formulation) the

174

Polyol

HO —| *Polyester* or *Polyether* |— OH

OCN —| |— NCO
diisocyanate

OCN —| |— NCO
diisocyanate

OCN —| |— N - C - O ∿ *Polyester* or *Polyether* ∿ O - C - N —| |— NCO

urethane group

urethane group

diisocyanate prepolymer

chain extender (diol)

triol

chain extender (diamine)

Polyurethane

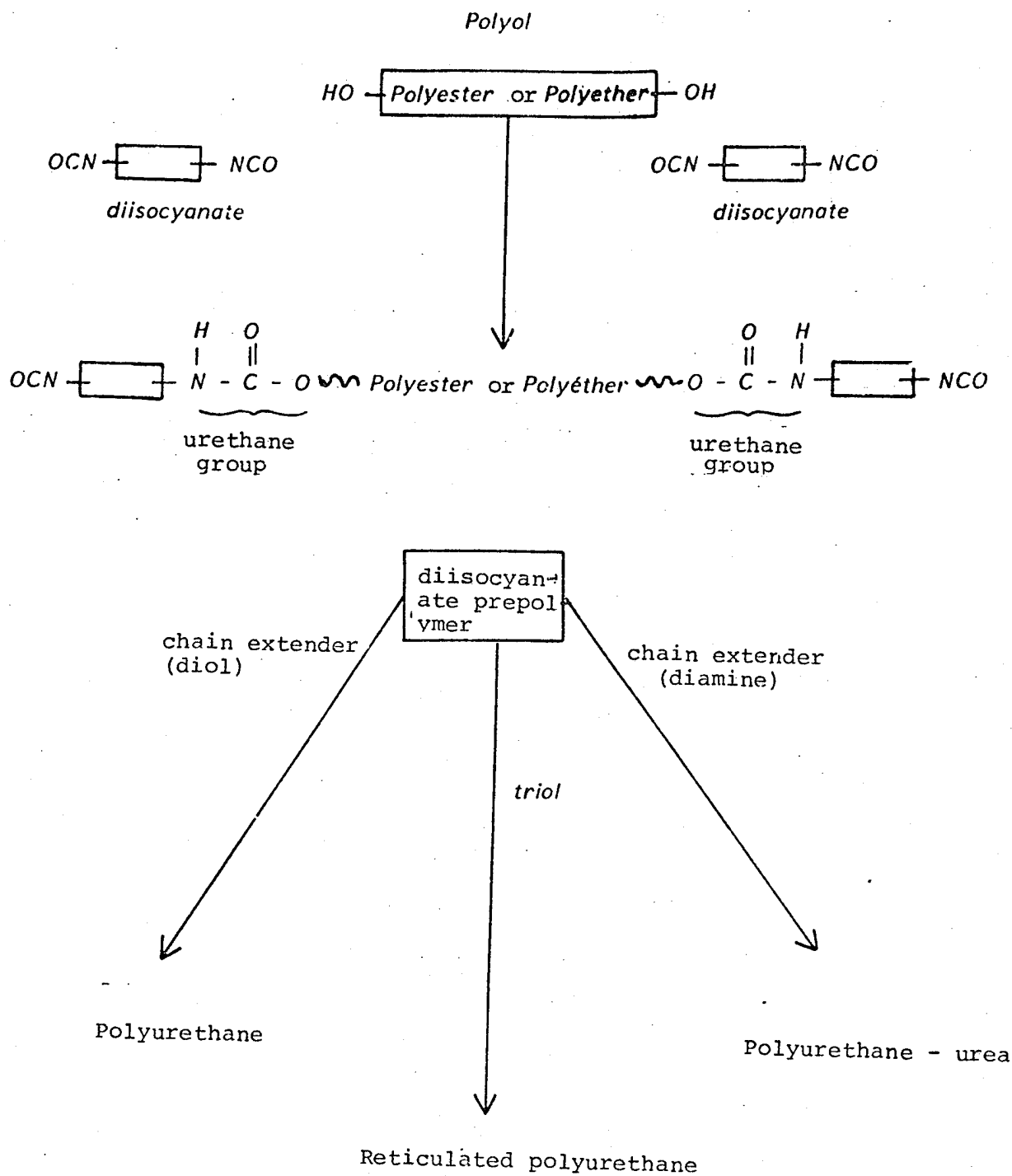Reticulated polyurethane

Polyurethane – urea

Figure 87 – Obtaining a PUR – General Diagram

175

synthetic reactions occur in mass. We designed a special mold to carry out the synthesis of composites in the best operating conditions. We give more details in chapter II on composites.

5) STATIC MECHANICAL PROPERTIES

This part concerns both polyurethane dies and composites.

5)1 - Static Mechanical Measurements on the Die

The mechanical properties are studied on a tensile machine (JJ. LLOYD Instruments).

The elongation at rupture is accomplished at the rate of 30 mm/mn on samples about 1 mm thick and whose shape complies with standard H_3.
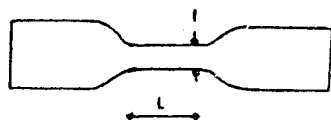
I = 4 mm
L = 17 mm

The tearing strength is determined on the samples which have the following shape:

The curves giving the stresses as a function of the deformation are recorded. The curves showing the tensile or tearing properties of polyurethane, such as the modulus of elasticity (E_o), the rupture strain σ_r, the elongation at rupture ϵ_r, etc. are recorded.

5) 2 - Static Mechanical Measurements on Composites

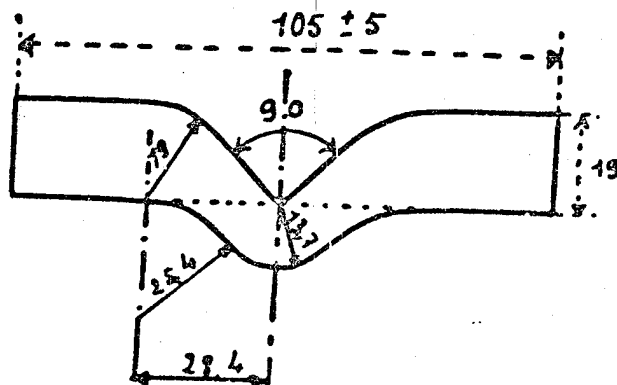We did not use tensile tests to study the static mechanical properties, as the first tests could not be processed for technical reasons. Actually, the rupture in the samples often began in the jaws.

The static mecahnical measurements are therefore performed   /189
by 3-point bending measurements using an assembly installed on a J.J. LLOYD tensile machine. We performed the measurements as a function of the temperature using a J.J. LLOYD environmental chamber.

Figure 88 shows a diagram of the bending test as well as the dimensions of the test samples.
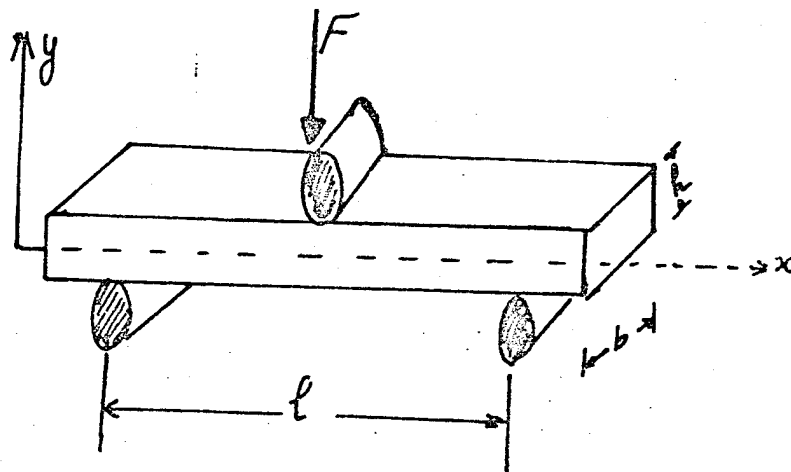

Figure 88 - Bending Test on 3 Points

with b = width of test sample
     h = thickness of test sample
     1 = distance between the support points (50 mm)

Experimentally, one records at the rate of 5 mm/mn the curve (force - f(deflection)) from which the rupture stress σ_r (or strain for a specific stress F) and the modulus of elasticity under bending E may be calculated. The characteristics are given by the following equations:

$$\sigma_r = \frac{3\,Fr\,l}{2\,b\,h^2} \quad ; \quad E = \frac{F\,l^3}{4\,b\,h^3\,\delta}$$

with F: force corresponding to the deflection δ in the linear range in the vicinity of the origin.

6) DYNAMIC MECHANICAL PROPERTIES

The dynamic mechanical properties are determined on the DDV II B Rheovibron viscoelasticimeter on both the die and on the corresponding composite.

The DDV IIB Rheovibron viscoelasticimeter (Figure 89) brings to evidence the dependency of the preservation modulus, the dissipation modulus and the angle of loss with the temperature at four frequencies (3,5; 11, 35 and 110 Hz). The temperature range spreads from -120°C to 200°C. This apparatus provides a direct reading of the angle of loss (tg δ).

A sinusoidal deformation is applied to one end of the test sample and the force transmitted is measured on the other end. This is therefore a tensile test. The phase shift between the strain and deformation is directly determined.

The force transmitted and the value of the phase shift are read to calculate the real and imaginary parts of the dynamic tensile modulus.

C-3
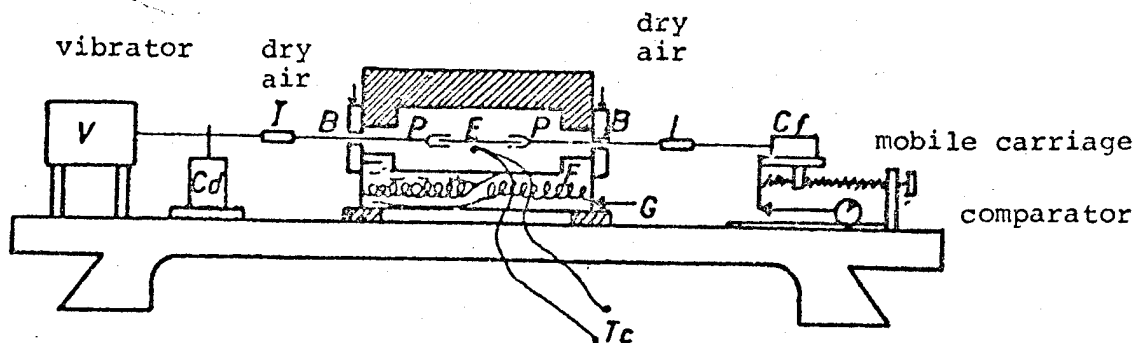
E - Test Sample   F - Thermostatic Fluid

P - Clip   G - Circulation of Conditioning Gas

T_c - Thermocouple C_d - Displacement Sensor

I - Thermal Insulator C_f - Force Sensor

Figure 89 - Diagram of DDV II Rheovibron

$$E^* = E' + iE''$$
$$E' = |E^*| \cos \delta$$
$$E'' = |E'| \sin \delta$$

$$tg \; \delta = \frac{E''}{E'}$$

The measurable Tg δ values range from 10^{-2} to 1.8 with an   /191
accuracy of 2%. As for the modulus, the measurements may range
from 10^5 to 5.10^9 N/m^2 with an accuracy of 10%.

The samples used have the following dimensions, on the average:
length = 40 mm, width = 4 mm, thickness = 1 mm.

The measurements are performed by lowering the temperature
by 5°C/mn and by raising the temperature by 3°C/mn.

7) DIELECTRIC MEASUREMENTS

The dielectric measurements are performed using a cell made up of a 4274 A - LCR Mettler type Hewlett Packard automatic bridge, in a fairly broad temperature range (-100°C -> + 100°C) and with a frequency ranging from 100 Hz to 10 KHz.

The samples in the form of films or thin plates are metallized under vacuum to improve the contact with the measuring electrodes.

8) EXAMINATION IN THE MICROSCOPE

Our laboratory is equipped with a Wild MSA type stereoscopic microscope.

We can also use an electronic scanning microscope (MEB) to study the rupture surfaces. We made a few photos on the polyurethane composites (fiber arrangement, breaks and rupture surface).

GENERAL CONCLUSION

There is no published result on composite materials with a polyurethane matrix reinforced with long unidirectional fibers. The only known work is on rigid, high-density polyurethane foams, reinforced with ground or cut fibers. Our study is the first one carried out on the behavior of such materials.

1) The first part of this work defined the structure-property relationships as a function of the type of chain extender for various prepared polyurethanes (laboratory and commercial formulations).

The characteristics of the basic reagents (diol α,ω oligomers or diisocyanate prepolymers, chain extenders) may influence the structure of the final material.

In order to understand the behavior of the various commercial

formulations, we undertook a study on the influence of the chain
extender types on the polyurethane properties. We derived the
following information:

The properties of polyurethane elastomers depend little on
the crystallinity of the rigid nodules, but mainly on the type
and number of interactions beteen rigid segments and the ability
of these segments to move in their amorphous state. For example,
by comparing decanediol and butanediol as chain extender, the
high-temperature creep of the corresponding polyurethanes occurs
at temperatures below the melting point of the corresponding rig-
id crystalline segments.

Use of an aromatic diol instead of a linear aliphatic diol
as chain extender gives the corresponding polyurethanes a better
high temperature performance. This is also true when an aromatic
diol is replaced by an aromatic diamine (Moca).

The commercial formulations cover an entire range of elastomer
properties.

The polyether prepolymers (L and M adiprenes) give the polv-
urethanes relatively low vitreous transitions (Tg) (-60°C; -50°C),
whereas with polyesters (cyanaprenes), the polyurethane Tg is - 35°C
approximately.

Polyurethanes obtained by using armomatic diamine (Moca)
as chain extender have a good high temperature behavior. However,
the "lifespan in the pot" of the reactional mixture is generally
short (1 - 10 minutes).

Use of diol (or triol) chain extenders in the commercial form-
ulations increases the "lifespan in the pot" of the reaction and
gives the corresponding polyurethanes lower rubber modulus values.

The relaxation of the flexible segments occurs in a narrow temperature range, with higher values for the maximum relaxation peak.

2 - The second part of the study devoted to polyurethane composites leads to the following conclusions:

The extraction and differential thermal analysis tests give us precious information on the quality of the die in the composites and therefore on the adhesion of the die to the fibrous reinforcements.

The calorimetric measurements show that the vitreous transition of flexible polyurethane segments does not change significantly. In the case of glass fibers, it spreads over a wide temperature range. /1! This may indicate that the chain relaxation is relatively disturbed by the chemcial attachment between the surface of the fiber and the die. The impact of the type of reinforcement on the die quality is also shown by the extraction tests coupled to infrared analyses. The presence of Kevlar fiber fabric has a catastrophic impact on the rate of advancement of the reaction and we are able to extract about 90% of the soluble fractions. For carbon fibers, the soluble extracts are not negligible: 20% . In IR one sees urea bonds in lower percentages than for an urea polyurethane prepared without carbon fibers. Glass fibers give a different result. The soluble extracts are comparable to extracts from the die alone. The oiling type (coupling agent) present on the fiber surface as well as the water molecules participate in the reactions with isocyanate functions. Furthermore, when the isocyanate functions are provided by diphenyl methane diisocyanate MDI, there is a formation of isocyanurate cycles, probably due to the trimeridation of the functions (NCO) in the presence of basic sites on the glass fiber surface.

The static mechanical properties determined under bending conditions provide an additional element in terms of the impact

182

C-3

of the reinforcement. Actually, the curves recorded show a fragile carbon composite behavior for a ductile glass composite behavior and this is for tests performed at low temperatures (10°C below the vitreous transition of the die). The Kevlar composites exhibit low modulus values and a poor high temperature behavior.

The difference in the longitudinal and transverse modulus values compared to the mathematical models used is greatest for carbon composites.

3 - Dynamic mechanical measurements performed with the viscoelastometer provided us with an additional experimental element on whether or not a second relaxation exists beyond the vitreous transition. Our conclusion in this regard is based on PLAZEK's studies [78] and states that the "relaxation" observed is not associated with a molecular phenomenon, but to the entire composite system.

4 - Composites with a polyurethane elastomer matrix should find many applications because of their combined properties of flexibility and rigidity.

The reinforcement of polyurethane elastomers with long fibers leads to a rigid material in the fiber direction and allowing certain movements in any other direction. The amplitude of this will be maximum in the direction perpendicular to the reinforcements.

5 - Finally, we propose glass fibers based on commercial formulations (V-L100 and V-M400) to be used as testing materials by SNIAS on mechanical structures. The two polyurethane matrices selected have comparable elastomer properties. However, the absorption characterized by the angle of loss values tg (θ) is greater in polyurethane PUR-M400.

Future studies should focus on certain research areas to improve the interfacial properties with carbon and aramide fibers and the implementation conditions. For example, the chemical blockage of excessively reactive isocyanate functions and their release prevents impregnation problems caused by the lifespan in the reaction pot, and makes it possible to prepare preimpregnated polyurethane-fiber systems.

The results on the quality of the matrix disturbed in the presence of carbon and araminde fibers are surprising. To our knowledge, the influence of such reinforcements on other dies, such as polyurethane, has not be elicited in literature. In this light, a thorough study should be conducted.

184

REFERENCES

1. D.J. Lyman. "Step Growth Polymerization", Vol. 3, 95, 1972, D.H. Solomon, Editor

2. J.H. Saunders, K.C. Frisch. High Polymers, Vol. 16, Part I, "Polyurethanes Chemistry and Technology", Interscience Publishers, 1962.

3. J. Robin. Information Chimie, 176, 203 (1978)

4. L.H. Peebles Jr. Macromolecules, 7(6), 872 (1974).

5. D.J. Lyman. J. Polym. Sci., 45, 49 (1960).

6. K.A. Pigott. Encyclopedia of a Polymer Science and Technology, Vol. 11, p. 506 (1969), Interscience Publishers.

7. H. Ulrich. J. Polym. Sci., Macromol. Rev., 11, 93 (1976).

8. Lipatov. Adv. Ureth. Sci. Technol., 4, 1 (1974), K.C. Frisch, S.C. Reegen, Editors.

9. R.R. Aitken, G.M.F. Jeffs. Polymer, 18, 197 (1977).

10. D.R. Andrews, T.J. Hammack. J. Polym. Sci., B(3), 665 (1965).

11. T. Tanaka, T. Yokoyama, Y. Yamguchi. J. Polym. Sci., A-1(6), 2153 (1968).

12. A.M. North, J.C. Reid. Europ. Polym. J., 8, 1129 (1972).

13. W.J. Macknight, M.Yan. J. Polym. Sci., C(42), 817 (1973).

14. R.W. Seymour, S.L. Cooper. Macromolecules, 6, 48 (1973).

15. C.H.M. Jacques. Polymers Alloys, D. Klemper, K.C. Frisch, Editors, 1 (1977).

16. S.L. Cooper, J.C. West, R.W. Seymour. Encyclopedia of Polymer Science and Technology, Supplement No. 1, John Wiley and Sons, 521 (1976).

17. S.L. Cooper, A.V. Tobolsky. J. Appl. Polym. Sci., 10, 1837 (1966).

18. R. Bonnart. J. Macromolec. Sci., B(2), 115 (1968).

19. J.M. Estes, R.W. Seymour, D.S. Huh; S.L. Cooper. Polym. Eng. and Sci., 9(6), 383 (1969).

20. I.O. Sayer, R.T. Jefferson, J.V. Pustinger, J.L. Schwendeman Organic coatings preprints, 32(1), 288, (1972).

21. H.N. Ng, A.E. Allegrezza, R.W. Seymour, S.L. Cooper, Polymer, 14, 255, (1973).

22. S.L. Samuels, G.L. Wilkes, J. Polym. Sci., 43, 149 (1973).

23. C.E. Wilkes, C.S. Yusek, J. Macromol. Sci. Phys., 7, 579 (1973).

24. R.W. Seymour, A.E. Allegrezza Jr., S.L. Cooper, Macromolecules, 6(6) 896 (1973).

25. N.S. Schneider, C.S. Paik Sung, R.W. Matton, J.L Illinger, Macromolecules, 8(1), 62, (1975).

26. J. Koutsky, Polym. Letters 8, 353 (1970).

27. Y. Camerlin, J. Gole, J.P. Pascault, Die Angew. Makromol. Chem., 95, 67 (1981).

28. Y. Camberlin, A. Chakar, J.P. Pascault, Caoutchoucs et Plastiques No. 261, 153 (1982).

29. G.G. Seefried, J.V. Koleske and F.E. Critchfield, J. Appl. Polym. Sci., 19, 2493 (1975).

30. S. Lin, J. Biranowski and D.H. Lorenz, Advances in Urethane Science and Technology, D.C. Frisch and K. Klemper, Eds., Vol. 8, 105, (1981).

31. G. Trappe, Advances in Polyurethane Technology, Eds. J.M. Buist and H. Gudgeon, Chap. 3, (1968).

32. C.S. Schollemberger, Polyurethane Technology, P. Bruins, Ed., Chap. 10, (1969).

33. J.H. Saunders, Rubb. Chem. Tech. 33(5), 1259 (1960).

34. K. Pigott, B.F. Frye, K.R. Allen, S. Steingiser, W.C. Darr and J.H. Saunders, J. Chem. Eng. Data, 5(3), 391 (1960).

35. R.J. Athey, J.G. Dipinto and J.S. Rugg, Adiprene L, A liquid Urethane Elastomer, Dev. Prod. Rep. no. 10, DuPont (1968).

36. N.V. Steere, Handbook of Laboratory Safety, 2nd ed., Chemical Rubber Company (1971).

37. D. Klempner and K.C. Frisch, Advances in Urethane Science and Technology, Vol. 8, p. 93 (1981).

38. Y. Camberlin, J.P. Pascault, J.M. Letoffe and P. Claudy, J. Polym. Sci. Polym. Chem. Ed. 20, 383, (1982).

186

39. Y. Chamberlin, J.P. Pascault, J.M. Letoffe and P. Claudy, J. Polym. Sci. Polym. Chem. Ed. 20, 1445 (1982).

40. Y. Chamberlin and J.P. Pascault, J. Polym. Chem. Ed. 21, 415 (1983).

41. C.S. Paik Sung, T.W. Smith, C.B. Hu, Nak-Ho SUNG, Macromolecules, 12, 538 (1979).

42. B.D. Agarwall, L.J. Broutman, Analysis and Performance of Fiber Composites (1980).

43. P. Lefranc, (Fiber and glass reinforcement), Plastiques A9, Techniques de l'Ingenieur.

44. G. Debicki, Doctoral Thesis in Engineering, INSA-Lyon (1978).

45. J. Verdu, Long-term plastics behavior, Techniques de l'Ingenieur, Vol. 19.

46. R.M. Gerkin, L.F. Lawler, E.G. Schwarty, Reinforcement Systems of high modulus RRIM urethane composites, SPI Urethane Div., Meeting Oct. 1978.

47. D.L. Simpkins, Reinforced Reaction Injection Moulding Process and Materials for Automatic Body Panels S.A.E. Tech. Paper Series, Fevrier-Mars 1979, Detroit.

48. K.W. Schulte, H. Boden, K. Seel, C. Weber, Glass Fiber Reinforced RIM Polyurethanes - Properties and Processing Techniques, Kunstoffe 68. 9, 1978, pp. 510-515.

49. A.B. Isham, Reaction Injection Moulding with Glass Fiber Reinforcement S.A.E. Tech. Paper Series, Fevrier-Mars 1978, Detroit.

50. D.G. Gluck, J.R. Hagan and D.E Hipchen, Journal of Cellular Plastics, May-June 1980, pp. 159-170.

51. B. Dewimille, Doctoral Thesis in Engineering, Paris 1980.

52. H.S. Loveless, Journal of Testing and Evaluation STEVA, Vol. 1, No. 6, 532-537 (1973).

53. M. Coquet, Industrial Control Revue No. 114. Apr.. 45-49 (1982).

54. L.B. Grezczuk, Theoretical and Experimental Studies and Properties and Behavior of Filamentary Composites. Report No. 3550, (1966).

55. Puck, Loading and deformation of layered fiber reinforced plastic bars, Kunstoffe, 1967.

56. S.W. Tsai, Structural Behavior of Composite Materials-Aeroneutronic Publication No. U-2122 (1963).

57. S.W. Tsai, Stuctural Behavior of Composite Materials, NASA, CR 71, (1964).

58. J.C. Ekwall, Structural Dynamics and Materials Conf. Palm Springs, Calif., (1966).

59. M. Schrader, Modern Plastic 195 (1967).

60. G.E. Vogel, 22nd Conf. S.P.I.R.P/C Section 13 B (1967).

61. M. Das, J. Appl. Polym. Sci., 17, 1019 (1973).

62. Bomo, Doctoral Thesis in Engineering, Mulhouse (1983).

63. J.P. Bayoux, Doctoral Thesis in Science, Lyon (1980).

64. H. Manson and M. Sperling, Polmer Blends and Composites, Plenum Press N.Y. (1977).

65. A.T. Dang Thi, Y. Camberlin, T.M. Lam, J.P. Pascault, Matrix Angew, Makrom. Chem., 111, 29 (1983).

66. R. Battistella, Doctoral Thesis in Science, Strasburg (1971).

67. A.T. Dang Thi, Doctiral Thsis in Science, Lyon (1982).

68. A.L. Chang, R.M. Briller, E.L. Thomas, R.J. Zadrahaler, F.E. Critchfield, Polymer 23, 1060 (1982).

69. T.H. Farebrother and J.A. Raymond, Polymer Engineering Composite, (1977) Chap. 4.

70. S. Fischer, I. Roman, H. Harel, G. Marom and H.D. Wagner, Journal of Testing and Evaluation, Sept. 303-307 (1981).

71. R.E. Chambers and F.J. McGarry, ATSM Bulletin No. 238, 38 (1969).

72. J.J. Herque, Doctoral Thesis in Engineering, Mulhouse (1975).

73. A.S. Kenyon, J. Coll. Interf. Sci. 27, 761, (1968).

74. P.W.R. Beaumont, J. of Adhesion 6, 107, (1974).

75. K. Reed, Polym. Composites 1, 44 (1980).

76. Yong Sok O, Doctoral Thesis in Science (in progress).

77. J.K. Gilham, J.A. Benci and R.F. Boyer, Polym. Eng. Sci. 16, 357 (1976).

78. L.E. Neilsen, Polym. Eng. Sci. 17, 713, (1977).

79. D.J. Plazek et al., J. Polym. Sci. Phys., 20, pp. 1533-1583 (1983).

80. Analytical Chemistry of the Polyurethanes, Interscience, Vol. 16, part III.

81. G. Fages and Q.T. Pham, Die Makromol. Chem., 179, 1011 (1978).

82. Y. Camberlin, J.P. Pascault and Q.T. Pham, Die Makromol. Chem., 180, 397 (1979).

83. J. Consaga, J. Appl. Polym. Sci., 24, 2147 (1970).

84. G. Fages and T. Pham, Die Makromol. Chem., 180, 2435 (1979).

85. A.T. Dang Thi, J.P. Pascault and Q.T. Pham, Makromol. Chem. Rapid Commun., 3, 49, (1982).

END

DATE

FILMED

MAR 15 1985